N° d'ordre : 41680

THESE

présentée en vue
d'obtenir le grade de

DOCTEUR

en

Spécialité : Automatique et Informatique Industrielle

Par

LOUAJRI Hanane

**DOCTORAT DELIVRE CONJOINTEMENT
PAR MINES DOUAI ET L'UNIVERSITE DE LILLE 1**

Titre de la thèse :

Centralized and Decentralized Fault Diagnosis of a Class of Hybrid Dynamic Systems: Application to Three Cell Converter

Soutenue le 5 Fevrier devant le jury:

President	*Bruno FRANCOIS*	*Professeur à l'Ecole Centrale de Lille*
Rapporteur	*Audine SUBIAS*	*Maître de conférences (HDR) à l'INSA de Toulouse*
Rapporteur	*Dimitri LEFEBVRE*	*Professeur à l'Université du Havre*
Examinateur	*Ghaleb HOBLOS*	*Enseignant chercheur (HDR) à l'ESIGELEC de Rouen*
Directeur de thèse	*Moamar SAYED-MOUCHAWEH*	*Professeur à l'Ecole des Mines de Douai*

Laboratoire(s) d'accueil : Département Informatique Automatique, Mines Douai
Ecole Doctorale SPI 072 (Lille I, Lille III, Artois, ULCO, UVHC, Centrale Lille)

ACKNOWLEDGEMENTS

Despite appearances, this page is the most difficult to write. How to say in a few words my gratitude to those who have always encouraged me in making this work.

First of all, I would like to thank my thesis supervisor, Professor Moamar SAYED-MOUCHAWEH, for his valuable suggestions and assistance during the preparation of this thesis. Without his guidance and support, this thesis might not have presented here.

I would also like to thank Professor Stéphane LECOEUCHE, the research director, and Mr. Philippe HASBROUCQ, head of the laboratory at the automatic department for their help and availability.

Special thanks goes to Ms. Audine SUBIAS, Professors Dimitri LEFEBVRE and Bruno FRANCOIS and Mr. Ghaleb HOBLOS for their comments on the research presented in this dissertation.

From simple readers to people who have devoted their time and energy to help me in this work, to all of these people, I want to express my thanks.

Finally, I dedicate this work to my parents who supported and encouraged me during all these years. I thank them from the bottom of my heart for allowing me to go so far in my studies. Also thank you to all my family and friends for their love, encouragement and support during those years.

Contents

List of Tables

List of Figures

Chapter 1

General introduction

1.1 Context and motivation

Online fault diagnosis of complex dynamical systems is crucial to ensure safe operation in spite of faults impacting the system behaviors. A fault can be defined as a non-permitted deviation of at least one characteristic property of a system, or one of its components, from its normal or intended behavior. Consequences of the occurrence of faults can be severe and result in human casualties, environmentally harmful emissions, high repair costs, or economical losses caused by unexpected stops in production lines. Therefore, early detection and isolation of faults is the key to maintaining system performance, ensuring system safety, and increasing system life.

Many complex dynamical systems are embedded in the sense that they consist of a physical plant with a discrete controller. Therefore, the system has several discrete changes between different configuration modes through the actions of the controller exercised on the system plant (e.g., actuators). This kind of system, called discretely controlled continuous systems (DCCS), is modeled as hybrid dynamic systems (HDS). In the latter, the dynamic behavior evolves continuously with time according to the discrete mode in which the system is. When a change in the system discrete mode, or configuration, occurs, the continuous dynamic behavior will evolve differently. Consequently, model based diagnosis approaches need to take into account both the continuous and discrete dynamics of the system as well as the interactions between them in order to achieve the fault diagnosis.

The general principal of model based diagnosis approaches is based on the use of a mode of the system normal and/or fault behaviors. Discrete-event model diagnosis based approaches describe the system as discrete modes changes in response to the occurrence of discrete events. Therefore, they ignore the continuous dynamics of the system. Continuous model diagnosis based approaches represent the system dynamics as a continuous time evolution using differential or difference equations. However, they do not take into account the discrete changes of the system discrete modes or configurations. Consequently, these both approaches cannot be used to achieve the fault diagnosis of HDS since in the latter both continuous and discrete dynamics (evolutions) and the interactions between them must be taken into account. In addition, faults may impact both the continuous and discrete dynamics. Therefore, the diagnosis module, generally called diagnoser, must deal with these faults. Indeed, fault can be characterized by abnormal changes in system parameters describing the system continuous dynamics. This type of faults are called

parametric faults. Furthermore, faults can cause undesired or unpredicted changes in the system discrete mode or configuration. This type of faults is termed as discrete faults. Consequently, HDS fault diagnosis approaches need to handle both parametric and discrete fault. Finally, many real HDS contain a huge number of discrete modes. Therefore, constructing a global model of the system can be very hard and complex. Thus, it is important to develop an approach which scale well to the system size (to discrete modes).

Consequently based on all these issues, diagnosis of HDS is a challenging task. For this reason, the contributions of this dissertation aims at achieving the parametric and discrete faults diagnosis of HDS, in particular DCCS, with multiple discrete modes.

1.2 Contributions

This dissertation develops an event based scheme for parametric and discrete faults in HDS, in particular DCCS, Louajri et al. (2013), Louajri and Sayed-Mouchaweh (2014a), Louajri and Sayed-Mouchaweh (2014b), Louajri and Sayed-Mouchaweh (2014c), Louajri and Sayed-Mouchaweh (2014d). This scheme is based on the decomposition of the system into several discrete and continuous components in order to exploit the modularity property of the system. The goal is to construct local hybrid models for the system hybrid components. Each local hybrid model is build by the combination of a discrete component with its interacting continuous components (i.e., components that change its continuous dynamic evolution according to the discrete state of this discrete component). These local hybrid models are used to:

- facilitate the construction of the system global model in order to achieve the centralized fault diagnosis;
- construct the local diagnosers in order to achieve the decentralized fault diagnosis for large scale systems.

The specific contributions of this dissertation are as follows:

1. **Modular parametric and discrete faults centralized diagnosis approach**. This approach builds one global hybrid diagnoser based on the use of one global model of the system. The global model is constructed based on the synchronous composition between the different hybrid local models. The use of the latter facilitates significantly the construction of the global model as well as the centralized diagnoser.

2. **Parametric and discrete faults decentralized diagnosis approach without the need to a global model**. In this approach, local hybrid diagnosers are constructed based on the local hybrid models. Each hybrid diagnoser aims at diagnosing the parametric and discrete faults that can occur in its associated hybrid component. In order to achieve a diagnosis performance

equivalent to the one of the centralized diagnosis structure, a coordinator is defined. The latter merges the local diagnosis decisions in order to obtain one global diagnosis decision equivalent to the one of the centralized diagnoser. The local diagnosers and the coordinator are constructed without the use of a global model but only the local models. Therefore, this approach scales well to large scale systems with multiple discrete modes.

3. **Hybrid diagnosability and co-diagnosabilty notions**. For the centralized hybrid diagnoser, a hybrid diagnosability notion is defined. The latter aims at verifying if the system model is rich enough in information in order to allow the diagnoser to infer the occurrence of parametric and discrete faults within a bounded delay after their occurrence. This hybrid diagnosability notion is an extension of the diagnosability notion defined for discrete event systems, Sampath et al. (1996). Likewise, a hybrid co-diagnosability notion is defined to verify whether the set of local hybrid diagnosers with their coordinator can infer the occurrence of parametric and discrete faults that the centralized hybrid diagnoser can infer. These two notions are based on the use of hybrid events traces which combine discrete events and the events generated by the continuous dynamics. Therefore, they show clearly the interest of using the events generated by the continuous dynamics in order to enhance the diagnosis capacity of the system for both parametric and discrete faults.

4. **Experimental case study for parametric and discrete faults decentralized diagnosis of three cell converter**. A benchmark of three cell converter is developed using Matlab-Simulink^{TM} environment and Stateflow^{TM} toolbox. This benchmark is used in order to validate the performance of the proposed parametric and discrete faults decentralized diagnosis approach. To this end, several normal and fault scenarios are generated. In these scenarios, parametric and discrete faults are generated in different time instances and different discrete modes as well as different orders. In addition, noises are added in order to be close as much as possible to real operation conditions.

1.3 Organization

Chapter 2 presents an overview of HDS and their related model based diagnosis approaches. Firstly, the basic definitions and classes of HDS are provided. Then, the major HDS modeling tools are presented. Next, general scheme of HDS fault diagnosis, problem formulation and challenges are detailed. Finally, the HDS fault diagnosis approaches, in particular DCCS, are studied and compared. They are classified into three main categories: parametric fault diagnosis, discrete fault diagnosis and parametric and discrete faults diagnosis approaches. A simple example of one tank level water control system is used throughout the chapter in order to illustrate and compare these approaches of literature.

Chapter 3 presents the principal scheme and steps of the proposed modular hybrid centralized diagnosis approach. Firstly, the different steps to build the local

models of discrete, continuous and hybrid system components are detailed. Then, the construction of the system global model, based on the synchronous composition of the hybrid local models, is described. Finally, the steps of hybrid centralized diagnoser construction are explained. The simple example of one tank level water control system is used throughout the chapter in order to illustrate the proposed approach.

Chapter 4 presents the motivations, principal scheme and steps of the proposed hybrid decentralized fault diagnosis approach. Firstly, the different steps of the decentralized hybrid diagnosis approach are presented. Then, the procedure to build the local hybrid diagnoser for each hybrid component of the system is detailed. Then, the steps to merge the local diagnosis decisions through a coordinator are discussed. Finally, centralized and decentralized diagnosis structures are compared. The example of one tank level water control system is used throughout the chapter in order to illustrate the proposed approach and to compare it with the centralized diagnosis approach detailed in Chapter 3.

Chapter 5 presents the experimentation of the decentralized fault diagnosis approach developed in chapter 4. Firstly, the three cell converter system is presented. Then, the different steps to build the decentralized hybrid diagnosis structure, developed in Chapter 4, for the three cell converter are detailed. Next, the simulation results are presented and discussed. Finally, the performance of centralized and decentralized diagnosis structures, developed respectively in Chapter 3 and Chapter 4, is compared in order to show the interest of using decentralized diagnosis approach for large scale systems.

Chapter 6 summarizes the contributions of this dissertation, discuss the current limitations of the proposed approaches and presents the future directions of this work in order to improve these approaches.

Chapter 2

Related work in hybrid dynamic systems diagnosis

Contents

2.1 Introduction

Model-based diagnosis approaches achieve fault diagnosis by detecting a difference between expected behavior defined by a system model and observed behavior provided by the sensors. The model represents the system nominal (desired) behavior as well as the faulty behaviors in response to faults belonging to a predefined set of failure modes. A failure mode gathers a set of faults in a system which has the same effect according to either the configuration or maintaining procedure. Model-based diagnosis approaches can be classified according to the used modeling representation tool. Generally, they can be divided into discrete-event, continuous and hybrid dynamic systems approaches. Discrete event systems approaches, Bhowal

et al. (2007), abstract time by modeling system behavior as a sequence of discrete events and states and the fault diagnosis task is achieved based on analyzing observed event sequences. Continuous systems approaches , Cocquempot et al. (2004), employ a continuous or discrete-time representation of the system, and use quantitative and/or qualitative methods for diagnosis. Hybrid dynamic systems (HDS) approaches combine continuous and event-based behaviors, and are the most general, but also the most complex.

This dissertation focuses on diagnosis of HDS. The latter change its continuous dynamics from one discrete mode to another discrete mode in response to the occurrence of discrete events. HDS cover a wide class of systems and can be applied to a broad class of applications. Examples of HDS are tanks water level control system, multiple collisions, Coulomb friction, power converter and constrained pendulum, Van Der Schaft et al. (2000).

In HDS, faults can occur as abnormal change in the value of parameters describing the continuous dynamics and are called parametric faults. Faults can also occur as unexpected, abnormal, changes in system discrete mode and are called discrete faults. Discrete event systems approaches deal with discrete faults; while continuous systems approaches deal with parametric faults. HDS approaches must deal with both parametric and discrete faults.

Chapter 2 is organized as follows. Firstly, the definition, motivation and classes of HDS are presented. Then, the problem formulation and challenges of the diagnosis in HDS are handled. Finally, major fault diagnosis approaches of HDS are studied and their performance is compared. The goal of this comparison is to emphasize the interest and the progress beyond the state of the art of the proposed approaches, developed in Chapters 3 and 4 in this dissertation. In order to illustrate and compare the presented modeling tools and diagnosis approaches of the literature, the well-known one tank water level control system (Fig.2.1) is used.

2.2 Hybrid dynamic systems

2.2.1 Definition and motivation

Many physical systems are HDS. The term 'hybrid dynamic system' has many meanings, one of which is a dynamical system whose evolution depends on a coupling between variables that take values in a continuum and variables that take values in a finite or countable set, Van Der Schaft et al. (2000). Therefore, a HDS are a dynamic systems that exhibits both continuous and discrete dynamic behaviors.

Example 2.1 ***The one tank water level control system as a hybrid dynamic system***

The one tank water level control system (Fig.2.1) exhibits the continuous dynamics represented by the level of the tank and the discrete dynamics represented by the discrete modes of the pump (pump on (Pon), pump off ($Poff$)) and the valve (valve opened (VO), valve closed (VC)). The discrete mode of the pump or the valve is changed in response to a discrete control command event sent by the

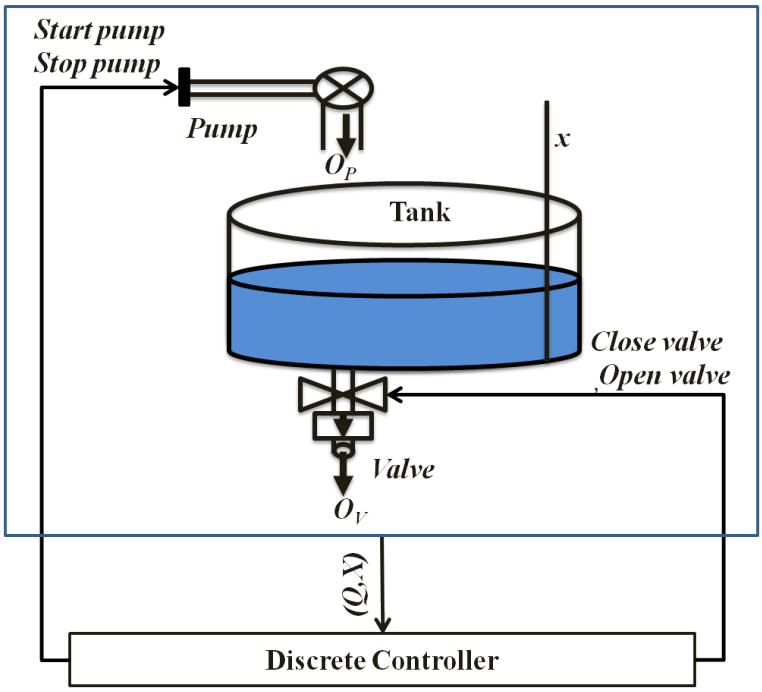

Figure 2.1: One tank water level control system.

discrete controller. As an example, if the initial discrete mode of the pump, respectively the valve, is 'pump off', respectively 'valve closed', the control command event 'start pump', respectively 'open valve', will change the pump discrete mode to 'pump on', respectively 'valve open'. The continuous dynamic evolution of the tank level x depends on the discrete modes of the pump and the valve. The tank filling is assured by flow rate O_P/s_T when the pump is on, where s_T is the tank surface,. The tank emptying is assured by flow rate O_V when the valve is opened. Therefore, the one tank water level control system is a HDS.

2.2.2 Classes of hybrid dynamic systems

Three particular classes of HDS can be distinguished:

1. **Jump linear systems (JLS)**, Farhood and Beck (2014), are defined as a family of HDS with randomly jumping parameters (usually governed by a Markov jump process) and are used to model systems subject to failures or structure changes. JLS are characterized by a hybrid state (q, x) consisting of a discrete state q whose evolution is governed by uncontrollable external discrete inputs (unknown) and a continuous variable x whose evolution is represented by a differential equation without input (an autonomous system). JLS operates in multiple discrete modes. The individual modes are linear. However, the switching between these modes introduces non-linearity into the whole system description. Many HDS are a subject to random abrupt variations such as a manufacturing system and a networked control system, Zhang and Boukas

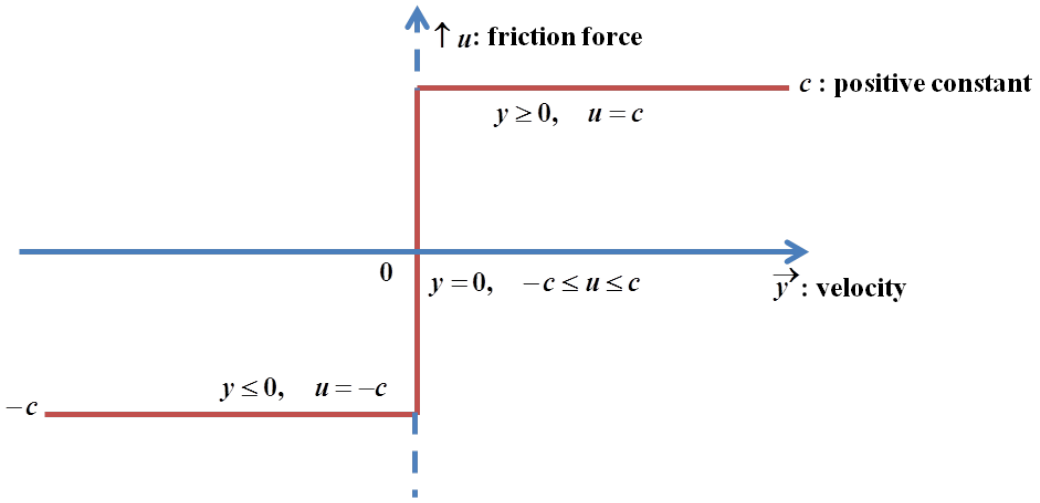

Figure 2.2: Coulomb friction characteristics.

(2009). Let consider a manufacturing system producing a product with a constant demand rate d, Gupta et al. (2009). The system is, however, subject to occasional breakdowns and so at any time t_k, the system can be in one of two discrete modes. The first mode is normal one in which the number of produced products x_{k+1} at time t_{k+1} is equal to the products x_k produced at time t_k plus the production u_k minus the demand rate d ($x_{k+1} = x_k + u_k - d$). In the failure discrete mode (breakdowns), the number of products x_{k+1} will be equal to $x_k + u_k$.

2. **Piecewise affine systems (PWAS)**, Eren et al. (2014), are a special class of HDS in which the continuous dynamics within each discrete mode are affine and the mode switching always occurs at specific subsets of the state space that are known a priori. PWAS are also an important modeling class for nonlinear systems because a wide variety of non-linearities are either piecewise-affine (e.g., a saturated linear actuator characteristic) or can be approximated as piecewise-affine functions, Rodrigues and How (2003). PWAS are obtained by partitioning the state and input set into a finite number of polyhedral regions, and by considering linear/affine subsystems sharing the same continuous state in each region, Bemporad et al. (2005). As an example of PWAS, we can cite the Coulomb friction system, Van Der Schaft et al. (2000). In this system, the velocity y has three discrete modes characterized by three different segments of piecewise linear characteristics (see Fig.2.2).

3. **Discretely controlled continuous systems (DCCS)**, Palejiya et al. (2014), are a special class of HDS widely used in the literature. These systems are composed of a set of continuous variables arranged in a feedback loop with a discrete event controller. In these systems, the changes in discrete modes are achieved by discrete control commands, e.g. opening or closing a valve

(see Fig.2.1) . As examples of this class of HDS, we can cite temperature and water level (see Fig.2.1) control systems, Van Der Schaft et al. (2000).

The class of HDS considered in this dissertation is a DCCS.

2.3 Hybrid dynamic systems modeling

There are three major modeling tools widely used in the literature to model HDS. These tools are briefly presented in the next subsections.

2.3.1 Hybrid Petri nets

Petri nets are widely used to model discrete event systems. Continuous Petri nets model continuous systems or approximate discrete systems. Hybrid Petri nets (HPN), Gomez et al. (2010), model HDS by combining discrete and continuous parts. HPN is formally defined by the tuple:

$$HPN = \{P, T, h, Pre, Post\} \tag{2.1}$$

where

- $P = \{P_1,\ P_2,\ \cdots,\ P_k\}$ is a finite, not empty, set of places;
- $T = \{T_1,\ T_2,\ \cdots,\ T_m\}$ is a finite, not empty, set of transitions;
- $h : P \bigcap T \rightarrow \{D, C\}$ called 'hybrid function', indicates for every node whether it is a discrete node (D) or a continuous node (C). Node represent transitions (indicated by bars) and places (indicared by circles);
- $Pre : P_i \times T_j \rightarrow \Re^+$ *or* $\aleph$ is a function that defines an arc from a place P_i to a transition T_j;
- $Post : P_i \times T_j \rightarrow \Re^+$ *or* $\aleph$ is a function that defines an arc from a transition T_j to a place P_i;

Example 2.2 ***Hybrid Petri net for the one tank system example***

HPN for the one tank system example is depicted in Fig.2.3. HPN is composed of one continuous place P_1 represented by a double circle, two continuous transitions represented by empty bars, T_1 and T_2, four discrete places P_2, P_3, P_4 and P_5 represented by a circle and four discrete transitions represented by full bars T_3, T_4, T_5 and T_6. P_1 describes the level x of tank, P_2 and P_3 describe, respectively, the position closed and opened of the valve and P_4 and P_5 describe, respectively, the position off and on of the pump. Continuous transitions T_1 and T_2 describe, respectively, the filling and the emptying of the tank. Discrete transitions T_3, T_4, T_5 and T_6 describe, respectively, the controller commands to open and to close the valve and to start and to stop the pump.

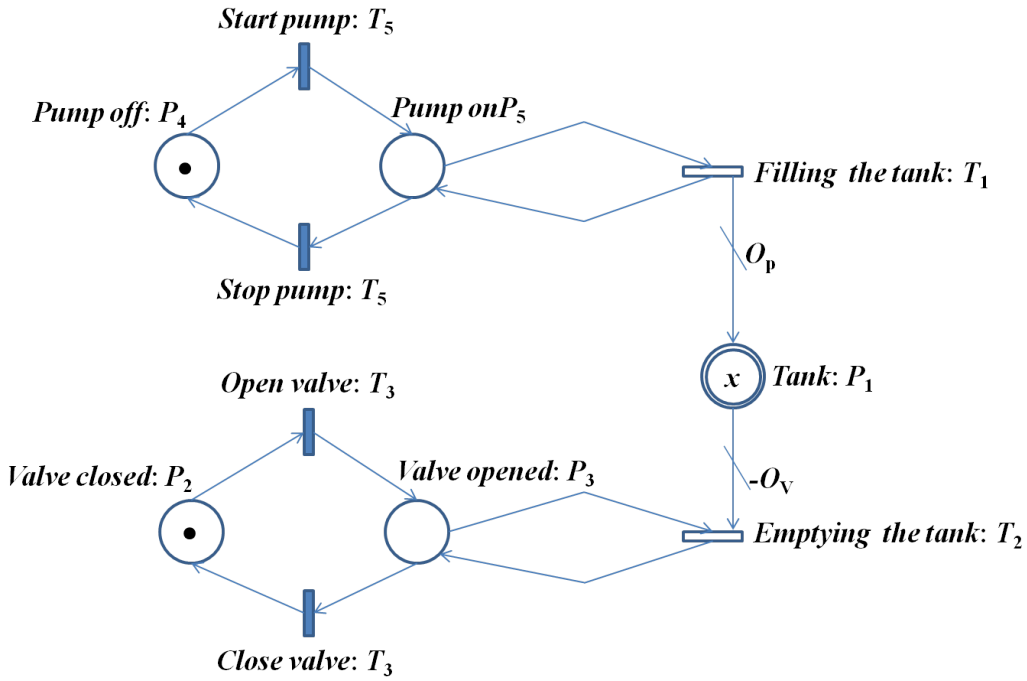

Figure 2.3: Hybrid Petri net for the one tank system example.

2.3.2 Hybrid automata

A hybrid automaton is a mathematical model for HDS, which combines, in a single formalism, transitions for capturing discrete change with differential equations for capturing continuous change. A hybrid automaton is a finite state machine with a finite set of continuous variables whose values are described by a set of ordinary differential equations. A hybrid automaton is defined by the tuple, Lynch et al. (2003):

$$G = (Q, \Sigma, X, flux, Init, \delta) \tag{2.2}$$

where,

- Q: is the set of hybrid model states of the system;
- Σ: is the set of system events;
- X: is a finite set of continuous variables describing the continuous dynamics of the system;
- $flux : Q \times X \rightarrow \Re^n$: is a function characterizing the continuous dynamic evolution of X in each state q;
- $\delta : Q \times \Sigma \rightarrow Q$: is the state transition function of the system. A transition $\delta(q, e) = q^+$ corresponds to a change from state q to state q^+ after the occurrence of discrete event $e \in \Sigma$;

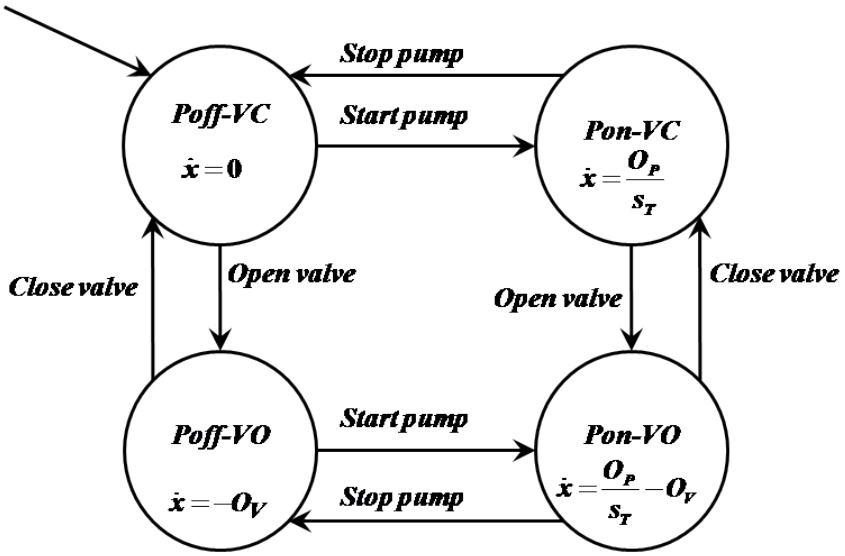

Figure 2.4: Hybrid automaton for the one tank system example.

- $Init = (q_1 \in Q,\ X(q_1),\ flux(q_1))$: is the set of initial conditions.

Example 2.3 ***Hybrid automaton for the one tank system example***

Hybrid automaton for the one tank system example is depicted in Fig.2.4 and is defined by the tuple:

$$G = (Q, \Sigma, X, flux, Init, \delta)$$

where,

- $Q = \{Poff - VC,\ Pon - VC,\ Pon - VO,\ Poff - VO\}$. represents, respectively, pump off and valve closed, pump on and valve closed, pump on and valve opened and pump off and valve opened;
- $\Sigma = \{Start\ pump,\ Stop\ pump,\ Open\ valve,\ Close\ valve\}$;
- $flux$: is the dynamic evolution $\dot{x}$ of the tank level in each discrete state;
- δ: is the state transition function. As an example $\delta(Poff-VC, Start\ pump) = Pon - VC$;
- $Init:\ (Poff - VC,\ \dot{x} = 0)$;

2.3.3 Hybrid bond graphs

brid bond graph), Roychoudhury et al. (2009), are a graphical description of a physical dynamic systems with discontinuities. Similar to a regular bond graph, it is an energy-based technique. Hybrid bond graph are directed graphs defined by a set

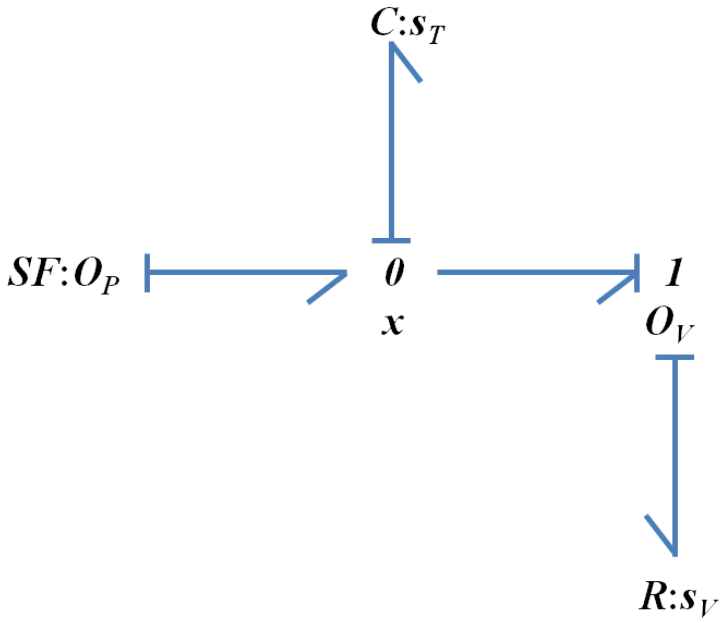

Figure 2.5: Hybrid bond graph for the one tank system example.

of summits and a set of edges. Summits represent components. The edges, called bonds (drawn as half arrows), represent ideal energy connections between the components. However, it allows instantaneous switching of the junction structure, which may violate the principle of continuity of power. Hybrid bond graph extend bond graphs to a hybrid modeling framework, in a way that they produce physically verifiable hybrid models of system behavior. Controlled junctions act as ideal switches, enabling a junction to be in either the 'on' or the 'off' state.

Example 2.4 ***Hybrid bond graph for the one tank system example***

Hybrid bond graph for the one tank system example, Fichou (2004), is depicted in Fig.2.5. The input flow into the tank, assured by the pump, is represented as flow source SF. The two important pressures are the input flow O_P and the output flow O_V. A 0-junction defines each of these variables (pressures) and connects to the storage element that represent the tank capacity (C) according the the section s_T of the tank. The dissipative element represented by the valve section s_V is connected to the 1-junction to represent the emptying of the tank through the valve.

The molding tools used in this dissertation to model HDS is a hybrid automaton.

2.4 Hybrid dynamic systems fault diagnosis

Fault diagnosis is very important because it can provide accurate fault information and defined the diagnosability of the system.The diagnosability consists in determining if the system model is rich enough in information in order to allow the diagnoser to infer the occurrence of predefined faults within a finite observable events after

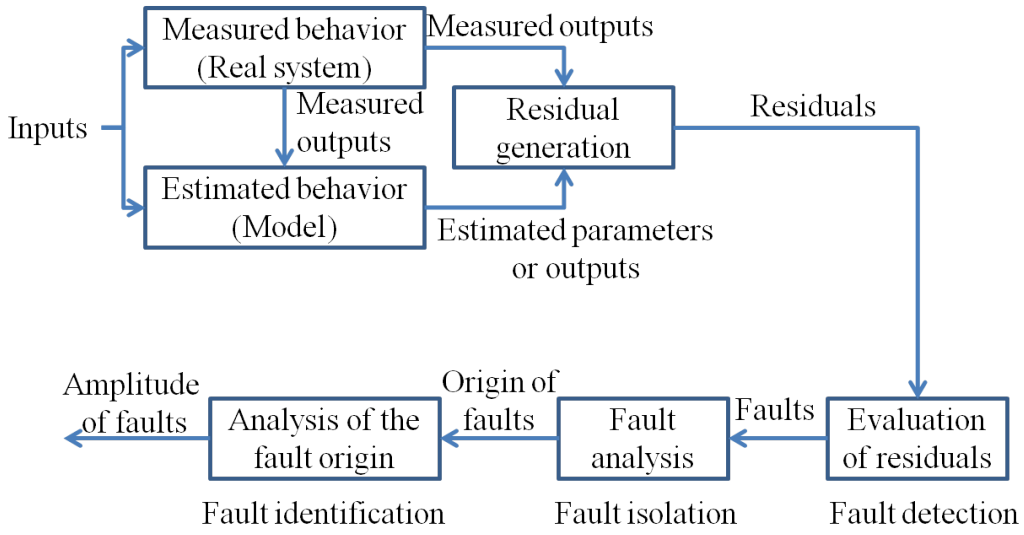

Figure 2.6: General scheme for model-based diagnosis of hybrid systems.

their occurrence. The overall aim of this section is to provide a general scheme of HDS fault diagnosis, the problem formulation and challenges of the diagnosis of this type of systems and definition of the classes of faults that can occur in HDS.

2.4.1 General scheme of hybrid dynamic systems fault diagnosis

Fig.2.6 presents the general scheme used by the different approaches of the literature to achieve the fault diagnosis in HDS. Three main tasks are achieved by these approaches. These tasks are developed in the following section.

2.4.1.1 Fault estimation

In HDS, the behavior evolves over time. Therefore, continuous monitoring is necessary in order to predict the time-varying behavior and to compare it to the real one. This comparison helps to generate indicators about fault behaviors. Generally, two techniques are used to characterize the time varying behavior:

- Output estimation, Daigle (2008) ,which is an algorithm that uses a series of measurements observed over time, containing noise (random variations) and other inaccuracies, and produces estimates of unknown outputs that tend to be more precise than those based on a single measurement alone.

- Parameter estimation, Ding et al. (2014),which consists in determining the parameters and states of the mathematical model of the system that can be associated with possible faults in the system. The parameter estimation is achieved in three steps: establishment of the mathematical model of the system's normal behavior, determination of the relationship between the model

parameters and the physical system parameters and estimation of the model parameters from the input/ output measurements.

2.4.1.2 Fault detection

Given both measured and estimated parameters or outputs, observed differences are computed, and a decision must be made fault occurrence or not since these differences implicate the presence of a fault in the system. Fault detection, Pisano et al. (2014), takes as input the difference between expected and actual parameters or outputs, defined as residual, and issues a true or false value indicating fault presence. Therefore, fault detection consists in designing a residual enabling one to make a binary decision indicating the occurrence or not of a fault in the system.

2.4.1.3 Fault isolation and identification

Given that a fault has occurred, fault isolation, Zouari et al. (2014), reasons about the differences between model-predicted and observed behaviors, and establishes possible candidates as combinations of faults that can explain the observed behavior. Therefore, fault isolation consists of determining the localization (sources or origins) of different faults. In single fault diagnosis, the goal is to obtain a unique single fault that can explain the observations. In multiple fault diagnosis, the goal is expanded to obtain sets of faults that, taken together, explain the observations.

If fault isolation discovers a fault, then fault identification computes the magnitudes of the faults that match the observations most closely.

This dissertation focuses only on single fault scenarios.

2.4.2 Classes of faults

The faults are abnormalities that affect one or more properties of the system, which can lead to a failure or to a breakdown of the system. They can occur in different parts of the system. The objective of diagnosis is to establish which possible faults or combinations of faults match the observed system behavior. In the literature, faults are classified according to their location, their time evolution or their nature.

2.4.2.1 Classification of faults according to their location

As shown in Fig.2.7, faults may manifest in different parts of the system, namely, the actuators, the system, the sensors and controller.

1. **Actuator faults**, Bouibed et al. (2014), act at the operational part and deteriorate the signal input of the system. They represent a total or partial failure of an actuator acting on the system. An example of total failure of one actuator is an actuator which remains 'stuck' at a position resulting in an inability to control the system through the actuator. Partial failure actuators are actuators reacting similarly to the rated speed but only partly, that is with some degradation in their action on the system (loss of engine power, leakage in a cylinder ...). For the one tank water level system, the actuator faults are

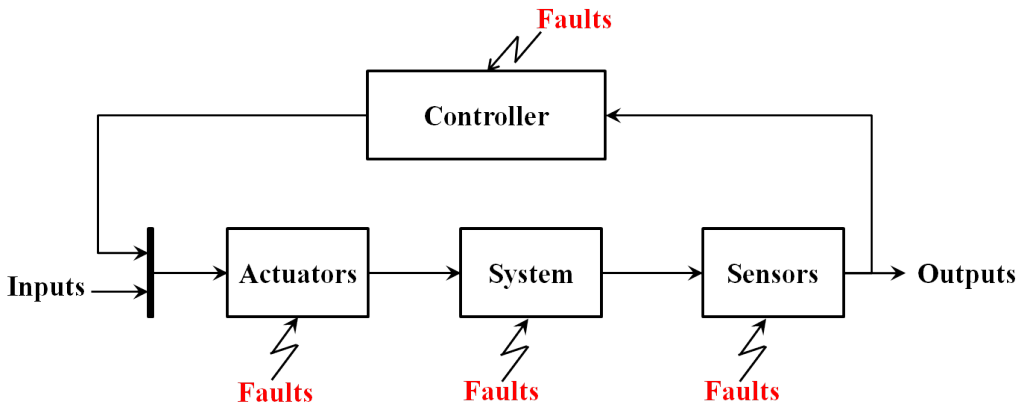

Figure 2.7: Location of faults in hybrid dynamic systems.

the failed on or failed off of the pump and the stuck opened or stuck closed of the valve. They are total failure impacting the actuators pump and valve.

2. **Sensor faults**, Cha and Agrawal (2014), are the cause of a bad image of the physical state of the system. A partial failure sensor produces a signal with varying degrees of consistency with the true value of the variable to be measured. This can result in a reduction of the displayed value relative to the true value, or the presence of a skew or increased noise preventing proper reading. A total failure sensor produces a value that is not related to the measured variable. For the one tank water level system, the sensor fault is the breakdown of the continuous sensor x measuring the water level. The sensor cannot provide anymore a measure about the water level in the tank.

3. **System faults**, Cha and Agrawal (2014), are faults resulting in breakage or deterioration of a system component reducing its capacity to perform a task. For the one tank water level system, the system fault is represented by the leakage in the tank. The occurrence of leakage fault will change the system parameters.

4. **Controller faults**, Savkin and Evans (2002), impact the controller outputs. Indeed in this case, the controller does not respond properly to its inputs sensor reading . As an example for the one tank system, when the water level is above a certain threshold, the controller must react by opening the valve. When the controller is in a faulty mode, it will not respond when the level is high. In this dissertation controller faults are not considered

2.4.2.2 Classification of faults according to their time evolution

As shown in Fig.2.8, faults can be abrupt, intermittent or gradual.

1. **Abrupt faults**, Yoo (2014), manifest at full magnitude immediately. Abrupt faults are defined as a malfunction of a component that must be replaced or

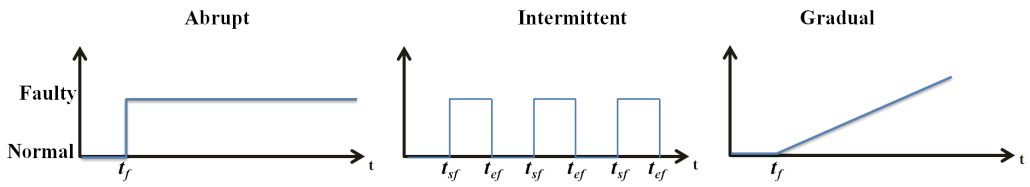

Figure 2.8: Classification of faults according to their time evolution.

repaired. This type of faults is characterized by a discontinuity in the temporal evolution of the variable. This evolution is characteristic of an abrupt fault of the corresponding element. For the one tank water level system, the failed on or failed off of the pump and the stuck opened or stuck closed of the valve are abrupt faults.

2. **Intermittent faults**, Xu et al. (2014), are a special case of abrupt faults with the property that the signal returns randomly to its normal value. In this dissertation intermittent faults are not considered.

3. **Gradual faults**, Sun et al. (2014), represent slow degradations. Gradual faults are very difficult to detect. For the one tank water level system example, a leakage in the tank is a gradual fault, since the leakage section s_{lg} is increased gradually.

2.4.2.3 Classification of faults according to their nature

In HDS, faults can occur as parameter value changes in continuous dynamics, and are called parametric faults. Faults can also occur in the form of mode-changing behavior, which are represented as unexpected changes in system mode and are called discrete faults. Therefore, two types of faults may be considered for hybrid dynamical systems depending on the dynamics that are affected by faults (parametric or discrete). In both cases, they entail unpredicted, abnormal, changes in the system configuration:

1. **Parametric faults**, Isermann (2006), are associated with changes in parameter values, and are useful for modeling degradations in system components. For example, the occurrence of a leakage in the tank water level control system (see Fig.2.1) adds a new parameter to the dynamic evolution (section of leakage).

2. **discrete faults**, Daigle (2008), affect the system discrete dynamics and are considered either as the occurrence of unobservable events and/or reaching discrete fault modes. For example, valve can become stuck closed by itself.

Example 2.5 ***Parametric and discrete faults for the one tank system example***

For the one tank system, six faults can be considered for this system (see Table 2.1).

Table 2.1: Faults for the diagnosis of one tank level control system.

Fault types	***Fault labels***	***Fault description***
Discrete faults	F_1	Valve stuck opened
	F_2	Valve stuck closed
	F_3	Pump failed off
	F_4	Pump failed on
	F_5	Breakdown of the continuous sensor x
Parametric fault	F_6	Leakage in the tank ($s_{lg} \neq 0$)

2.4.3 Problem formulation and challenges in diagnosis of hybrid dynamic systems

HDS comprise several discrete modes. In each one of the latter, particular continuous dynamics are defined. Generally, they are characterized by a set of differential equations. The transition from one mode to another one occurs in response to the occurrence of the external observable events as controller events, or internal events as discrete faults. The parametric faults impacting the continuous dynamics' parameters can also be represented as unobservable internal events entailing a transition towards new modes. In both cases, the problem of fault diagnosis in HDS is to distinguish normal and fault (discrete and parametric) modes based on observable discrete events and continuous measurements issued from continuous dynamics.

Therefore, several challenges are arisen to achieve fault diagnosis in HDS as:

- HDS have both complex, hybrid dynamics and a relatively large number of components that can interact in a large scale system, Koutsoukos et al. (2002);
- The space of possible candidates is exponential in the number of faults. Therefore, space and time complexity of diagnosis algorithms becomes exponential in the general case;
- HDS have several distinct operational modes. The latter correspond to different dynamical models, whereby each model has different governing dynamics. Each dynamical model can correspond to a nominal or faulty operating mode and no distinction is made about whether the transition between modes is normal or due to the occurrence of a fault event, Kan John et al. (2009);
- Different types of faults (parametric and discrete) affect the continuous and discrete dynamics and generate unobservable autonomous transitions. This increase significantly the complexity of fault diagnosis.

2.5 Hybrid dynamic systems fault diagnosis approaches

Because of the different types of faults and the different modeling representation tools, fault diagnosis can be performed in many different ways. In order to situate

the contribution of this dissertation according to the state of the art, model-based diagnosis approaches of HDS, in particular DCCS, are classified into three main categories:

1. approaches for the diagnosis of parametric faults,
2. approaches for the diagnosis of discrete faults,
3. approaches for the diagnosis of both parametric and discrete faults.

2.5.1 Parametric fault diagnosis approaches

In this category, Cocquempot et al. (2004), Alavi et al. (2011), Kamel et al. (2012), Van Gorp (2013), parametric faults are considered to be abnormal deviations of parameter values in continuous modes of operation. Functional redundancy between the model and the sensor measurements are exploited in order to achieve the fault diagnosis. Relations over observable variables are computed in order to generate residuals sensitive to a certain subset of parametric faults. In order to take into account the changes in system dynamics due to discrete mode changes, residuals are generated for each of these modes. However, since they consider all discrete events as observable, discrete faults entailing abnormal changes in discrete modes cannot be diagnosed. In addition, since residuals are defined in each discrete mode, the system global model including all its discrete modes is required to achieve the parametric fault diagnosis. This increases significantly the approaches complexity in the case of large scale systems. In the latter, the global model contains a huge number of discrete modes.

Fig.2.9 illustrates the general principle of parametric fault diagnosis approaches in HDS, in particular DCCS. An observer is used in order to estimate the continuous variables $\hat{X}$ characterizing the continuous dynamics in each discrete mode. The latter is identified based on the discrete control command events issued by the controller. Then, residuals $r_{q(t)}$ sensitive to a predefined set of parametric faults are generated at each discrete mode q based on the use of real, X (measured) and estimated, $\hat{X}$ (by the observer) values of continuous variables as well as the input vector $u(t)$.

Example 2.6 ***Parametric fault diagnosis for the one tank example***

Let us take the approach proposed by, Van Gorp (2013), as an example of parametric fault diagnosis approaches and let us applied it to achieve the diagnosis of a leakage in the tank (parametric fault defined by the leakage section s_{lg}). The different discrete operating modes must be defined. For the one tank example, four discrete modes are defined:

1. Pump off and valve closed;
2. Pump on and valve closed;
3. Pump on and valve opened;

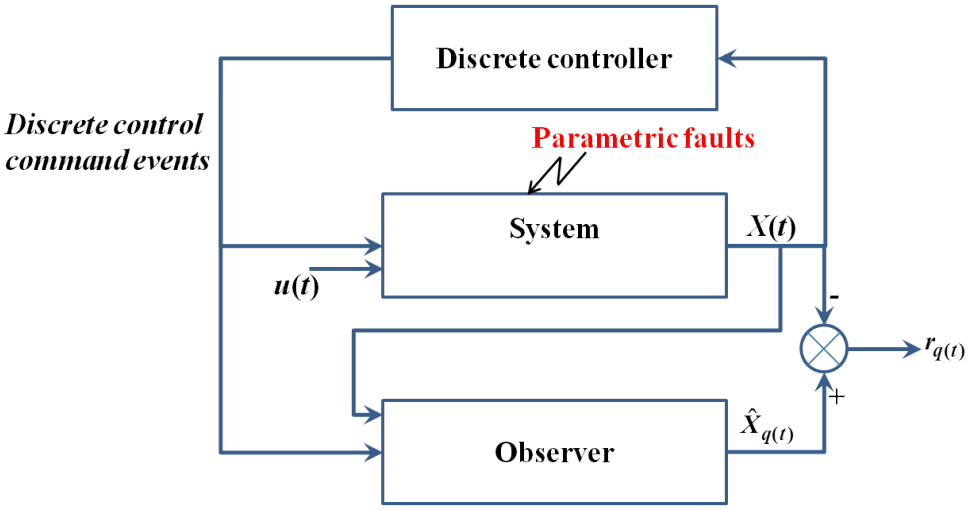

Figure 2.9: General principle of parametric fault diagnosis approaches for DCCS.

4. Pump off and valve opened;

These discrete modes are determined by the observer based on the discrete control command events (Open valve, Close valve, Start pump, Stop pump) issued by the controller. In each discrete mode, residual r sensitive to the tank leakage is defined as follows:

$$r_{q(t)} = \hat{x}_{q(t)} - x(t) \tag{2.3}$$

where $r_{q(t)}$ is the residual at discrete mode q, $x(t)$ is the measured value of the water level at instant t and $\hat{x}_{q(t)}$ is the estimated value of the water level. The dynamic evolution, $\dot{x}$, of the water level, x, is defined by, Van Gorp (2013):

$$\dot{x} = A_{q(t)}x(t) + B_{q(t)}u(t) + K_{q(t)}f_c(t) \tag{2.4}$$

where u is the input vector equal to O_p (see Fig.2.1), $A_{q(t)}$ and $B_{q(t)}$ are constant matrices characterizing the dynamic evolution of x. $A_{q(t)}$ and $B_{q(t)}$ change in each discrete mode q according to the pump, P, and valve, V, discrete modes. $K_{q(t)}f_c(t)$ indicates the occurrence or not of the leakage. f_c is the parametric fault matrix. Therefore, f_c is equal to the leakage flow, $Q_{lg} = -\frac{s_{lg}\sqrt{2g}}{2s_T\sqrt{x_0}}x(t)$. In the case of leakage in the tank, $K_{q(t)}$ is equal to 1 and equal to zero otherwise. Thus, (2.4) is rewritten as follows, Cocquempot et al. (2004):

$$\dot{x} = -V\frac{s_V\sqrt{2g}}{2s_T\sqrt{x_0}}x + P\frac{O_P}{s_T} - K_{q(t)}\frac{s_{lg}\sqrt{2g}}{2s_T\sqrt{x_0}}x(t) \tag{2.5}$$

where, x_0 is the initial level of the tank, $A_{q(t)}$ is equal to $V\frac{s_V\sqrt{2g}}{2s_T\sqrt{x_0}}$, and $B_{q(t)}$ is equal to $P\frac{1}{s_T}$. P is equal to 0 when the pump is off and is equal to 1 when the pump is on. V is equal to 0 when the valve is closed and is equal to 1 when the valve is opened. Therefore, $A_{q(t)}$ is equal to 0 when the valve is closed and equal to $-\frac{s_V\sqrt{2g}}{2s_T\sqrt{x_0}}$ when

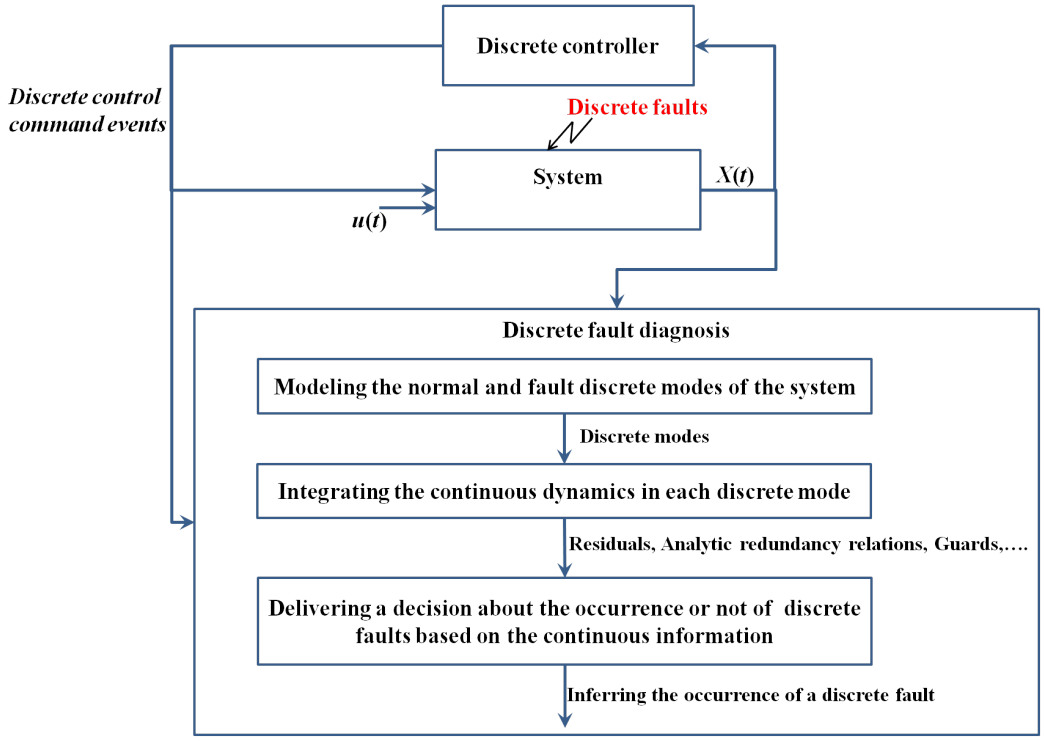

Figure 2.10: General principle of discrete fault diagnosis approaches for DCCS.

the valve is opened. $B_{q(t)}$ is equal to 0 when the pump is off and equal to $\frac{1}{s_T}$ when the pump is on.

The estimated value of $\hat{x}$ is calculated through a sliding mode observer, Van Gorp (2013). The estimated evolution in each discrete mode is calculated as follows:

$$\dot{\hat{x}} = A_{q(t)}\hat{x}_{q(t)} + B_{q(t)}u(t) + v_{q(t)} \tag{2.6}$$

where $v_{q(t)}$ is the correction term used in order to overcome the noises problem. $v_{q(t)}$ is calculated in each discrete mode as follows:

$$v_{q(t)} = -K_1 \left|r_{q(t)}\right|^{\frac{1}{2}} sign\left(r_{q(t)}\right) \tag{2.7}$$

where K_1 is a constant defined in $\Re^+$.

2.5.2 Discrete fault diagnosis approaches

In these approaches, the discrete faults are considered to be unobservable discrete events leading to unpredicted changes in the system configuration. They exploit the system continuous dynamics in order to generate observable events. The latter are then used to convert unobservable transitions, fired by discrete faults, into observable transitions. Consequently, These observable events allow to diagnose or to enhance the diagnosability of discrete faults (see Fig.2.10). According to how the

observable events are extracted from the continuous dynamics and how they are used to achieve the discrete fault diagnosis, these approaches can be divided into three subcategories: estimated continuous dynamics defined in normal modes based approaches, estimated continuous dynamics defined in normal and fault modes based approaches and guards based approaches. These three subcategories are developed in the following subsections.

2.5.2.1 Estimated continuous dynamics in normal modes based approaches

Estimated continuous dynamics in normal modes based approaches, Rahiminejad et al. (2012), Defoort et al. (2011), define in each expected, normal, discrete mode a set of residuals. All expected mode transitions are fired by the occurrence of observable discrete events. The residuals are equal to zero if the system remains in the same normal discrete mode. Thus, in the case of a normal observable discrete mode change, the residuals in the new discrete mode are equal to zero. If unpredicted change occurs due to the occurrence of unobservable discrete fault, the residuals, defined in the discrete mode before the fault occurrence, will be different of zero in the new (unpredicted) discrete mode. This change of residuals' values from zero indicates the occurrence of a discrete fault. The main drawback of these approaches is that each discrete fault requires the definition of at least one sensitive residual to the occurrence of this fault. This hypothesis is hard to satisfy in the most of real systems, in particular for large scale systems with huge number of discrete modes.

Example 2.7 ***Estimated continuous dynamics in normal modes based approaches for the one tank example***

In order to illustrated how these approaches achieve the discrete fault diagnosis, let us take the example of one tank level control system. Let us consider that only the discrete fault '*Pump failed on*' can occur. One residual is defined as the difference between the estimated $\hat{x}$ and measured x water level. In each discrete mode, the dynamic evolution of the measured water level is defined as follows:

$$\dot{x} = -VO_V + P\frac{O_P}{s_T} \tag{2.8}$$

V is equal to 1, respectively to 0, when the valve is opened, respectively closed. P is equal to 1, respectively to 0, when the pump is on, respectively off. Similarly in each discrete mode, the dynamic evolution of the estimated water level is calculated as follows:

$$\dot{\hat{x}} = -\hat{V}O_V + \hat{P}\frac{O_P}{s_T} \tag{2.9}$$

$\hat{V}$ is equal to 1, respectively to 0, when the valve should be opened, respectively closed. $\hat{P}$ is equal to 1, respectively to 0, when the pump should be on, respectively off.

In each discrete mode (q), a residual, $r_{q(t)}$, is defined as follows:

$$r_{q(t)} = \hat{x} - x \tag{2.10}$$

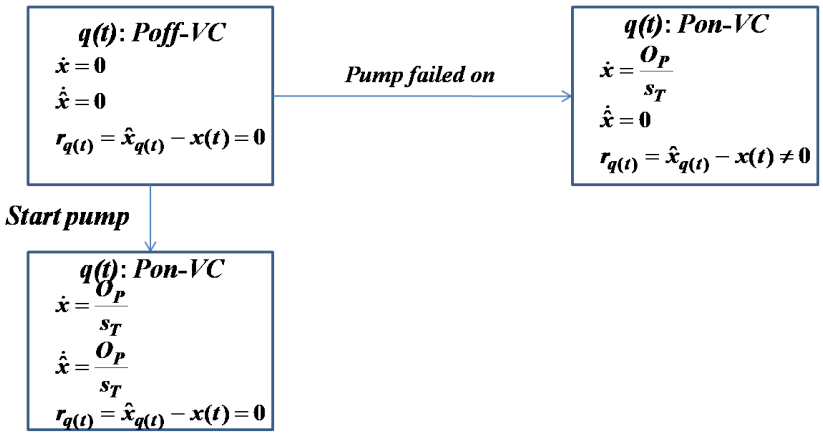

Figure 2.11: Estimated continuous dynamics in normal modes based approaches for Example 2.7.

In the case of the normal change of the system from discrete mode '$Poff - VC$' to discrete mode '$Pon - VC$' (due to the control command event *Start pump*), residual $r_{q(t)}$ in the new discrete mode '$Pon - VC$' is equal to zero (see Fig.2.11). Since the transition to the new discrete mode is observed, the dynamic evolution of the estimated water level, $\dot{\hat{x}}$, takes into account this discrete mode change. In the case of the unpredicted (abnormal) change of the system from discrete mode '$Poff - VC$' to discrete mode '$PFon - VC$' (due to discrete fault '*Pump failed on*'), residual $r_{q(t)}$ in this new discrete mode, '$PFon - VC$', is different from zero (see Fig.2.11). This is due to the fact that the transition to this new discrete mode is unobservable. Therefore, the dynamic evolution of the estimated water level, $\dot{\hat{x}}$, does not take into account this discrete mode change. Consequently, $r_{q(t)}$ will be different from zero. The change of residual value from zero generates an observable event used in order to detect the occurrence of the discrete fault '*Pump failed on*'.

2.5.2.2 Estimated continuous dynamics in normal and fault modes based approaches

Estimated continuous dynamics in normal and fault modes based approaches, Bayoudh et al. (2006), define in each normal or fault discrete mode a set of residuals. These residuals are defined based on a set of analytic redundancy relations (ARR) between system continuous variables. Value domain of each residual includes 0, 1 or *und* when the residual value is, respectively, zero, different of zero and undefined. The latter represents the case when the associated residual is not defined in the new active mode. A discrete fault is isolated by determining in which discrete fault mode the system is. This determination is based on the values domain of all the residuals in both normal and faulty modes. Therefore, these approaches require a sufficient number of residuals in order to discriminate all the fault discrete modes from normal discrete modes. This hypothesis is hard to satisfy for large scale systems with multiple discrete modes.

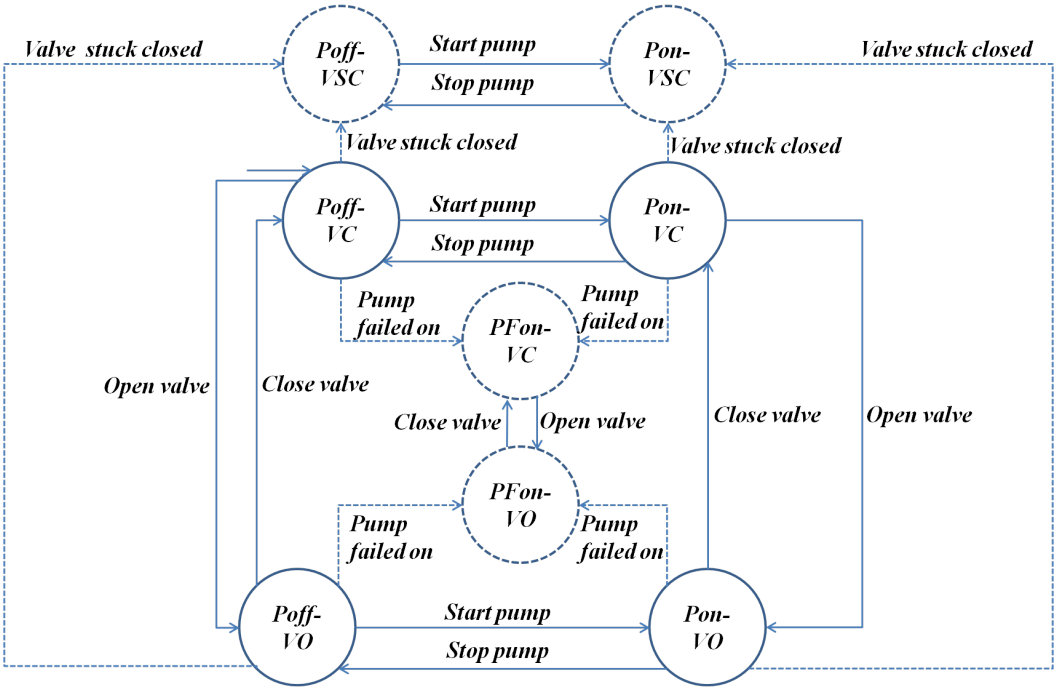

Figure 2.12: Hybrid automaton for Example 2.8.

Table 2.2: Table of analytic redundancy relations classified by mode.

System mode	*The corresponding analytic redundancy relations*
$Poff - VC$	$ARR_1 : \hat{\dot{x}} = 0$
$Pon - VC$	$ARR_2 : \hat{\dot{x}} = \frac{O_P}{s_T}$
$Pon - VO$	$ARR_3 : \hat{\dot{x}} = -O_V + \frac{O_P}{s_T}$
$Poff - VO$	$ARR_4 : \hat{\dot{x}} = -O_V$
$Poff - VSC$	$ARR_1 : \hat{\dot{x}} = 0$
$Pon - VSC$	$ARR_2 : \hat{\dot{x}} = \frac{O_P}{s_T}$
$PFon - VO$	$ARR_3 : \hat{\dot{x}} = -O_V + \frac{O_P}{s_T}$
$PFon - VC$	$ARR_2 : \hat{\dot{x}} = \frac{O_P}{s_T}$

Example 2.8 ***Estimated continuous dynamics in normal and fault modes based approaches for the one tank example***

For the one tank water level control system example, let us consider the discrete faults '$Valve\ stuck\ closed$' (VSC) indicated by fault label F_1 and '$Pump\ failed\ on$' ($PFon$) indicated by fault label F_2. Let us apply the approach proposed by Bayoudh et al. (2006), to achieve the diagnosis of these faults. The system is modeled using the automaton of Fig.2.12. It is supposed that these discrete faults can occur from any discrete mode. The analytic redundancy relations (ARR) of the system are

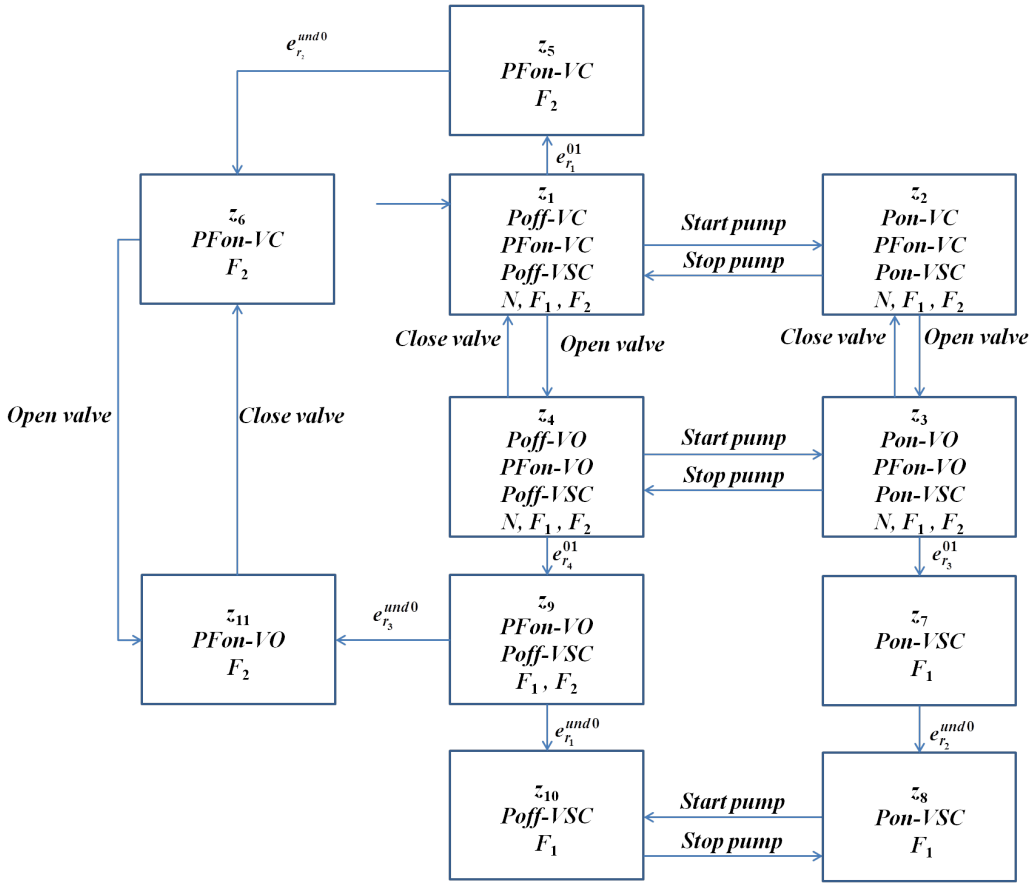

Figure 2.13: Diagnoser for the model defined in Fig.2.12.

computed in each of the four normal modes ($Poff-VC$, $Pon-VC$, $Pon-VO$, $Poff-VO$) and of the four faulty modes ($Poff-VSC$, $Pon-VSC$, $PFon-VO$, $PFon-VC$) (see Table 2.2). The global diagnoser is presented in Fig.2.13. From the initial state $Poff-VC$, the diagnoser infers with certainty the occurrence of discrete fault '*Pump failed on*' by using the continuous information. When the discrete fault '*Pump failed on*' occurred, residual r_1, calculated using ARR_1 ($r_1 = \hat{\dot{x}} - \dot{x}$) (see Table 2.2), changes its value from 0 to 1 and residual r_2, calculated using ARR_2 (see Table 2.2), changes its value from *und* (not defined in the normal discrete mode '$Poff-VC$') to 0. This change enabled the diagnoser to infer the occurrence of discrete fault, '*Pump failed on*'. The same reasoning is applied to infer the occurrence of discrete fault, '*Valve stuck closed*'.

2.5.2.3 Guards based approaches

Guards based approaches, Bhowal et al. (2007), Biswas et al. (2006), defined the normal discrete mode transitions as controlled or autonomous. Controlled transitions depend only on external events issued by the controller while autonomous transi-

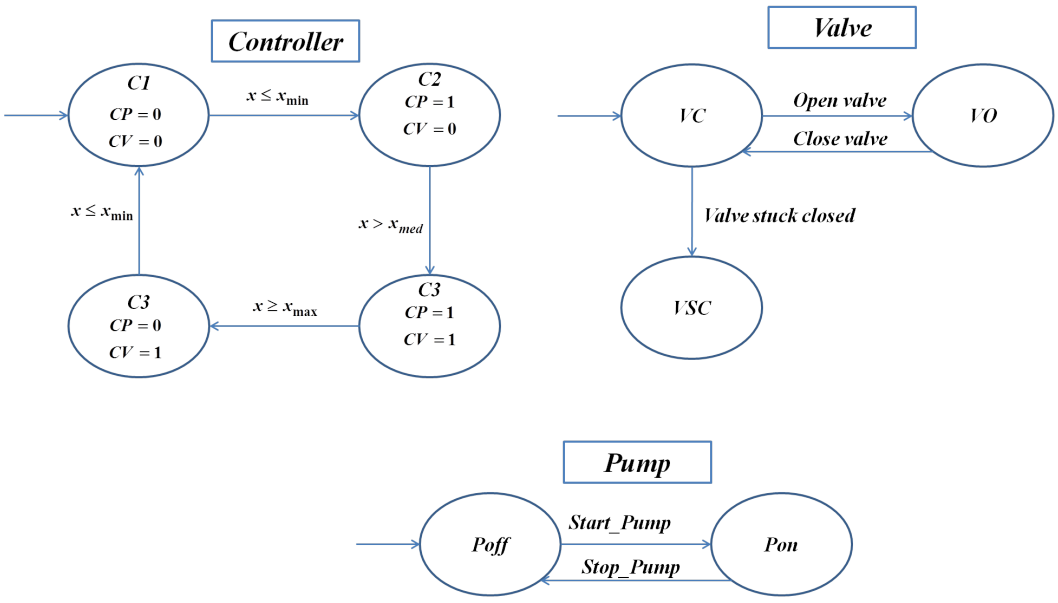

Figure 2.14: Discrete controller, valve and pump models for Example 2.9.

tions depend on internal system continuous variables. Transition guards are defined as linear inequalities based on these continuous variables. When a guard is satisfied, its corresponding mode transition is enabled. The diagnoser is constructed based on the set of transitions labeled by control command events as well as the guards defined by the system continuous variables. The diagnoser aims at distinguishing between the normal and faulty sequences (set of events and guards) based on the observable events and measured variables. The interest of these approaches is to enhance the diagnosability of discrete faults by integrating the continuous dynamics. Indeed, the transitions labeled by guards can help to enhance the diagnosability of discrete faults by integrating the continuous dynamics. Each discrete mode of the system is characterized by a different evolution of continuous variables and each transition validates certain number of guards associated to these variables. Consequently, in an indeterminate cycle, the evolution of continuous dynamics of these variables changes. This change will entail the violation (non-satisfaction) of some guards associated to certain states in this cycle and therefore allows to leave the indeterminate cycle. An indeterminate cycle is a sequence of uncertain states in which the diagnoser is unable to decide with certainty and within a finite number of observable events the occurrence of a fault. Thus, the system will get out of this indeterminate cycle within a finite time. However, these approaches do not scale to systems with a large number of discrete modes, since the diagnoser is built using the global model of the system.

Example 2.9 ***Guards based approaches for the one tank example***

For the one tank water level control system example, let us considered the discrete fault '*Valve stuck closed*' (VSC) indicated by fault label F_1. Let us apply the

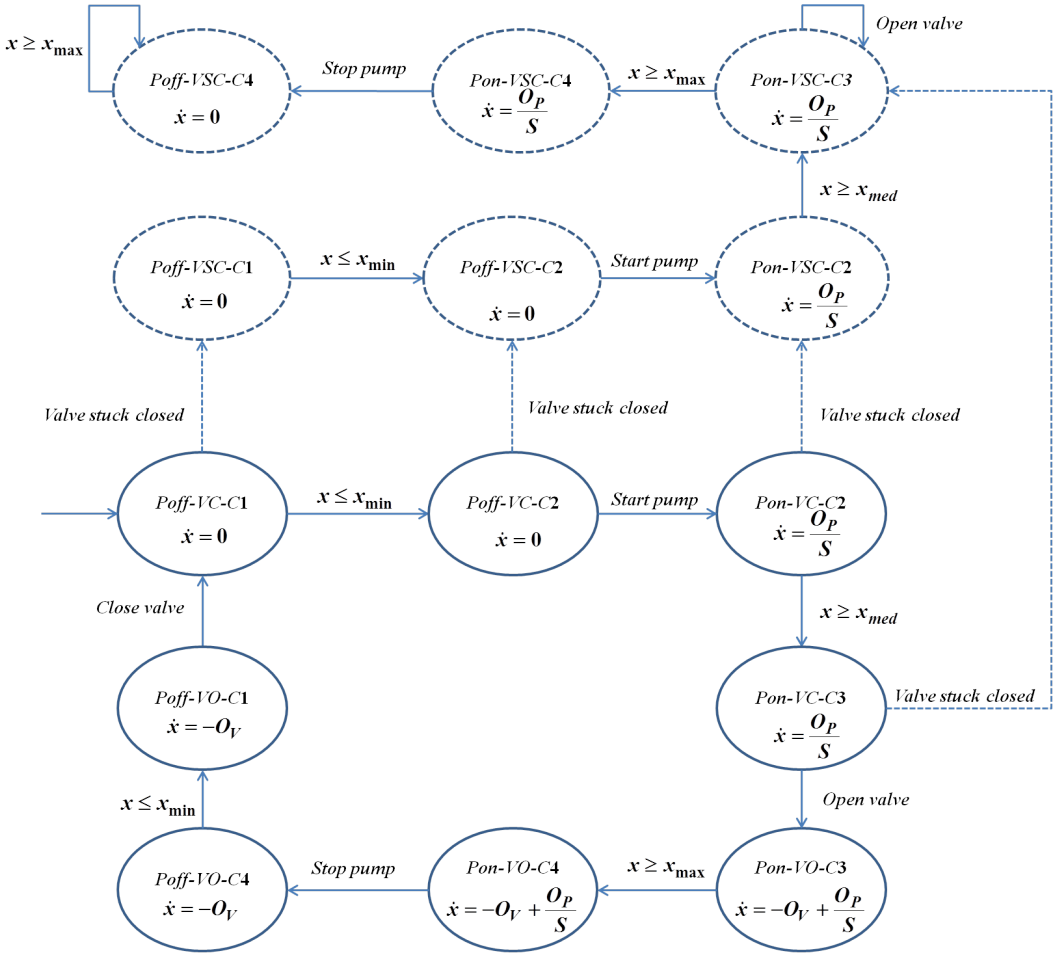

Figure 2.15: Hybrid model for Example 2.9.

approach proposed by Bhowal et al. (2007), to achieve the diagnosis of this fault. The model of the system is represented by a hybrid automaton as illustrated in Fig.2.15. The observable transitions between the normal discrete modes are assured by the control command events and the internal system continuous variables. The pump is controlled to be on if the water level is lower than the minimal level x_{min} and is controlled to be stopped if the water level is above the maximal level x_{max}. The valve is controlled to be opened when the water level is above the medium level x_{med} and is controlled to be closed when the level is lower than the minimal level x_{min}. The controller states are represented by $C1$, $C2$, $C3$ and $C4$. The discrete controller issues the control command events '$Start_P$' when the controller variable CP change from 0 to 1, '$Stop_P$' when the controller variable CP change from 1 to 0, '$Openvalve$' when the controller variable CV change from 0 to 1 and '$Closevalve$' when the controller variable CV change from 1 to 0 (see Fig.2.14). The global automaton is a result of the synchronization of the discrete automata of the discrete controller, the valve and the pump and the continuous dynamics evolution

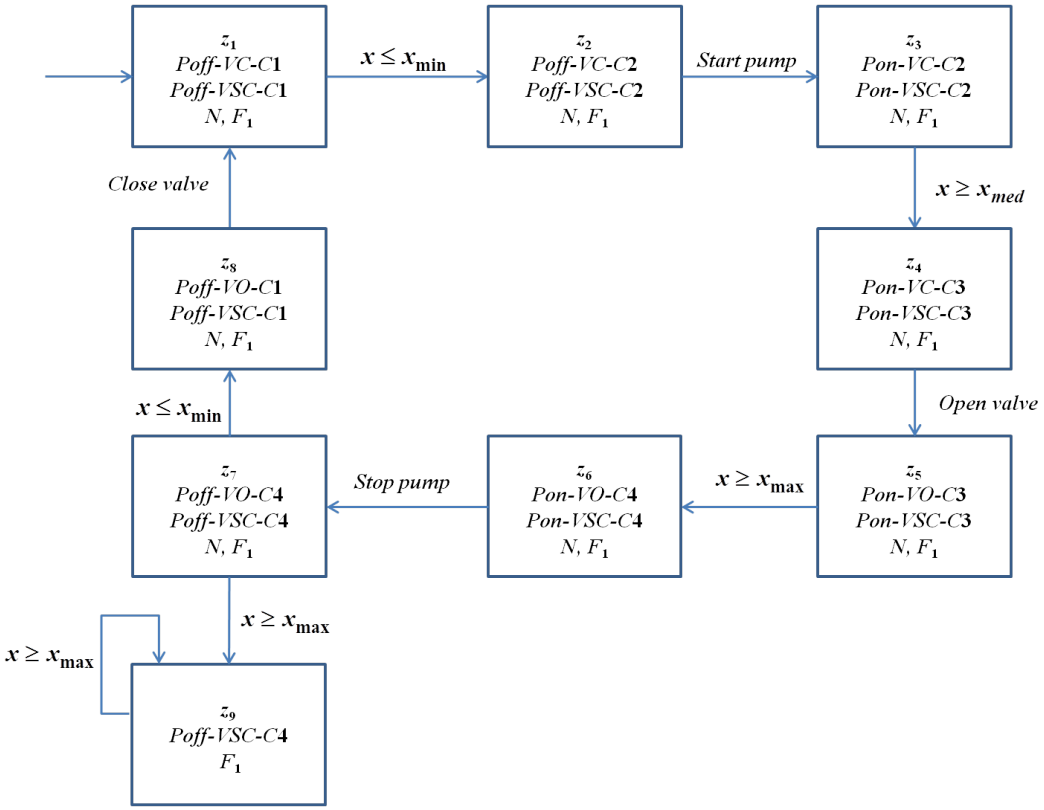

Figure 2.16: Diagnoser of the global model defined in Fig.2.15.

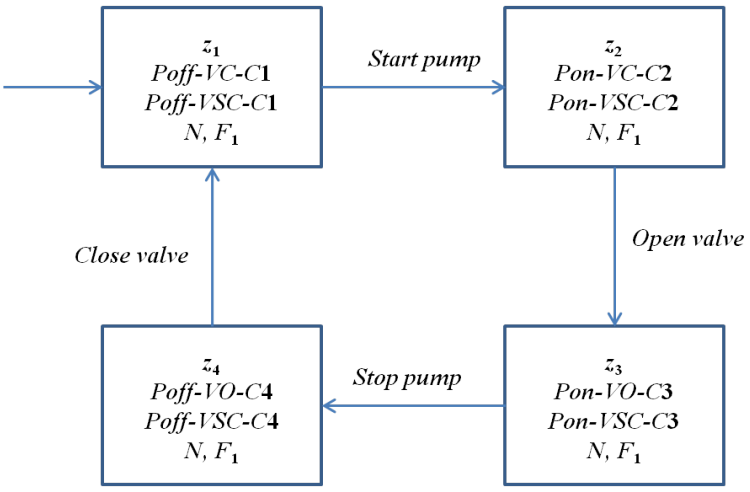

Figure 2.17: Diagnoser of the global model defined in Fig.2.15 excluding the continuous information.

corresponding to each global discrete mode. For the sake of simplicity, the discrete fault '*Valve stuck closed*' occurs starting only from the states where the valve is closed. We suppose that the flow of the pump id greater than the flow of the valve.

The global diagnoser diagnoses the discrete faults by generating a decision D_z. Every state z_i of the diagnoser is of the form ([state], [labels]), where labels indicate the system operating status (faulty, normal). The diagnoser is built based on the global model of the system. The diagnoser transition consists of only the observable events and the measurable continuous variables of the global model. A state z_i of the diagnoser includes the states having the same observable discrete output. The observable output is defined based on the controller command events. As an example, when pump is controlled to be on, the observable pump discrete state output is $P = 1$. The global diagnoser of the one tank water level control system is represented in Fig.2.16. As shown in Fig.2.16, the diagnoser states z_1, z_2, z_3, z_4, z_5, z_6, z_7 and z_8 form an indeterminate cycle indicating an uncertain decision 'N, F_1'. In the case of the occurrence of discrete fault '*Valve stuck closed*', the level in the tank will not decrease. Therefore, a guard $x \leq x_{min}$ will not be satisfied. The satisfaction of guard $x \geq x_{max}$ allows the diagnoser to leave the indeterminate cycle and to diagnose with certainty the occurrence of discrete fault '*Valve stuck closed*' (see Fig.2.16). If we remove the continuous information from the model, the diagnoser will remain in the indeterminate cycle (see Fig.2.17)

2.5.3 Parametric and discrete faults diagnosis approaches

This category includes few approaches for the diagnosis of both parametric and discrete faults. In these approaches, the discrete faults are considered to be unobservable discrete events leading to abnormal changes in the system discrete mode and the parametric faults are considered to be unobservable discrete events leading to unpredicted changes in the system parameters. They exploit the system continuous dynamics in order to diagnose parametric faults and to enhance the diagnosability of discrete faults; while they use the system discrete dynamics in order to diagnose discrete faults and to enhance the diagnosability of parametric faults (see Fig.2.18). According to how they extract the information allowing the diagnosis of parametric and discrete faults, these approaches can be divided into three subcategories: events time occurrence based approaches, continuous and discrete symbols based approaches and hybrid structure based diagnosis approaches.

2.5.3.1 Events time occurrence based approaches

Events time occurrence based approaches, Derbel (2009) and the references therein, capture the continuous dynamics by integrating the occurrence time of the system discrete events. They consider that the occurrence of discrete or parametric faults does not change events ordering but only alters their timing characteristics. Therefore, a discrete or parametric fault is diagnosed when predicted events occur too late or too early or they do not occur at all during their predefined time intervals. The main drawback of these approaches is that only parametric and discrete faults violating temporal constraints or specifications between events' time occurrences can

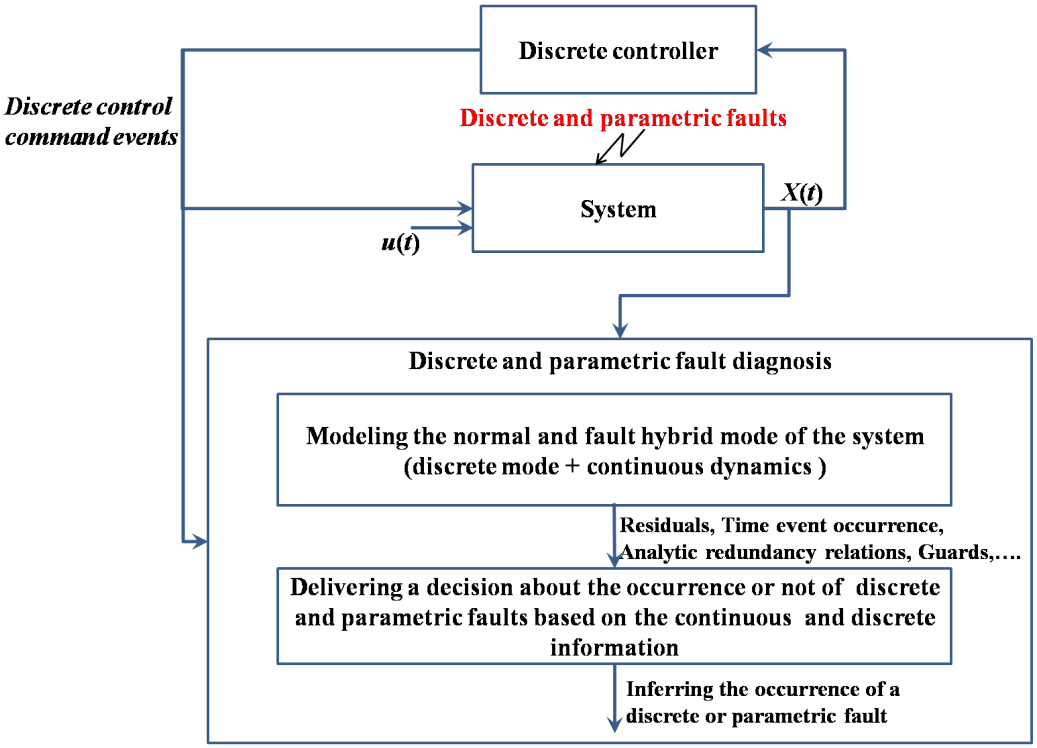

Figure 2.18: Parametric and discrete faults diagnosis structure.

be diagnosed.

Example 2.10 ***Events time occurrence based approaches for the one tank system example***

For the one tank water level control system example, let us consider the discrete fault $'Pump\ failed\ off'$ $(PFoff)$ indicated by fault label F_1 and the parametric fault $'Leakage\ in\ the\ tank'$ indicated by fault label F_2. Let us apply the approach proposed by Derbel (2009), in order to achieve the diagnosis of these faults. The system is modeled using the automaton of Fig.2.19. The system is considered to be equipped by three discrete sensors capturing respectively the minimal water level $(x = 0)$, medium water level $(x = 250)$ and maximal water level $(x = 500)$. When the level is equal to $x = 0$, $x = 250$ or $x = 500$, the events $S1$, $S2$ and $S3$ will be respectively, generated by the corresponding sensors. The time required to reach the predefined levels $(0,\ 250,\ 500)$ is computed based on the estimated flows of the pump $(\frac{O_P}{s_T})$ and the valve (O_V). Therefore, $\dot{x}$ is equal to $(\frac{O_P}{s_T} - O_V)$. This time is measured by a clock, x_1, initiated at each state of the system model. The pump is controlled to be on if event $S1$ is generated and is controlled to be stopped when event $S3$ is generated. The valve is controlled to be opened when event $S2$ is generated and is controlled to be closed when event $S1$ is generated. The diagnosis of the parametric and discrete faults is based on the time of the occurrence of

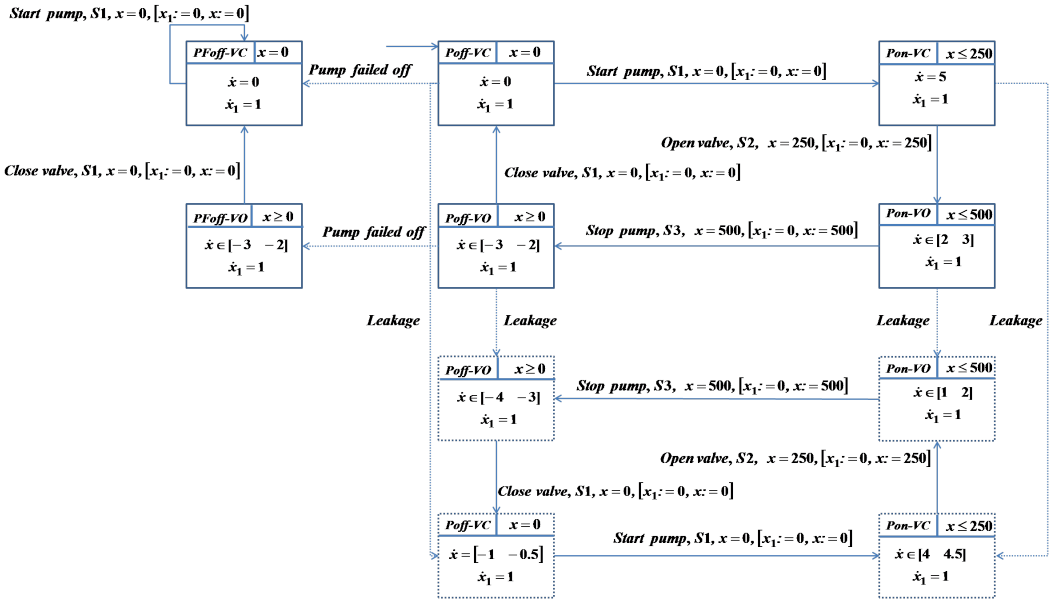

Figure 2.19: Events time occurrence based model for Example 2.10.

discrete events. The estimated required times, e.g., $x_1 = 50$, or time intervals, e.g., $x_1 = \begin{bmatrix} 83 & 125 \end{bmatrix}^T$, in the normal and fault operating conditions are used in order to infer the occurrence of both parametric and discrete faults (see Fig.2.20) .The discrete fault $'Pump\ failed\ off'$ is diagnosed when event $S2$ or $S3$ does not occur (see Fig.2.19 and Fig.2.20). The parametric fault $'Leakage\ in\ the\ tank'$ is diagnosed when event $S2$, respectively $S3$, occurs too late if the system is in the state '$Pon-VC$', respectively '$Pon-VO$' (see Fig.2.19 and Fig.2.20). While this fault is diagnosed when event $S1$ occurs too early if the system is in the state '$Poff-VO$' (see Fig.2.19 and Fig.2.20).

2.5.3.2 Continuous and discrete symbols based approaches

Continuous and discrete symbols based approaches, Daigle et al. (2010a), Daigle et al. (2010b), construct the temporal causal graphs (TCG) for each normal and fault discrete mode based on the use of a global hybrid bond graph. TCG separates out the variables and signals from the bond graph and makes clear the relationships between variables. When measurement deviations, caused by a fault occurrence, are observed through residuals, TCG are used to determine the effects that faults will have on the measurements as well as the temporal order in which they deviate. Then, a fault signature is defined for each fault as the qualitative value of the magnitude and the first non-zero derivative change which can be observed in the residuals. They are defined by $(+, -, 0)$ symbols to indicate increasing/decreasing/stable values for the residuals. In order to distinguish parametric from discrete faults, the signatures are extended by adding discrete symbols. They describe the discrete change behavior represented as a change from nonzero to zero (N) or a change from

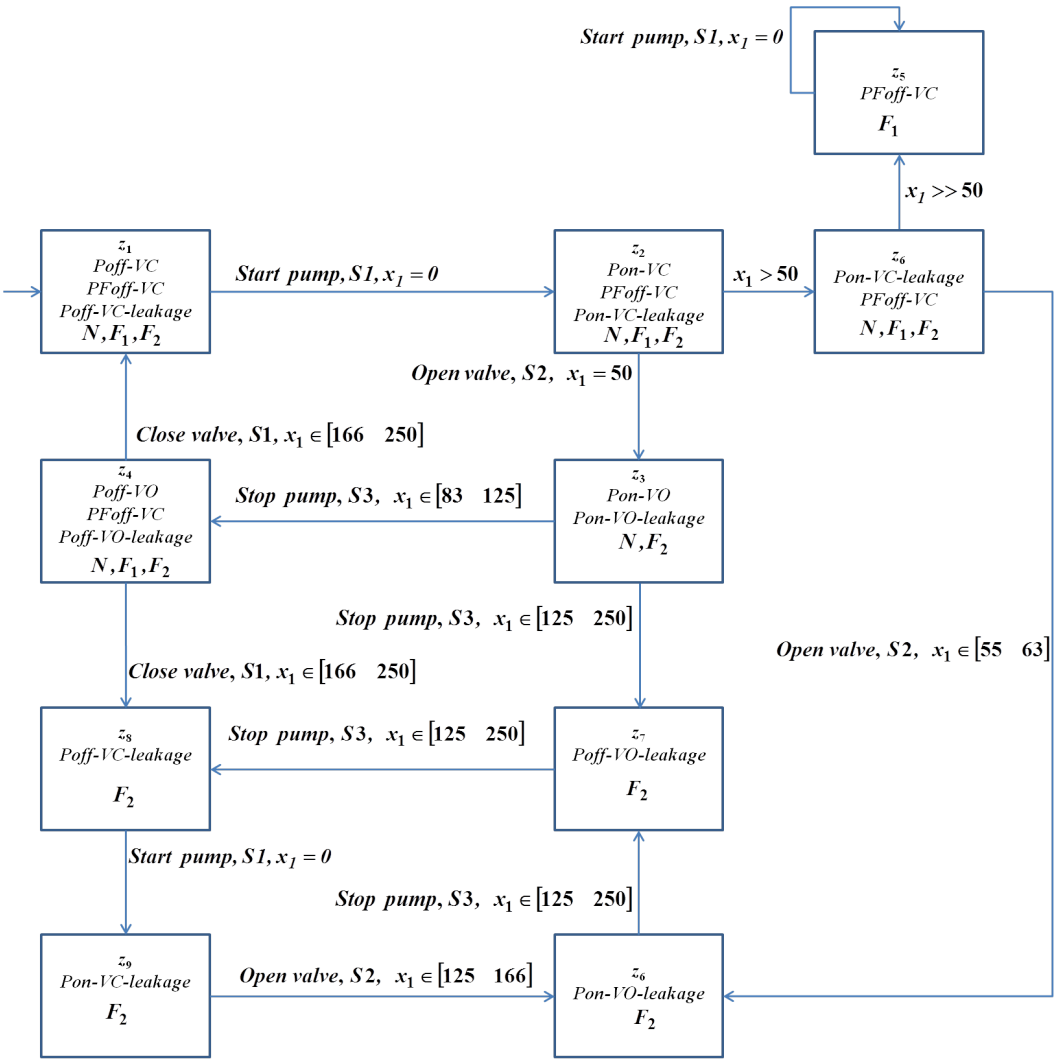

Figure 2.20: Diagnoser of the global model defined in Fig.2.19.

zero to nonzero (Z). The third symbol, (X), denotes the case when no discrete change is observed. These symbols provide additional discriminatory information. Indeed, discrete faults cause abrupt changes while parametric faults cause progressive changes with a finite change in variables magnitude. An individual diagnoser for each fault in each discrete mode is constructed based on the use of its fault signature. Then, in order to integrate the control commands, the individual diagnosers for the set of faults that one wants to diagnose are combined leading to obtain one global hybrid diagnoser for these faults (parametric and discrete). Nevertheless, this approach suffers from the need to a global model, hybrid bond graph, to achieve the diagnosis. In addition, since an individual diagnoser is constructed for each mode, this approach does not scale to large scale systems containing a huge number of discrete modes. Furthermore, this approach is based on an ideal symbol generation

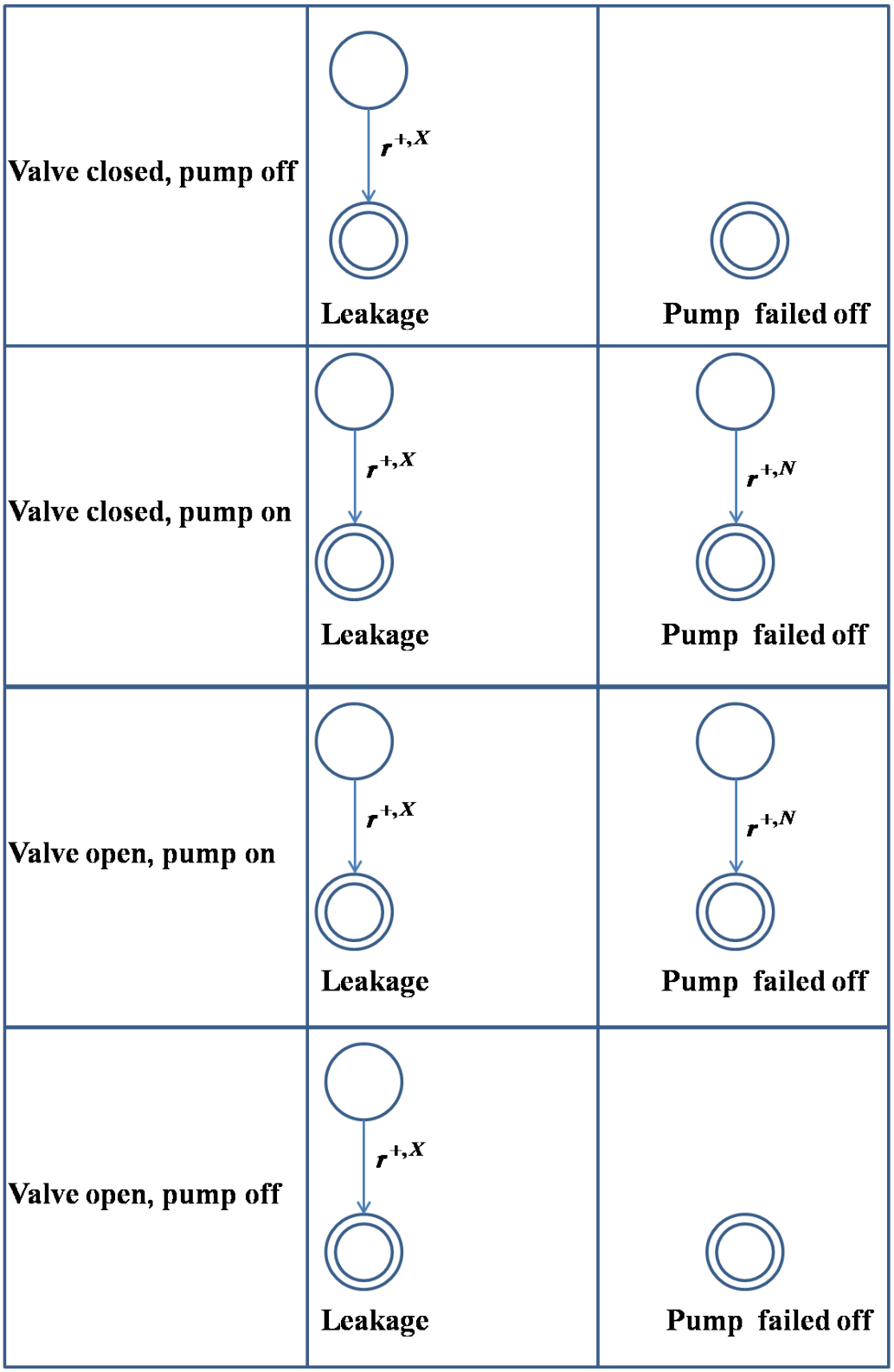

Figure 2.21: Parts of diagnoser corresponding to each of the faults ('*Pump failed off*' and '*Leakage in the tank*') in each discrete mode for Example 2.11.

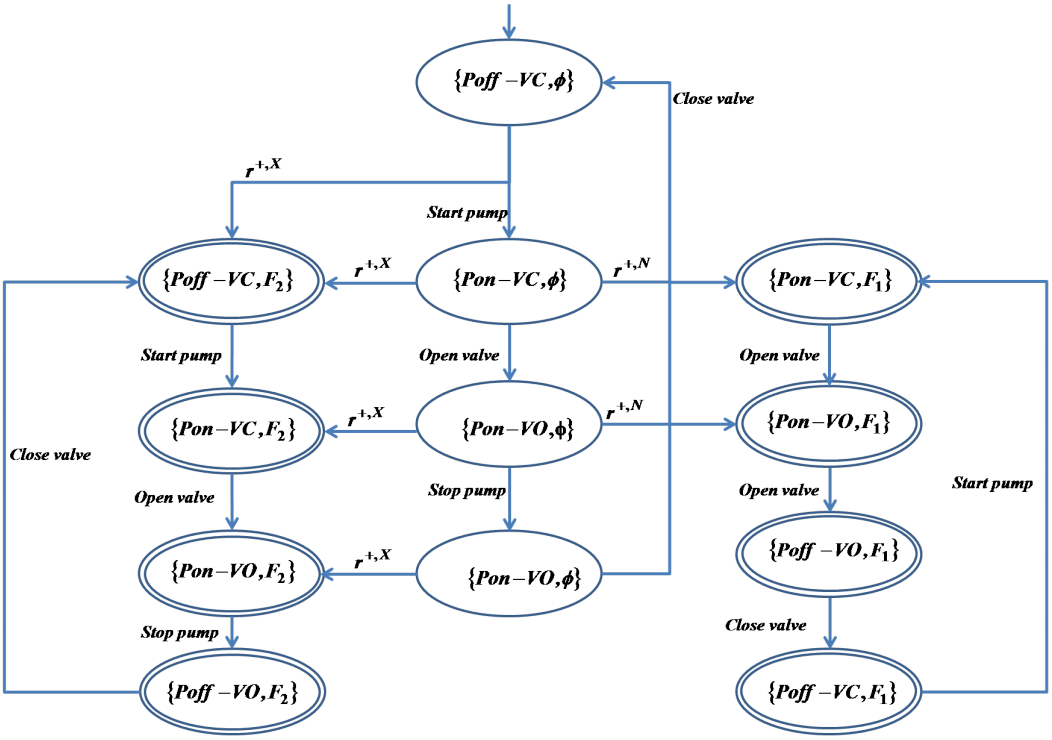

Figure 2.22: Global diagnoser for Example 2.11.

considering that the order that a fault impacts the system variables is known at the point of the first deviation. This may not be true due to the fault propagation delay. Therefore, diagnosability analysis of the system may not be correct. In addition, discrete symbols do not distinguish between two negative, respectively two positive, changes due to two different discrete faults, e.g., '*Pump filed off*' and '*Valve stuck-opened*', respectively '*Pump failed on*' and '*Valve stuck closed*'.

Example 2.11 ***Continuous and discrete symbols based approaches***

For the one tank water level control system example, let us consider the discrete fault '*Pump failed off*' ($PFoff$) indicated by fault label F_1 and the parametric fault '*Leakage in the tank*' indicated by fault label F_2. Let us apply the approach proposed by Daigle et al. (2010b), in order to diagnose the predefined faults. The system is modeled using a Hybrid bond graph (see Fig.2.5). The parts of diagnoser corresponding to each considered fault in each discrete mode are depicted in Fig.2.21. In the case of the occurrence of parametric fault '*Leakage in the tank*' the level of water decreases progressively. This change is represented by a continuous symbol $(+)$ and a discrete symbol (X) (non abrupt observable change). In the case of the occurrence of the discrete fault '*Pump failed off*', the input flow will be removed. The dynamic evolution of the water level will change from non zero value to zero value. Therefore, the level of the water decreases abruptly due to the occurrence of this fault. This change is represented by a continuous symbol $(+)$ and a discrete

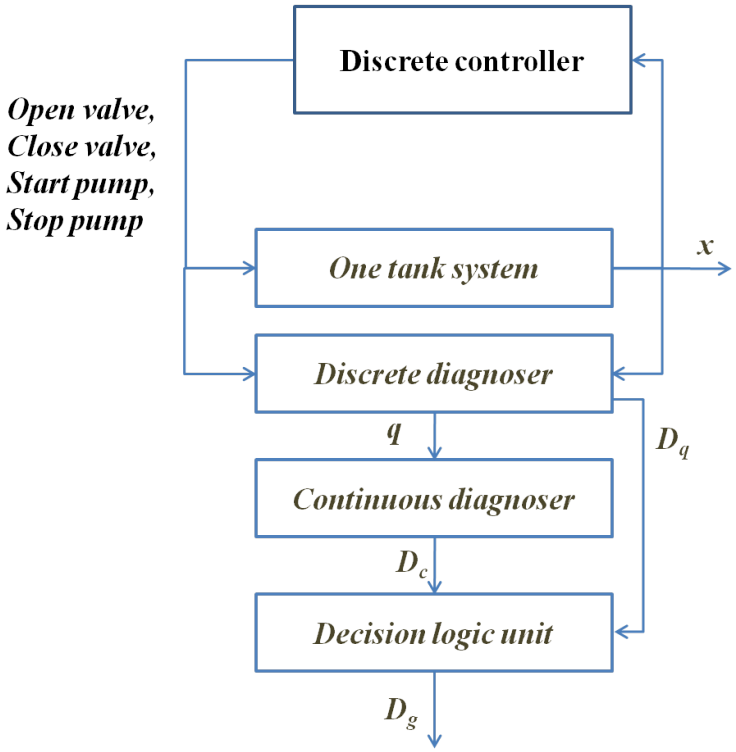

Figure 2.23: Hybrid structure diagnoser general scheme for the one tank system example.

symbol (N). The global diagnoser to diagnose discrete fault '*Pump failed off*' and parametric fault '*Leakage in the tank*' including the control commands is represented in Fig.2.22. The symbol $\phi = \{N, F_1, F_2\}$ indicates the case of uncertain decision.

2.5.3.3 Hybrid structure based diagnosis approaches

Hybrid structure based diagnosis approaches, Fourlas et al. (2002), Fourlas (2009) and Fourlas (2014), divide the diagnoser into three parts: the discrete diagnoser, the continuous diagnoser and the decision logic unit. The discrete diagnoser exploits the information extracted from the system continuous dynamics to get rid of diagnosis ambiguity due to the system behavior abstraction. The continuous diagnoser generates residuals. The latter compare the measured and nominal values of each continuous variable in order to diagnose the parametric faults in each discrete mode. The information about the discrete mode is provided to the continuous diagnoser thanks to the information extracted from the discrete dynamics. Finally, the decision logic unit is used to produce the final diagnosis statement (discrete and parametric fault labels) which is expressed as a combination of discrete (discrete faults labels) and continuous (parametric fault labels) sub-statements issued from the discrete and continuous diagnosers. However, these approaches do not scale to the systems with a large number of discrete mode, since the discrete diagnoser is

Figure 2.24: Hybrid model for Example 2.12.

built using the global model of the system.

Example 2.12 ***Hybrid structure based diagnosis approaches for the one tank system example***

For the one tank water level control system example, let us consider the discrete fault '*Valve stuck closed*' (VSC) indicated by fault label F_1 and the parametric fault '*Leakage in the tank*' indicated by fault label F_2. Let us apply the approach proposed by Fourlas (2014), to achieve the diagnosis of the considered faults (see Fig.2.23). The system is modeled using a hybrid automaton (see Fig.2.24). The discrete diagnoser (similar of the diagnoser of Fig.2.16) is constructed based on the global model of the system. The decision of a discrete diagnoser allows to diagnose the discrete fault in the system and to estimate its discrete mode.

The continuous diagnoser is based on the residual ($r = \hat{x} - x$) in order to diagnose the parametric fault of the system. The residual is calculated over time based on the continuous measurement x issued by the sensor capturing the water level x and based on the discrete mode defined by the discrete diagnoser. Since the discrete diagnoser detects the occurrence of a fault of type F_1, the residual, r, is equal to zero.

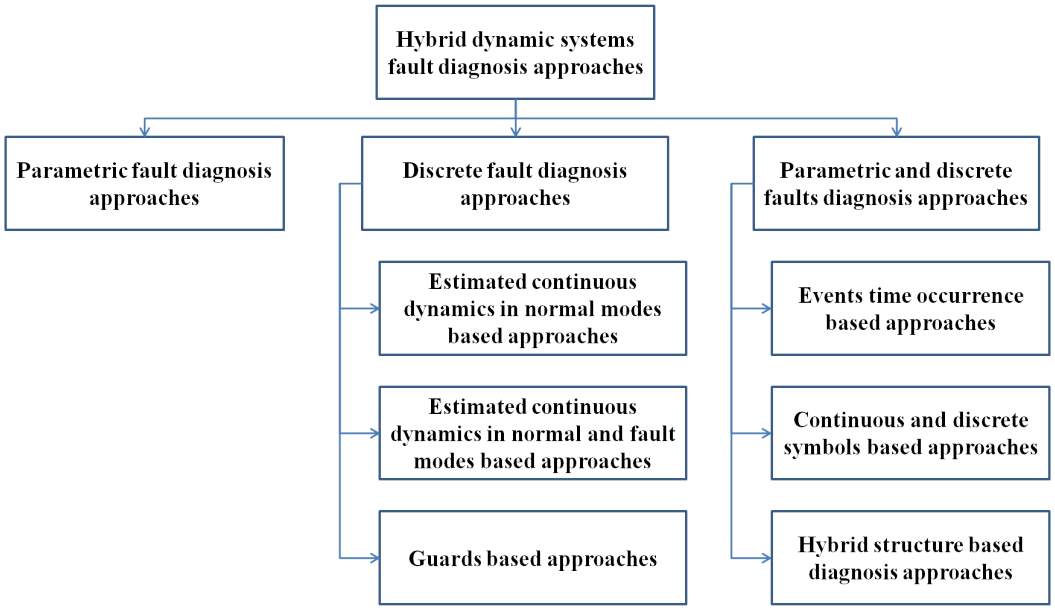

Figure 2.25: Classification of hybrid dynamic systems fault diagnosis approaches.

The logic decision unite issues the global decision (D_g) as the union of the discrete diagnoser (D_d) and continuous diagnoser (D_c): $D_g = D_d \cup D_c$. In the case of a discrete fault of type F_1, the discrete diagnoser issues $D_d = F_1$ and the continuous diagnoser issues $D_c = N$. The global decision is $D_g = F_1$. The same reasoning is applied in the case of a parametric fault of type F_2 ($D_g = F_2$).

2.6 Summary

In this chapter, the basic definitions and the classes of HDS are presented. Then, the different approaches of the literature to achieve the fault diagnosis of HDS, in particular DCCS are studied. They are classified into three main categories: parametric fault diagnosis, discrete fault diagnosis and parametric and discrete fault diagnosis approaches (see Fig.2.25).

As shown in this chapter, HDS are complex systems in which the discrete and continuous dynamics cohabit. The challenge of the fault diagnosis of this type of systems is to take into account the discrete and the continuous dynamics as well as the interaction between them. Many HDS fault diagnosis approaches take benefit of the discrete dynamics in order to enhance the diagnosis of only parametric faults. Other HDS fault diagnosis approaches exploits the continuous dynamics in order to enhance the diagnosis of only discrete faults. However, few approaches to diagnose both parametric and discrete faults are developed. This is due to the complexity of distinguishing discrete and continuous fault behaviors from the normal ones using the same observation of the system. In addition, the approaches of these three categories suffer from the drawback that they do not scale well to large scale systems

Table 2.3: Comparison between hybrid dynamic systems fault diagnosis approaches.

Characteristics	***Discrete approaches***	***Parametric approaches***	***Discrete and parametric approaches***
Modular approach	No	No	No
Complexity of the diagnoser	Exponential with respect to the number of components	Exponential with respect to the number of components	Exponential with respect to the number of components
Diagnosis of discrete faults	Yes	No	Yes
Diagnosis of parametric faults	No	Yes	Yes
Robustness	Weak robustness	Weak robustness	Weak robustness

with a huge number of discrete modes. Table 2.3 compares the major characteristics of the HDS fault diagnosis approaches of the literature.

Consequently, in Chapter 3, a parametric and discrete faults diagnosis approach is proposed. In this approach, the modularity of the system is exploited in order to facilitate the construction of the system global model as well as the diagnoser. This modularity is taken into account through the decomposition of the system into a set of interacting hybrid (discrete and continuous) components as we will see in Chapter 3.

Chapter 3

Hybrid centralized fault diagnosis and diagnosability

Contents

3.1 Introduction

In this chapter, an approach for the diagnosis of both parametric and discrete faults in a discretely controlled continuous systems (DCCS) is proposed, Louajri et al. (2013), Louajri and Sayed-Mouchaweh (2014d). This approach exploits the system discrete and continuous dynamics as well as the interactions between them in order to enhance the diagnosability of parametric and discrete faults. In addition, this approach takes benefits of the modularity of the system in order to facilitate the construction of the system global model (see Fig.3.1). The system is considered to be composed of L interacting hybrid components (HCs). Each HC_j is composed of a discrete component (Dc_j) associated to its interacting continuous components (Ccs). A local discrete model DG^j, $j \in \{1, \cdots, L\}$, is constructed for each Dc_j. The latter includes nominal and faulty states reached due to the occurrence of faults (considered as unobservable events) in its associated component. While each Cc_i, $i \in \{1, \cdots, n\}$, is represented by the nominal $\tilde{\dot{x}}_i$ and real $\dot{x}_i$ dynamic evolutions of continuous variable x_i. For each Cc_i, a residual r_i is defined as a

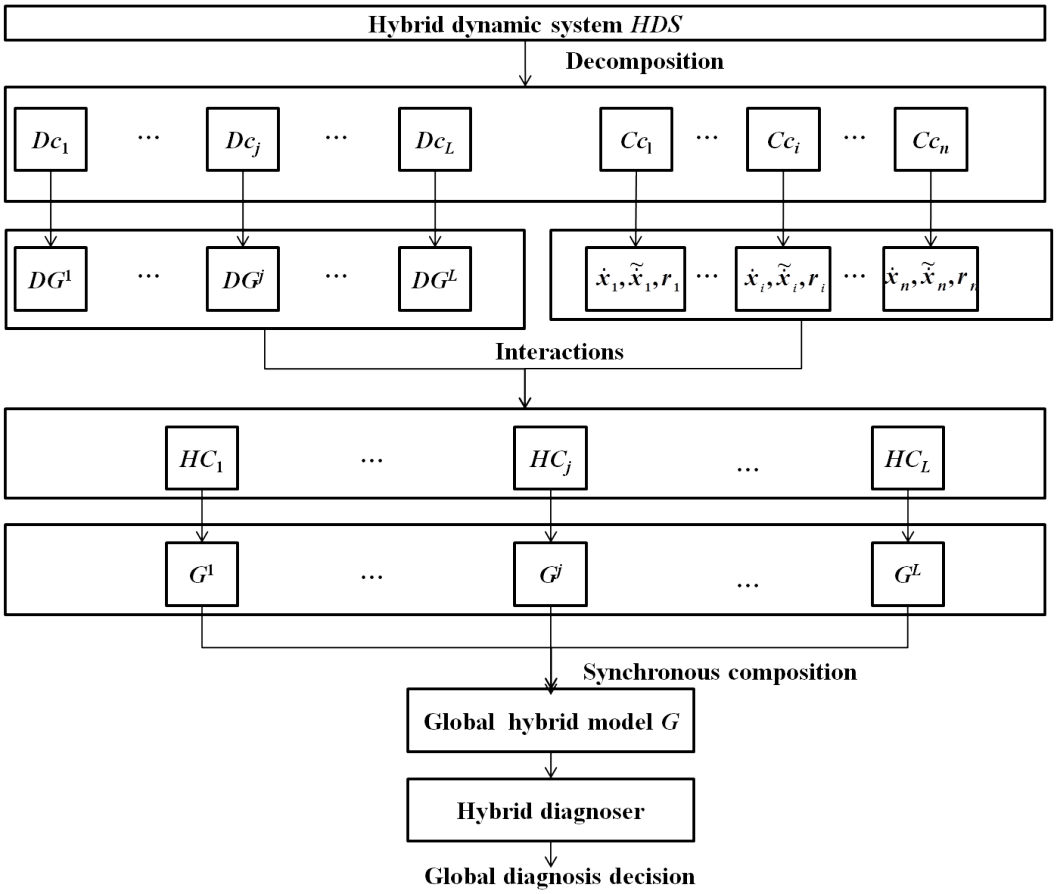

Figure 3.1: Steps of the proposed approach to achieve the centralized hybrid diagnosis.

difference between $\dot{x}_i$ and $\dot{\tilde{x}}_i$ in each discrete state in order to diagnose parametric faults related to Cc_i. The set of n residuals, $r_i,\ i \in \{1, \cdots, n\}$, defines the global residual r. The set of n nominal $\dot{\tilde{x}}_i,\ i \in \{1, \cdots, n\}$, and real $\dot{x}_i,\ i \in \{1, \cdots, n\}$, dynamic evolutions of continuous variable $x_i,\ i \in \{1, \cdots, n\}$ define, respectively, the global nominal $\dot{\tilde{X}}$ and real $\dot{X}$ dynamic evolutions of continuous variables X. The local hybrid model G^j, where $j \in \{1, \cdots, L\}$, is obtained for each HC_j by a combination of the local discrete model DG^j of Dc_j and the dynamic evolutions of its associated continuous components. G^j includes nominal and faulty states reached due to the occurrence of parametric and discrete faults (considered as unobservable events) in its associated discrete and continuous components. The global model G is obtained by the synchronous composition of the local hybrid models $\{G^j\},\ j \in \{1, \cdots, L\}$.

The following assumptions hold:

- The system continuous dynamics are defined by linear differential equations (L.D.E) allowing describing normal and faulty continuous behaviors;

- The considered faults can affect sensors, actuators or the system. Controller faults are not considered;
- The considered faults are permanent and single (multiple faults are not considered);
- The parametric faults are considered to be incipient faults (i.e., slow abnormal change in parameters value as for example a consequence of aging effects).

Chapter 3 is organized as follows. Firstly, the different steps to build the local models of discrete, continuous and hybrid system components are detailed. Then, the construction of the system global model, based on hybrid local models is described. Finally, the steps of hybrid centralized diagnoser construction are explained. A simple example of one tank level water control system is used throughout the chapter in order to illustrate the proposed approach.

3.2 System modeling

DCCS consist of continuous components (Ccs) whose operating modes are switched by a feedback of discrete states of discrete components (Dcs). In the following subsections, the modeling of these components is detailed. Then, the system global model is constructed based on the use of these components models as well as the interactions between them.

Example 3.1 ***System decomposition for the one tank system example***

For the one tank water level control system (Fig.3.2). The system is composed of one continuous component Cc and two discrete components Dc_1 and Dc_2. Cc is represented by the tank of section s_T. Its continuous dynamics are represented by the water level x of the tank. Dc_1 and Dc_2 are, respectively, the discrete behaviors of the valve, V, of section s_V and the pump, P.

3.2.1 Discrete components modeling

The nominal and faulty behaviors of each discrete component $Dc_j, j \in \{1, \cdots, L\}$ is modeled using discrete automaton DG^j defined by the tuple:

$$DG^j = (Q_D^j, h_q^j, \tilde{h}_q^j, \Sigma_D^j, DSL^j, \delta_D^j, Init_D^j) \tag{3.1}$$

where,

- $Q_D^j = \{q_k^j, k \in \{1, \cdots, g\}\}$: is a finite set of discrete states of Dc_j. A normal operating mode is represented by one state in DG^j while a failure mode can be represented by several states;
- The output of state q_k^j is characterized by real discrete output vector $h_q^j : Q_D^j \rightarrow \{0, 1\}$ and nominal discrete output vector $\tilde{h}_q^j : Q_D^j \rightarrow \{0, 1\}$. At normal discrete mode, h_q^j is equal to $\tilde{h}_q^j$ while in faulty modes h_q^j is different from $\tilde{h}_q^j$;

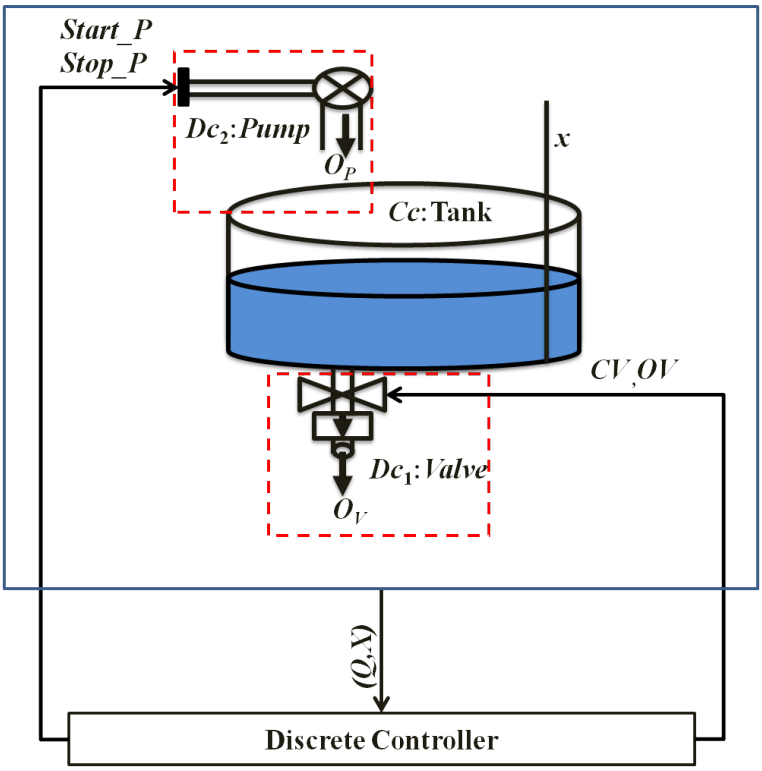

Figure 3.2: One tank water level control system decomposition.

- $\Sigma_D^j = \Sigma_{Do}^j \cup \Sigma_{Du}^j$: is the discrete event set of Dc_j. It includes observable discrete events Σ_{Do}^j corresponding to control command events and unobservable discrete events Σ_{Du}^j. Σ_{Du}^j includes discrete fault events Σ_{Df}^j that can occur at Dc_j as well as normal but unobservable discrete events;

- The set of failure events is divided into dd^j different failure types or modes indicated by the following discrete status labels $DSL^j = \{DN_j, F_1, F_2, \cdots, F_{dd^j}\}$, where DN_j denotes the absence of discrete faults related to Dc_j. Each state q_k^j of Dc_j has its proper discrete status label DSL_k^j;

- $\delta_D^j : Q_D^j \times \Sigma_D^j \rightarrow Q_D^j$: is the state transition function. A transition $\delta_D^j(q^j, e) = q^{j+}$ corresponds to a change from state q^j to state q^{j+} after the occurrence of discrete event e;

- $Init_D^j = (q_1^j \in Q_D^j,\ h_q^j(q_1^j) = h_{q_1^j}^j,\ \tilde{h}_q^j(q_1^j) = \tilde{h}_{q_1^j}^j,\ DSL^j(q_1^j) = DSL_1^j)$: is the initial conditions;

- K is the language representing the controller output. It is defined as the set of control command event sequences generated by the controller and sent to the different Dcs. The set of control command event sequences sent to Dc_j is represented by K^j;

- The global model of discrete components is obtained by synchronizing the local discrete automata using parallel or synchronous composition operator. It builds the system global model from its individual component models. In this parallel or synchronous composition, a common event between two components can only be executed if both components execute it simultaneously, Cassandras and Lafortune (2008). However, the private events which can be executed by only one component can be executed whenever possible.

Example 3.2 ***Discrete components modeling for the one tank system example***

Let us take the one tank water level control example of Fig.3.2. Let us consider, for the sake of simplicity, that the valve V can fail in stuck opened failure mode. Discrete automaton DG^1 characterizing valve V discrete dynamics is defined by the tuple (see Fig.3.3):

$$DG^1 = (Q_D^1, h_q^1, \tilde{h}_q^1, \Sigma_D^1, DSL^1, \delta_D^1, Init_D^1) \tag{3.2}$$

where,

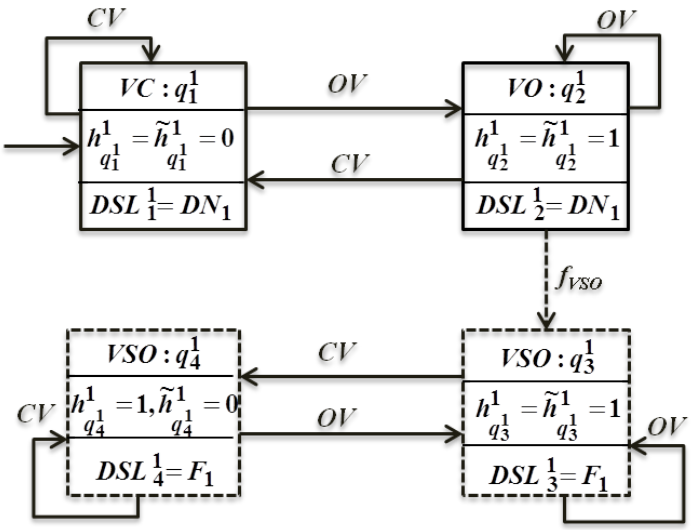

Figure 3.3: Discrete automaton DG^1 for valve V.

- $Q_D^1 = \{q_1^1,\ q_2^1,\ q_3^1,\ q_4^1\}$. q_1^1 and q_2^1 represent, respectively, the valve closed, VC, and the valve opened, VO, in normal operating conditions. q_3^1 and q_4^1 characterize the valve stuck opened failure mode, VSO;

- $\Sigma_D^1 = \Sigma_{Do}^1 \bigcup \Sigma_{Du}^1$: is the set of valve discrete events. $\Sigma_{Do}^1 = \{CV$ (close V), OV (open $V)\}$, $\Sigma_{Du}^1 = \Sigma_{Df}^1 = \{f_{SO}$ (fault event leading to V stuck opened failure mode)$\}$. The fault, f_{VSO}, can occur at the state where the valve is opened;

- $h_q^1 : Q_D^1 \rightarrow \{0,1\} = \{0\ (V \text{ closed}),\ 1\ (V \text{ opened})\}$;
- $\tilde{h}_q^1 : Q_D^1 \rightarrow \{0,1\} = \{0\ (V \text{ should be closed}),\ 1\ (V \text{ should be opened})\}$;
- $DSL^1 = \{DN_1 \text{ (valve in normal discrete mode)}, F_1 \text{ (valve stuck opened)}\}$. As an example status label for q_1^1, DSL_1^1, is equal to DN_1;
- $\delta_D^1 : Q_D^1 \times \Sigma_D^1 \rightarrow Q_D^1$: is the valve state transition function. As an example $\delta_D^1(q_1^1, OV) = q_2^1$ (see Fig.3.3);
- $Init_D^1 :\ (q_1^1,\ h_{q_1^1}^1 = \tilde{h}_{q_1^1}^1 = 0,\ DSL^1(q_1^1) = DSL_1^1 = DN_1)$.

For the one tank system example of Fig.3.2 The discrete automaton DG^2 characterizing the discrete dynamics of the pump, is defined by the tuple (3.3) (see Fig.3.4). We consider, for the sake of simplicity, that the pump can fail in pump failed off failure mode.

$$DG^2 = (Q_D^2, \Sigma_D^2, DSL^2, \delta_D^2, Init_D^2) \tag{3.3}$$

where,

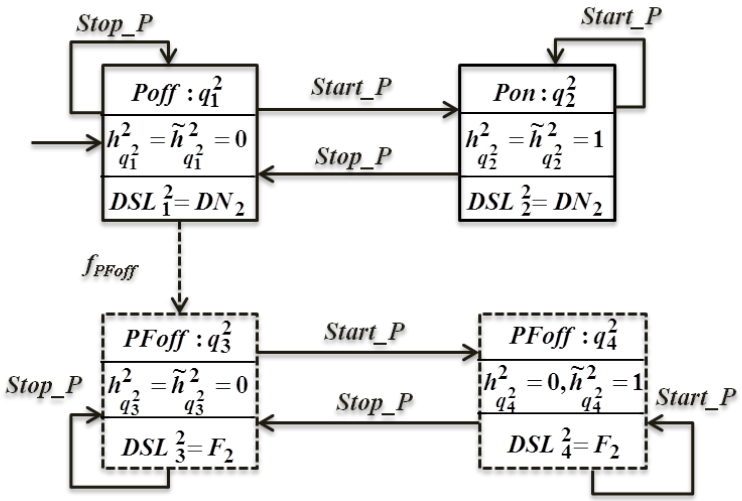

Figure 3.4: Discrete automaton DG^2 for pump P.

- $Q_D^2 = \{q_1^2,\ q_2^2,\ q_3^2,\ q_4^2\}$. q_1^2 and q_2^2 represent, respectively, pump off, $Poff$, and the pump on, Pon, in normal operating conditions. q_3^2 and q_4^2 characterize the pump failed off failure mode, $PFoff$;
- $h_q^2 : Q_D^2 \rightarrow \{0,1\} = \{0\ (\text{ pump stopped}),\ 1\ (\text{pump started})\}$;
- $\tilde{h}_q^2 : Q_D^2 \rightarrow \{0,1\} = \{0\ (\text{ pump should be stopped})\ 1\ (\text{pump should be started})\}$;

- $\Sigma_D^2 = \Sigma_{Do}^2 \bigcup \Sigma_{Du}^2$: is the set of pump discrete events. $\Sigma_{Do}^2 = \{Start\_P$ (start pump), $Stop\_P$ (stop pump)$\}$. $\Sigma_{Du}^2 = \Sigma_{Df}^2 = \{f_{PFoff}$ (fault event leading to pump failed off failure mode) $\}$. The fault, f_{PFoff}, can occur at the state where the pump is stopped;
- $DSL^2 = \{DN_2$ (pump in normal discrete mode), F_2 (pump failed off)$\}$. As an example status label for q_3^2, DSL_3^2, is equal to F_2;
- $\delta_D^2 : Q_D^2 \times \Sigma_D^2 \rightarrow Q_D^2$: is the state transition function. As an example, $\delta_D^2(q_1^2, Start\_P) = q_2^2$ (see Fig.3.4);
- $Init_D^2 :\ (q_1^2,\ hq1^2 = \tilde{h}q1^2 = 0,\ DSL^2(q_1^2) = DSL_1^2 = DN_2)$.

3.2.2 Continuous components modeling

The real continuous dynamic evolutions is supposed to be described in each discrete state q by the following L.D.E:

$$\dot{X} = A_{(q)} X + B_{(q)} u$$

$$\dot{X} = \begin{bmatrix} \dot{x}_1 \\ \vdots \\ \dot{x}_i \\ \vdots \\ \dot{x}_m \\ \vdots \\ \dot{x}_n \end{bmatrix} = \begin{bmatrix} A^1_{(q)1} & \cdots & A^i_{(q)1} & \cdots & A^m_{(q)1} & \cdots & A^n_{(q)1} \\ \vdots & \ddots & & & \ddots & & \vdots \\ A^1_{(q)i} & \cdots & A^i_{(q)i} & \cdots & A^m_{(q)i} & \cdots & A^n_{(q)i} \\ \vdots & \ddots & & & \ddots & & \vdots \\ A^1_{(q)m} & \cdots & A^i_{(q)m} & \cdots & A^m_{(q)m} & \cdots & A^n_{(q)m} \\ \vdots & \ddots & & & \ddots & & \vdots \\ A^1_{(q)n} & \cdots & A^i_{(q)n} & \cdots & A^m_{(q)n} & \cdots & A^n_{(q)n} \end{bmatrix} \begin{bmatrix} x_1 \\ \vdots \\ x_i \\ \vdots \\ x_m \\ \vdots \\ x_n \end{bmatrix} + \begin{bmatrix} B_{(q)1} \\ \vdots \\ B_{(q)i} \\ \vdots \\ B_{(q)m} \\ \vdots \\ B_{(q)n} \end{bmatrix} u \tag{3.4}$$

u is the input vector, $A_{(q)}$ is equal to $[A_{(q)1} \cdots A_{(q)i} \cdots A_{(q)m} \cdots, A_{(q)n}]^T$ and $B_{(q)}$ is equal to $[B_{(q)1} \cdots B_{(q)i} \cdots, B_{(q)m} \cdots B_{(q)n}]^T$. $A_{(q)i}$ and $B_{(q)i}$ are constant matrices of appropriate dimensions characterizing the dynamics of x_i, $i \in \{1, \cdots, n\}$.

For each x_i, (3.4) is reduced as:

$$\dot{x}_i = A_{(q)i} X + B_{(q)i} u \tag{3.5}$$

where $A_{(q)i}$ is equal to $[A^1_{(q)i} \cdots A^i_{(q)i} \cdots A^m_{(q)i} \cdots A^n_{(q)i}]$.

Based on (3.5), we can conclude that the dynamic evolution $\dot{x}_i$ of each continuous variable x_i depends on the system global discrete state q, the continuous variables X and the input vector u. q is obtained as a combination of the discrete states $(q^1, q^2 \cdots, q^L)$ of the discrete components Dc_j, $j \in \{1, \cdots, L\}$.

Each discrete state $q = [q^1 \cdots q^j \cdots q^L]$ is characterized by its corresponding real output vector $h_q = [h_q^1 \cdots h_q^j \cdots h_q^L]$. X is the combination of the set of continuous variables x_m, $m \in \{1, \cdots, n\}$: $X = [x_1 \cdots x_i \cdots x_m \cdots x_n]^T$.

$A^m_{(q)i}$ represents the influence of x_m on $\dot{x}_i$ at discrete state q. $A^m_{(q)i}$ is decomposed into two parts: A^m_{ci} and A^m_i. A^m_{ci} defines the influence of x_m on $\dot{x}_i$ whatever the

discrete state is; while A_i^m represents the influence of x_m on $\dot{x}_i$ when the system is in discrete state $q = [q^1 \cdots q^j \cdots q^L]$. Therefore, $A_{(q)i}^m$ can be written as follows:

$$A_{(q)i}^m = h_q^1 A_i^{m1} + \cdots + h_q^j A_i^{mj} + \cdots + h_q^L A_i^{mL} + A_{ci}^m = \sum_{j=1}^{L} h_q^j A_i^{mj} + A_{ci}^m \tag{3.6}$$

A_i^{mj}, $j \in \{1, \cdots, L\}$ represents the influence of x_m on $\dot{x}_i$ at Dc_j discrete state q^j when $h_q^j = 1$.

Likewise, $B_{(q)i}$ represents the influence of u on $\dot{x}_i$ when the system is in discrete state $q = [q^1 \cdots q^j \cdots q^L]$. Since input vector u depends on $q = [q^1 \cdots q^j \cdots q^L]$, therefore $B_{(q)i}$ can be written as follows:

$$B_{(q)i} = h_q^1 B_i^1 + \cdots + h_q^j B_i^j + \cdots + h_q^L B_i^L = \sum_{j=1}^{L} h_q^j B_i^j \tag{3.7}$$

where B_i^j represents the influence of u on $\dot{x}_i$ at Dc_j discrete state q^j when $h_q^j = 1$. Based on (3.6) and (3.7), (3.5) is developed as follows:

$$\begin{cases}
\dot{x}_i = A_{(q)i} X + B_{(q)i} u \\
\quad = \left[A_{(q)i}^1 \cdots A_{(q)i}^i \cdots A_{(q)i}^m \cdots A_{(q)i}^n\right] [x_1 \cdots x_i \cdots x_m \cdots x_n]^T + \\
\quad \left(h_q^1 B_i^1 + \cdots + h_q^j B_i^j + \cdots + h_q^L B_i^L\right) u \\
\\
\quad = \Big[\left(h_q^1 A_i^{11} + \cdots + h_q^j A_i^{1j} + \cdots + h_q^L A_i^{1L} + A_{ci}^1\right) \cdots \left(h_q^1 A_i^{i1} + \cdots + h_q^j A_i^{ij} + \right. \\
\quad \left. \cdots + h_q^L A_i^{iL} + A_{ci}^i\right) \cdots \left(h_q^1 A_i^{m1} + \cdots + h_q^j A_i^{mj} + \cdots + h_q^L A_i^{mL} + A_{ci}^m\right) \cdots \\
\quad \left(h_q^1 A_i^{n1} + \cdots + h_q^j A_i^{nj} + \cdots + h_q^L A_i^{nL} + A_{ci}^n\right)\Big] [x_1 \cdots x_i \cdots x_m \cdots x_n]^T \\
\quad + \left(h_q^1 B_i^1 + \cdots + h_q^j B_i^j + \cdots + h_q^L B_i^L\right) u \\
\\
\quad = \left[\left(\sum_{j=1}^{L} h_q^j A_i^{1j} + A_{ci}^1\right) \cdots \left(\sum_{j=1}^{L} h_q^j A_i^{ij} + A_{ci}^i\right) \cdots \left(\sum_{j=1}^{L} h_q^j A_i^{mj} + A_{ci}^m\right)\right. \\
\quad \left. \cdots \left(\sum_{j=1}^{L} h_q^j A_i^{nj} + A_{ci}^n\right)\right] [x_1 \cdots x_i \cdots x_m \cdots x_n]^T + \sum_{j=1}^{L} h_q^j B_i^j u \\
\\
\quad = \left(\sum_{j=1}^{L} h_q^j A_i^{1j} + A_{ci}^1\right) x_1 + \cdots + \left(\sum_{j=1}^{L} h_q^j A_i^{ij} + A_{ci}^i\right) x_i + \cdots + (\sum_{j=1}^{L} h_q^j A_i^{mj} \\
\quad + A_{ci}^m)\, x_m + \cdots + \left(\sum_{j=1}^{L} h_q^j A_i^{nj} + A_{ci}^n\right) x_n + \sum_{j=1}^{L} h_q^j B_i^j u
\end{cases}$$

Thus, the real dynamic evolution of x_i is written as follows:

$$\dot{x}_i = \sum_{m=1}^{n} \left(\left(\sum_{j=1}^{L} h_q^j A_i^{mj} + A_{ci}^m\right) x_m\right) + \sum_{j=1}^{L} h_q^j B_i^j u \tag{3.8}$$

When the system is in discrete state $q = [q^1 \cdots q^j \cdots q^L]$, characterized by $h_q = [h_q^1 = 0 \cdots h_q^j = 0 \cdots h_q^L = 0]$, then $\dot{x}_i$ is equal to $A_{ci}X$, where $A_{ci} = [A_{ci}^1 \cdots A_{ci}^i \cdots A_{ci}^m \cdots A_{ci}^n]$. If the system changes its discrete state from $q = [q^1 \cdots q^j \cdots q^L]$ characterized by $h_q = [h_q^1 = 0 \cdots h_q^j = 0 \cdots h_q^L = 0]$ to $q^+ = [q^1 \cdots q^{j+} \cdots q^L]$ characterized by $h_q = [h_q^1 = 0 \cdots h_q^{j+} = 1 \cdots h_q^L = 0]$, then $\dot{x}_i$ is equal to $\left(A_i^j + A_{ci}\right) X + B_i^j u$, where $A_i^j = [A_i^{1j} \cdots A_i^{ij} \cdots A_i^{mj} \cdots A_i^{nj}]$. Therefore, this decomposition allows defining a change in $\dot{x}_i$, $i \in \{1, \cdots, n\}$, as a function of a change in the system discrete state. This decomposition is useful in order to take benefit of an abnormal change, due to a discrete fault, in the system discrete mode to enhance the system discrete fault diagnosability as we will see later in subsection 3.3.3.

In order to describe the influence of each discrete component Dc_j on $\dot{x}_i$, (3.8) is decomposed as follows:

$$
\begin{cases}
\dot{x}_i = \sum\limits_{m=1}^{n} \left(\left(\sum\limits_{j=1}^{L} h_q^j A_i^{mj} + A_{ci}^m \right) x_m \right) + \sum\limits_{j=1}^{L} h_q^j B_i^j u \\
\\
= \left(\sum\limits_{j=1}^{L} h_q^j A_i^{1j} + A_{ci}^1 \right) x_1 + \cdots + \left(\sum\limits_{j=1}^{L} h_q^j A_i^{ij} + A_{ci}^i \right) x_i + \cdots + \\
\left(\sum\limits_{j=1}^{L} h_q^j A_i^{mj} + A_{ci}^m \right) x_m + \cdots + \left(\sum\limits_{j=1}^{L} h_q^j A_i^{nj} + A_{ci}^n \right) x_n + \sum\limits_{j=1}^{L} h_q^j B_i^j u \\
\\
= \sum\limits_{j=1}^{L} h_q^j A_i^{1j} x_1 + A_{ci}^1 x_1 + \cdots + \sum\limits_{j=1}^{L} h_q^j A_i^{ij} x_i + A_{ci}^i x_i + \sum\limits_{j=1}^{L} h_q^j A_i^{mj} x_m + \\
A_{ci}^m x_m + \cdots + \sum\limits_{j=1}^{L} h_q^j A_i^{nj} x_n + A_{ci}^n x_n + \sum\limits_{j=1}^{L} h_q^j B_i^j u \\
\\
= \sum\limits_{j=1}^{L} h_q^j \left(A_i^{1j} x_1 + \cdots + A_i^{ij} x_i + \cdots + A_i^{mj} x_m + \cdots + A_i^{nj} x_n \right) + \\
\sum\limits_{j=1}^{L} h_q^j B_i^j u + \left(A_{ci}^1 x_1 + \cdots + A_{ci}^i x_i + \cdots + A_{ci}^m x_m + \cdots + A_{ci}^n x_n \right) \\
\\
= \sum\limits_{j=1}^{L} \left(\sum\limits_{m=1}^{n} h_q^j A_i^{mj} x_m + h_q^j B_i^j u \right) + \sum\limits_{m=1}^{n} A_{ci}^m x_m
\end{cases}
$$

Thus, (3.8) is decomposed as follows:

$$\dot{x}_i = \sum_{j=1}^{L} \dot{x}_i^j + \dot{x}_{ci} \tag{3.9}$$

where $\dot{x}_i^j = \sum\limits_{m=1}^{n} h_q^j A_i^{mj} x_m + h_q^j B_i^j u$ and $\dot{x}_{ci} = \sum\limits_{m=1}^{n} A_{ci}^m x_m$. This decomposition allows determining the part that can change due to discrete control (influence of Dc_j on Cc_i). In the case of a system commutation due to a controller command, only the part of $\dot{x}_i$ sensitive to this command will be changed. The other parts of $\dot{x}_i$ will not change.

As for the real continuous dynamic evolutions $\dot{X}$, nominal continuous dynamic evolutions $\dot{\tilde{X}}$ of continuous variables X is defined as follows:

$$\dot{\tilde{X}} = \tilde{A}_{(q)}X + \tilde{B}_{(q)}u \tag{3.10}$$

where $\tilde{A}_{(q)}$ and $\tilde{B}_{(q)}$ are the nominal constant matrices in the nominal state. For each x_i, (3.10) is reduced as:

$$\dot{\tilde{x}}_i = \tilde{A}_{(q)i}X + \tilde{B}_{(q)i}u \tag{3.11}$$

Thus, based on (3.11), the nominal dynamic evolution of x_i is written as follows:

$$\dot{\tilde{x}}_i = \sum_{m=1}^{n} \left(\left(\sum_{j=1}^{L} \tilde{h}_q^j \tilde{A}_i^{mj} + \tilde{A}_{ci}^m \right) x_m \right) + \sum_{j=1}^{L} \tilde{h}_q^j \tilde{B}_i^j u \tag{3.12}$$

In order to describe the influence of each discrete component Dc_j on $\dot{\tilde{x}}_i$, (3.12) is decomposed as follows:

$$\dot{\tilde{x}}_i = \sum_{j=1}^{L} \dot{\tilde{x}}_i^j + \dot{\tilde{x}}_{ci} \tag{3.13}$$

where $\dot{\tilde{x}}_i^j = \sum_{m=1}^{n} \tilde{h}_q^j \tilde{A}_i^{mj} x_m + \tilde{h}_q^j \tilde{B}_i^j u$ and $\dot{\tilde{x}}_{ci} = \sum_{m=1}^{n} \tilde{A}_{ci}^m x_m$.

In order to separate the nominal and faulty continuous operating modes, each continuous component Cc_i is modeled by the automaton, G_{ci}, depicted in Fig.3.5.

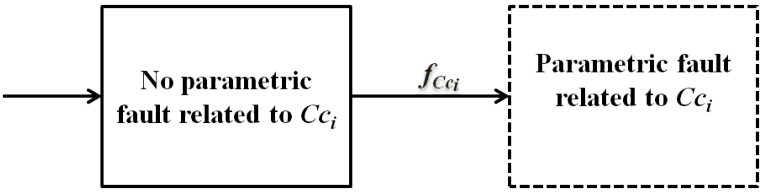

Figure 3.5: Continuous model of component Cc_i denoted by G_{ci}.

$$G_{ci} = (Q_{ci}, \Sigma_{ci}, \delta_{ci}, flux_i, r_i) \tag{3.14}$$

where,

- Q_{ci}: is the set of the continuous operating modes Cc_i;
- Σ_{ci}: is the event set of the parametric faults occurrence;
- $flux_i : Q_{ci} \times x_i \rightarrow \Re^n$: is a function characterizing the real evolution parts $\dot{x}_i$ and nominal evolution parts $\dot{\tilde{x}}_i$ of continuous variables x_i;
- r_i is the residual associated to x_i;

Example 3.3 ***Continuous component modeling for the one tank system example***

The continuous dynamics of the one tank water control system (see Fig.3.2) are characterized by continuous variable x (level of liquid in the tank). We consider as a parametric fault the leakage in the tank. This parametric fault is characterized by an output flow rate O_{lg}. O_{lg} depends on the leakage section s_{lg} and on the tank level x. Based on the definition of the dynamic evolutions of this system in the literature, Cocquempot et al. (2004), the system real and nominal dynamic evolutions of x are obtained as follows:

$$\begin{cases} \dot{x} = -h_q^1 \frac{s_V\sqrt{2g}}{2s_T\sqrt{x_0}}x + h_q^2\frac{O_P}{s_T} - \frac{s_{lg}\sqrt{2g}}{2s_T\sqrt{x_0}}x \\ \\ \tilde{\dot{x}} = -\tilde{h}_q^1 \frac{s_V\sqrt{2g}}{2s_T\sqrt{x_0}}x + \tilde{h}_q^2\frac{O_P}{s_T} \end{cases} \tag{3.15}$$

where, x_0 is the initial level of the tank and $O_{lg} = -\frac{s_{lg}\sqrt{2g}}{2s_T\sqrt{x_0}}x$. In nominal conditions, the leakage section s_{lg} is equal to 0. Thus, $\tilde{O}_{lg} = -\frac{\tilde{s}_{lg}\sqrt{2g}}{2s_T\sqrt{x_0}}x$ is equal to 0. (3.15) can be written as (3.8) as follows:

$$\begin{cases} \dot{x} = h_q^1A^1x + h_q^2A^2x + A_cx + h_q^1B^1u + h_q^2B^2u \\ \tilde{\dot{x}} = \tilde{h}_q^1\tilde{A}^1x + \tilde{h}_q^2\tilde{A}^2x + \tilde{A}_cx + \tilde{h}_q^1\tilde{B}^1u + \tilde{h}_q^2\tilde{B}^2u \end{cases} \tag{3.16}$$

where, $A^1 = \tilde{A}^1 = -\frac{s_V\sqrt{2g}}{2s_T\sqrt{x_0}} = -O_V$ (no parametric fault is considered in the valve section), $A^2 = \tilde{A}^2 = 0$ (the pump flow rate does not depend on the level of the tank, i.e., no influence of x in the pump flow rate), $A_c = -\frac{s_{lg}\sqrt{2g}}{2s_T\sqrt{x_0}} = -O_{lg}$, $\tilde{A}_c = 0$, $u = O_P$, $B^1 = \tilde{B}^1 = 0$ (the valve flow rate O_V is an output of the tank and therefore it does not depend on the input vector u) and $B^2 = \tilde{B}^2 = \frac{1}{s_T}$ (no parametric fault is considered for the section of the tank s_T). A_c represents the dynamic of the leakage does not depend on the system discrete state, while A^1 and B^2 depend on the discrete states of respectively, valve V and pump P.

In order to describe the influence of discrete components, the valve (Dc_1) and the pump (Dc_2), on $\dot{x}$ and $\tilde{\dot{x}}_i$, (3.16) is decomposed as follows:

$$\begin{cases} \dot{x} = \dot{x}^1 + \dot{x}^2 + \dot{x}_c \\ \tilde{\dot{x}} = \tilde{\dot{x}}^1 + \tilde{\dot{x}}^2 + \tilde{\dot{x}}_c \end{cases} \tag{3.17}$$

where:

- $\dot{x}^1 = h_q^1A^1x = -h_q^1O_Vx$ and $\tilde{\dot{x}}^1 = \tilde{h}_q^1\tilde{A}^1x = -\tilde{h}_q^1O_Vx$,
- $\dot{x}^2 = h_q^2B^2u = h_q^2\frac{O_P}{s_T}$ and $\tilde{\dot{x}}^2 = \tilde{h}_q^2\tilde{B}^2u = \tilde{h}_q^2\frac{O_P}{s_T}$,
- $\dot{x}_c = -O_lg$ and $\tilde{\dot{x}}_c = 0$.

Cc is modeled by G_c shown in Fig.3.6.

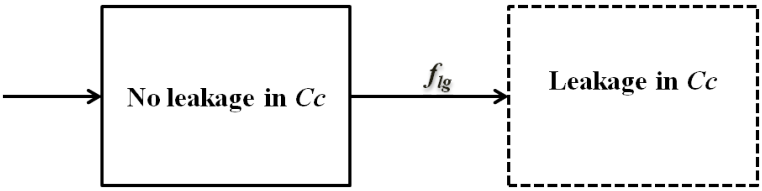

Figure 3.6: Cc automaton denoted by G_c for the one tank example.

3.2.3 Residuals generation

Based on (3.8) and (3.12), residual r_i of x_i is calculated as follows:

$$\begin{cases} r_i = \tilde{\dot{x}}_i - \dot{x}_i \\ \quad = \left(\tilde{A}_{(q)i}X + \tilde{B}_{(q)i}u\right) - \left(A_{(q)i}X + B_{(q)i}u\right) \\ \quad = \left(\tilde{A}_{(q)i} - A_{(q)i}\right)X + \left(\tilde{B}_{(q)i} - B_{(q)i}\right)u \end{cases}$$

Therefore, residual r_i is defined as follows:

$$\begin{cases} r_i = \left(\sum_{m=1}^{n}\left(\left(\sum_{j=1}^{L}\tilde{h}_q^j\tilde{A}_i^{mj} + \tilde{A}_{ci}^m\right)x_m\right) + \sum_{j=1}^{L}\tilde{h}_q^j\tilde{B}_i^j u\right) - \\ \qquad \left(\sum_{m=1}^{n}\left(\left(\sum_{j=1}^{L}h_q^j A_i^{mj} + A_{ci}^m\right)x_m\right) + \sum_{j=1}^{L}h_q^j B_i^j u\right) \end{cases} \tag{3.18}$$

$r = [r_1 \cdots r_i \cdots r_m \cdots r_n]^T$ is a set of the system residuals.

Parametric and discrete faults impact the system continuous dynamics characterized by matrices $A_{(q)i}$ and $B_{(q)i}$ in each discrete state q. The residual r_i is sensitive to the difference between the nominal $\tilde{A}_{(q)i}$, $\tilde{B}_{(q)i}$ and real $A_{(q)i}$, $B_{(q)i}$ values of system parameters. If there is no fault, then $\tilde{A}_{(q)i}$ is equal to $A_{(q)i}$ and $\tilde{B}_{(q)i}$ is equal to $B_{(q)i}$. In this case, r_i will be equal to zero. While, if there is a fault impacting $A_{(q)i}$ and $B_{(q)i}$, then for the measured values of X, $A_{(q)i}X$ and $B_{(q)i}u$ will be different from the values of $\tilde{A}_{(q)i}X$ and $\tilde{B}_{(q)i}u$. Therefore, r_i will be different from zero. In order to describe the influence of each discrete component Dc_j on the value of residual r_i, (3.18) is rewritten as follows:

$$\begin{aligned} r_i &= \left(\tilde{A}_{(q)i}X + \tilde{B}_{(q)i}u\right) - \left(A_{(q)i}X + B_{(q)i}u\right) \\ &= \left(\sum_{m=1}^{n}\left(\sum_{j=1}^{L}\tilde{h}_q^j\tilde{A}_i^{mj} + \tilde{A}_{ci}^m\right)x_m + \sum_{j=1}^{L}\tilde{h}_q^j\tilde{B}_i^j u\right) - \\ &\left(\sum_{m=1}^{n}\left(\sum_{j=1}^{L}h_q^j A_i^{mj} + A_{ci}^m\right)x_m + \sum_{j=1}^{L}h_q^j B_i^j u\right) \\ &= \left(\sum_{m=1}^{n}\sum_{j=1}^{L}\tilde{h}_q^j\tilde{A}_i^{mj}x_m + \sum_{m=1}^{n}\tilde{A}_{ci}^m x_m + \sum_{j=1}^{L}\tilde{h}_q^j\tilde{B}_i^j u\right) - \\ &\left(\sum_{m=1}^{n}\sum_{j=1}^{L}h_q^j A_i^{mj}x_m + \sum_{m=1}^{n}A_{ci}^m x_m + \sum_{j=1}^{L}h_q^j B_i^j u\right) \\ &= \left(\sum_{j=1}^{L}\left(\sum_{m=1}^{n}\tilde{h}_q^j\tilde{A}_i^{mj}x_m + \tilde{h}_q^j\tilde{B}_i^j u\right) - \sum_{j=1}^{L}\left(\sum_{m=1}^{n}h_q^j A_i^{mj}x_m + h_q^j B_i^j u\right)\right) \end{aligned}$$

$$
\begin{aligned}
&+\left(\sum_{m=1}^{n}\tilde{A}_{ci}^{m}x_m-\sum_{m=1}^{n}A_{ci}^{m}x_m\right)\\
&=\left(\sum_{j=1}^{L}\left(\sum_{m=1}^{n}\tilde{h}_q^j\tilde{A}_i^{mj}x_m+\tilde{h}_q^j\tilde{B}_i^j u-\sum_{m=1}^{n}h_q^jA_i^{mj}x_m+h_q^jB_i^ju\right)\right)\\
&+\left(\sum_{m=1}^{n}\tilde{A}_{ci}^{m}x_m-\sum_{m=1}^{n}A_{ci}^{m}x_m\right)\\
&=\left(\sum_{j=1}^{L}\left(\sum_{m=1}^{n}\left(\tilde{h}_q^j\tilde{A}_i^{mj}-h_q^jA_i^{mj}\right)x_m+\left(\tilde{h}_q^j\tilde{B}_i^j-h_q^jB_i^j\right)u\right)\right)\\
&+\left(\sum_{m=1}^{n}\left(\tilde{A}_{ci}^{m}-A_{ci}^{m}\right)x_m\right)
\end{aligned}
$$

Therefore, residual r_i is rewritten as follows:

$$r_i=\sum_{j=1}^{L}r_i^j+r_{ci} \tag{3.19}$$

where r_i^j is the part of residual r_i associated to Dc_j such as $r_i^j=(\tilde{\dot{x}}_i^j-\dot{x}_i^j)$.

Example 3.4 ***Residual generation for the one tank system example***

Based on the real $\dot{x}$ and nominal $\tilde{\dot{x}}$ dynamic evolutions of x calculated on the example 3.3, residual r for one tank water level control system (see Fig.3.2) is written as follows:

$$
\begin{cases}
r=\tilde{\dot{x}}-\dot{x}\\
\quad=\left(-\tilde{h}_q^1\frac{s_V\sqrt{2g}}{2s_T\sqrt{x_0}}x+\tilde{h}_q^2\frac{O_P}{s_T}\right)-\left(-\frac{h_q^1s_V\sqrt{2g}}{2s_T\sqrt{x_0}}x+h_q^2\frac{O_P}{s_T}-\frac{s_{lg}\sqrt{2g}}{2s_T\sqrt{x_0}}x\right)\\
\quad=-(\tilde{h}_q^1-h_q^1)\frac{s_V\sqrt{2g}}{2s_T\sqrt{x_0}}x+(\tilde{h}_q^2-h_q^2)\frac{O_P}{s_T}+(0+\frac{s_{lg}\sqrt{2g}}{2s_T\sqrt{x_0}}x)
\end{cases} \tag{3.20}
$$

In order to describe the influence of each discrete component Dc_j on residual r, (3.20) is rewritten as follows:

$$r=r^1+r^2+r_c \tag{3.21}$$

where $r^1=-(\tilde{h}_q^1-h_q^1)\frac{s_V\sqrt{2g}}{2s_T\sqrt{x_0}}x$, $r^2=(\tilde{h}_q^2-h_q^2)\frac{O_P}{s_T}$ and $r_c=(0+\frac{s_{lg}\sqrt{2g}}{2s_T\sqrt{x_0}}x)$.

- Let us consider the occurrence of a fault of type F_1, i.e., when the controller sends the command $'CV'$, the valve remains in its stuck opened, VSO, failure mode ($\tilde{h}_q^1=0$ while $h_q^1=1$). The occurrence of a fault of type F_1 will affect r as follows: $r=-\left((\tilde{h}_q^1=0)-(h_q^1=1)\right)\frac{s_V\sqrt{2g}}{2s_T\sqrt{x_0}}x+\left(\tilde{h}_q^2-h_q^2\right)\frac{O_P}{s_T}+\left(0+\frac{s_{lg}\sqrt{2g}}{2s_T\sqrt{x_0}}x\right)$. Since, there is no leakage, s_{lg} is equal to zero. Therefore, r will be written as follows: $r=-\left((\tilde{h}_q^1=0)-(h_q^1=1)\right)\frac{s_V\sqrt{2g}}{2s_T\sqrt{x_0}}x+\left(\tilde{h}_q^2-h_q^2\right)\frac{O_P}{s_T}$. Since the pump is in normal operating conditions, then $\tilde{h}_q^2$ is equal to h_q^2. Consequently r can be written as follows: $r=r^1=\frac{s_V\sqrt{2g}}{2s_T\sqrt{x_0}}x$.

- Let us now consider the occurrence of a fault of type F_2, i.e., when the controller sends the command $'Start\_P'$, the pump remains in its failed off failure mode, $PFoff$, ($\tilde{h}_q^2 = 1$ while $h_q^2 = 0$). The occurrence of a fault of type F_2 will affect the residuals r as follows: $r = -\left(\tilde{h}_q^1 - h_q^1\right)\frac{s_V\sqrt{2g}}{2s_T\sqrt{x_0}}x + \left((\tilde{h}_q^2 = 1) - (h_q^2 = 0)\right)\frac{O_P}{s_T} + \left(0 + \frac{s_{lg}\sqrt{2g}}{2s_T\sqrt{x_0}}x\right)$. Since there is no leakage, s_{lg} is equal to zero. Therefore, r is written as follows: $r = -\left(\tilde{h}_q^1 - h_q^1\right)\frac{s_V\sqrt{2g}}{2s_T\sqrt{x_0}}x + \left((\tilde{h}_q^2 = 1) - (h_q^2 = 0)\right)\frac{O_P}{s_T}$. Since the valve is in normal operating conditions, then $\tilde{h}_q^1$ is equal to h_q^1. Consequently, r can be written as follows: $r = r^2 = \frac{O_P}{s_T}$.
- Let us now consider the occurrence of a parametric fault of type F_3, i.e., leakage in the tank. Based on (3.20), this fault does not depend on the discrete state of the system. This fault will increase slowly r outside the normal interval. Since the valve and the pump are in normal operating conditions, then, $\tilde{h}_q^1$ and $\tilde{h}_q^2$ are equal, respectively, to h_q^1 and h_q^2. Consequently, $r = r_c = \frac{s_{lg}\sqrt{2g}}{2s_T\sqrt{x_0}}x$.

Parameters O_P, s_T and s_V are known nominal values that can be determined in advanced. Thus, as an example in the case of the occurrence of fault event of type F_2 the deference $\dot{\tilde{x}} - \dot{x}$ will be equal to this predefined value $\frac{O_P}{s_T}$.

3.2.4 Hybrid components modeling

A hybrid component $HC_j,\ j \in \{1, \cdots, L\}$, is composed of one discrete component $Dc_j,\ j \in \{1, \cdots, L\}$, with the set of $g,\ g \leq n$, continuous components (Ccs) whose continuous dynamic behavior is changed according to Dc_j discrete states. Therefore, the local hybrid model G^j of HC_j is obtained by a combination of the discrete local model of Dc_j, (DG^j), and the continuous dynamic evolutions of continuous components Ccs belonging to HC_j. Thus, the local hybrid model of the component HC_j is obtained by synchronizing the discrete local automaton DG^j of Dc_j and the set of local automata $G_{cji},\ i \in \{1, \cdots, g\}$, modeling Ccs belonging to HC_j using parallel or synchronous composition operator. The latter builds the hybrid component model from its individual components models. Therefore, $G^j = DG^j||G_{cj1}|| \cdots ||G_{cjg}$. The state corresponding to the multiple faults are removed from the hybrid local model.

The nominal and faulty behaviors of each hybrid component $HC_j, j \in \{1, \cdots, L\}$ is modeled using hybrid automaton G^j defined by the tuple (see Fig.3.7):

$$G^j = (Q^j, h_q^j, \tilde{h}_q^j, \Sigma^j, \delta^j, X^j, flux^j, r^j, r_c^j, HSL^j, Init^j) \tag{3.22}$$

where,

- Q^j: is the set of local hybrid model states of HC_j. Parametric and discrete faults occurred in the components of HC_j are included as states in the local hybrid automaton G^j of HC_j. Hence, the local hybrid model includes nominal operating modes, discrete faulty modes of Dc_j and parametric faulty modes of Ccs belonging to HC_j. A normal operating mode is represented by one local hybrid state in G^j while a failure mode can be represented by several

states. Consequently, Q^j is equal to $Q_D^j \times Q_c^j$, where Q_D^j is a finite set of local states representing the normal and faulty operating modes of Dc_j. $Q_c^j = Q_{cj1}^j \times \cdots \times Q_{cjg}^j$ is a finite set of local states representing the normal and faulty operating modes of Ccs belonging to HC_j;

- The output of each local state q^j is characterized by real discrete output vector $h_q : Q^j \to \{0,1\}$ and nominal discrete output vector $\tilde{h}_q^j : Q^j \to \{0,1\}$. At normal discrete modes, h_q is equal to $\tilde{h}_q$; while in faulty discrete modes h_q^j is different from $\tilde{h}_q$;

- $\Sigma^j = \Sigma_D^j \cup \Sigma_c^j$: is the event set of hybrid component HC_j. It includes the set of discrete events Σ_D^j and events indicating the parametric faults occurrence (Σ_c^j) in all Ccs belonging to HC_j. $\Sigma^j = \Sigma_o^j \cup \Sigma_u^j$. Σ_o^j includes control command events sent to Dc_j and other observable discrete events. Σ_u^j denotes the set of fault events Σ_f^j (parametric and discrete) that can occur in hybrid component HC_j;

- $\delta^j : Q^j \times \Sigma^j \to Q^j$: is the state transition function of HC_j. A transition $\delta^j(q^j, e) = q^{j+}$ corresponds to a change from state q^j to state q^{j+} after the occurrence of discrete event $e \in \Sigma^j$;

- $X^j \subset X$: is a finite set of continuous variables $x = [x_1 \cdots x_g]^T$ associated to the set of Ccs belonging to HC_j;

- $flux^j : Q \times X^j \to \Re^n$: is a function characterizing the real evolution parts $\left\{\dot{X}^j = [\dot{x}_1^j \cdots \dot{x}_g^j]^T,\ \dot{X}_c^j = [\dot{x}_{c1} \cdots \dot{x}_{cg}]^T\right\}$ and nominal evolution parts $\left\{\dot{\tilde{X}}^j = [\dot{\tilde{x}}_1 \cdots \dot{\tilde{x}}_g]^T,\ \dot{\tilde{X}}_c^j = [\dot{\tilde{x}}_{c1} \cdots \dot{\tilde{x}}_{cg}]^T\right\}$ of continuous variables X in each hybrid state q^j (see (3.9));

- $r^j = [r_1^j \cdots r_g^j]^T$ and $r_c^j = [r_{c1} \cdots r_{cg}]^T$ are a set of parts of residuals generated at each HC_j state q^j;

- The set of parametric and discrete fault events is divided into d^j different fault types or modes indicated by the following hybrid status labels: $HSL^j = \{N_j, F_1, F_2, \cdots F_{d^j}\}$ where N_j is the label indicating the absence of parametric and discrete faults in HC_j, i.e., normal operating conditions of HC_j;

- $Init^j = (q_1^j \in Q^j,\ h_q^j(q_1^j) = h_{q_1^j}^j,\ \tilde{h}_q^j(q_1^j) = \tilde{h}_{q_1^j}^j,\ \dot{X}^j(q_1^j),\ \dot{X}_c^j(q_1^j),$ $\dot{\tilde{X}}^j(q_1^j),\ \dot{\tilde{X}}_c^j(q_1^j),\ HSL^j(q_1^j))$: is the set of initial conditions.

Example 3.5 ***Hybrid components modeling for the one tank system example***

Let us take the discrete and continuous components defined, respectively, in Example 3.2 and Example 3.3. As we have seen in (3.15) in Example 3.3, the nominal and real continuous dynamic evolutions of this system are written as follows:

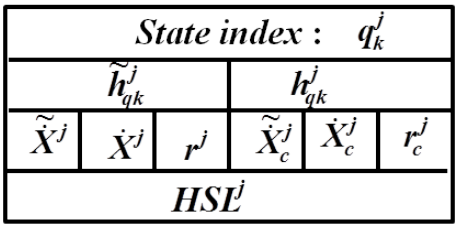

Figure 3.7: Hybrid state of local hybrid model G^j.

$$\begin{cases} \dot{x} = -h_q^1 \frac{s_V\sqrt{2g}}{2s_T\sqrt{x_0}}x + h_q^2 \frac{O_P}{s_T} - \frac{s_{lg}\sqrt{2g}}{2s_T\sqrt{x_0}}x \\ \\ \dot{\tilde{x}} = -\tilde{h}_q^1 \frac{s_V\sqrt{2g}}{2s_T\sqrt{x_0}}x + \tilde{h}_q^2 \frac{O_P}{s_T} \end{cases}$$

As shown in these equations, the dynamic evolution of x, representing the continuous component Cc, is influenced by the discrete state output of the valve, Dc_1, and discrete state output of the pump, Dc_2. Thus, the one tank water level control system is decomposed into two interacting HCs as shown in Fig.3.8:

- HC_1 is composed of valve V (Dc_1) and the tank (Cc);
- HC_2 is composed of pump P (Dc_2) and the tank (Cc).

Local hybrid automaton G^1 characterizing HC_1 hybrid dynamics is defined by the tuple (see Fig.3.9 and Fig.3.10):

$$G^1 = (Q^1, h_q^1, \tilde{h}_q^1, \Sigma^1, X^1, flux^1, r^1, r_c^1, \delta^1, HSL^1, Init^1) \tag{3.23}$$

where,

- $Q^1 = \{q_1^1,\ q_2^1,\ q_3^1,\ q_4^1, q_5^1, q_6^1\}$. q_1^1 and q_2^1 represent, respectively, the valve closed, ($VC(no\ leakage)$), and the valve opened, ($VO(no\ leakage)$), in normal operating conditions (of the valve and the tank). q_3^1 and q_4^1 characterize the valve stuck opened discrete failure mode, ($VSO(no\ leakage)$). $Q_c^1 = \{q_5^1,\ q_6^1\}$ characterize leakage failure mode in each hybrid discrete mode of HC_1 ($VC(leakage)$) and ($VO(leakage)$);
- $h_q^1 : Q^1 \to \{0,1\} = \{0\ (V$ closed), $1\ (V$ opened)$\}$;
- $\tilde{h}_q^1 : Q^1 \to \{0,1\} = \{0\ (V$ should be closed), $1\ (V$ should be opened)$\}$;
- $\Sigma^1 = \Sigma_o^1 \bigcup \Sigma_u^1$: is the set of HC_1 discrete events. $\Sigma_o^1 = \{CV$ (close V), OV (open V)$\}$, $\Sigma_u^1 = \Sigma_f^1 = \{f_{SO}$ (fault event leading to V stuck opened discrete failure mode), f_{lg} (fault event indicating the occurrence of the leakage in the tank)$\}$. The fault, f_{VSO}, can occur at the state where the valve is opened. While f_{lg} can occur whatever the discrete mode of HC_1 is.
- $\delta^1 : Q^1 \times \Sigma^1 \to Q^1$: is the HC_1 state transition function. As an example $\delta^1(q_2^1, CV) = q_1^1$ (see Fig.3.10);

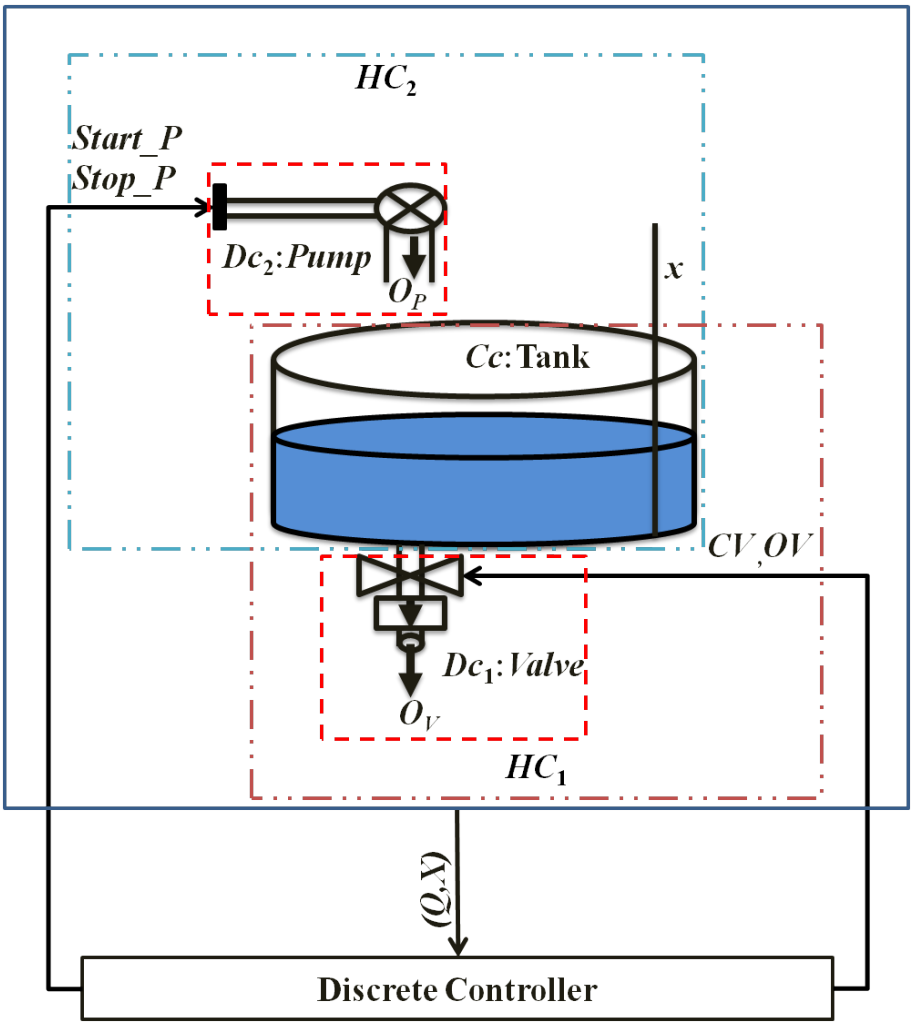

Figure 3.8: Hybrid components of the one tank water level control system.

- $X^1 = x$: represents the tank level;
- $flux^1 = \{\dot{x}^1,\ \tilde{\dot{x}}^1,\ \dot{x}_c,\ \tilde{\dot{x}}_c\}$: are the real $\dot{x}^1 = -h_q^1 \frac{s_V\sqrt{2g}}{2s_T\sqrt{x_0}}x$ and nominal $\tilde{\dot{x}}^1 = -\tilde{h}_q^1 \frac{s_V\sqrt{2g}}{2s_T\sqrt{x_0}}x$ dynamic evolution parts of x according to discrete state of the valve and the real $\dot{x}_c = -\frac{s_{lg}\sqrt{2g}}{2s_T\sqrt{x_0}}x$ and nominal $\tilde{\dot{x}}_c = 0$ dynamic evolution parts of x whatever the discrete mode of the system is;
- $r^1 = -\left(\tilde{h}_q^1 - h_q^1\right)\frac{s_V\sqrt{2g}}{2s_T\sqrt{x_0}}x = -\left(\tilde{h}_q^1 - h_q^1\right)O_V$ is the part of residual r generated in the valve discrete states. $r_c = \left(0 + \frac{s_{lg}\sqrt{2g}}{2s_T\sqrt{x_0}}x\right) = (0 + O_{lg})$ is the part of residual r generated whatever the valve discrete mode is;
- $HSL^1 = \{N_1$ (Absence of the faults in HC_1), F_1 (valve stuck opened), F_3 (leakage in the tank)$\}$. As an example status label for q_1^1, HSL_1^1, is equal to N_1;

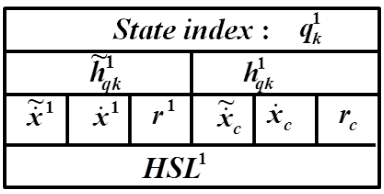

Figure 3.9: Local hybrid state of HC_1.

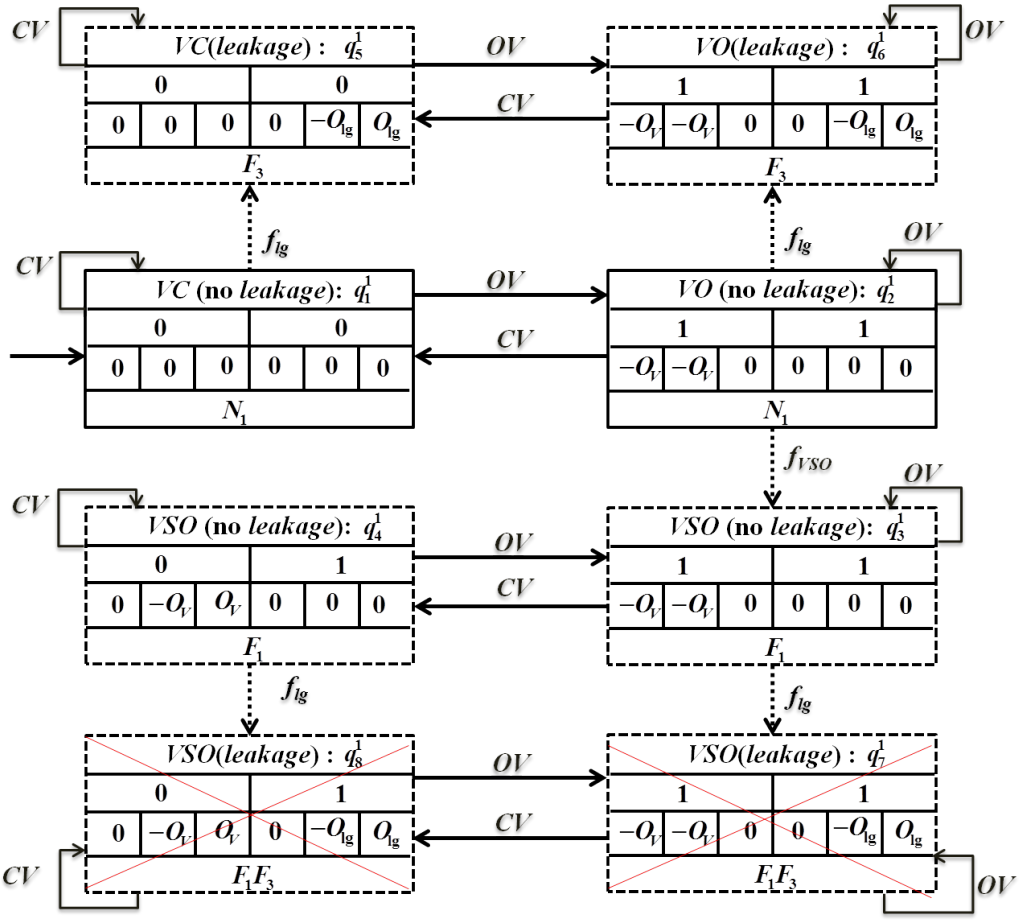

Figure 3.10: Hybrid automaton G^1 for HC_1.

- $Init^1$: $(q_1^1,\ h_{q_1^1}^1 = \tilde{h}_{q_1^1}^1 = 0,\ \dot{x}^1 = \tilde{\dot{x}}^1 = 0,\ \dot{x}_c = \tilde{\dot{x}}_c = 0,\ HSL_{q_1^1} = N_1)$: is the set of initial conditions.

Hybrid states q_7^1 and q_8^1 and the events loading to these states are removed from hybrid automaton G^1 of HC_1 because multiple faults are not considered (see Fig.3.10).

Likewise, local hybrid automaton G^2 characterizing HC_2 hybrid dynamics is

defined by the tuple (see Fig.3.11):

$$G^2 = (Q^2, h_q^2, \tilde{h}_q^2, \Sigma^2, X^2, flux^2, r^2, r_c^2, \delta^2, HSL^2, Init^2) \tag{3.24}$$

where,

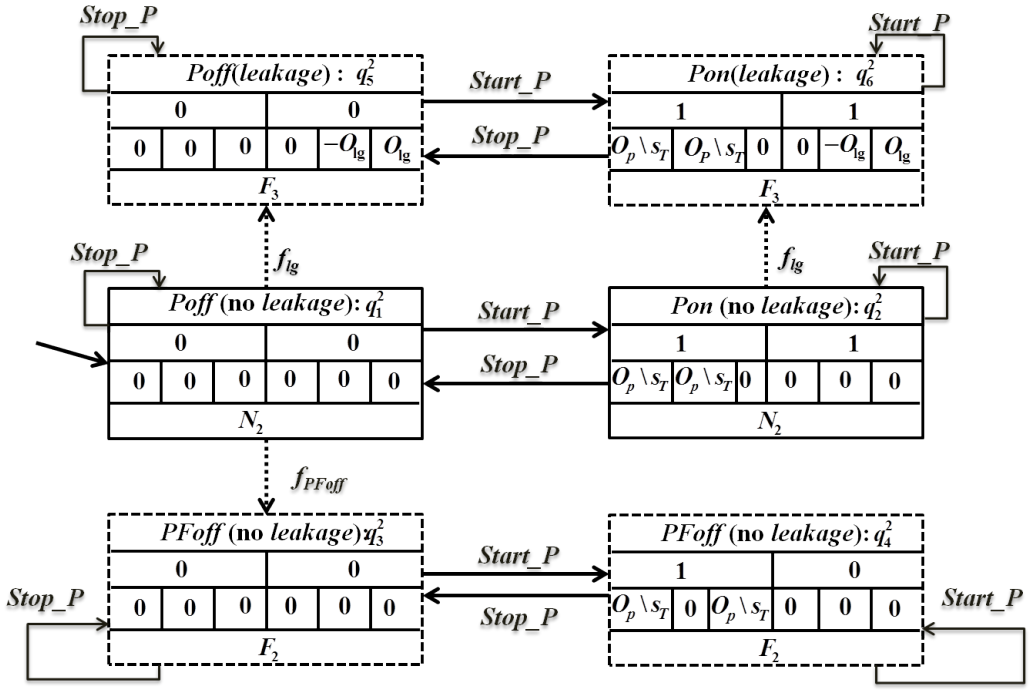

Figure 3.11: Hybrid automaton G^2 for HC_2.

- $Q^2 = \{q_1^2,\ q_2^2,\ q_3^2,\ q_4^2, q_5^2, q_6^2\}$. q_1^2 and q_2^2 represent, respectively, pump off, $(Poff(no\ leakage))$, and the pump on, $(Pon(no\ leakage))$, in normal operating conditions. q_3^2 and q_4^2 characterize the pump failed off failure mode, $(PFoff(no\ leakage))$. $Q_c^2 = \{q_5^2,\ q_6^2\}$ characterize leakage failure mode in each discrete mode of HC_2, $(Pon(leakage))$ and $(Poff(leakage))$;
- $h_q^2 : Q^2 \rightarrow \{0,1\} = \{0$ (pump stopped), 1 (pump started)$\}$;
- $\tilde{h}_q^2 : Q^2 \rightarrow \{0,1\} = \{0$ (pump should be stopped) 1 (pump should be started)$\}$;
- $\Sigma^2 = \Sigma_o^2 \bigcup \Sigma_u^2$: is the set of HC_2 events. $\Sigma_o^2 = \{Start\_P$ (start pump), $Stop\_P$ (stop pump)$\}$. $\Sigma_u^2 = \Sigma_f^2 = \{f_{PFoff}$ (fault event leading to pump failed off failure mode), f_{lg} (fault indicating the occurrence of leakage in the)$\}$. The fault, f_{PFoff}, can occur at the state where the pump is stopped. While f_{lg} can occur whatever the discrete mode of HC_2 is.
- $\delta^2 : Q^2 \times \Sigma^2 \rightarrow Q^2$: is the HC_2 state transition function. As an example, $\delta^2(q_1^2, Start\_P) = q_2^2$ (see Fig.3.11);

- $X^2 = x$: represents the tank level;
- $flux^2 = \{\dot{x}^2,\ \tilde{\dot{x}}^2,\ \dot{x}_c,\ \tilde{\dot{x}}_c\}$: are the real $\dot{x}^2 = h_q^2 \frac{O_P}{s_T}$ and nominal $\tilde{\dot{x}}^2 = \tilde{h}_q^2 \frac{O_P}{s_T}$ dynamic evolution parts of x according to discrete state of the pump and the real $\dot{x}_c = -\frac{s_{lg}\sqrt{2g}}{2s_T\sqrt{x_0}}x$ and nominal $\tilde{\dot{x}}_c = 0$ dynamic evolution parts of x whatever the discrete mode of the system is;
- $r^2 = \left(\tilde{h}_q^2 - h_q^2\right)\frac{O_P}{s_T}$ is the part of residual r generated in the pump discrete states. $r_c = \left(0 + \frac{s_{lg}\sqrt{2g}}{2s_T\sqrt{x_0}}x\right) = (0 + O_{lg})$ is the part of residual r generated whatever the pump discrete mode is;
- $HSL^2 = \{N_2$ (Absence of faults in HC_2), F_2 (pump failed off), F_3 (leakage in the tank)$\}$. As an example status label for q_1^2, HSL_1^2, is equal to N_2;
- $Init^2 :\ (q_1^2,\ h_{q_1^2}^2 = \tilde{h}_{q_1^2}^2 = 0,\ \dot{x}^2 = \tilde{\dot{x}}^2 = 0,\ \dot{x}_c = \tilde{\dot{x}}_c = 0,\ HSL_{q_1^2} = N_2)$: is the set of initial conditions.

3.2.5 Global system modeling

The global hybrid model of the HDS is obtained by synchronizing the local hybrid automata, $G^j,\ j \in \{1, \cdots, L\}$, using parallel or synchronous composition operator. The latter builds the hybrid global model from its individual component models. In this parallel or synchronous composition, a common event between two hybrid components can only be executed if both components execute it simultaneously. However, the private events which can be executed by only one hybrid component can be executed whenever possible. Therefore, G is equal to $G^1||G^2||\cdots||G^L$. The continuous dynamics in each state are calculated based on (3.9), (3.13) and (3.19). The state corresponding to the multiple faults are removed from the hybrid global model.

The hybrid dynamics of the system are modeled by a linear hybrid automaton defined by the tuple (see Fig.3.12 and Fig.3.14):

$$G = (Q, h_q, \tilde{h}_q, \Sigma, X, flux, r, Init, \delta, GSL) \tag{3.25}$$

where,

- Q: is the set of hybrid model states obtained by synchronizing the local hybrid states of $G^j,\ j \in \{1, \cdots, L\}$. Therefore, Q is equal to $Q^1 \times \cdots \times Q^L$;
- The output of each hybrid global state q is characterized by real discrete output vector $h_q : Q \to \{0,1\}^L$ and nominal discrete output vector $\tilde{h}_q : Q \to \{0,1\}^L$. At normal discrete modes, h_q is equal to $\tilde{h}_q$ while in faulty modes h_q is different from $\tilde{h}_q$;
- $\Sigma = \Sigma^1 \cup \cdots \cup \Sigma^j \cup \cdots \cup \Sigma^L$: is the set of system events. $\Sigma = \Sigma_o \cup \Sigma_u$, where Σ_o includes control command events and other observable discrete events. Σ_u denotes the set of fault events Σ_f (parametric and discrete) that can occur in the system as well as normal but unobservable discrete events;

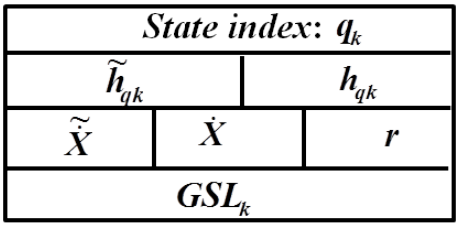

Figure 3.12: Hybrid state of global hybrid model G.

- X: is a finite set of continuous variables $X = [x_1 \cdots x_i \cdots x_n]^T$ describing the continuous dynamics of the system;
- $flux : Q \times X \rightarrow \Re_n$: is a function characterizing real evolution $\dot{X}$ and nominal evolution $\tilde{\dot{X}}$ of continuous variables X in each state q;
- $r = [r_1, \cdots, r_n]^T$: is a set of residuals generated at each hybrid state q and used as consistency indicators;
- $\delta : Q \times \Sigma \rightarrow Q$: is the state transition function of the system. A transition $\delta(q, e) = q^+$ corresponds to a change from state q to state q^+ after the occurrence of discrete event $e \in \Sigma$;
- The set of parametric and discrete fault events is divided into d different fault types or modes indicated by the following global status labels: $GSL = \{N, F_1, F_2, \cdots F_d\}$ where N is the label indicating the absence of parametric and discrete faults in the system, i.e., normal operating conditions of the system;
- $Init = (q_1 \in Q,\ h_q(q_1),\ \tilde{h}_q(q_1),\ \dot{X}(q_1),\ \tilde{\dot{X}}(q_1),\ GSL(q_1))$: is the set of initial conditions.

the multiple faults global states and the events loading to these states are removed from the global automaton because multiple faults are not considered.

Example 3.6 ***Global system modeling of the one tank system example***

The hybrid global model of the one tank water level system of Fig.3.2 is modeled by linear hybrid automaton defined by the tuple (see Fig.3.13):

$$G = (Q, h_q, \tilde{h}_q, \Sigma, X, flux, r, Init, \delta, GSL) \tag{3.26}$$

where,

- $Q = \{q_1,\ q_2,\ q_3,\ q_4,\ q_{11},\ q_{12},\ q_{13},\ q_{14},\ q_{21},\ q_{22},\ q_{23},\ q_{24},\ q_{31},\ q_{32},\ q_{33},\ q_{34}\}$. q_1, q_2, q_3 and q_4 represent, respectively, valve closed and pump off $(VCPoff(no\ leakage))$, valve closed and pump on $(VCPon(no\ leakage))$, valve opened and pump on $(VOPon(no\ leakage))$, and valve opened and pump off $(VOPoff(no\ leakage))$, in normal operating conditions. q_{11}, q_{12}, q_{13} and

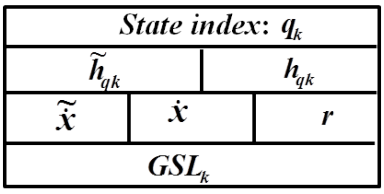

Figure 3.13: Global hybrid state of on tank water level control system.

q_{14} characterize the valve stuck opened failure mode ($VSOPoff(no\ leakage)$, $VSOPon(no\ leakage)$). q_{21}, q_{22}, q_{23} and q_{24} characterize the pump off failure mode ($VCPFoff(no\ leakage)$, $VOPFoff(no\ leakage)$). $\{q_{31}, q_{32}, q_{33}, q_{34}\}$ characterize leakage failure mode in discrete normal mode ($VCPoff(leakage)$, $VCPon(leakage)$, $VOPon(leakage)$ and $VOPoff(leakage)$);

- $h_q : Q \rightarrow 0,1^2$ is equal to $h_q^1 h_q^2$ and $\tilde{h}_q : Q \rightarrow 0,1^2$ is equal to $\tilde{h}_q^1 \tilde{h}_q^2$;
- $\Sigma = \Sigma^1 \cup \Sigma^2 \cup \Sigma^c = \Sigma_o \cup \Sigma_u$. $\Sigma_o = \{CV, OV, Start\_P, Stop\_P\}$. $\Sigma_u = \Sigma_f = \{f_{VSO}, f_{PFoff}, f_{lg}$ (fault event indicating the occurrence of leakage in the tank)$\}$;
- $X = x$: represents the tank level;
- $flux = \{\dot{x}, \tilde{\dot{x}}\}$: is the real $\dot{x} = \dot{x}^1 + \dot{x}^2 + \dot{x}_c$ and nominal $\tilde{\dot{x}} = \tilde{\dot{x}}^1 + \tilde{\dot{x}}^2 + \tilde{\dot{x}}_c$ evolutions of x in each global hybrid state;
- $r = -\left(\tilde{h}_q^1 - h_q^1\right) \frac{s_V\sqrt{2g}}{2s_T\sqrt{x_0}} x + \left(\tilde{h}_q^2 - h_q^2\right) \frac{O_P}{s_T} - \left(0 - \frac{s_{lg}\sqrt{2g}}{2s_T\sqrt{x_0}} x\right) = -\left(\tilde{h}_q^1 - h_q^1\right) O_V + \left(\tilde{h}_q^2 - h_q^2\right) \frac{O_P}{s_T} - (0 - O_{lg})$: is the residual generated in each hybrid state, where $O_V = \frac{s_V\sqrt{2g}}{2s_T\sqrt{x_0}} x$ and $O_{lg} = \frac{s_{lg}\sqrt{2g}}{2s_T\sqrt{x_0}} x$;
- GSL is equal to $\{N, F_1, F_2, F_3\}$ (see Table 3.1). N is the label indicating the absence of faults of types F_1, F_2 and F_3 in one tank water level control system;
- $Init$: $(q_1, h_q = \tilde{h}_q = 00, \dot{x} = \tilde{\dot{x}} = 0, GSL_{q_1} = N)$;

The global model of one tank water level control system (Fig.3.2) is depicted in (Fig.3.14). Hybrid model G contains 16 hybrid states (4 normal states and 4*3 faulty states) and 38 transitions (32 observable transitions and 6 unobservable transitions) (see Fig.3.14).

3.3 Hybrid diagnoser construction

3.3.1 Fault signature construction

A qualitative signature is constructed by abstracting the different residuals. This abstraction is achieved by continuous and discrete symbols generation. Continuous

Table 3.1: Faults for the diagnosis of one tank level control system.

Fault types	*Fault labels*	*Fault description*
Discrete faults	F_1	V stuck opened
	F_2	Pump failed off
Parametric fault	F_3	leakage in the tank ($s_{lg} \neq 0$)

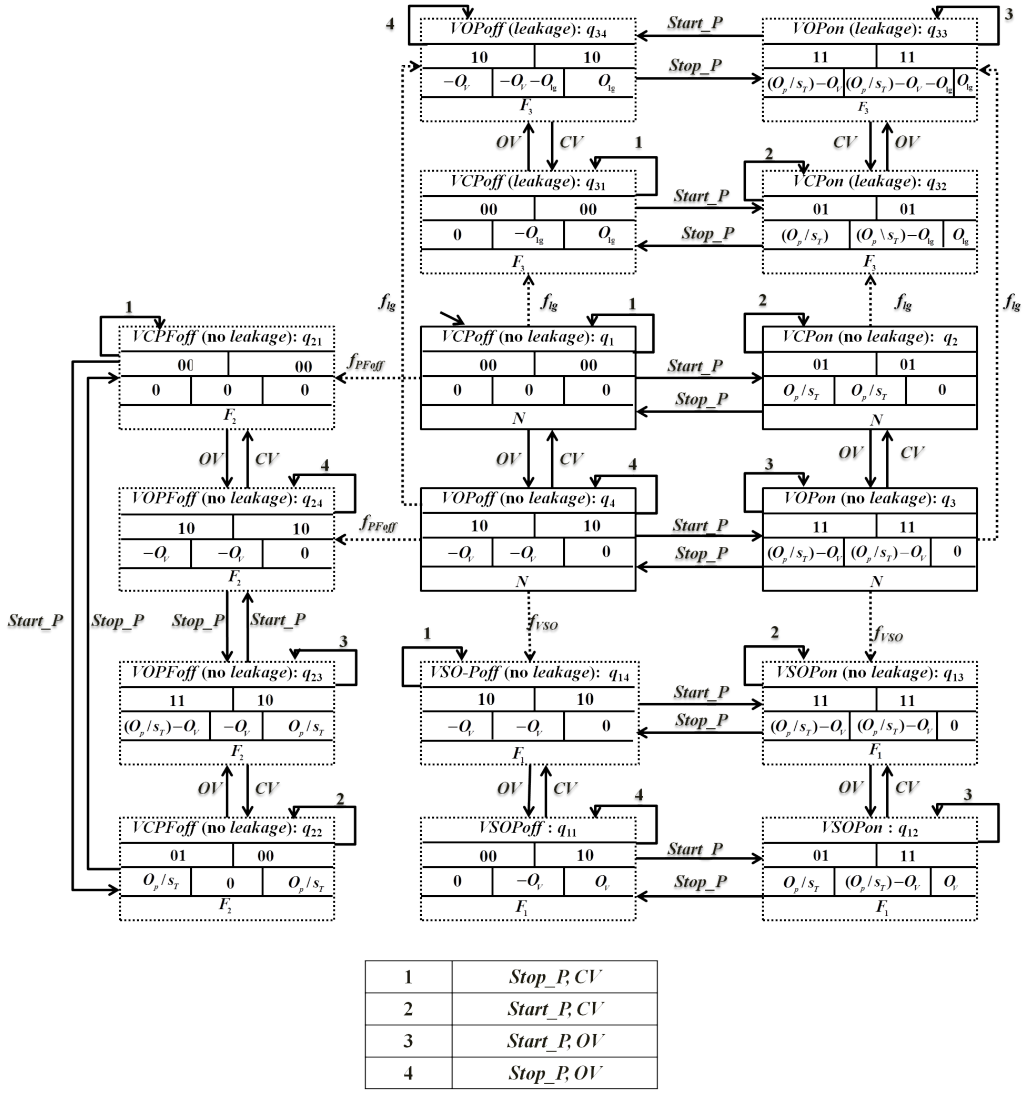

Figure 3.14: Automaton of composite model.

symbols $CS(r_i) \in \{0, -, +\}$ represent the qualitative abstraction of residual values into stable/decreasing/increasing ones (Fig.3.15):

- $r_i^0 : r_i(t)$ belongs to the nominal interval;

- $r_i^- : r_i(t)$ is below the nominal interval;
- $r_i^+ : r_i(t)$ is above the nominal interval.

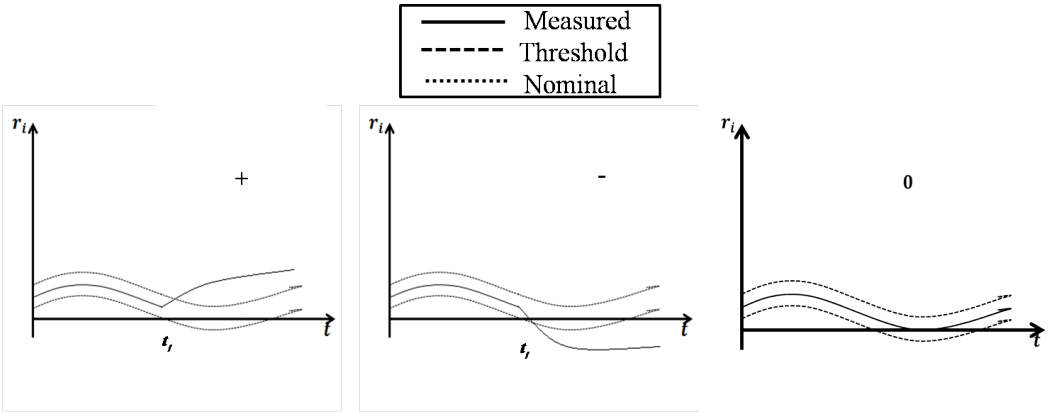

Figure 3.15: Continuous symbols generation.

Terms in (3.18) ($h_q^j A_i^{mj} x_m$ and $h_q^j B_i^j u$, $j \in \{1, \cdots, L\}$), describe the interactions between continuous and discrete components for the dynamic evolution ($\dot{x}_i, i \in \{1, \cdots, n\}$) of each continuous variable x_i. They can exhibit an abrupt change in the continuous dynamics due to unpredicted change (abnormal) in Dc_j discrete mode. This change is characterized by the absence ($h_q^j = 0$ while $\tilde{h}_q^j = 1$) or the addition ($h_q^j = 1$ while $\tilde{h}_q^j = 0$) of $A_i^{mj} x_m$ and $B_i^j u$. Parametric faults may be characterized as abrupt, i.e, discontinuous change, or incipient, i.e, slow changes. Incipient faults are more difficult to deal with. Therefore, in this thesis, parametric faults are considered to be incipient due to ageing effects for example. Consequently parametric incipient faults cannot cause an abrupt change with a finite change in magnitude. Therefore, they are indicated by a progressive abnormal change of parameter value in A_i^{mj} and B_i^j as well as in the term, A_{ci}^m. In order to take into account this discriminative information, discrete symbols $DS(r_i)$ are added for the abstraction of each residual r_i in order to distinguish between parametric and discrete faults as follows (Fig.3.16):

- $PC_i^j = +Val$: denotes an abrupt positive change in residual r_i due to a discrete fault caused by Dc_j. $+Val$ is equal to the absolute value of $A_i^{mj} x_m$ or $B_i^j u$ associated to h_q^j;
- $NC_i^j = -Val$: denotes an abrupt negative change in residual r_i due to a discrete fault caused by Dc_j;
- UC_i: denotes that there is no observed abrupt change in residual r_i.

A fault signature Sig_z at global discrete state q is the combination of continuous and discrete symbols of the different residuals as follows:

$$sig_z = \left(r_1^{CS(r_1)}, DS(r_1)\right) \& \cdots \& \left(r_i^{CS(r_i)}, DS(r_i)\right) \& \cdots \& \left(r_n^{CS(r_n)}, DS(r_n)\right) \tag{3.27}$$

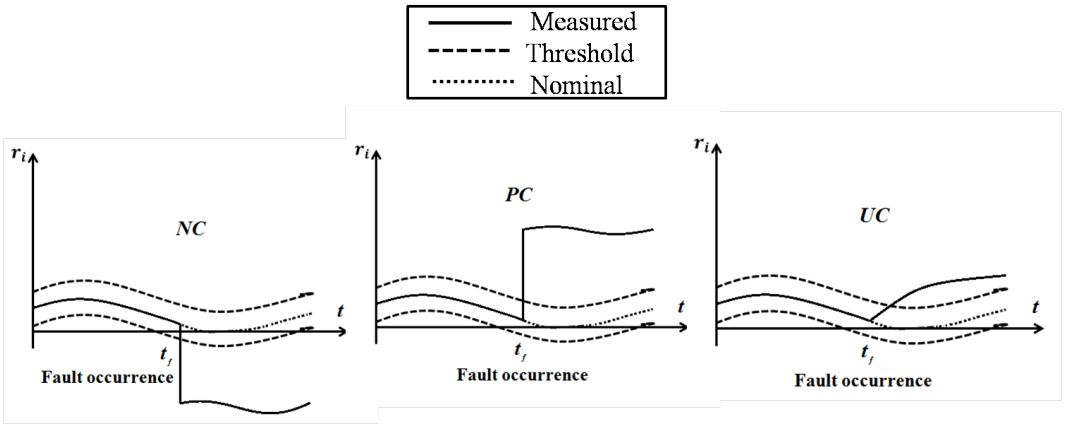

Figure 3.16: Discrete symbols generation.

Example 3.7 ***Fault signature generation for the one tank system example***

For the one tank water level control example, the system generates a specific fault signature in each hybrid global state according to the residual defined in this state. These fault signatures are generated using the continuous dynamic evolutions in each hybrid global state. In normal operating mode, the system generates a normal fault signature $sig_0 = (r^0, UC)$, e.g., hybrid states q_1, q_2, q_3 and q_4 of Fig.3.14 (the residual in these states is equal to zero: there is no change in a residual). The fault signature sig_0 is generated also in discrete faults states where the residual does not yet change its value: Indeed when a discrete fault occurs, the continuous dynamic evolution will not be change until a control command event changes the discrete mode. As an example when the discrete fault f_{PFoff} occurred at the initial state 'q_1' with the normal mode '$VCPoff(no\ leakage)$', the system will move to the state q_{21} with the failure mode '$VCPFoff(no\ leakage)$'. the continuous dynamic evolution in these two states, q_1 and q_{21} (see Fig.3.14), is the same. Thus, the fault signature is the same for both states. However, the occurrence of control command event $Start_P$ will move the system to state q_{22}. The continuous dynamic evolution in this state is different from one of q_1. Therefore, a different fault signature is generated at this state. In the other faulty operating modes the system generates a fault signature different from sig_0. e.g., in faulty state $(q_{12} : VSOPon(no\ leakage))$ the system generates a fault signature equal to $sig_1 = (r^+,\ PC^1)$. This positive change PC^1 is equal to $(O_V = \frac{s_V\sqrt{2g}}{2s_T\sqrt{x_0}}x)$ (see Fig.3.14 and Table 3.2). The thresholds are defined based on the system discrete faults. We consider that the section of leakage is less than the section of valve: $s_V \gg s_{lg}$. Therefore, when a leakage occurred, the residual r increases slowly outside the normal interval. This increase is less than one produced by the discrete fault related to the valve. Thus the change due to the discrete fault related to the valve is considered abrupt while the parametric fault

due to the leakage is considered to be progressive. Table 3.2 shows the global fault signatures used by the centralized hybrid diagnoser to achieve its diagnosis.

Table 3.2: Faults signature table.

Signature name	***Residual value***	***Fault signature***
sig_0	0	(r^0, UC)
sig_1	$\frac{s_V\sqrt{2g}}{2s_T\sqrt{x_0}}x$	(r^+, PC^1)
sig_2	$\frac{O_P}{s_T}$	(r^+, PC^2)
sig_3	$\frac{s_{lg}\sqrt{2g}}{2s_T\sqrt{x_0}}x$	(r^+, UC)

3.3.2 Centralized hybrid diagnoser construction

The objective of the centralized hybrid diagnoser (CHD) is to detect and isolate the occurrence of parametric and discrete faults affecting the system (see Fig.3.17). CHD is built based on the global model, G, of the system. Initial state z_1 of CHD is composed of initial state q_1 of G and all states q_k of G reached from q_1 by the occurrence of unobservable events. Then, the G states that are reached from any G state belonging to z_1, through either the same control command event or the same fault signature, are gathered into the same state z_2. By following the same reasoning, the other states of CHD are constructed. Thus, the transition function of the CHD can be defined by:
$\delta_z = Z \times Sig \times \Sigma \rightarrow Z$
where, Z is the set of all CHD states and Sig denotes the set of all CHD fault signatures generated by the system. A fault signature generates a new kind of observable events tanks to the system continuous dynamic evolution in each discrete mode. This new kind of observable events enhances the diagnosis capacity of parametric and discrete faults of the system.

Each state z_k of the CHD is of the form:
$z_k = \{Q_k,\ \tilde{h}_z,\ \dot{\tilde{X}},\ GSL_{z_k}\}$
where, $Q_k = \{q_b, \cdots, q_l\}$ is the set of model states belonging to the CHD state z_k, $\tilde{h}_z$ is the nominal state output of z_k, $GSL_{z_k} = \{GSL_{q_b}, \cdots, GSL_{q_l}\}$ gathers the set of labels of z_k states. $\dot{\tilde{X}}$ is the nominal dynamic evolutions of the continuous variables in the states of z_k.

CHD contains only transitions labeled by observable events (control command events or fault signatures). This is the essential difference between G and CHD. Each state of the hybrid diagnoser is of the form of Fig.3.18.

Definition 3.1 *Hybrid diagnoser state z_k is called normal, if $GSLz_k$ is equal to $\{N\}$.*

Definition 3.2 *Hybrid diagnoser state z_k is called F_w-certain ,$w \in \{1, \cdots, d\}$, if $GSLz_k$ is equal to $\{F_w\}$.*

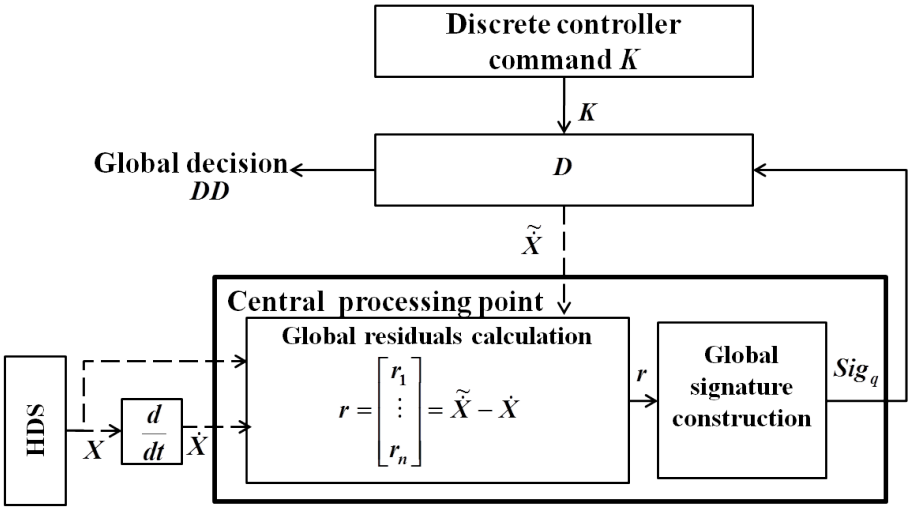

Figure 3.17: Implementation of global diagnoser D online.

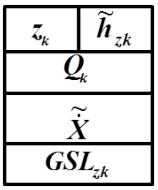

Figure 3.18: State of centralized hybrid diagnoser (CHD).

Definition 3.3 *Hybrid diagnoser state z_k is called F_w-uncertain, if $GSLz_k$ contains different labels beside fault label F_w.*

Definition 3.4 *An indeterminate cycle is a sequence of F_w-uncertain states in which the hybrid diagnoser is unable to decide with certainty and within a finite number of observable transitions the occurrence of a fault of type $F_w, w \in \{1, \cdots, d\}$. Therefore, a cycle is F_w-indeterminate if the following two conditions are satisfied:*

- *It is F_w-uncertain cycle in the hybrid diagnoser;*
- *Its states form two cycles in the model, the states of the first cycle have the normal label while the states of the second cycle have fault label F_w.*

Example 3.8 ***Centralized hybrid diagnoser of the one tank system example***

CHD model of one tank water level control system is carried out in a conventional way. For the sake of simplicity, only a part of CHD is shown in Fig.3.20. The global hybrid diagnoser is shown in Fig.3.21. A detailed description of each state and transition of CHD is represented by states and transition tables. The hybrid diagnoser state table (Table 3.3) provides a detailed description of the contents of

each hybrid diagnoser state. Hybrid diagnoser transition table (Table 3.4) defines the initial state, the final state and the description of each hybrid diagnoser transition.

The hybrid diagnoser is constructed based on the use of hybrid automaton G of Fig.3.14 as follows:

- Initial state z_1 (Fig.3.19), characterized by (Q_1, $\tilde{h}_{z_1}$, $\tilde{\dot{x}}$, GSL_{z_1}), is composed of the following G states: q_1 (G initial state), q_{21} reached from q_1 by the occurrence of fault event 'f_{PFoff}' (fault of type F_2) and q_{31} reached from q_1 due to the occurrence of fault event 'f_{lg}' (fault of type F_3). Thus, Q_1 is equal to $\{q_1,\ q_{21},\ q_{31}\}$. $\tilde{h}_{z_1}$ is equal to the nominal output of the states of Q_1. As we can see in Fig.3.14 and Fig.3.19, $\tilde{h}_{q_1}, \tilde{h}_{q_{21}}$ and $\tilde{h}_{q_{31}}$ in, respectively, q_1, q_{21} and q_{31} are equivalent and equal to 00. Thus, $\tilde{h}_{z_1}$ is equal to 00. GSL_{z_1} gathers the normal and fault labels associated to the states belonging to Q_1. Therefore, GSL_{z_1} is equal to $\{N,\ F_2,\ F_3\}$. Finally, $\tilde{\dot{x}}$ gathers $\tilde{\dot{x}}$ of all the states q_k of Q_1. Since states q_{21} and q_{31} are reached from q_1 due to the occurrence of unobservable event (a fault)(see Fig.3.14), $\tilde{\dot{x}}$ in these states are equivalent and equal to 0 (see Fig.3.19).

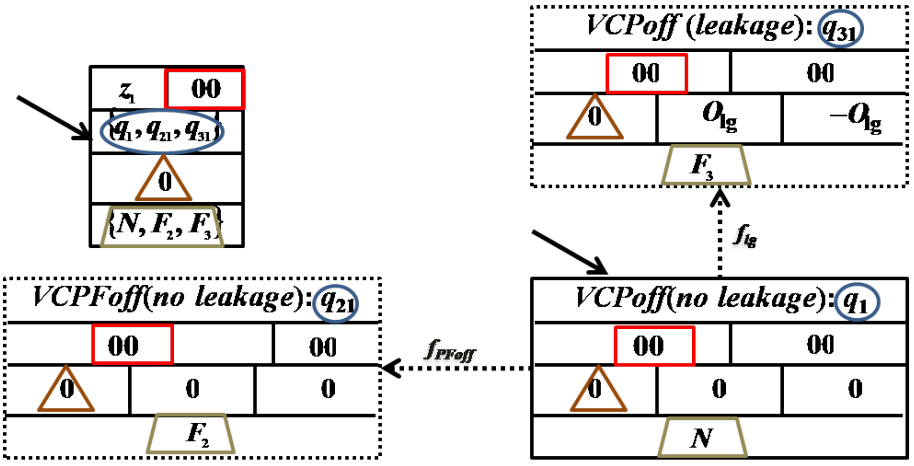

Figure 3.19: Initial state z_1 of centralized hybrid diagnoser (CHD).

- Continuous dynamic evolutions of states belonging to Q_1 will allow to generate a set of fault signatures as we can see in Fig.3.20. These fault signatures allow detecting and isolating parametric fault of type F_3 as follows. q_{31} of G (reached due to the occurrence of a fault of type F_3) generates fault signature sig_3 through the residual calculated in this state (see Fig.3.14 and Table3.2). This fault signature is used as an observable transition to isolate the occurrence of a fault of type F_3 by moving to diagnoser state z_{31} (see Fig.3.20). The other states of Q_1, $\{q_1, q_{21}\}$, generate fault signature sig_0 (the continuous dynamic evolutions in these states does not evolve). sig_0 is used as transition to z_1';
- z_1' is characterized by (Q_1', $\tilde{h}_{z_1'}$, $\tilde{\dot{x}}$, $GSL_{z_1'}$). Q_1' is composed of states of Q_1 excluding the state isolated from z_1 (q_{31}: fault of type F_3). Thus, Q_1' is equal

to $\{q_1,\ q_{21}\}$. Then, all the states of G reached from $Q_1^{'}$ due to the occurrence of unobservable events are added to $Q_1^{'}$ (see Fig.3.14). Based on Fig.3.14, f_{lg} is the only unobservable event that can occur from the states of $Q_1^{'}$. This fault event can occur from state q_1 (see Fig.3.14). f_{lg} moves the system model from state q_1 to state q_{31}. Therefore, $Q_1^{'}$ is equal to $\{q_1,\ q_{21},\ q_{31}\}$. $\tilde{h}_{z_1^{'}}$ is equal to 00. $GSL_{z_1^{'}}$ is equal to $\{N,\ F_2,\ F_3\}$. $\tilde{\tilde{x}}$ is equal to 0. Consequently, $z_1^{'}$ is equivalent to z_1. Thus, sig_0 is used as a self transition to loop in the same hybrid diagnoser state z_1.

Table 3.3: Hybrid diagnoser states table for Example 3.8.

Hybrid diagnoser state z	***Global model states*** q	$\tilde{h}_z$	$\tilde{\tilde{x}}$	***Fault* label** GSL_z
z_1	$\{q_1,\ q_{21},\ q_{31}\}$	00	0	$\{N,\ F_2,\ F_3\}$
z_2	$\{q_2,\ q_{22},\ q_{32}\}$	01	$\frac{O_P}{s_T}$	$\{N,\ F_2,\ F_3\}$
z_3	$\{q_2,\ q_{32}\}$	01	$\frac{O_P}{s_T}$	$\{N,\ F_3\}$
z_4	$\{q_3,\ q_{13},\ q_{33}\}$	11	$\frac{O_P}{s_T} - O_V$	$\{N,\ F_1,\ F_3\}$
z_5	$\{q_2,\ q_{12},\ q_{32}\}$	01	$\frac{O_P}{s_T}$	$\{N,\ F_1,\ F_3\}$
z_6	$\{q_4,\ q_{14},\ q_{24},\ q_{34}\}$	10	$-O_V$	$\{N,\ F_1,\ F_2,\ F_3\}$
z_7	$\{q_1,\ q_{11},\ q_{21},\ q_{31}\}$	00	0	$\{N,\ F_1,\ F_2,\ F_3\}$
z_8	$\{q_3,\ q_{13},\ q_{23},\ q_{33}\}$	11	$\frac{O_P}{s_T} - O_V$	$\{N,\ F_1,\ F_2,\ F_3\}$
z_9	$\{q_{11}\}$	00	0	$\{F_1\}$
z_{10}	$\{q_{12}\}$	01	$\frac{O_P}{s_T}$	$\{F_1\}$
z_{11}	$\{q_{13}\}$	11	$\frac{O_P}{s_T} - O_V$	$\{F_1\}$
z_{12}	$\{q_{14}\}$	10	$-O_V$	$\{F_1\}$
z_{13}	$\{q_{21}\}$	00	0	$\{F_2\}$
z_{14}	$\{q_{22}\}$	01	$\frac{O_P}{s_T}$	$\{F_2\}$
z_{15}	$\{q_{23}\}$	11	$\frac{O_P}{s_T} - O_V$	$\{F_2\}$
z_{16}	$\{q_{24}\}$	10	$-O_V$	$\{F_2\}$
z_{17}	$\{q_{31}\}$	00	0	$\{F_3\}$
z_{18}	$\{q_{32}\}$	01	$\frac{O_P}{s_T}$	$\{F_3\}$
z_{19}	$\{q_{33}\}$	11	$\frac{O_P}{s_T} - O_V$	$\{F_3\}$
z_{20}	$\{q_{34}\}$	10	$-O_V$	$\{F_3\}$

- The states of hybrid diagnoser reached due to the occurrence of each control command are computed. The occurrence of control command $'Start\_P'$ transits the hybrid diagnoser from z_1 to z_2 characterized by $(Q_2,\ \tilde{h}_{z_2},\ \tilde{\tilde{x}},\ GSL_{z_2})$. Q_2 is equal to all the states reached from Q_1 due to the occurrence of $'Start\_P'$. Thus, Q_2 is equal to $\{q_2,\ q_{22},\ q_{32}\}$ (see Fig.3.14). Then, all the states of G reached from Q_2 due to the occurrence of unobservable event are added to Q_2. No other unobservable events can occur from the states of Q_2 (see Fig.loop1). Therefore, Q_2 remains equal to $\{q_2, q_{22}, q_{32}\}$. $\tilde{h}_{z_2}$ is equal to the nominal output of the states of Q_2. Consequently is equal to 01 (the pump is considered to

be started), GSL_{z_2} is equal to the set of fault labels of the states of Q_2. Thus, GSL_{z_2} is equal to $\{N,\ F_2,\ F_3\}$ while $\tilde{\dot{x}}$ is equal to the nominal continuous evolution of x in the states of Q_2. Thus, $\tilde{\dot{x}}$ is equal to $\frac{O_P}{s_T}$ (see Fig.3.14).

- Continuous dynamic evolutions of the states belonging to Q_2 will allow to generate a set of fault signatures as we can see in Fig.3.20. These fault signatures allow converting unobservable transitions into observable ones. Consequently, they are used in order to detect and isolate discrete fault F_2 and parametric faults F_3 as follows. q_{22} of G (reached from the faulty state q_{31} due to controlled event $'Start\_P'$) generates fault signature sig_2. This fault signature is used as an observable transition to isolate the occurrence of a fault of type F_2 by moving the diagnoser to state z_{22}. q_{32} of G (reached due to the occurrence of fault of type F_3) generates fault signature sig_3. This fault signature is used as an observable transition to isolate the occurrence of a fault of type F_3 by moving the diagnoser to state z_{32}. In normal operating conditions, q_2 generates fault signature sig_0. sig_0 is used as an observable transition to move CHD to state z_3.

- z_3 is characterized by $(Q_3,\ \tilde{h}_{z_3},\ \tilde{\dot{x}},\ GSL_{z_3})$. Q_3 is composed of states of Q_2 excluding the states isolated from z_2 (q_{22}: fault of type F_2) and q_{32}: fault of type F_3)). Thus, Q_3 is equal to $\{q_2\}$. Then, all the states of G reached from Q_3 due to the occurrence of an unobservable event are added to Q_3. The only unobservable event that can occur at q_2 is fault event f_{lg}. Therefore, Q_3 is equal to $\{q_2,\ q_{32}\}$. $\tilde{h}_{q_2}$ and $\tilde{h}_{q_{32}}$for, respectively, states q_2 and q_{32} is equal to 01. Consequently, $\tilde{h}_{z_3}$ is equal to 01. Similarly, GSL_{z_3} is equal to $\{N,\ F_3\}$ and $\tilde{\dot{x}}$ is equal to $\frac{O_P}{s_T}$ (see Fig.3.14).

  Likewise, the other hybrid diagnoser states can be constructed as for z_0, z_1, z_2 and z_3. The complete CHD is depected in Fig.3.21

Table 3.4: Hybrid diagnoser transitions table for Example 3.8.

CHD transition	***Curent state z***	***Future state z^+***		***CHD transition***	***Curent state z***	***Future state z^+***
sig_0	z_1	z_1		$Stop\_P$	z_1	z_1
CV	z_1	z_1		sig_3	z_1	z_{17}
$Start\_P$	z_1	z_2		OV	z_1	z_6
sig_3	z_2	z_{18}		sig_2	z_2	z_{14}
sig_0	z_2	z_3		sig_0	z_3	z_3
$Start\_P$	z_3	z_3		CV	z_3	z_3
sig_3	z_3	z_{18}		$Stop\_P$	z_3	z_1
OV	z_3	z_4		sig_0	z_4	z_4
OV	z_4	z_4		$Start\_P$	z_4	z_4
sig_3	z_4	z_{19}		$Stop\_P$	z_4	z_6
CV	z_4	z_5		sig_0	z_5	z_3

sig_3 ***CHD transition***	z_5 ***Curent state*** z	z_{18} ***Future state*** z^+		sig_1 ***CHD transition***	z_5 ***Curent state*** z	z_{10} ***Future state*** z^+
sig_0	z_6	z_6		$Stop\_P$	z_6	z_6
OV	z_6	z_6		sig_3	z_6	z_{20}
CV	z_6	z_7		$Start\_P$	z_6	z_8
sig_0	z_7	z_1		sig_1	z_7	z_9
sig_3	z_7	z_{17}		sig_0	z_8	z_4
sig_2	z_8	z_{15}		sig_3	z_8	z_{19}
sig_1	z_9	z_9		$Stop\_P$	z_9	z_9
CV	z_9	z_9		$Start\_P$	z_9	z_{10}
sig_1	z_{10}	z_{10}		$Start\_P$	z_{10}	z_{10}
CV	z_{10}	z_{10}		$Stop\_P$	z_{10}	z_9
OV	z_{10}	z_{11}		sig_0	z_{11}	z_{11}
OV	z_{11}	z_{11}		$Start\_P$	z_{11}	z_1
CV	z_{11}	z_{10}		$Stop\_P$	z_{11}	z_{12}
sig_0	z_{12}	z_{12}		OV	z_{12}	z_{12}
$Stop\_P$	z_{12}	z_{12}		$Start\_P$	z_{12}	z_{11}
CV	z_{12}	z_9		OV	z_9	z_{12}
sig_0	z_{13}	z_{13}		CV	z_{13}	z_{13}
$Stop\_P$	z_{13}	z_{13}		$Start\_P$	z_{13}	z_{14}
sig_2	z_{14}	z_{14}		CV	z_{14}	z_{14}
$Start\_P$	z_{14}	z_{14}		$Stop\_P$	z_{14}	z_{13}
OV	z_{14}	z_{15}		sig_2	z_{15}	z_{15}
$Start\_P$	z_{15}	z_{15}		OV	z_{15}	z_{15}
CV	z_{15}	z_{14}		$Stop\_P$	z_{15}	z_{16}
sig_0	z_{16}	z_{16}		$Stop\_P$	z_{16}	z_{16}
OV	z_{16}	z_{16}		CV	z_{16}	z_{13}
OV	z_{13}	z_{16}		sig_3	z_{17}	z_{17}
$Stop\_P$	z_{17}	z_{17}		CV	z_{17}	z_{17}
$Start\_P$	z_{17}	z_{18}		sig_3	z_{18}	z_{18}
$Start\_P$	z_{18}	z_{18}		CV	z_{18}	z_{18}
$Stop\_P$	z_{18}	z_{17}		OV	z_{18}	z_{19}
sig_3	z_{19}	z_{19}		OV	z_{19}	z_{19}
$Start\_P$	z_{19}	z_{19}		CV	z_{19}	z_{18}
$Stop\_P$	z_{19}	z_{20}		sig_3	z_{20}	z_{20}
OV	z_{20}	z_{20}		$Stop\_P$	z_{20}	z_{20}
$Start\_P$	z_{20}	z_{19}		CV	z_{20}	z_{17}
OV	z_{17}	z_{20}				

3.3.3 Hybrid diagnosability notion

Discrete faults are structural faults leading to new operating modes. Parametric faults can be structural faults corresponding to new faulty modes with their own

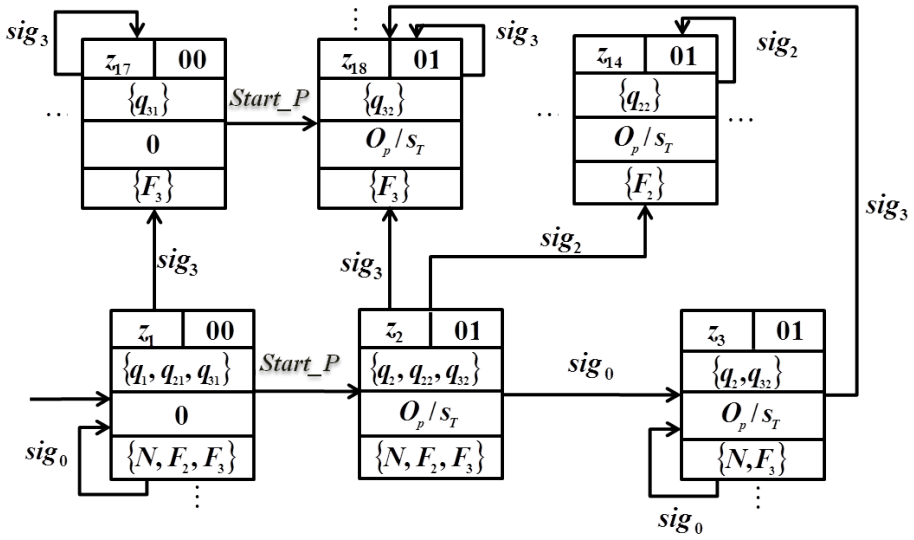

Figure 3.20: Part of centralize hybrid diagnoser (CHD).

continuous dynamics and non-structural faults characterized as disturbances on the operating mode of HDS. In all cases, parametric and discrete faults are defined in the system hybrid model G as states in the associated automaton. Therefore, the parametric and discrete faults diagnosability notion is defined as the ability to distinguish each of the faulty states from the normal ones (mode tracking). This distinguishability is based on the observable discrete events Σ_o and continuous measurements X. The measurements are used to generate residuals in each state. Then, these residuals are abstracted in order to obtain so-called fault signature events. These fault signature events may turn transitions with unobservable events into observable ones. The distinguishability of two modes depends on the fact that two faults of two different types must produce different effect. These effects are defined by a set of controlled mode change events (controllable events) interleaved with the fault signature events. These event sequences are called hybrid traces or hybrid event sequences and define the language generated by the occurrence of faults of type $F_w, w \in \{1, \cdots, d\}$. A hybrid trace is composed of fault signatures interleaved by control command events. Each one of the latter must be preceded and followed by a fault signature. Therefore, the notion of diagnosability, Gomez et al. (2010) requires that two faults belonging to two different types with respect to an initial discrete mode at the time of fault occurrence must produce different observable languages or hybrid event sequences. The hybrid diagnosability notion consists in determining whether the system model is rich enough in information in order to allow the hybrid diagnoser to infer the occurrence of predefined faults within a finite number of observable events and finite time of measurement deviations in one discrete mode.

Diagnosability notion defined for discrete event systems (SED), Sampath et al. (1996), Sampath (1995), is developed in order to integrate the parametric fault and the hybrid aspect of the considered system. Our aim is to take benefit of the continuous dynamic evolutions in order to get rid of the existence of indeterminate

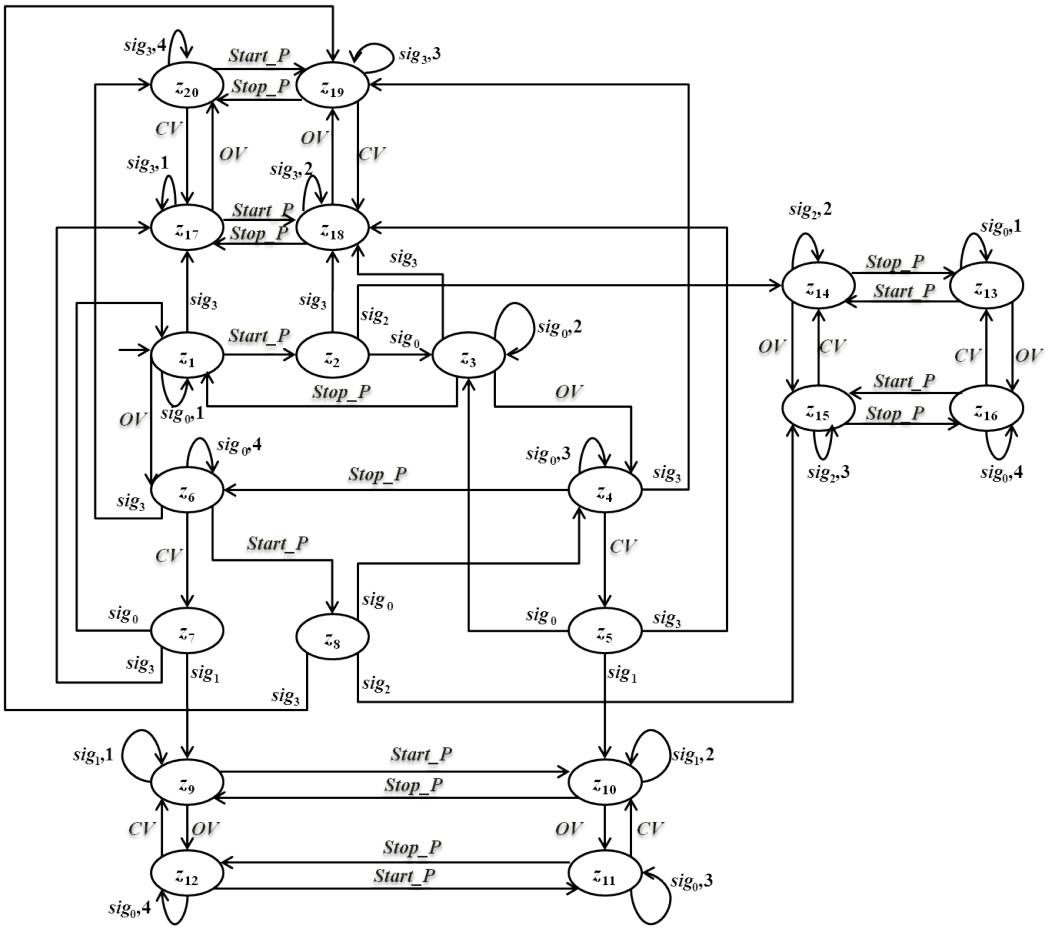

1	*Stop_P, CV*
2	*Start_P, CV*
3	*Start_P, OV*
4	*Stop_P, OV*

Figure 3.21: Centralize hybrid diagnoser (CHD) model.

cycles. Thus, an extended notion of diagnosabilty of discrete faults for HDS is defined as follows:

Definition 3.5 *HDS is said to be diagnosable with respect to projection function P and to fault labels $\{F_1, F_2, \cdots, F_d\}$ if the following holds:*
$(\exists v \in \aleph)(\forall w \in \{1, \cdots, d\})(\forall s \in \psi_{\Sigma_{F_w}})(\forall t \in htrace(HDS)/s)(|t| \geq v) \Rightarrow Diag$
where the hybrid diagnosability condition Diag is:

$$\forall y \in P^{-1}[P(st)] \Rightarrow \Sigma_{F_w} \in y \tag{3.28}$$

where,
$htrace(HDS) \subseteq (\Sigma \cup Sig)^*$ denotes the set of all the hybrid traces (hybrid event sequences) generated by HDS;
$htrace(HDS)/s = \{t \in htrace(HDS) | st \in htrace(HDS)\}$: denotes the set of hybrid event sequences after s. $|t|$ is the number of events in t;
$\psi_{\Sigma_{F_w}}$: is the set of all hybrid event sequences of HDS that end with a event of Σ_{F_w}. Σ_{F_w} is a set of fault events of type F_w;
$P^{-1}[P(st)]$: corresponds to all the hybrid event sequences which have an observable projection $P(st)$, i.e. an observable hybrid event sequences similar to the one of st;

The above definition means that the HDS, generating $htrace(HDS)$, is diagnosable with respect to a set of faults of type F_w, $w \in \{1, \cdots, d\}$, if and only if all the hybrid traces containing a fault of type F_w have a finite observable part different from those of all the other hybrid event sequences generated by the system.

Generally, the interest of this definition is the use of continuous information (the set of faults signature events) in order to increase the diagnosability of discrete faults and diagnose the parametric faults tanks to the use of fault signature events generated due to the occurrence of parametric fault.

Each hybrid state of the system is characterized by a different evolution of continuous variables and each transition is enabled by certain number of faults signature events associated to these variables. Consequently, in the case of existence of indeterminate cycle in a hybrid diagnoser, the evolution of continuous dynamics of these variables will entail the occurrence of fault signature events associated to certain states in this cycle. Thus, the system will get out of this indeterminate cycle within a finite number of observable events.

Example 3.9 ***Comparison of the diagnosability between continuous, discrete event and hybrid dynamic systems using the one tank system example***

For the one tank system example, the hybrid diagnoser allows diagnosing the set of considered faults (Table 3.1) that can occur in the system (see Fig.3.21 and Table 3.3). In order to show the utility of the use of both continuous and discrete dynamics in the hybrid diagnoser, the continuous, the discrete event and the hybrid diagnosers are compared in this example using the controlled event sequence $'Start\_P'$ $'Stop\_P'$ (Fig.3.22).

- The continuous diagnoser uses a set of residuals in order to achieve the fault diagnosis. Since a continuous systems is considered to include one discrete mode,

the residuals are calculated for this mode. Therefore, they are sensitive to the faults that occur in this discrete mode. Consequently, if the system changes its discrete mode, these residuals become uncorrected for the fault diagnosis in this new discrete mode. For the leakage fault, residual r, calculated by (3.20) in Example 3.4, is sensitive to this parametric fault according to the tank system discrete mode. If the the tank system is in $(VCPoff(no\ leakage))$, r is equal to $-(0-h_q^1)\frac{s_V\sqrt{2g}}{2s_T\sqrt{x_0}}x+(0-h_q^2)\frac{O_P}{s_T}+(0+\frac{s_{lg}\sqrt{2g}}{2s_T\sqrt{x_0}}x$ $(\tilde{h}_q^1=\tilde{h}_q^2=0)$. If the tank system changes its discrete mode due to controller command event '$Start\_P$', then r is equal to $-(0-h_q^1)\frac{s_V\sqrt{2g}}{2s_T\sqrt{x_0}}x+(1-h_q^2)\frac{O_P}{s_T}+(0+\frac{s_{lg}\sqrt{2g}}{2s_T\sqrt{x_0}}x$ $(\tilde{h}_q^1=0$ and $\tilde{h}_q^2=0)$. Therefore, r must take into account the discrete mode in order to be sensitive to leakage fault according to the new discrete mode.

- The discrete diagnoser, shown in the right side of Fig.3.22, has the indeterminate cycle defined by $(Start\_P\ Stop\_P)^*$. When the discrete diagnoser observes $'Start\_P'$, it transits from uncertain state dz_1 (dz_1 denotes the initial discrete diagnoser state) with $GLS_{dz_1}=\{N,\ F_2\}$ to uncertain state dz_2 with $GLS_{dz_2}=\{N,\ F_2\}$. The latter moves the hybrid diagnoser from z_1 into z_{17} with $(GLS_{z_{17}}=F_3)$. Then, the occurrence of $'Stop\_P'$ moves the discrete diagnoser from dz_2 into dz_1. Therefore, the discrete diagnoser may remain indefinitely in this cycle without being able to decide with certainty the occurrence or not of a fault of type F_2. Moreover, it cannot diagnose the parametric fault 'leakage', indicated by fault label F_3, since this fault is related to the system continuous dynamics.

- Form initial state z_1, the hybrid diagnoser shown in the left side of Fig.3.22, diagnoses with certainty the occurrence of a fault of type F_3 due to the observation of the fault signature event sig_3. The latter moves the hybrid diagnoser from z_1 into z_{17} with $(GLS_{z_{17}}=F_3)$. sig_3 is generated thanks to the abstraction of residual r calculated based on the continuous dynamics in z_1. The hybrid diagnoser moves from z_1 to z_2 by the occurrence of $'Start\_P'$. In z_2, the hybrid diagnoser isolates with certainty the occurrence of a fault of types F_2 or F_3 thanks to the observation of, respectively, sig_2 or sig_3. In addition, the hybrid diagnoser can infer the absence of a fault of type F_2 tanks to the observation of fault signature event sig_0 (see Fig.3.22).

We can conclude that, the hybrid diagnoser is able to diagnose with certainty the occurrence of the set of faults of Table 3.1 tanks to the use of both the continuous and discrete dynamics.

3.3.4 Parametric faults Identification

After isolating a parametric fault, a phase of identification is necessary to define its amplitude, Brito Palma et al. (2005). When the parametric fault is detected, the system is assumed to be in faulty state and it is modeled by a linear differential equation (L.D.E) (3.8) with faulty matrices (A_i^{mj}, A_{ci}^m and B_i^j, $j\in\{1,\cdots,L\}$, $i\in\{1,\cdots,n\}$). The parameter identification is done through two steps. In the first

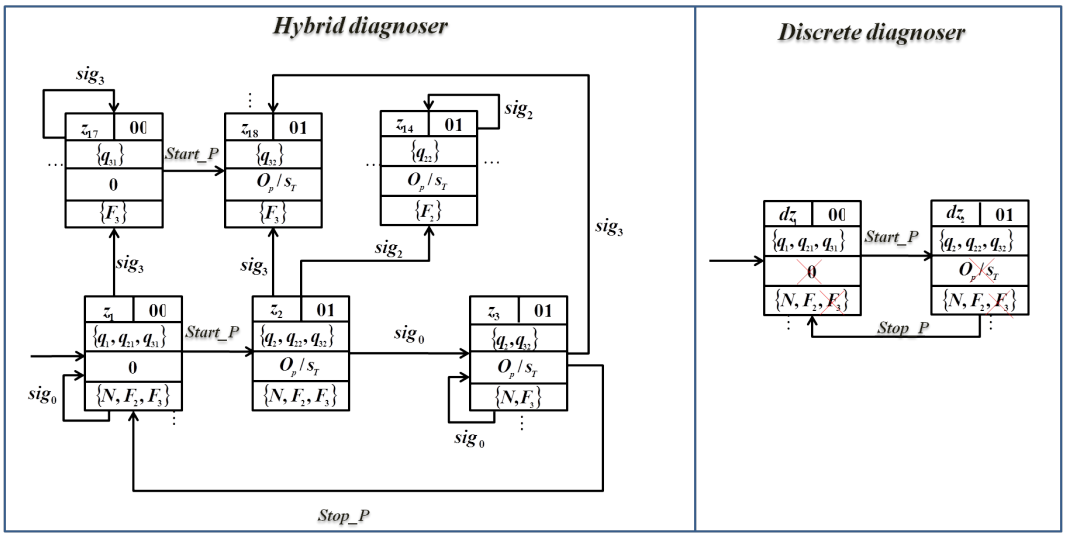

Figure 3.22: Comparison of discrete and hybrid diagnosers in response to the observation of controller command squence '$Start\_P$"$Stop\_P$'.

step, the L.D.E are exploited in order to determine the sensitive residuals to this fault. Then, these residuals are analyzed in order to identify the fault parameters.

Example 3.10 ***Parametric faults Identification for one tank system example***

In the one tank system example (Fig.3.2), one parametric fault is considered (leakage in the tank: fault of type F_3). After the detection of the occurrence of this fault, the real value of leakage section s_{lg} has to be determined. For this example, the system is modeled through one continuous variable x (the water level) and one residual r is generated by the system. By analyzing the L.D.E of this system (3.15), the relationship between r and L.D.E in the case of occurrence of a parametric fault of type F_3 is defined as follows:

$r = -(\tilde{h}_q^1 - h_q^1)\frac{s_V\sqrt{2g}}{2s_T\sqrt{x_0}}x + (\tilde{h}_q^2 - h_q^2)\frac{O_P}{s_T} - (0 - \frac{s_{lg}\sqrt{2g}}{2s_T\sqrt{x_0}}x)$

Since only simple fault scenarios are considered and in the case of the occurrence of a fault of type F_3, i.e., leakage in the tank $\tilde{h}_q^1$ and $\tilde{h}_q^2$ are equal, respectively, to h_q^1 and h_q^2. Therefore, residual r in this case is equal to:

$$\begin{cases} r = & 0 & + & 0 & - (0 - \frac{s_{lg}\sqrt{2g}}{2s_T\sqrt{x_0}}x) \\ r = & \frac{s_{lg}\sqrt{2g}}{2s_T\sqrt{x_0}}x & & & \end{cases} \tag{3.29}$$

Based on (3.29), s_{lg} is calculated as follows:

$$s_{lg} = \frac{2s_T\sqrt{x_0}}{x\sqrt{2g}}r \tag{3.30}$$

3.4 Summary

As discussed in Chapter 2, many HDS diagnosis approaches, diagnose only parametric or only discrete faults. While, the approaches that diagnose both parametric and discrete faults do not scale well to large scale systems. In our approach, we take benefit of the modularity of the system in order to facilitate the construction of the system global model. The latter is decomposed into a set of interacting hybrid components. The local hybrid model is built for each hybrid component. The system global model is obtained by synchronizing the set of local hybrid models. Then, the hybrid diagnoser is constructed based on the system global model. The hybrid diagnoser exploits the continuous and discrete dynamics as well as the interactions between them in order to enhance the diagnosability of discrete faults as well as parametric faults. Indeed, the hybrid diagnoser exploits the system continuous dynamic evolution in each discrete mode in order to generate a new kind of observable events called fault signatures. The latter allow converting unobservable transitions into observable ones. Thus, fault signatures are used in order to enhance the diagnosis capacity of parametric and discrete faults.

The number of the system global states, gs, increases exponentially with respect to the number, $ls^j,\ j \in 1, \cdots, L$, of the local states of system hybrid components since gs is equal to $ls^1 \cdots \times ls^j \times \cdots \times ls^L$. Therefore, the use of the global model in order to construct the diagnoser can be very hard in the case of large scale systems. with multiple discrete states In order to overcome this problem, a hybrid decentralized fault diagnosis structure for large scale HDS are proposed in Chapter 4.

Chapter 4

Decentralized hybrid diagnosis and co-diagnosability

Contents

4.1 Introduction

Fault diagnosis approaches of the literature do not scale to HDS with a large number of discrete modes because they achieve fault diagnosis using one centralized diagnosis module, i.e., diagnoser. The latter is built using a global model of the system. Centralized diagnosis approaches entail two problems:

1. the weak robustness in the sense that, when the global diagnoser fails, this may bring down the entire diagnosis task;
2. the system global model can be too huge to be physically constructed. As an example, the global model of telecommunication networks, as the one studied in Pencolé and Cordier (2005), has a size of the order of $2^{10} \times 4^{300}$. Therefore, constructing a global model for this type of large scale systems is physically unfeasible.

Consequently, in this chapter, the proposed approach of Chapter 3, Louajri et al. (2013), Louajri and Sayed-Mouchaweh (2014d), is developed in order to achieve the diagnosis of parametric and discrete faults in decentralized manner using several local hybrid diagnosers, Louajri and Sayed-Mouchaweh (2014b), based on the following steps (Fig.4.1):

- Decomposition of the system into a set of L interacting hybrid components, $HC_j,\ j \in \{1, \cdots, L\}$. As shown in subsection 3.2.4 of Chapter 3, each Hybrid component HC_j is composed of one discrete component Dc_j with the set of $g,\ g \leq n$, continuous components (Ccs) whose continuous dynamic behavior is changed according to Dc_j discrete states;
- Construction of local hybrid models, $G^1, \cdots, G^L$, for the system hybrid components $HC_1, \cdots, HC_L$. The details of this step can be found in Chapter 3, subsection 3.2.4;
- Construction of local hybrid diagnoser $D_j,\ j \in \{1, \cdots, L\}$, based on local model $G^j,\ j \in \{1, \cdots, L\}$, of each hybrid component HC_j. The objective of this local hybrid diagnoser is to detect and isolate the occurrence of parametric and discrete faults that can occur in HC_j.
- Construction of a coordinator in order to merge the different local diagnosers' decisions and to issue one global diagnosis decision equivalent to the one provided by the centralized diagnoser. This decisions merging is based on the use of rules allowing overcoming the decision ambiguity that can be arisen due to the partial observability of the system by each local hybrid diagnoser.

Two major differences can be stated between the centralized diagnosis approach, studied in Chapter 3, and the decentralized diagnosis approach:

1. the fault diagnosis is achieved by a set of local diagnosers, and not by one global diagnoser. Therefore, the diagnosis robustness is enhanced in the sense that when one local diagnoser is failed, the other local diagnosers remain operational and continue to assure their fault diagnosis.
2. the local diagnosers are constructed based on the use of local models. The complexity for constructing the local diagnosers is polynomial in the size of local models. Therefore, no need to use a global model to achieve the fault diagnosis of the system. This helps to overcome the problem of handling a huge number of discrete modes in the case of large scale HDS.

Chapter 4 is organized as follows. Firstly, the different steps of the decentralized hybrid diagnosis approach are presented. Then, the procedure to build the local hybrid diagnoser for each hybrid component of the system is detailed. Then, the steps to merge the local diagnosis decisions through a coordinator are discussed. Finally, the comparison between centralized and decentralized diagnosis structure is presented. The example of one tank level water control system is used throughout the chapter in order to illustrate the proposed approach and to compare it with the centralized approach detailed in Chapter 3.

4.2 Local hybrid diagnoser

Local hybrid diagnoser $D_j,\ j \in \{1, \cdots, L\}$, is built based on local model G^j of each hybrid component HC_j. The objective of D_j is to detect and isolate the occurrence

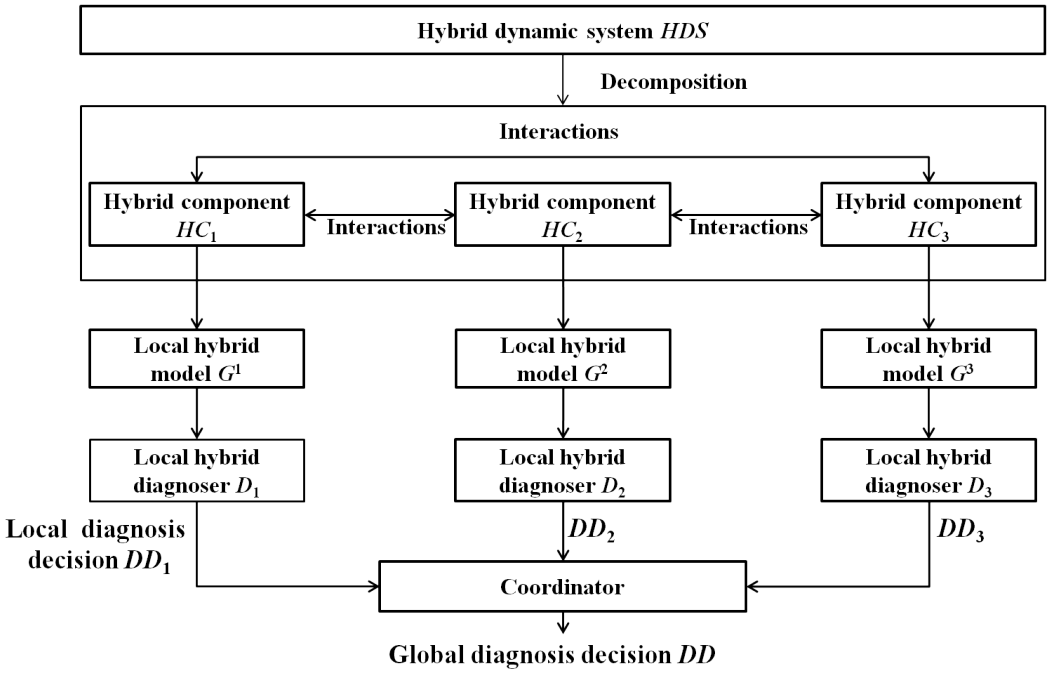

Figure 4.1: Decentralized hybrid diagnosis structure for a HDS composed of 3 interacting HCs.

of parametric and discrete faults that can occur in HC_j. D_j observes in each local discrete state q^j a part ($\dot{X}^j$ and $\tilde{\dot{X}}^j$) of the system real and nominal continuous dynamic evolutions $\dot{X}$ and $\tilde{\dot{X}}$. Therefore, D_j states are defined based on q^j, $\dot{X}^j$ and $\tilde{\dot{X}}^j$. In the next subsections,the details required to construct D_j are presented.

4.2.1 Local fault signature construction

Let us consider the set of residuals $r_i,\ i \in \{1, \cdots, n\}$, generated by the global system, G, in each global discrete state q, as developed in subsection 3.2.3 of Chapter 3:

$$r_i = \tilde{\dot{x}}_i - \dot{x}_i$$
$$r_i = \sum_{j=1}^{L} r_i^j + r_{ci}$$

where,

$$r_i^j = \sum_{m=1}^{n} \left(\tilde{h}_q^j \tilde{A}_i^{mj} - h_q^j A_i^{mj} \right) x_m + \left(\tilde{h}_q^j \tilde{B}_i^j - h_q^j B_i^j \right) u$$
$$r_{ci} = \sum_{m=1}^{n} \left(\tilde{A}_{ci}^m - A_{ci}^m \right) x_m$$

Based on (3.27), the set of residuals defined in global state q belonging to the diagnoser state z are abstracted into a global fault signature as follows (see subsection 3.3.1 of Chapter 3):

$sig_z = \left(r_1^{CS(r_1)}, DS(r_1)\right) \& \cdots \& \left(r_i^{CS(r_i)}, DS(r_i)\right) \& \cdots \& \left(r_n^{CS(r_n)}, DS(r_n)\right)$
Based on (3.9) and (3.13) (see subsection 3.2.2 of Chapter 3 for more details), the normal and global dynamic evolutions in $q = (q^1 \cdots q^j \cdots q^L)$ are defined as follows:
$\dot{x}_i = \sum_{j=1}^{L} \dot{x}_i^j + \dot{x}_{ci}$
$\tilde{\dot{x}}_i = \sum_{j=1}^{L} \tilde{\dot{x}}_i^j + \tilde{\dot{x}}_{ci}$
where,
$\dot{x}_i^j = \sum_{m=1}^{n} h_q^j A_i^{mj} x_m + h_q^j B_i^j u$
$\dot{x}_{ci} = \sum_{m=1}^{n} A_{ci}^m x_m$
$\tilde{\dot{x}}_i^j = \sum_{m=1}^{n} \tilde{h}_q^j \tilde{A}_i^{mj} x_m + \tilde{h}_q^j \tilde{B}_i^j u$
$\tilde{\dot{x}}_{ci} = \sum_{m=1}^{n} \tilde{A}_{ci}^m x_m$

As defined in subsection 3.2.4 of Chapter 3, each hybrid component HC_j is composed of one discrete component Dc_j and the set of $\{Cc_g\}$, $g \leq n$, continuous components (Ccs) whose continuous dynamic behavior is changed according to Dc_j discrete states. Therefore, the set of continuous variables associated to the set of Ccs belonging to HC_j is equal to:
$X^j = [x_{g_1} \cdots x_{g_g}]^T$
The set of parts of real continuous dynamic evolutions that change according to the discrete state q^j of Dc_j is described as follows:
$\dot{X}^j = [\dot{x}_{g_1}^j \cdots \dot{x}_{g_g}^j]^T$
where, $\dot{x}_i^j$, $i \in \{g_1, \cdots, g_g\}$, describes the part of $\dot{x}_i$ that changes according to the Dc_j discrete state (q^j).
The set of real parts of continuous dynamic evolutions of X^j, related to Dc_j, that does not change according to the discrete state of the system is defined as follows:
$\dot{X}_c^j = [\dot{x}_{cg_1} \cdots \dot{x}_{cg_g}]^T$
Likewise, the set of parts of nominal continuous dynamic evolutions that change according to discrete state q^j of Dc_j is described as follows:
$\tilde{\dot{X}}^j = [\tilde{\dot{x}}_{g_1}^j \cdots \tilde{\dot{x}}_{g_g}^j]^T$
where, $\tilde{\dot{x}}_i^j$, $i \in \{g_1, \cdots, g_g\}$, describes the part of $\tilde{\dot{x}}_i$ that changes according to the nominal Dc_j discrete state.
The set of nominal parts of continuous dynamic evolutions that does not change according to the discrete state of the system:
$\tilde{\dot{X}}_c^j = [\tilde{\dot{x}}_{cg_1} \cdots \tilde{\dot{x}}_{cg_g}]^T$

Therefore, the set of parts $r^j + r_c^j$ of residuals r associated to HC_j is defined as follows:

$$r = \left(\tilde{\dot{X}}^j + \tilde{\dot{X}}_c^j\right) - \left(\dot{X}^j + \dot{X}_c^j\right)$$

$$
\begin{aligned}
&= \left(\tilde{\dot{X}}^j - \dot{X}^j\right) + \left(\tilde{\dot{X}}_c^j - \dot{X}_c^j\right) \\
&= \left(\begin{bmatrix} \tilde{\dot{x}}_{g_1}^j \\ \vdots \\ \tilde{\dot{x}}_i^j \\ \vdots \\ \tilde{\dot{x}}_{g_g}^j \end{bmatrix} - \begin{bmatrix} \dot{x}_{g_1}^j \\ \vdots \\ \dot{x}_i^j \\ \vdots \\ \dot{x}_{g_g}^j \end{bmatrix}\right) + \left(\begin{bmatrix} \tilde{\dot{x}}_{cg_1} \\ \vdots \\ \tilde{\dot{x}}_{ci} \\ \vdots \\ \tilde{\dot{x}}_{cg_g} \end{bmatrix} - \begin{bmatrix} \dot{x}_{cg_1} \\ \vdots \\ \dot{x}_{ci} \\ \vdots \\ \dot{x}_{cg_g} \end{bmatrix}\right) \\
&= \begin{bmatrix} r_{g_1}^j \\ \vdots \\ r_i^j \\ \vdots \\ r_{g_g}^j \end{bmatrix} + \begin{bmatrix} r_{cg_1} \\ \vdots \\ r_{ci} \\ \vdots \\ r_{cg_g} \end{bmatrix} \\
r &= r^j + r_c^j \\
&= r^j + r_c^j
\end{aligned}
$$

Let M_j be the masque function defining the continuous dynamic evolutions impacted by discrete state q^j of HC_j. $M_j(r)$ is equal to the part of residual r related to the discrete and continuous dynamics defined by the HC_j components. Therefore, for each hybrid component HC_j, $M_j(r)$ is defined as follows (see Fig.4.2):

$$M_j(r) = r^j + r_c^j \tag{4.1}$$

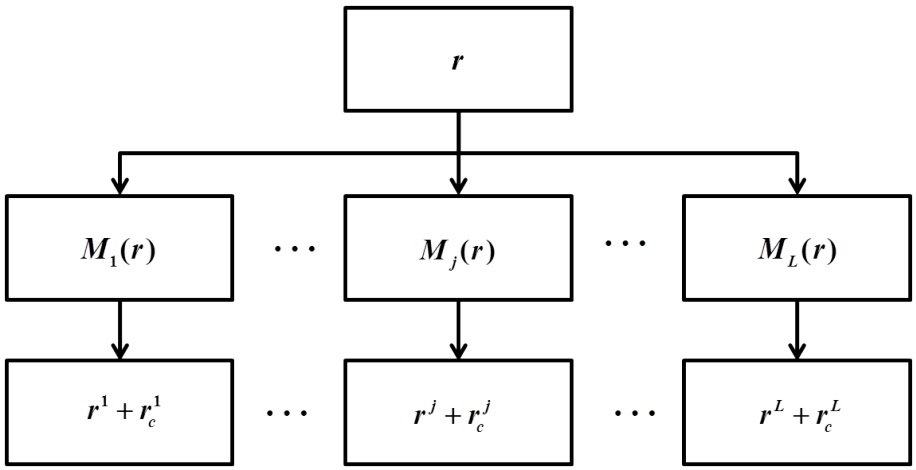

Figure 4.2: Local residuals related to HC_j, $j \in \{1, \cdots, L\}$.

The local fault signatures are obtained by abstracting the different parts of residuals defined in the local hybrid states of G^j. This abstraction is achieved by continuous and discrete symbols generation as the one defined for the global residual r (see subsection 3.3.1 of Chapter 3 for more details). By analogy to the global fault signature at global diagnoser state z defined by (3.27), local fault signature sig_{z^j} at local hybrid state z^j is the combination of continuous and discrete symbols of the

different g residual parts as follows:
$M_j(sig_z) = sig_{z^j} = \left(M_j(r_1)^{CS(M_j(r_1))}, DS(M_j(r_1))\right) \& \cdots \& \left(M_j(r_i)^{CS(M_j(r_i))}, DS(M_j(r_i))\right) \& \cdots \& \left(M_j(r_n)^{CS(M_j(r_n))}, DS(M_j(r_n))\right)$
If $r_k,\ k \notin \{g_1, \cdots, gg\} \Rightarrow M_j(r_k) = \Phi$.

Based on (4.1), sig_{z^j} is written as follows:

$$sig_{z^j} = \left((r^j_{g_1} + r_{cg_1})^{CS(r^j_{g_1}+r_{cg_1})}, DS(r^j_{g_1} + r_{cg_1})\right) \& \cdots \& \left((r^j_i + r_{ci})^{CS(r^j_i+r_{ci})}, DS(r^j_i + r_{ci})\right) \& \cdots \& \left((r^j_{g_g} + r_{cg_g})^{CS(r^j_{g_g}+r_{cg_g})}, DS(r^j_{g_g} + r_{cg_g})\right) \tag{4.2}$$

Local continuous symbols $CS(r^j_i + r_{ci}) \in \{0, -, +\}$ represent the qualitative abstraction of the part $(r^j_i + r_{ci})$ of residual r_i observed by HC_j into stable/ decreasing/ increasing ones:

- $0 : r^j_i(t)$ and $r^j_{ci}(t)$ belongs to the nominal interval;
- $- : r^j_i(t)$ or $r^j_{ci}(t)$ is below the nominal interval;
- $+ : r^j_i(t)$ or $r^j_{ci}(t)$ is above the nominal interval;
- Φ: if r_i is defined for a continuous component Cc_iwhich does not belong to HC_j ($Cc_i \notin HC_j$).

Local discrete symbols $DS(r^j_i + r_{ci}) \in \{PC^j_i, NC^j_i, UC^j_i\}$ represent the abstraction of each residual part $(r^j_i + r_{ci})$ in order to distinguish between parametric and discrete faults as follows:

- $PC^j_i = +Val$: denotes an abrupt positive change in r^j_i due to a discrete fault caused by Dc_j. $+Val$ is equal to the absolute value of $A^{mj}_i x_m$ or $B^j_i u$ associated to h^j_q;
- $NC^j_i = -Val$: denotes an abrupt negative change in part of residual r^j_i due to a discrete fault caused by Dc_j;
- UC^j_i: denotes that there is no observed abrupt change in r^j_i;
- Φ:if $Cc_i \notin HC_j$.

Example 4.1 ***Local fault signatures for the one tank system example***

As shown in Example 3.5 of Chapter 3, the one tank system is decomposed into two hybrid components:

- HC_1 composed of valve V (Dc_1) and the tank (Cc);
- HC_2 composed of pump P (Dc_2) and the tank (Cc).

The residual r of this system is defined, as we can see in Example 3.4, as follows:

$$\begin{cases} r = \tilde{\dot{x}} - \dot{x} \\ \quad = \left(-\tilde{h}_q^1 \frac{s_V\sqrt{2g}}{2s_T\sqrt{x_0}}x + \tilde{h}_q^2 \frac{O_P}{s_T}\right) - \left(-\frac{h_q^1 s_V\sqrt{2g}}{2s_T\sqrt{x_0}}x + h_q^2\frac{O_P}{s_T} - \frac{s_{lg}\sqrt{2g}}{2s_T\sqrt{x_0}}x\right) \\ \quad = -(\tilde{h}_q^1 - h_q^1)\frac{s_V\sqrt{2g}}{2s_T\sqrt{x_0}}x + (\tilde{h}_q^2 - h_q^2)\frac{O_P}{s_T} + (0 + \frac{s_{lg}\sqrt{2g}}{2s_T\sqrt{x_0}}x) \\ \quad = r^1 + r^2 + r_c \end{cases}$$

where,

$$\begin{aligned} r^1 &= -(\tilde{h}_q^1 - h_q^1)\tfrac{s_V\sqrt{2g}}{2s_T\sqrt{x_0}}x = (\tilde{h}_q^1 - h_q^1)O_V \\ r^2 &= (\tilde{h}_q^2 - h_q^2)\tfrac{O_P}{s_T} \\ r_c &= (0 + \tfrac{s_{lg}\sqrt{2g}}{2s_T\sqrt{x_0}}x) = (0 + O_{lg}) \end{aligned} \tag{4.3}$$

where, O_V is the valve flow rate, O_{lg} is the leakage flow rate and O_P is the pump flow rate.
Since HC_1 is composed of valve V (Dc_1) and the tank (Cc), the masque function $M_1(r)$ is defined as follows:
$M_1(r) = r^1 + r_c$
Since HC_2 is composed of pump P (Dc_2) and the tank (Cc), the masque function $M_2(r)$ is defined as follows:
$M_2(r) = r^2 + r_c$
Based on Fig.3.10 of Example 3.5, the local fault signatures for HC_1 can be calculated as follows:

- In normal operating mode of hybrid component HC_1 (q_1^1 and q_2^1 of Fig.3.10), the parts (r^1 and r_c) of residual r defined in these states (q_1^1 and q_2^1) are equal to zero (because $\tilde{h}_q^1 = h_q^1$ and $s_{lg} = 0$). By abstracting the value of $(r^1 + r_c)$ in these states, HC_1 generates the following normal local fault signature:
  $sig_0^1 = \left((r^1 + r_c)^0, UC^1\right)$

- Faulty local state ($q_4^1 : VSO(no\ leakage)$) corresponds to the occurrence of discrete fault 'valve stuck open'. Therefore, based on (4.3), the part r^1 of residual r defined in this state is equal to O_V (because $\tilde{h}_q^1 = 0$ while $h_q^1 = 1$) and r_c is equal to zero (because $s_{lg} = 0$). By abstracting $(r^1 + r_c)$ in this state, HC_1 generates the following local fault signature:
  $sig_1^1 = \left((r^1 + r_c)^+, PC_1^1\right)$
  This positive change PC_1^1 is equal to ($O_V = \frac{s_V\sqrt{2g}}{2s_T\sqrt{x_0}}x$) (see Fig.3.10).

- Faulty local states ($q_5^1 : VC(leakage)$ and $q_6^1 : VO(leakage)$), corresponding to the occurrence of a leakage, the part r^1 of residual defined in these states is equal to zero (because $\tilde{h}_q^1 = h_q^1$) and r_c is equal to O_{lg} (because $s_{lg} \neq 0$). By abstracting the value of $(r^1 + r_c)$ in these states, HC_1 generates the following local fault signature:
  $sig_3^1 = \left((r^1 + r_c)^+, UC^1\right)$
  As shown in Example 3.7 of Chapter 3, the parametric fault representing the

leakage is considered to be progressive. The parameter of this fault corresponds to the leakage section.

Based on the same reasoning used to construct the fault signatures of HC_1, the fault signature of HC_2 can be computed using Fig.3.11 of Example 3.5

- In normal operating mode of hybrid component HC_2 (q_1^2 and q_2^2 of Fig.3.11), the parts (r^2 and r_c) of residual r defined in these states are equal to zero. By abstracting the value of $(r^2 + r_c)$ in these states, HC_2 generates the following normal local fault signature:
  $sig_0^2 = \left(\left(r^2 + r_c\right)^0, UC^2 \right)$

- Faulty local state ($q_4^2 : PFoff(no\ leakage)$) corresponds to the occurrence of discrete fault 'pump failed off'. Therefore, based on (4.3), the part r^2 of r defined in these states is equal to $\frac{O_P}{s_T}$ and r_c is equal to zero. By abstracting $(r^2 + r_c)$ in these states, HC_2 generates the following local fault signature:
  $sig_2^2 = \left(\left(r^2 + r_c\right)^+, PC_2^2 \right)$
  This positive change PC_2^2 is equal to $\frac{O_P}{s_T}$ (see Fig.3.11).

- Faulty local states ($q_5^2 : Poff(leakage)$ and $q_6^2 : Pon(leakage)$), the part r^2 of residual r defined in these states is equal to zero and r_c is equal to O_{lg}. By abstracting the value of $(r^2 + r_c)$ in these states, HC_2 generates the following local fault signature:
  $sig_3^2 = \left(\left(r^2 + r_c\right)^+, UC^2 \right)$

4.2.2 Local hybrid diagnoser construction

The objective of local hybrid diagnoser D_j of HC_j is to detect and isolate the occurrence of parametric and discrete faults affecting the dynamics of hybrid component HC_j. D_j is built based on the local model, G^j, of HC_j. Initial state z_1^j of D_j is composed of initial state q_1^j of G^j and all states q_k^j of G^j reached from q_1^j by the occurrence of unobservable events. Then, the G^j states that are reached from any G^j state belonging to z_1^j, through either the same control command event or the same local fault signature, are gathered into the same state z_2^j. By following the same reasoning, the other D_j states are constructed. Thus, D_j transition function can be defined by:

$$\delta_z^j = Z^j \times Sig^j \times \Sigma^j \rightarrow Z^j \tag{4.4}$$

where, Z^j is the set of all D_j states and Sig^j denotes the set of all D_j local fault signatures sig_{z^j} generated by its HC_j.

Each state z_k^j of D_j is of the form (see Fig.4.3):

$z_k^j = \left\{ Q_k^j,\ \tilde{h}_z^j,\ \tilde{\dot{X}}^j,\ HSL_{z_k^j}^j \right\}$

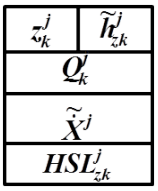

Figure 4.3: Local state of decentralized hybrid diagnoser D_j.

where, $Q_k^j = \{q_b^j, \cdots, q_l^j\}$ is the set of model local states belonging to the D_j state z_k^j, $\tilde{h}_z^j$ is the nominal local state output of z_k^j, $HSL_{z_k^j}^j = \{HSL_{q_b^j}^j, \cdots, HSL_{q_l^j}^j\}$ gathers the set of labels of z_k^j states and $\tilde{\dot{X}}^j = \left[\tilde{\dot{x}}_1^j, \cdots, \tilde{\dot{x}}_n^j\right]^T$ is the nominal parts of dynamic evolutions of the continuous variables in the local states of z_k^j.

D_j contains only the transitions labeled by observable events (control command events or fault signatures). This is the essential difference between G^j and D_j.

Definition 4.1 *The state z_k^j of local hybrid diagnoser D_j is called normal, if $HSL_{z_k^j}^j$ is equal to $\{N_j\}$.*

Definition 4.2 *The state z_k^j of local hybrid diagnoser D_j is called F_w-certain ,$w \in \{1, \cdots, d^j\}$, if $HSL_{z_k^j}^j$ is equal to $\{F_w\}$.*

Definition 4.3 *The state z_k^j of local hybrid diagnoser D_j is called F_w-uncertain, if $HSL_{z_k^j}^j$ contains at least one other label in addition to fault label F_w.*

Definition 4.4 *An F_w indeterminate cycle is a sequence of F_w-uncertain states in which the local hybrid diagnoser D_j is unable to decide with certainty and within a finite number of observable transitions the occurrence of a fault of type $F_w, w \in \{1, \cdots, d^j\}$. Therefore, a cycle is F_w-indeterminate if the following two conditions are satisfied:*

- *It is F_w-uncertain cycle in the local hybrid diagnoser D_j;*
- *Its states form two cycles in the model G^j, the states of the first cycle have the normal label N^j while the states of the second cycle have fault label F_w.*

Example 4.2 ***Local hybrid diagnoser of one tank system example***

For the one tank system example, two local hybrid diagnosers D_1 and D_2 are constructed for, respectively, HC_1 and HC_2 .

D_1 is constructed based on the use of local hybrid automaton G^1 of Fig.3.10 as follows:

- Initial state z_1^1 (Fig.4.4), characterized by (Q_1^1, $\tilde{h}_{z_1^1}^1$, $\tilde{\dot{x}}^1$, $HSL_{z_1^1}^1$), is composed of the following G^1 states: q_1^1 (G^1 initial state), q_5^1 reached from q_1^1 by the

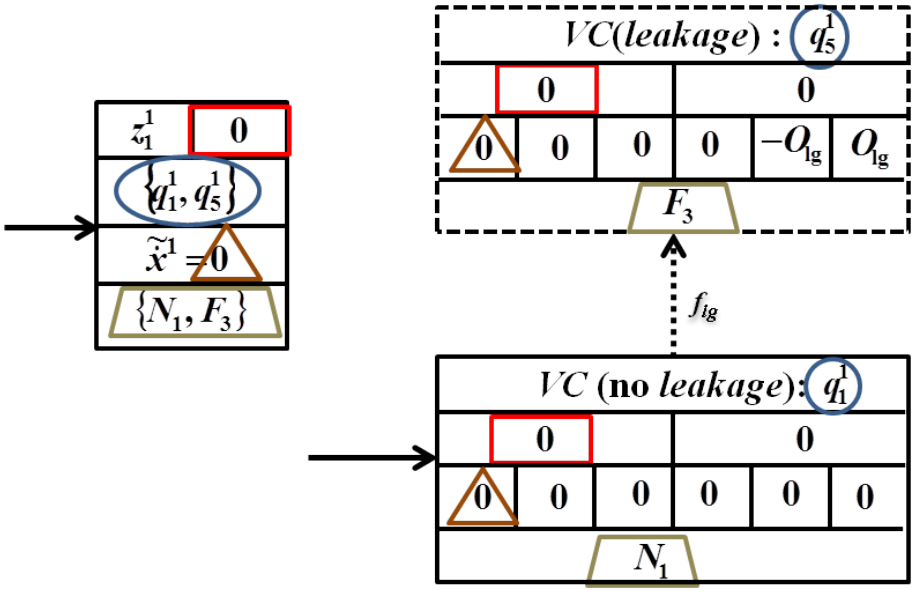

Figure 4.4: Initial state z_1^1 of local hybrid diagnoser D_1.

occurrence of fault event f_{lg} (fault of type F_3). Thus, Q_1^1 is equal to $\{q_1^1,\ q_5^1\}$. $\tilde{h}^1_{z_1^1}$ is equal to the nominal output of the states of Q_1^1. As we can see in Fig.3.10 and Fig.4.4, $\tilde{h}^1_{q_1^1}$ and $\tilde{h}^1_{q_5^1}$ in, respectively, q_1^1 and q_5^1 are equivalent and equal to 0. Thus, $\tilde{h}^1_{z_1^1}$ is equal to 0. $HSL^1_{z_1^1}$ gathers the normal and fault labels associated to the states belonging to Q_1^1. Therefore, $HSL^1_{z_1^1}$ is equal to $\{N_1,\ F_3\}$. Finally, $\tilde{x}^1$ gathers $\tilde{x}^1$ of all the states q_k^1 of Q_1^1. Since state q_5^1 is reached from q_1^1 due to the occurrence of unobservable event (a fault)(see Fig.3.10), $\tilde{x}^1$ in q_1^1 and q_5^1 are equivalent and equal to 0 (see Fig.4.4).

- Continuous dynamic evolutions of states belonging to Q_1^1 will allow to generate a set of fault signatures as we can see in Fig.4.5. These fault signatures allow detecting and isolating parametric faults of type F_3 as follows. q_5^1 of G^1 (reached due to the occurrence of a fault of type F_3) generates fault signature sig_3^1 through the part $(r^1 + r_c)$ of residual r calculated in this state ($r^1 = 0$ and $r_c = O_{lg}$)(see Fig.3.10 and Table 4.1). sig_3^1 is used as an observable transition to isolate the occurrence of a fault of type F_3 by moving to diagnoser state z_4^1 (see Fig.4.5). The other state of Q_1^1, q_1^1, generates fault signature sig_0^1 (the parts $(r^1 + r_c)$ of residual r in these state does not evolve yet ($r^1 = 0$ and $r_c = 0$)). sig_0^1 is used to label the transition to $z_1^{1'}$;

- $z_1^{1'}$ is characterized by $(Q_1^{1'},\ \tilde{h}^1_{z_1^{1'}},\ \tilde{x}^1,\ HSL^1_{z_1^{1'}})$. $Q_1^{1'}$ is composed of states of Q_1^1 excluding the state isolated from z_1^1 (q_5^1: fault of type F_3). Thus, $Q_1^{1'}$ is equal to $\{q_1^1\}$. Then, all the states of G^1 reached from $Q_1^{1'}$ due to the occurrence of unobservable events are added to $Q_1^{1'}$ (see Fig.3.10). Based on Fig.3.10, f_{lg} is the only unobservable event that can occur from the states of

$Q_1^{1'}$. This fault event can occur from state q_1^1 (see Fig.3.10). f_{lg} moves HC_1 model from state q_1^1 to state q_5^1. Therefore, $Q_1^{1'}$ is equal to $\{q_1,\ q_5^1\}$. $\tilde{h}^1_{z_1^{1'}}$ is equal to 0. $HSL^1_{z_1^{1'}}$ is equal to $\{N_1,\ F_3\}$. $\tilde{x}^1$ is equal to 0. Consequently, $z_1^{1'}$ is equivalent to z_1^1. Thus, sig_0^1 is used as a self transition to loop in the same local hybrid diagnoser state z_1^1 (see Fig.4.4).

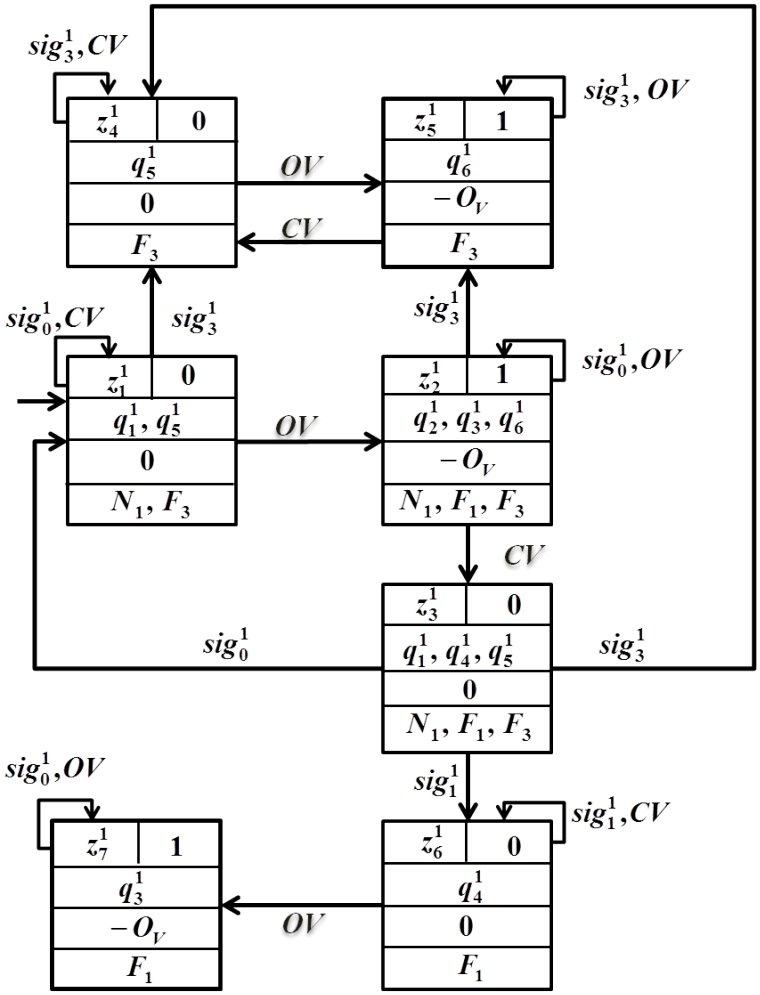

Figure 4.5: Local hybrid diagnoser D_1 of HC_1.

- The states of D_1 reached due to the occurrence of each control command are computed. The occurrence of control command OV moves D_1 from z_1^1 to z_2^1 characterized by $(Q_2^1,\ \tilde{h}^1_{z_2^1},\ \tilde{x}^1,\ HSL^1_{z_2^1})$. Q_2^1 is equal to all the states reached from Q_1^1 due to the occurrence of $'OV'$. Thus, Q_2^1 is equal to $\{q_2^1,\ q_6^1\}$ (see Fig.3.10). Then, all the states of G^1 reached from Q_2^1 due to the occurrence of unobservable event are added to Q_2^1. The unobservable event, other than f_{lg}, that can occur at q_2^1 is fault event f_{VSO}. Therefore, Q_2 is equal to $\{q_2^1,\ q_3^1,\ q_6^1\}$. $\tilde{h}^1_{z_2^1}$ is equal to the nominal output of the states of Q_2^1. Consequently, $\tilde{h}^1_{z_2^1}$ is

equal to 1 (the valve is considered to be opened), $HSL^1_{z^1_2}$ is equal to the set of fault labels of the states of Q^1_2. Thus, $HSL^1_{z^1_2}$ is equal to $\{N_1,\ F_1,\ F_3\}$ while $\tilde{\dot{x}}^1$ is equal to the nominal part of continuous evolution of x^1 in the states of Q^1_2. Thus, $\tilde{\dot{x}}^1$ is equal to $-O_V$ (see Fig.3.10).

- Continuous dynamic evolutions of the states belonging to Q^1_2 will allow to generate a set of local fault signatures as we can see in Fig.4.5. These fault signatures allow converting unobservable transitions into observable ones. Consequently, they are used in order to detect and isolate parametric faults of type F_3 as follows. q^1_6 of G^1 (reached from faulty state q^1_5 due to controlled event OV) generates fault signature sig^1_3. sig^1_3 is used as an observable transition to isolate the occurrence of a fault of type F_3 by moving the diagnoser to state z^1_5. The other states of Q^1_2, $\{q^1_2,\ q^1_3\}$, generate local fault signature sig^1_0 (the parts of continuous dynamic evolutions in these state do not evolve). sig^1_0 is used as a self transition to loop in the same local hybrid diagnoser state z^1_2.

- The occurrence of control command CV transits D_1 from z^1_2 to z^1_3 characterized by $(Q^1_3,\ \tilde{h}^1_{z^1_3},\ \tilde{\dot{x}}^1,\ HSL^1_{z^1_3})$. Q^1_3 is equal to all the states reached from Q^1_1 due to the occurrence of CV. Thus, Q^1_3 is equal to $\{q^1_1,\ q^1_4,\ q^1_5\}$ (see Fig.3.10). Then, all the states of G^1 reached from Q^1_3 due to the occurrence of unobservable events are added to Q^1_3. No other unobservable events can occur from the states of Q^1_3 (see Fig.3.10). Therefore, Q^1_3 remains equal to $\{q^1_1,\ q^1_4,\ q^1_5\}$. $\tilde{h}^1_{z^1_3}$ is equal to the nominal output of the states of Q^1_3. Consequently, $\tilde{h}^1_{z^1_3}$ is equal to 0 (the valve is considered to be closed), $HSL^1_{z^1_3}$ is equal to the set of fault labels of the states of Q^1_3. Thus, $HSL^1_{z^1_3}$ is equal to $\{N_1,\ F_1,\ F_3\}$ while $\tilde{\dot{x}}^1$ is equal to the nominal part of continuous evolution of x^1 in the states of Q^1_3. Thus, $\tilde{\dot{x}}^1$ is equal to 0 (see Fig.3.10).

- Continuous dynamic evolutions of the states belonging to Q^1_3 will allow to generate a set of fault signatures as we can see in Fig.4.5. These fault signatures allow converting unobservable transitions into observable ones. Consequently, they are used in order to detect and isolate a discrete faults of type F_1 and parametric faults of type F_3 as follows. q^1_4 of G^1 (reached from faulty state q^1_3 due to controlled event CV) generates fault signature sig^1_1. sig^1_1 is used as an observable transition to isolate the occurrence of a fault of type F_1 by moving D_1 to state z^1_6. q^1_5 of G^1 (reached from the faulty state q^1_6 due to controlled event $'CV'$) generates fault signature sig^1_3. sig^1_3 is used as an observable transition to isolate the occurrence of a fault of type F_3 by moving the diagnoser to state z^1_4. The other state of Q^1_3, q^1_1, generates fault signature sig^1_0 (the parts of continuous dynamic evolutions in these state do not evolve). sig^1_0 is used as a transition to loop D_1 initial state z^1_1 (see Fig.4.5).

Based on the same reasoning used to construct local diagnoser D_1 of HC_1, D_2 of HC_2 can be constructed as we can see in Fig.4.6.

Table 4.1 and Table 4.2 represent, respectively, the local fault signatures used by local hybrid diagnosers $D1$ and $D2$ in order to achieve their diagnosis.

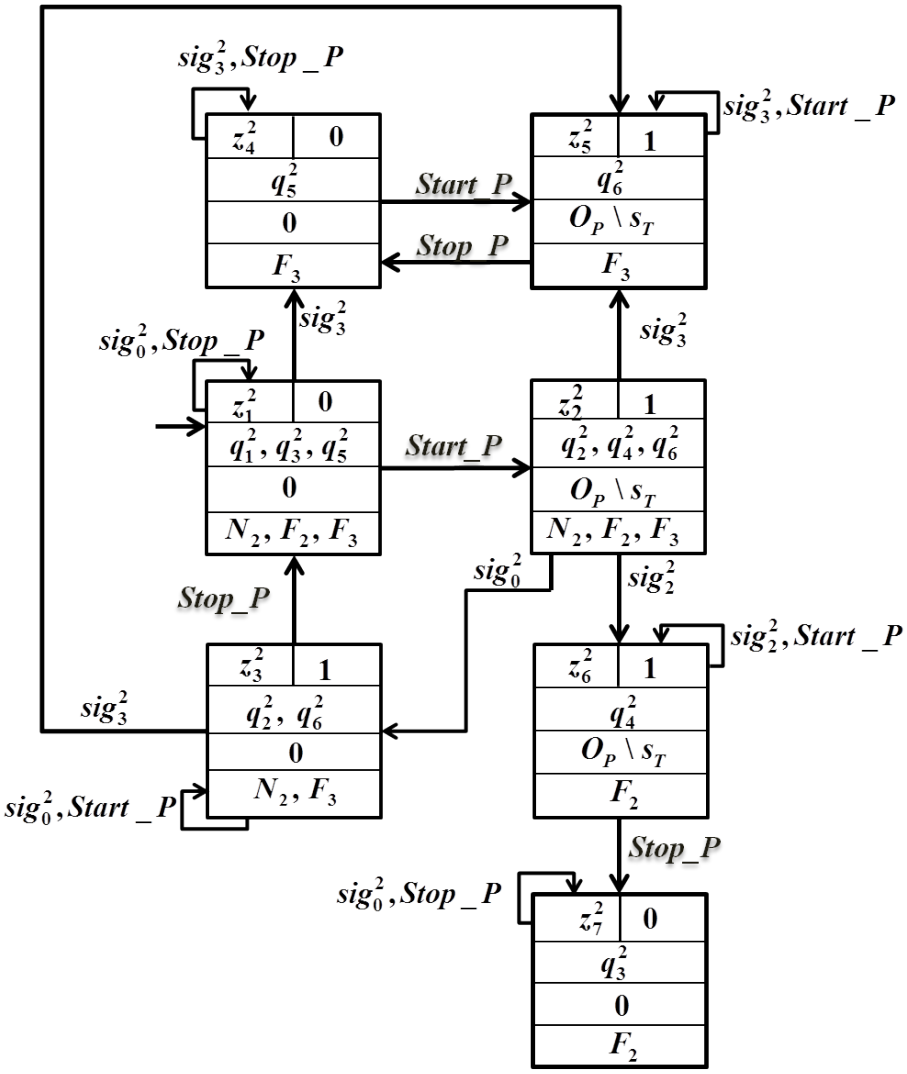

Figure 4.6: Local hybrid diagnoser D_2 of HC_2.

4.3 Coordinator construction

The coordinator aims at providing a global diagnosis decision equivalent to the one of a centralized diagnoser. It achieves that based on the use of local diagnosis decisions provided by the local diagnosers. The coordinator is composed of two main parts (see Fig.4.7):

1. Central processing point;

2. Decision merging point.

Table 4.1: Local fault signatures used by local hybrid diagnoser D_1.

Local fault signature name	***Part of residual value*** $r^1 + r_c$	***Local fault signature***
sig_0^1	0	$\left((r^1 + r_c)^0, UC^1\right)$
sig_1^1	$\frac{s_V\sqrt{2g}}{2s_T\sqrt{x_0}}x$	$\left((r^1 + r_c)^+, PC^1\right)$
sig_3^1	$\frac{s_{lg}\sqrt{2g}}{2s_T\sqrt{x_0}}x$	$\left((r^1 + r_c)^+, UC^1\right)$

Table 4.2: Fault signatures used by local hybrid diagnoser of HC_2 to achieve its diagnosis.

Local fault signature name	***Part of residual value*** $r^2 + r_c$	***Local fault signature***
sig_0^2	0	$\left((r^2 + r_c)^0, UC^2\right)$
sig_2^2	$\frac{O_P}{s_T}$	$\left((r^2 + r_c)^+, PC^2\right)$
sig_3^2	$\frac{s_{lg}\sqrt{2g}}{2s_T\sqrt{x_0}}x$	$\left((r^2 + r_c)^+, UC^2\right)$

4.3.1 Central processing point construction

As shown in subsection 4.2.2, local diagnoser D_j takes benefit of the local fault signatures in order to enhance the diagnosability of the parametric and discrete faults that can occur in its associated HC_j. Indeed, these fault signatures are used to convert unobservable transitions into observable ones. This conversion helps to isolate the occurrence of certain parametric and discrete faults by distinguishing their corresponding failure mode states from the other ones. To achieve that, D_j requires its associated local fault signatures. Since $\dot{X}$ is not measurable at the level of local diagnosers ($\dot{X}^j,\ j \in \{1, \cdots, L\}$, is not measurable), the part $(r^j + r_c^j)$ of residuals r is not measurable. Consequently, the local fault signatures cannot be calculated at the level of local diagnosers. Indeed, only the global residual $r = \tilde{\dot{X}} - \dot{X}$ can be calculated. Thus, a central processing point is defined in order to construct observable local fault signatures based on the use of global residuals r (see Fig.4.8). To achieve that, the central processing point computes first the global residuals r. Then, its replaces the unmeasurable local residuals $(r^j + r_c^j)$ in the local fault signatures by r. This allows calculating observable fault signatures.

4.3.1.1 Global residual computing

The global residuals r is computed at the central processing point as follows (see Fig.4.8):

- The parts $\{\tilde{\dot{X}}^1, \cdots, \tilde{\dot{X}}^j, \cdots, \tilde{\dot{X}}^L\}$ of nominal continuous dynamic evolutions $\tilde{\dot{X}}$ are sent by the local diagnosers $\{D_1, \cdots, D_j, \cdots, D_L\}$ to the central processing point;

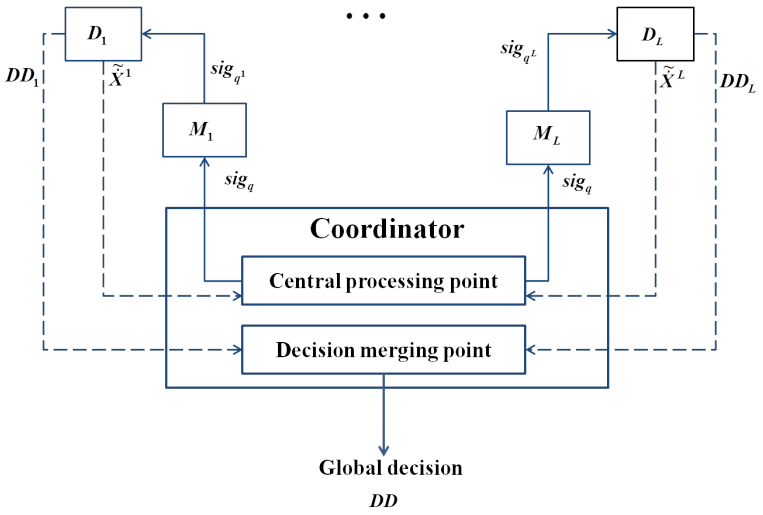

Figure 4.7: Coordinator to compute the global decision DD.

- The part $\dot{\tilde{X}}_c$ of $\dot{\tilde{X}}$ that does not change according to the discrete state of the system is registered in the central processing point (see Fig.4.8);
- The global nominal continuous dynamic evolution $\dot{\tilde{X}}$ is computed as the sum of the parts $\{\dot{\tilde{X}}^1, \cdots, \dot{\tilde{X}}^j, \cdots, \dot{\tilde{X}}^L\}$ and $\dot{\tilde{X}}_c$;
- The global residual r is calculated as the difference between nominal $\dot{\tilde{X}}$ and real $\dot{X}$ continuous dynamic evolutions;

4.3.1.2 Equivalence between global and local residuals

Through this subsection the equivalence between the global and local residual will be demonstrated as follows.

Based on (3.19), the set of residuals $\{r_i\},\ i \in \{1, \cdots, n\}$, generated by the global system G in each global discrete state q, is decomposed into a set of L parts r_i^j and r_{ci}. Therefore, we can write:

$$r_i = \sum_{j=1}^{L} r_i^j + r_{ci}$$

$$r_i = r_i^1 + \cdots + r_i^j + \cdots + r_i^L + r_{ci}$$

- Let us consider the occurrence of a discrete fault related to Dc_j ($\tilde{h}_q^j \neq h_q^j$). Based on (3.19), the residual r_i^j is computed for each $Cc_i \in HC_j$ as follows:
  $$r_i^j = \sum_{m=1}^{n} \left(\tilde{h}_q^j \tilde{A}_i^{mj} - h_q^j A_i^{mj}\right) x_m + \left(\tilde{h}_q^j \tilde{B}_i^j - h_q^j B_i^j\right) u$$
  where, r_i^j is different from zero since $\tilde{h}_q^j$ different from h_q^j.
  Since one fault can occur at the same time, $r_i^k,\ k \neq j$, and r_{ci} are equal to zero. Consequently, we can write:
  $r_i = 0 + \cdots + 0 + r_i^j + 0 + \cdots + 0$

$r_i = r_i^j \Rightarrow r_i = r_i^j + r_{ci}$ (since r_{ci}=0).
For each $Cc_m \notin HC_j$, the residual r_m is equal to zero (the discrete state of Dc_j does not influence the dynamic evolution of CC_m).
Thus, we can write:

$$\left\{\begin{array}{l} \forall Cc_i \in HC_j, \\ \quad r_i^j + r_{ci} = r_i \\ \quad \forall Cc_m \notin HC_j \\ \quad\quad r_m^j + r_{cm} = \Phi \\ \forall k \in \{1, \cdots, L\},\ k \neq j \\ \quad \forall Cc_v \in HC_k \\ \quad\quad r_v^k + r_{cv} = 0 \end{array}\right. \tag{4.5}$$

- Let us now consider the occurrence of a parametric fault related to the change in the value of parameter A_{ci}^m for $Cc_i \in HC_j$. Based on (3.19), we can write:
$r_{ci} = \sum_{m=1}^{n} \left(\tilde{A}_{ci}^m - A_{ci}^m\right) x_m$
r_{ci} is different from zero. Since one fault can occur at the same time, $r_i^j,\ j \in \{1, \cdots, L\}$, and $r_m \neq r_i$ are equal to zero. Consequently, we can write:
$r_i = 0 + \cdots + 0 + \cdots + 0 + r_{ci}$
$r_i = r_{ci} \Rightarrow r_i = r_i^j + r_{ci}$ (since $r_i^j = 0$).
Likewise, for each $HC_k, k \neq j$ that contains Cc_i, $r_i^k + rci = r_i$. Thus, we can write:

$$\left\{\begin{array}{l} \forall j \in \{1, \cdots, L\},\ Cc_i \in HC_j \\ \quad r_i^j + r_{ci} = r_i \\ \quad \forall Cc_m \neq Cc_i \\ \quad\quad r_m^j + r_{cm} = 0 \\ \forall k \in \{1, \cdots, L\},\ k \neq j,\ Cc_i \in HC_k \\ \quad r_i^k + r_{ci} = r_i \\ \quad \forall Cc_m \neq Cc_i \\ \quad\quad r_m^k + r_{cm} = 0 \\ \forall s \in \{1, \cdots, L\},\ s \neq j,\ s \neq k,\ Cc_i \notin HC_s \\ \quad \forall Cc_v \in HC_s \\ \quad\quad r_v^s + r_{cv} = 0 \end{array}\right. \tag{4.6}$$

4.3.1.3 Local residual computation

As developed in subsection 3.3.1, the global residuals allow discriminating the occurrence of parametric and discrete faults. As an example, a discrete fault in Dc_j causes an abrupt positive change in residual r_i equal to PC_i^j. Consequently, based on subsection 4.3.1.2, the central processing point replaces the local residuals $(r^j + r_c^j)$, which are not measurable, by the global residuals r as follows:

- when the global residuals $\{r_i\},\ i \in \{1, \cdots, n\}$, is equal to PC_i^j or NC_i^j (abrupt positive or negative change in global residuals $\{r_i\},\ i \in \{1, \cdots, n\}$, due to a discrete fault caused by Dc_j, the local residuals are computed by (4.5);

- when $r_i \neq 0$ and $r_m = 0,\ m \neq i,\ m \in \{1, \cdots, n\}$ and r_i is not equal to any defined PC_i^j or NC_i^j, $j \in \{1, \cdots, L\}$, (there is no observed abrupt change in residuals), this indicates the occurrence of a parametric fault in continuous component Cc_i. Thus, the local residuals are computed by (4.6);

- when the global residual $\{r_i\}\ i \in \{1, \cdots, n\}$ is equal to zero, i.e, normal operating mode, the local residuals are computed as follows:

$$\begin{cases} \forall j \in \{1, \cdots, L\},\ Cc_i \in HC_j \\ r_i^j + r_{ci} = 0 \end{cases} \tag{4.7}$$

Replacing the unmeasurable local residuals $(r^j + r_c^j)$ in the local fault signature sig_{z^j} by their corresponding measurable values and abstracting these values into discrete and continuous symbols, leads to obtain observable local fault signature sig_{z^j}. The latter, entails the evolution of D_j from one state to another one.

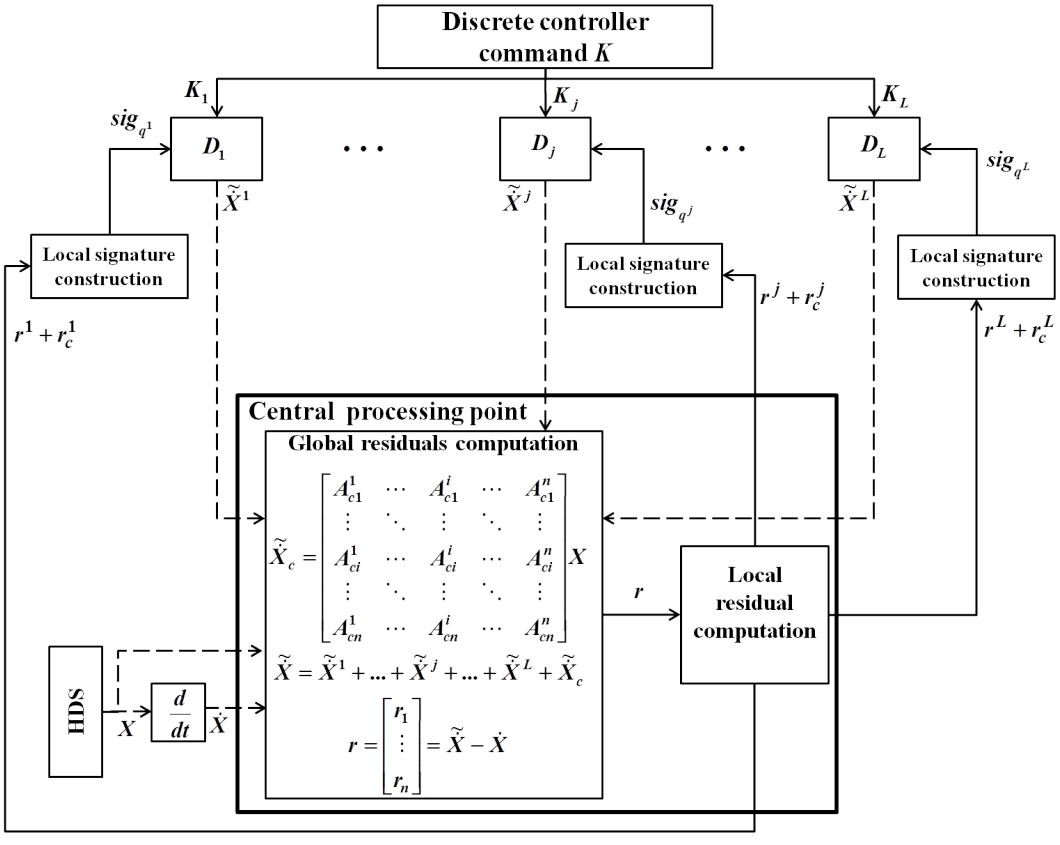

Figure 4.8: Central processing point used to compute the current global fault signature.

Example 4.3 ***Central processing point of one tank system example***

As shown in Example 4.2 for the one tank system example, two local hybrid diagnosers D_1 and D_2 are constructed for, respectively, HC_1 and HC_2. Each one of them sends its part of nominal continuous dynamic evolution to the central processing point. Therefore, D_1 sends $\tilde{\dot{x}}^1$; while D_2 sends $\tilde{\dot{x}}^2$. First, The central processing point calculates the nominal continuous dynamic evolution (see equation (3.17) in Example 3.3):
$\tilde{\dot{x}} = \tilde{\dot{x}}^1 + \tilde{\dot{x}}^2 + \tilde{\dot{x}}_c$
where, $\tilde{\dot{x}}_c = -\frac{\tilde{s}_{lg}\sqrt{2g}}{2s_T\sqrt{x_0}}x = 0$ ($\tilde{s}_{lg} = 0$).
The real continuous evolution is obtained by the system through the continuous sensor measuring the water level x in the tank. Second, The central processing point calculates residual r as a difference between the nominal and real continuous dynamic evolutions of x. Finally, the local residuals are computed as follows (see Fig.4.9):

- Based on (4.5), when r is equal to $\frac{s_V\sqrt{2g}}{2s_T\sqrt{x_0}}x = PC^1$ (see Table 4.1), the local residuals are computed as follows:

$$\begin{cases} r^1 + r_c = r \\ r^2 + r_c = 0 \end{cases} \tag{4.8}$$

- Based on (4.5), when r is equal to $\frac{Q_P}{s_T} = PC^2$ (see Table 4.2), the local residuals are computed as follows:

$$\begin{cases} r^1 + r_c = 0 \\ r^2 + r_c = r \end{cases} \tag{4.9}$$

- Based on (4.7), when r is equal to 0 (see Table 4.1 and Table 4.2), the local residuals are computed as follows:

$$\begin{cases} r^1 + r_c = 0 \\ r^2 + r_c = 0 \end{cases} \tag{4.10}$$

- Otherwise, i.e, there is no observed abrupt change in residual (parametric fault representing a leakage), the local residuals are computed by (4.6) as follows:

$$\begin{cases} r^1 + r_c = r \\ r^2 + r_c = r \end{cases} \tag{4.11}$$

4.3.2 Decision merging point construction

The system decomposition achieved by the proposed approach allows each local hybrid diagnoser to diagnose faults that can occur in its corresponding hybrid component. In order to obtain a decentralized diagnosis performance equivalent to a centralized diagnoser, a decision merging point is defined. It generates a global diagnosis decision by merging local diagnosis decisions provided by local hybrid diagnosers. Let $F^1, \cdots, F^j, \cdots, F^L$ denote the set of fault types that can occur, respectively, in $HC_1, \cdots, HC_j, \cdots, HC_L$. Global diagnosis decision DD is computed based on the following rules (see Table 4.3):

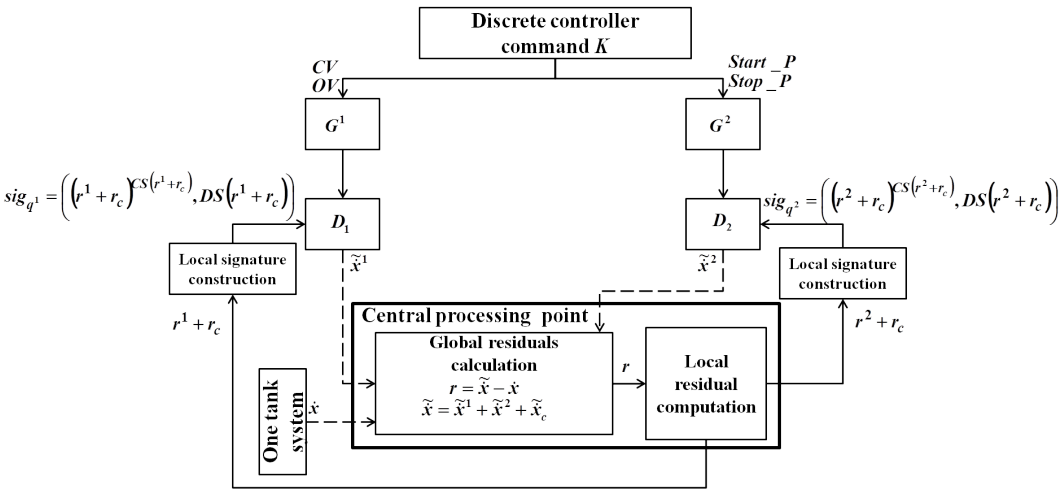

Figure 4.9: Central processing point for one tank system example.

- Rule 1: Global diagnoser D issues the decision DD equal to 'N' only if the system is in a normal operating mode. Thus, the global decision, DD, issued by the coordinator is equal to 'N' iff all the components of the system are in normal operating mode, i.e., all the local diagnosers $\{D_1, \cdots, D_j, \cdots, D_L\}$, declare a local decision $\{DD_1, \cdots, DD_j, \cdots, DD_L\}$, equal to '$N_1$', $\cdots$,'N_j', $\cdots$, 'N_L';

- Rule 2: If D issues DD equal to 'F_j', then local diagnoser D_j will declare with certainty the occurrence of a fault of type F_j by issuing the local decision DD_j equal to 'F_j'. The other local diagnosers $\{D_k\}$, $k \neq j$, $k \in \{1, \cdots, L\}$, will issue local diagnosis decision DD_k equal to 'N_k or Nothing' since they cannot diagnose a fault occurring in a component which is not associated to one of them;

- Rule 3: If the faults of two different types F_j, F_k cannot be distinguished by D, then DD is equal to 'F_j or F_k'. In decentralized diagnosis structure local diagnosers D_j and D_k issue, respectively, the local diagnosis decisions DD_j ='F_j' and DD_k ='F_k'. Since only simple fault scenarios are considered for the construction of local diagnosers, then DD issued by the decision merging point will be equal to 'F_j or F_k';

- Rule 4: When D is unable to decide with certainty the occurrence or not of a fault, its decision DD is equal to 'Nothing'. In this case, all local diagnosers $\{D_1, \cdots, D_L\}$ will be unable to decide with certainty the occurrence or not of a fault, $DD_1 = \cdots = DD_L$ ='Nothing'. The global diagnosis decision DD issued by the decision merging point will be equal to 'Nothing'.

These rules result from the equivalent between local and global disgnoers states as we will see in section 4.5.

Table 4.3: Rules to compute global diagnosis decision DD.

Rules	D_1	...	D_j	...	D_k	...	D_L	DD
1	N_1	...	N_j	...	N_k	...	N_L	N
2	N_1 or Nothing	...	F_j	...	N_k or Nothing	...	N_L or Nothing	F_j
	N_1 or Nothing	...	N_j or Nothing	...	F_k	...	N_L or Nothing	F_k
3	N_1 or Nothing	...	F_j	...	F_k	...	N_L or Nothing	F_j or F_k
4	Nothing	...	Nothing	...	Nothing	...	Nothing	Nothing

Table 4.4: Global diagnosis decision DD for the one tank system example.

Rules	***Local hybrid diagnoser*** D_1	***Local hybrid diagnoser*** D_2	***Global decision*** DD
2	F_1	Nothing	F_1
	Nothing	F_2	F_2
3	F_3	F_3	F_3
4	Nothing	Nothing	Nothing

Example 4.4 ***Coordinator construction for one tank system example***

The global decision DD for the one tank example is computed using Table 4.4. We must note that, the global diagnoser of this system is able to diagnose with certainty all the predefined faults (F_1, F_2 and F_3); there is no confusion between global fault signatures, i.e., faults of two different types do not own the same fault signature. In the Example 4.5 of section 4.5, we will demonstrate the equivalence between the global decisions issued by the centralized and decentralized diagnosers for this example.

4.4 Hybrid co-diagnosability notion

As in the global model of the system, the parametric and discrete faults are defined in their associated hybrid component models as faulty states. Therefore, the parametric and discrete faults co-diagnosability notion is defined as the ability to distinguish each of the faulty states,reached due to the occurrence of a fault of type F_w from the normal ones in decentralized manner. This distinguishability is based on observable discrete events Σ_0 and continuous measurements X through the use of a set of local hybrid diagnosers. Hybrid co-diagnosability notion allows verifying that each fault diagnosable by a centralized diagnoser is diagnosable by at least one local hybrid diagnoser based on its proper observation.

Definition 4.5 *HDS composed of L hybrid components* ($\{HC_j\}$, $j \in \{1, \cdots, L\}$) *is said to be co-diagnosable with respect to local projection functions* $P_1, \cdots, P_j, \cdots, P_L$ *and to fault labels* $\{F_1, \cdots, F_d\}$ *if the following holds:*

$(\exists v \in \aleph)(\forall w \in \{1, \cdots, d\})(\forall s \in \psi_{\Sigma^j_{F_w}})(\forall t \in htrace(HC_j)/s)(|t| \geq v) \Rightarrow Diag^j$
where the co-diagnosability condition $Diag^j$ *is:*

$$\forall y \in P_j^{-1}[P_j(st)] \Rightarrow \Sigma^j_{F_w} \in y \tag{4.12}$$

where,
$htrace(HC_j)$: denotes the set of all the hybrid traces (hybrid event sequences) generated by HC_j;
$htrace(HC_j)/s = \{t \in htrace(HC_j) | st \in htrace(HC_j)\}$: denotes the set of hybrid traces after s. $|t|$ is the number of events in t;
$\psi_{\Sigma^j_{F_w}}$: is the set of all hybrid traces of HC_j that end with a event of $\Sigma^j_{F_w}$. $\Sigma^j_{F_w}$ is a set of fault events of type F_w that can occur in HC_j;
$P_j^{-1}[P_j(st)]$: corresponds to all local hybrid traces ($htrace(HC_j)$) which have a projection P_j, i.e. an observable part, similar to the one of st;

The above definition means that the occurrence of a fault of type F_w, $w \in \{1, \cdots, d\}$, is diagnosable by at least one local hybrid diagnoser D_j after a finite number of observable events if and only if all the local hybrid traces containing a fault of type F_w have a finite observable part different from those of all the other local hybrid traces observed by D_j.

The above definition cannot always hold since it assumes that there is no communication between any pair of local hybrid diagnosers. Indeed, co-diagnosability property is stronger than diagnosability one. If a system is co-diagnosable, then it is diagnosable; while a diagnosable system does not ensure that it is co-diagnosable. This is due to the fact that, the local or partial observation of the system by local hybrid diagnosers may create ambiguity between their local diagnosis results. Therefore, limited communication through a coordinator is required to ensure that the system is co-diagnosable.

4.5 Centralized and decentralized structures equivalence

In order to demonstrate the equivalence between the centralized and decentralized diagnosis structures, the equivalence between a global hybrid trace $v \in htrace(HDS)$ and the synchronization of its local hybrid traces $v_1, \cdots, v_j \cdots, v_L$ (see Fig.4.10) must be demonstrated:

$$v = ||_{j=1}^{L} v_j \tag{4.13}$$

Indeed, when a global hybrid trace conducts the global diagnoser, D, from state z_k characterized by (Q_k, GSL_k) to state z_k^+ characterized by (Q_k^+, GSL_k^+), the set of local hybrid traces observed by the corresponding local diagnosers move them from states $(z_k^1 \cdots z_k^j \cdots z_k^L)$ characterized by $\{(Q_k^1, HSL_k^1), \cdots, (Q_k^j, HSL_k^j), \cdots, (Q_k^L, HSL_k^L)\}$ to states $(z_k^{1+} \cdots z_k^{j+} \cdots z_k^{L+})$ characterized by $\{(Q_k^{1+}, HSL_k^{1+}), \cdots, (Q_k^{j+}, HSL_k^{j+}), \cdots, (Q_k^{L+}, HSL_k^{L+})\}$.

As defined in subsection 3.3.3, $htrace(HDS) \subseteq (\Sigma \cup Sig)^*$, denotes the set of all the hybrid traces (hybrid event sequences) generated by HDS;

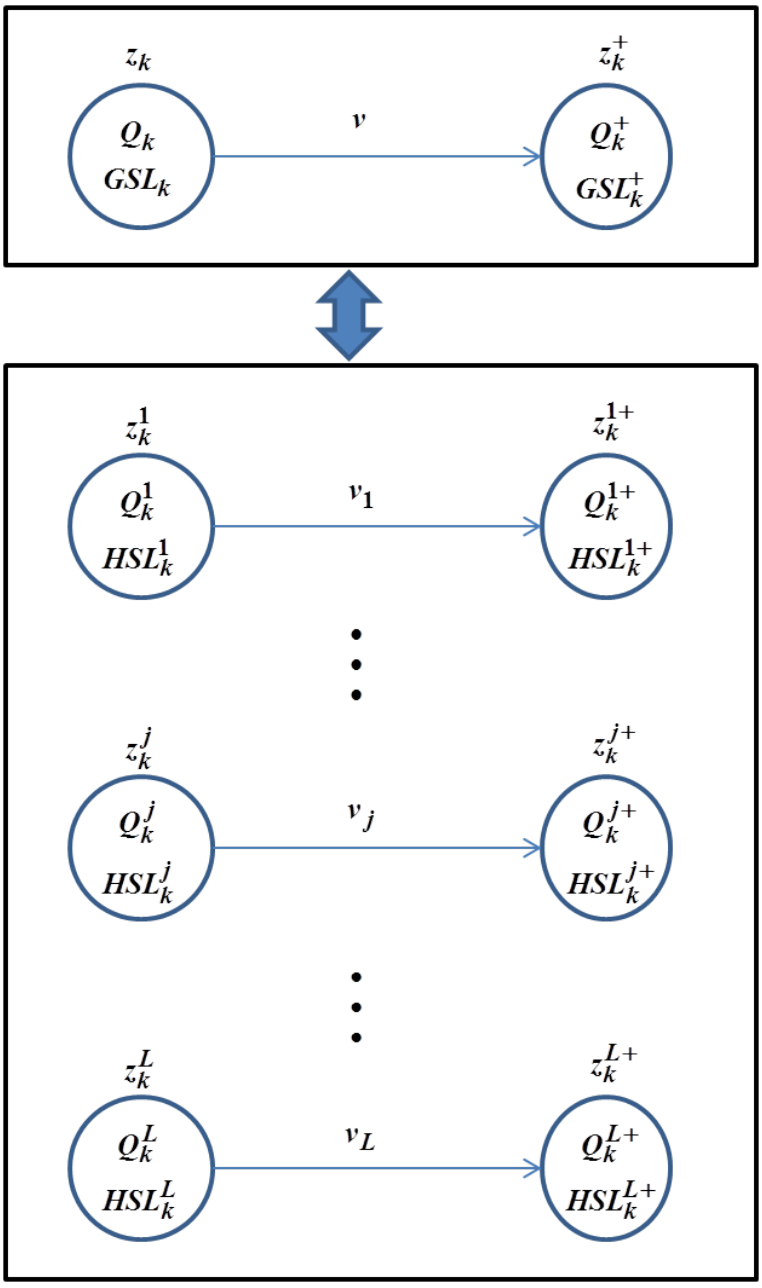

Figure 4.10: Global hybrid trace and its corresponding local hybrid traces.

where,

- Sig: denotes the set of global fault signatures $\{sig_z\}$ generated by the continuous dynamics at each state q of z ;
- $\Sigma = \Sigma^1 \cup \cdots \cup \Sigma^j \cup \cdots \cup \Sigma^L \cup \Sigma^c$ is the set of system discrete events;
- Σ^j is the set of HC_j discrete events;
- Σ^c is the set of events indicating the occurrence of parametric faults.

Thus each discrete event $e \in \Sigma$ belongs to at least one Σ^j and each $e \in \Sigma^j$ is also in Σ since $\Sigma = \cup_{j=1}^{L} \Sigma^j$.

Based on subsection 4.3.1.2, the equivalence between global and local fault signatures is demonstrated.

When (4.13) is demonstrated, the global diagnoser states z_k and z_k^+ will be equivalent to the combination of local diagnoser states $(z_k^1 \cdots z_k^j \cdots z_k^L)$ and $(z_k^{1+} \cdots z_k^{j+} \cdots z_k^{L+})$. The state equivalence means that:

- The global model states Q_k and Q_k^+ are equivalent to the combination of local model states $(Q_k^1 \cdots Q_k^j \cdots Q_k^L)$ and $(Q_k^{1+} \cdots Q_k^{j+} \cdots Q_k^{L+})$;
- The global decision labels GSL_k and GSL_k^+ are equal to the union of local decision labels $(HSL_k^1 \cdots HSL_k^j \cdots HSL_k^L)$ and $(HSL_k^{1+} \cdots HSL_k^{j+} \cdots HSL_k^{L+})$.

At diagnoser state z_k, two type of events can occur:

1. A control command event which changes the discrete mode of model states Q_k in z_k;
2. A fault signature sig_z generated by the continuous dynamics in model states Q_k in z_k. If the diagnoser does not detect a fault in z_k, the fault signature will be a self loop transition. If the diagnoser detect the occurrence of a discrete fault, the fault signature will move the diagnoser to another state z_k^+ with different discrete mode. If the diagnoser detect the occurrence of a parametric fault, the fault signature will move the diagnoser from z_k to another state z_k^+ with the same discrete mode.

As we have seen in subsection 4.3.1, the central processing point will calculate observable local signatures $(sig_z^1 \cdots sig_z^j \cdots sig_z^L)$ based on the global residuals r. These local signatures are equivalent to the global fault signature sig_z. Therefore, they are generated at the same time.

Fault signature sig_z can be generated in response to the occurrence of a fault of type F_w, $w \in \{1, \cdots, d\}$, or to the normal operating conditions. In the first case, sig_z is equal to sig_{F_w} while in the second case, sig_z is equal to sig_0.

In the decentralized diagnosis structure, the local fault signatures are calculated as follows (see Fig.4.11):

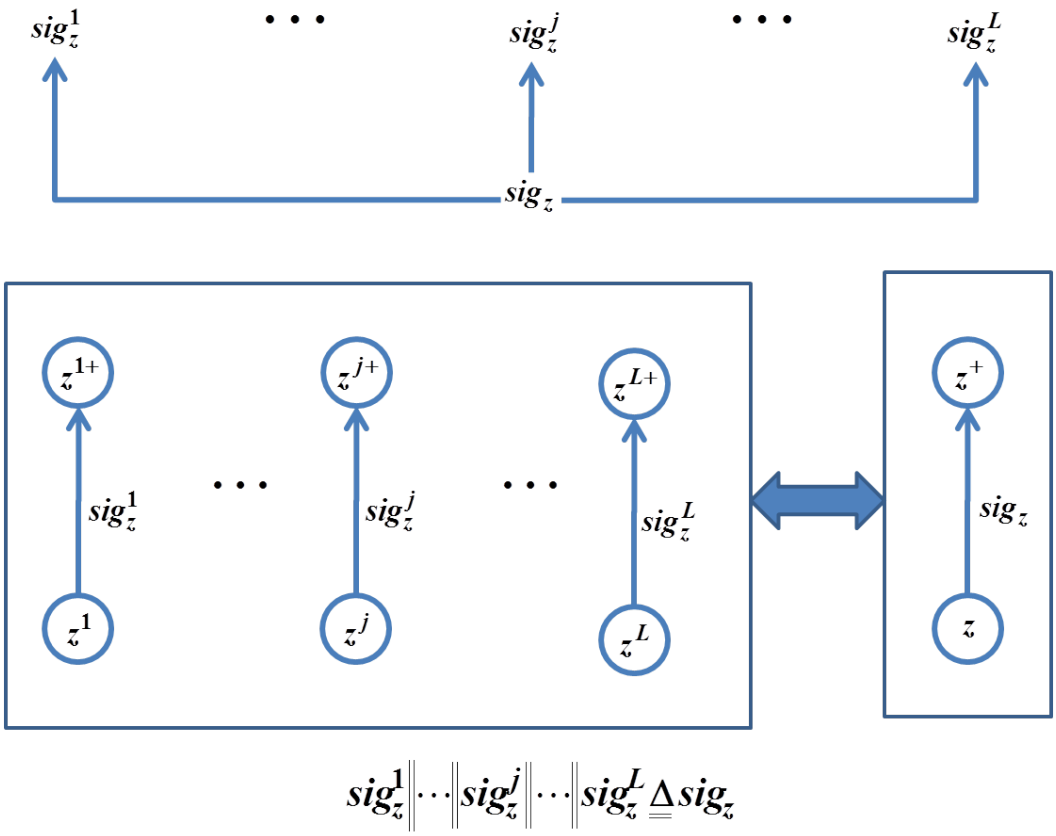

Figure 4.11: Equivalence between global and local fault signatures.

- If the global fault signature is sig_0, the centralized processing point will calculate the observable equivalent local fault signatures $sig_0^1 \cdots sig_0^j \cdots sig_0^L$. The latter will occur at the same time for all the local diagnosers. This means that sig_0^j cannot occur in D^j without the occurrence at the same time of the other $sig_0^k,\ k \neq j,\ k \in \{1, \cdots, L\}$.
- If the global fault signature is equal to sig_{F_w}, indicating the occurrence of a fault of type F_w in hybrid component HC_j, then the central processing point will calculate the observable local fault signatures $sig_0^1 \cdots sig_{F_w}^j sig_0^k \cdots sig_0^L$ since only the part of residuals related to HC_j is sensitive to this fault (see subsection 4.3.1.2).

The synchronous composition operator between the local fault signature can be defined as follows:

$$sig_z^1 || \cdots || sig_z^j || \cdots || sig_z^L \triangleq sig_z \tag{4.14}$$

since the execution at the same time of $sig_z^1 \cdots sig_z^j \cdots sig_z^L$ is equivalent to the execution of sig_z. $\triangleq$ denotes the equivalence symbol.

Let v be equal to $sig_0^*\ e\ sig_{F_w}^*$ (sig_0^* means that the fault signature sig_0 can occur zero or many times). Based on the definition of the projection function P_j in subsection 4.4, the local hybrid traces according to local hybrid diagnosers are calculated as follows. We suppose that $P_j(e) = e$; while $P_k(e) = \varepsilon,\ k \neq j\ k \in \{1, \cdots, L\}$ (see Fig.4.12) and a fault of type F_w occurred in HC_L.

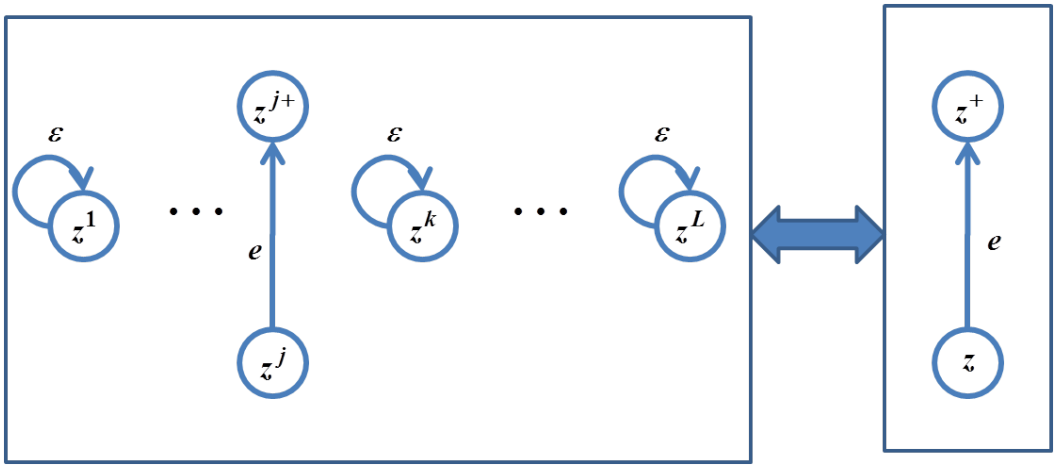

Figure 4.12: Local projection of the occurrence of event e observable by local hybrid diagnoser D_j.

$$\begin{cases} v_1 = sig_0^{1*}\ \varepsilon\ sig_0^{1*} \\ \vdots \\ v_j = sig_0^{j*}\ e\ sig_0^{j*} \\ \vdots \\ v_L = sig_0^{L*}\ \varepsilon\ sig_{F_w}^{L*} \end{cases} \tag{4.15}$$

Based on (4.14), (4.15) can be rewritten as follows:

$||_{j=1}^{L} v_j = \left(sig_0^1 \parallel \cdots \parallel sig_0^j \parallel \cdots \parallel sig_0^L\right)^*\ e\ \left(sig_0^1 \parallel \cdots \parallel sig_0^j \parallel \cdots \parallel sig_{F_w}^L\right)^*$

Thus, (4.15) is rewritten as follows:

$$||_{j=1}^{L} v_j = sig_0^*\ e\ sig_{F_w}^* \tag{4.16}$$

Therefore, the equivalence between global and local hybrid traces is demonstrated.

Example 4.5 ***Equivalence between centralized and decentralized diagnosers for the one tank system example***

For the one tank system example, let us consider the observation of global hybrid trace (see Fig.4.13):

$v = Start\_P\ sig_0\ OV\ sig_0$

Figure 4.13: Part of centralize hybrid diagnoser corresponding to global hybrid traces $Start\_P\ sig_0\ OV\ sig_0$.

Based on Fig.3.21 and Table 3.3, the initial states of this global hybrid trace is z_1, characterized by $Q_1 = \{q_1\ (VCPoff(no\ leakage)),\ q_{21}\ (VCPFoff(no\ leakage)),\ q_{31}\ (VCPoff(leakage))\}$ and $GSL_1 = \{N,\ F_2,\ F_3\}$. The final state of v is z_4, characterized by $Q_4 = \{q_3\ (VOPon(no\ leakage)),\ q_{13}\ (VSOPon(no\ leakage)),\ q_{33}\ (VOPon(leakage))\}$ and $GSL_4 = \{N,\ F_1,\ F_3\}$.

v is observed in decentralized diagnoser level as follows.

- The local hybrid diagnoser D_1 observes its corresponding part (see the definition of the projection function P_j in subsection 4.4):
  $P_1(v) = v_1 = \varepsilon\ M_1(sig_0)\ OV\ M_1(sig_0) = \varepsilon\ sig_0^1\ OV\ sig_0^1$
  The initial states of this local hybrid trace (see Fig.4.14) is z_1^1, characterized by $Q_1^1 = \{q_1^1\ (VC(no\ leakage)),\ q_5^1\ (VC(leakage))\}$ and $HSL_1^1 = \{N_1,\ F_3\}$. The final state of v_1 is z_2^1, characterized by $Q_2^1 = \{q_2^1\ (VO(no\ leakage)),\ q_3^1\ (VSO(no\ leakage)),\ q_6^1\ (VO(leakage))\}$ and $HSL_2^1 = \{N_1,\ F_1,\ F_3\}$.

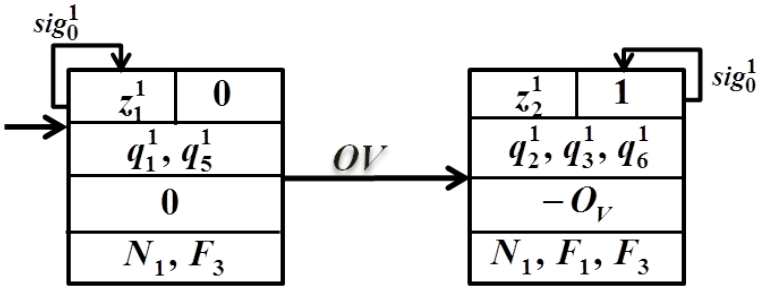

Figure 4.14: Part of D_1 corresponding to local hybrid traces $\varepsilon\ sig_0^1\ OV\ sig_0^1$.

- Likewise, the local hybrid diagnoser D_2 observes its corresponding part as follows:
  $P_2(v) = v_2 = Start\_P\ M_2(sig_0)\ \varepsilon\ M_2(sig_0) = Start\_P\ sig_0^2\ \varepsilon\ sig_0^2$
  The initial states of this local hybrid trace (see Fig.4.15) is z_1^2, characterized by $Q_1^2 = \{q_1^2\ (Poff(no\ leakage)),\ q_3^2\ (PFoff(no\ leakage)),\ q_5^2\ (Poff(leakage))\}$ and $HSL_1^2 = \{N_2,\ F_2,\ F_3\}$. The final state of v_2 is z_3^2, characterized by $Q_3^2 = \{q_2^2\ (Pon(no\ leakage)),\ q_6^2\ (Pon(leakage))\}$ and $HSL_3^2 = \{N_2,\ F_3\}$.

- The synchronization between local hybrid traces v_1 and v_2 is obtained as follows:

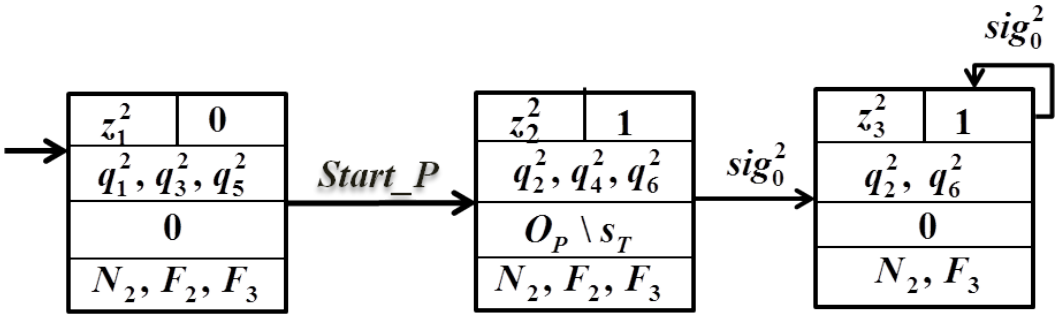

Figure 4.15: Part of D_2 corresponding to local hybrid traces $Start\_P\ sig_0^2\ \varepsilon\ sig_0^2$.

- Since local signatures sig_0^1 and sig_0^2 have to be observed at the same time by D_1 and D_2 (since they are generated through the same global residual r), the first event that can occur is $Start_P$ in D_2;
- sig_0^1 and sig_0^2 occur at the same time leading to evolve both D_1 and D_2. The execution of sig_0^1 and sig_0^2 is equivalent to the execution of sig_0 since they are calculated based on the same global residual r (see Example 4.3 and Fig.4.9);
- Since local signatures sig_0^1 and sig_0^2 have to be observed at the same time by D_1 and D_2 (since they are generated through the same global residual r), the following event that can be occurred is OV in D_1;
- sig_0^1 and sig_0^2 occur at the same time leading to evolve both D_1 and D_2. The execution of sig_0^1 and sig_0^2 is equivalent to the execution of sig_0 since they are calculated based on the same global residual r (see Example 4.3 and Fig.4.9);

Thus the global hybrid trace obtained by the synchronization of $P_1(v)$ and $P_2(v)$ is:
$Start\_P\ sig_0\ OV\ sig_0$
which is equivalent to the global hybrid trace v.

- The combination of the initial local states z_1^1, characterized by Q_1^1 equal to $\{q_1^1\ (VC(no\ leakage)),\ q_5^1\ (VC(leakage))\}$ and HSL_1^1 equal to $\{N_1,\ F_3\}$, and z_1^2, characterized by Q_1^2 equal to $\{q_1^2\ (Poff(no\ leakage)),\ q_3^2\ (PFoff(no\ leakage)),\ q_5^2\ (Poff(leakage))\}$ and HSL_1^2 equal to $\{N_2,\ F_2,\ F_3\}$, of the observed hybrid trace can be obtained as follows:
  - $q_1^1 q_1^2 = (VCPoff(no\ leakage)) \triangleq q_1 = (VCPoff(no\ leakage))$ and $\left(HSL_1^1 HSL_1^2 = N_1 N_2\right) \triangleq (GSL_1 = N)$;
  - $q_1^1 q_3^2 = (VCPFoff(no\ leakage)) \triangleq q_{21} = (VCPFoff(no\ leakage))$ and $\left(HSL_1^1 HSL_3^2 = N_1 F_2\right) \triangleq (GSL_1 = F_{21})$;
  - $q_1^1 q_5^2 = (VCPoff(leakage)) \triangleq q_{31} = (VCPoff(leakage))$ and $\left(HSL_1^1 HSL_5^2 = N_1 F_3\right) \triangleq (GSL_{31} = F_3)$;

- $q_5^1 q_1^2 = (VCPoff(leakage))$, $\underline{\underline{\Delta}}\ q_{31} = (VCPoff(leakage))$ and $\left(HSL_5^1 HSL_1^2 = F_3N_2\right)\ \underline{\underline{\Delta}}\ (GSL_{31} = F_3)$;
- $q_5^1 q_3^2 = (VCPFoff(leakage))$ can not be considered because is corresponding to multiple fault;
- $q_5^1 q_5^2 = (VCPoff(leakage))\ \underline{\underline{\Delta}}\ q_{31} = (VCPoff(leakage))$ and $\left(HSL_5^1 HSL_5^2 = F_3F_3\right)\ \underline{\underline{\Delta}}\ (GSL_{31} = F_3)$;

Thus the result of the combination of initial local states z_1^1 (Q_1^1, HSL_1^1) and z_1^2 (Q_1^2, HSL_1^2) is a global state characterized by $Q_k = \{q_1,\ q_{21},\ q_{31}\}$ and $GSL_k = \{N, F_2, F_3\}$. That means that the combination of initial local states z_1^1 and z_1^2 is equivalent to the global initial state z_1 (Q_1, GSL_1).

- Likewise, the combination of final local states z_2^1 characterized by $Q_2^1 = \{q_2^1\ (VO(no\ leakage)),\ q_5^1\ (VC(leakage))\}$ and $HSL_1^1 = \{N_1,\ F_3\}$, and z_1^2, characterized by $Q_1^2 = \{q_1^2\ (Poff(no\ leakage)),\ q_3^2\ (PFoff(no\ leakage)),\ q_5^2\ (Poff(leakage))\}$ and $HSL_1^2 = \{N_2,\ F_2,\ F_3\}$, and z_3^2, characterized by $Q_3^2 = \{q_2^2\ (Pon(no\ leakage)),\ q_6^2\ (Pon(leakage))\}$ and $HSL_3^2 = \{N_2,\ F_3\}$ of the observed hybrid trace can be obtained as follows:

  - $q_2^1 q_2^2 = (VOPon(no\ leakage))\ \underline{\underline{\Delta}}\ q_2 = (VOPon(no\ leakage))$ and $\left(HSL_2^1 HSL_2^2 = N_1N_2\right)\ \underline{\underline{\Delta}}\ (GSL_2 = N)$;
  - $q_2^1 q_6^2 = (VOPon(leakage))\ \underline{\underline{\Delta}}\ q_{33} = (VOPon(leakage))$ and $\left(HSL_2^1 HSL_6^2 = N_1F_3\right)\ \underline{\underline{\Delta}}\ (GSL_{33} = F_3)$;
  - $q_3^1 q_2^2 = (VSOPon(no\ leakage))\ \underline{\underline{\Delta}}\ q_{13} = (VSOPon(no\ leakage))$ and $\left(HSL_3^1 HSL_2^2 = F_1N_2\right)\ \underline{\underline{\Delta}}\ (GSL_{13} = F_1)$;
  - $q_3^1 q_6^2 = (VSOPon(leakage))$ can not be considered because is corresponding to multiple fault;
  - $q_6^1 q_2^2 = (VOPon(leakage))\ \underline{\underline{\Delta}}\ q_{33} = (VOPon(leakage))$ and $\left(HSL_6^1 HSL_2^2 = F_3N_2\right)\ \underline{\underline{\Delta}}\ (GSL_{33} = F_3)$;
  - $q_6^1 q_6^2 = (VOPon(leakage))\ \underline{\underline{\Delta}}\ q_{33} = (VOPon(leakage))$ and $\left(HSL_6^1 HSL_6^2 = F_3F_3\right)\ \underline{\underline{\Delta}}\ (GSL_{33} = F_3)$;

  Thus, the result of the combination of final local states z_2^1 (Q_2^1, HSL_2^1) and z_3^2 (Q_3^2, HSL_3^2) is a global state characterized by $Q_k^+ = \{q_2,\ q_{13},\ q_{33}\}$ and $GSL_k^+ = \{N, F_1, F_3\}$. That means that the combination of final local states z_2^1 and z_2^2 is equivalent to the final global stat z_4 (Q_4, GSL_4).

Therefore, the global and local hybrid diagnosers are equivalent.

4.6 Centralized and decentralized structures comparison

The centralized hybrid diagnosis approach presented in Chapter 3 allows exploiting the modularity of the system in order to diagnose the parametric and discrete faults that can occur in the system. However, it is necessary to build the global model in order to construct the diagnoser. This constraint implies that the use of this

approach for large scale systems remains difficult. Consequently, in this chapter, a decentralized approach for the diagnosis of parametric and discrete faults without the use of a global model is developed. The computation complexity of this approach is polynomial with the number of system components and the size of their local models.

Let $|G^j|$ be the number of states of local model G^j and $|G|$ be the number of states of global model G. Let $|\Sigma^j|$ be the number of events in Σ^j and $|\Sigma|$ be the number of events in Σ. the number of transitions is equal to $|G^j| \times |\Sigma^j|$ for G^j and $|G| \times |\Sigma|$ for G. Consequently, the complexity for constructing D_j is of the order $O\left(|G^j| \times |\Sigma^j|\right)$; while the complexity for constructing D is of the order $O\left(|G| \times |\Sigma|\right)$.

Let us assume that the system is composed of L local hybrid component $\{HC_j\}$. The number of global model states is equal to $|G| = |G^1| \times \cdots \times |G^j| \times \cdots \times |G^L| = |G^j|^L$ and the number of events is equal to $|\Sigma|$. Consequently, the complexity for constructing the L local diagnosers $\{D_j\}$, $j \in \{1, \cdots, L\}$, is of the order $O\left(L|G^j| \times |\Sigma|\right)$; while the complexity for constructing D is of the order $O\left(|G^j|^L \times |\Sigma|\right)$. Therefore, the complexity of the proposed decentralized diagnosis approach is polynomial in the number of the system components and the size of local model G^j; while the complexity of the proposed centralized diagnosis approach is exponential in the number of the system components and the size of local model G^j.

Remark 4.1 *In the centralized hybrid diagnosis approach, the fault diagnosis is achieved by one global hybrid diagnoser. When the latter fails, this bring down the entire diagnosis task. while, in the decentralized hybrid diagnosis approach the fault diagnosis is achieved by two local diagnosers, and not by one global diagnoser. Therefore, the diagnosis robustness is enhanced in the sense that when one local diagnoser is failed, the other local diagnosers remain operational and continue to assure their fault diagnosis.*

Table 4.5 shows a comparison between the centralized and decentralized proposed approaches.

Example 4.6 ***Comparison between centralized and decentralized approaches for the one tank system example***

For the one tank system example, the centralized hybrid diagnosis approach is developed throughout the Chapter 3. In this chapter, the decentralized hybrid diagnosis approach is applied to diagnose the same faults considered in Example 3.8. Based on Example 4.4, the decentralized fault diagnosis approach achieve a globl diagnosis decision equivalent to the one of centralized diagnoser. Table 4.6 represents the comparison between the major characteristics of the centralized and decentralized proposed approaches for the one tank system example. Based on remark 4.1, the decentralized proposed approach has the advantage to be robust because when D_1 fails, D_2 diagnoses the occurrence of faults F_2 and F_3; while, when D_2 fails, D_1 assures the diagnosis of the occurrence of faults F_1 and F_3.

Table 4.5: Comparison between the proposed centralized and decentralized approaches.

Characteristics	***Centralized approach***	***Decentralized approach***
Decomposition of the system	Yes In order to exploit the modularity of the system	Yes In order to construct the local diagnosers
The use of global model	Yes	No
Complexity of the diagnoser	Exponential with respect to the number of components	Polynomial with respect to the number of components
Diagnosis of discrete faults	Yes	Yes
Diagnosis of parametric faults	Yes	Yes
Robustness	Weak robustness (see remark 4.1)	Strong robustness (see remark 4.1)

Table 4.6: Comparison between the centralized and decentralized proposed approaches for the one tank system example.

Characteristics	***Centralized approach***	***Decentralized approach***
Decomposition of the system	Yes Into 2 hybrid components HC_1 and HC_2	Yes Into 2 hybrid components HC_1 and HC_2
The use of global model	Yes	No
The complexity of the diagnoser	$\|G^1\| \times \|G^2\|$	$\|G^1\| + \|G^2\|$
Diagnosis of discrete faults	Yes F_1 and F_2	Yes F_1 and F_2
Diagnosis of parametric faults	Yes F_3	Yes F_3
Robustness	Weak robustness (see remark 4.1)	Strong robustness (see remark 4.1)

4.7 Summary

As discussed in Chapter 2, many HDS diagnosis approaches diagnose only parametric or only discrete faults. While, the approaches that diagnose both parametric and discrete faults do not scale well to large scale systems. In Chapter 3, a new centralized diagnosis approach of both parametric and discrete fault is defined. This approach takes benefit of the modularity of the system in order to facilitate the construction of the system global model. Nevertheless, the number of system global states increases exponentially with respect to the number of the system hybrid components. Therefore, the use of the global model in order to construct the diagnoser can be very hard in the case of large scale systems.

In this chapter, a decentralized fault diagnosis of large scale HDS is proposed. This approach builds a local disgnoser for each hybrid component based on its local model. The local hybrid diagnoser exploits the continuous and discrete dynamics as well as the interactions between them in order to enhance the co-diagnosability of parametric and discrete faults. Indeed, the local hybrid diagnoser exploits the part of the system continuous dynamic evolutions defined in each local discrete mode in order to generate a new kind of observable events called local fault signatures. The latter were demonstrated to be equivalent to global fault signatures. These local fault signatures allow converting unobservable transitions into observable ones. Thus, fault signatures are used in order to enhance the diagnosis capacity of parametric and discrete faults that can occur in each hybrid component. In order to ensure a local diagnosis decision equivalent to the global one, the interactions between the different hybrid components must be taken into account. This is achieved by the use of a coordinator. The latter merges the local diagnosis decisions, issued by the local hybrid diagnosers, in order to issue a final decision about the origin of the fault and identifies its parameters. The advantage of the proposed approach is that local hybrid diagnosers as well as the coordinator are built using local models.

In order to demonstrate the efficiency of the proposed decentralized fault diagnosis approach, the latter is applied to achieve the parametric and discrete faults of the three-cell converter system in Chapter 5. Then, centralized and decentralized diagnosis structures are compared in order to show the interest of the use of decentralized approach.

Chapter 5

Case study: Diagnosis of three cell converter system

Contents

5.1 Introduction

In this chapter, the decentralized diagnosis approach developed in Chapter 4 is applied to achieve the fault diagnosis of the three cell converter, Louajri and Sayed-Mouchaweh (2014a). Through this chapter the three cell converter is used in order

to demonstrate the efficiency of the proposed decentralized diagnosis approach. The local diagnosers are constructed using the local model of each hybrid component of this system.

Chapter 5 is organized as follows. Firstly, the three cell converter system is presented. Then, the different steps to build the local models of discrete, continuous and hybrid system components are detailed. Next, the procedure to build the local hybrid diagnoser for each hybrid component of the system is developed. Then, the steps to merge the local diagnosis decisions through a coordinator are discussed. Next, the simulation results are presented. Finally, the performance of the proposed centralized and decentralized diagnosis structures is compared in order to show the interest of using the proposed decentralized diagnosis approach for large scale systems.

5.2 Three cell converter presentation

In order to illustrate the centralized and decentralized proposed approaches, the three cell converters, Shahbazi et al. (2013), Benzineb et al. (2013), Lezana et al. (2009), depicted in Fig.5.1, is used.

The continuous dynamics of the system are described by state vector $X = \left[\begin{array}{ccc} Vc_1 & Vc_2 & I \end{array}\right]^T$, where Vc_1 and Vc_2 represent, respectively, the floating voltage of capacitors C_1 and C_2 and I represents the load current flowing from source E towards the load (R, L) through three elementary switching cells $S_j,\ j \in \{1, 2, 3\}$. The latter represent the system discrete dynamics. Each discrete switch S_j has two discrete states: $\{S_j\}$ opened $(h_q^j = 0)$ or S_j closed $(h_q^j = 1)$, where h_q^j is the state discrete output of S_j. The control of this system has two main tasks:

1. balancing the voltages between the switches;
2. regulating the load current to a desired value.

To accomplish that, the controller changes the switches' states from opened to closed or from closed to opened by applying discrete commands 'close' or 'open' to each discrete switch $S_j,\ j \in \{1, 2, 3\}$ (see Fig.5.1). Thus, the considered example is a DCCS.

5.3 System modeling and decomposition

5.3.1 Discrete components modeling

In the literature, Defoort et al. (2011), Uzunova et al. (2012) and Gray et al. (2014), eight faults are considered for the diagnosis of the three cell converters system (see Table 5.1). Based on subsection 3.2.1 of Chapter 3, discrete automaton DG^1 characterizing switch S_1 discrete dynamics is defined by the tuple (see Fig.5.2):

$$DG^1 = (Q_D^1, h_q^1, \tilde{h}_q^1, \Sigma_D^1, DSL^1, \delta_D^1, Init_D^1) \tag{5.1}$$

where,

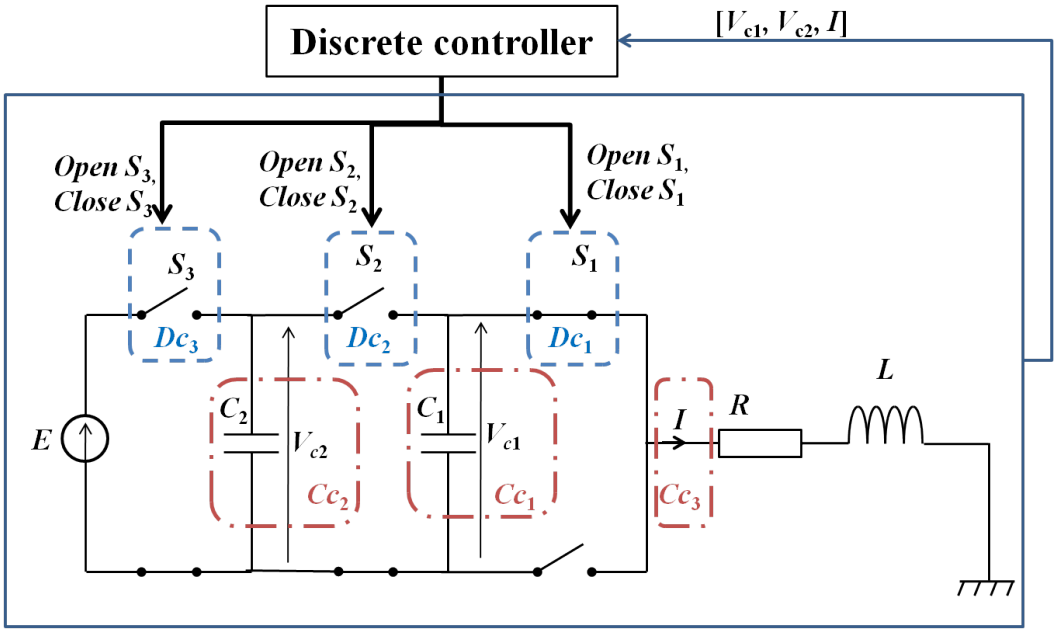

Figure 5.1: Three-cell converter system.

Table 5.1: Faults in the three cell converters.

Fault types	*Fault labels*	*Fault description*
Discrete faults	F_1	S_1 stuck opened
	F_2	S_1 stuck closed
	F_3	S_2 stuck opened
	F_4	S_2 stuck closed
	F_5	S_3 stuck opened
	F_6	S_3 stuck closed
Parametric faults	F_7	Change in the nominal parameter values of C_1 due to electrical chemical aging of C_1
	F_8	Change in the nominal parameter values of C_2 due to electrical chemical aging of C_2

- $Q_D^1 = \{q_1^1,\ q_2^1,\ q_3^1,\ q_4^1,\ q_5^1,\ q_6^1\}$. q_1^1 and q_2^1 represent, respectively, switch S_1 closed, S_1C, and switch S_1 opened, S_1O, in normal operating conditions. q_3^1 and q_4^1 characterize switch S_1 stuck opened failure mode, S_1SO. q_5^1 and q_6^1 characterize switch S_1 stuck closed failure mode, S_1SC;

- $\Sigma_D^1 = \Sigma_{Do}^1 \bigcup \Sigma_{Du}^1$: is the set of S_1 discrete events. $\Sigma_{Do}^1 = \{CS_1$ (close S_1), OS_1 (open S_1)$\}$, $\Sigma_{Du}^1 = \Sigma_{Df}^1 = \{f_{S_1SO}$ (fault event leading to S_1 stuck opened

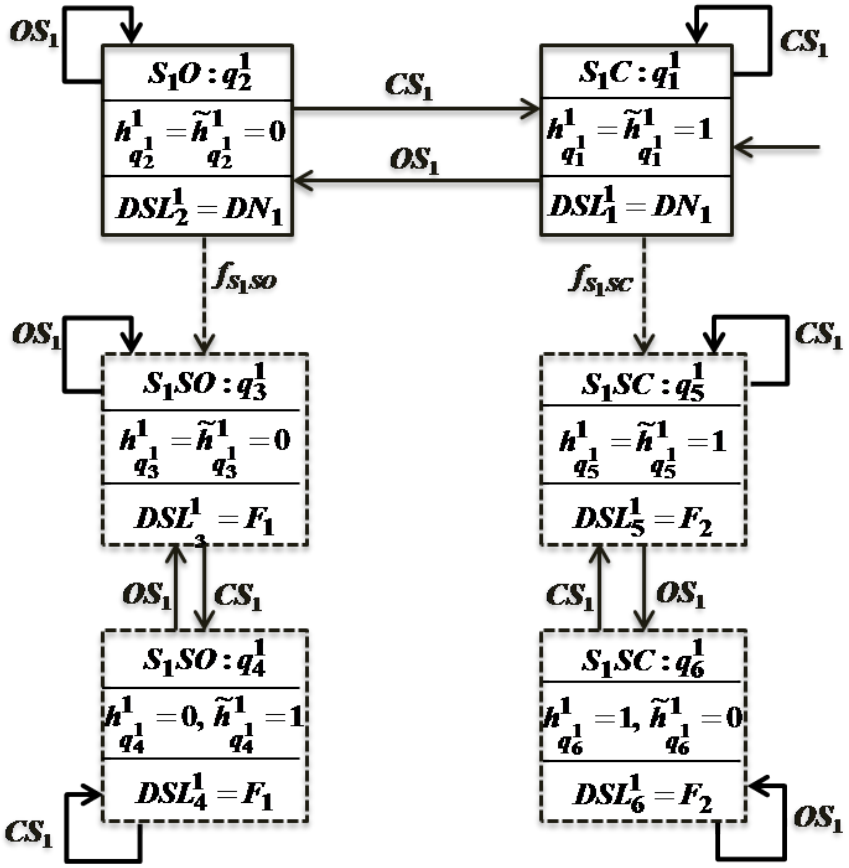

Figure 5.2: Discrete automaton DG^1 for switch S_1.

failure mode), f_{S_1SC} (fault event leading to S_1 stuck closed failure mode)}. The fault, f_{S_1SO}, can occur at the state where the valve is opened; while f_{S_1SC} can occur at the state where the valve is closed;

- $h_q^1 : Q_D^1 \rightarrow \{0,1\} = \{0$ (S_1 opened), 1 (S_1 closed)$\}$;
- $\tilde{h}_q^1 : Q_D^1 \rightarrow \{0,1\} = \{0$ (S_1 should be opened), 1 (S_1 should be closed)$\}$;
- $DSL^1 = \{DN_1$ (S_1 normal), F_1 (S_1 stuck opened), F_2 (S_1 stuck closed)$\}$. As an example, status label for q_1^1, DSL_1^1, is equal to DN_1 (see Fig.5.2);
- $\delta_D^1 : Q_D^1 \times \Sigma_D^1 \rightarrow Q_D^1$: is S_1 state transition function. As an example, $\delta_D^1(q_1^1, OS_1) = q_2^1$ (see Fig.5.2);
- $Init_D^1 : (q_1^1,\ h_{q_1^1}^1 = \tilde{h}_{q_1^1}^1 = 1,\ DSL^1(q_1^1) = DSL_1^1 = DN_1)$.

Likewise, discrete automaton DG^2 characterizing switch S_2 discrete dynamics is defined by the tuple (see Fig.5.3):

$$DG^2 = (Q_D^2, h_q^2, \tilde{h}_q^2, \Sigma_D^2, DSL^2, \delta_D^2, Init_D^2) \tag{5.2}$$

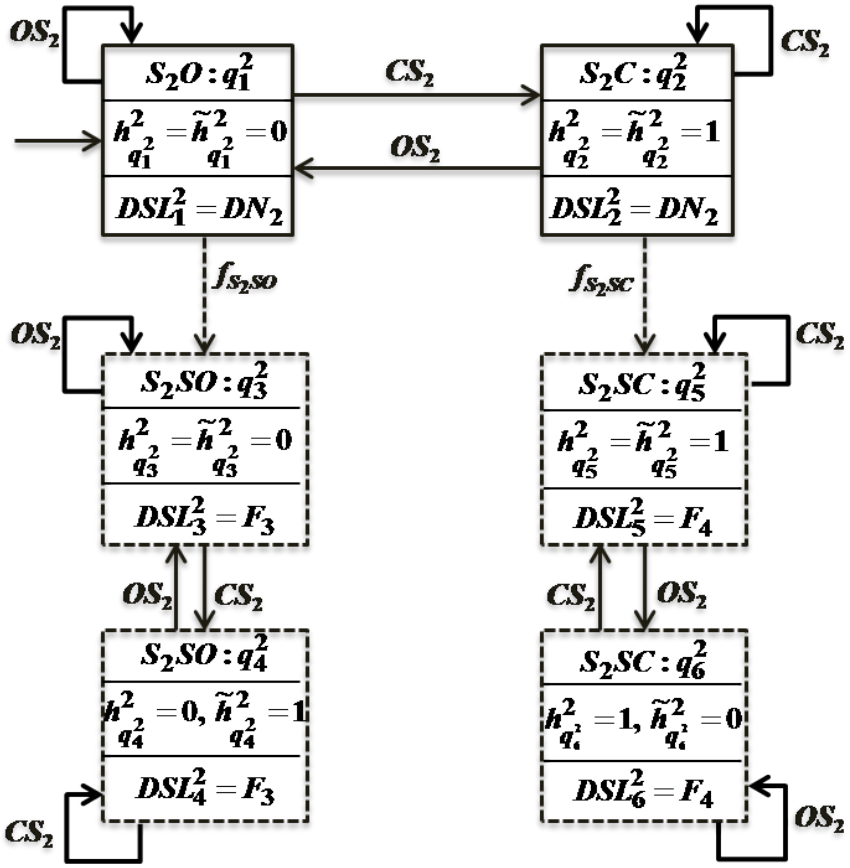

Figure 5.3: Discrete automaton DG^2 for switch S_2.

where,

- $Q_D^2 = \{q_1^2,\ q_2^2,\ q_3^2,\ q_4^2,\ q_5^2,\ q_6^2\}$. q_1^2 and q_2^2 represent, respectively, switch S_2 opened, S_2O, and switch S_2 closed, S_2C, in normal operating conditions. q_3^2 and q_4^2 characterize switch S_2 stuck opened failure mode, S_2SO. q_5^2 and q_6^2 characterize switch S_2 stuck closed failure mode, S_2SC;

- $\Sigma_D^2 = \Sigma_{Do}^2 \bigcup \Sigma_{Du}^2$: is the set of S_2 discrete events. $\Sigma_{Do}^2 = \{CS_2$ (close S_2), OS_2 (open S_2)$\}$, $\Sigma_{Du}^2 = \Sigma_{Df}^2 = \{f_{S_2SO}$ (fault event leading to S_2 stuck opened failure mode), f_{S_2SC} (fault event leading to S_2 stuck closed failure mode)$\}$. The fault, f_{S_2SO} can occur at the state where the valve is opened; while f_{S_2SC}, can occur at the state where the valve is closed;

- $h_q^2 : Q_D^2 \rightarrow \{0,1\} = \{0$ (S_2 opened), 1 (S_2 closed)$\}$;

- $\tilde{h}_q^2 : Q_D^2 \rightarrow \{0,1\} = \{0$ (S_2 should be opened), 1 (S_2 should be closed)$\}$;

- $DSL^2 = \{DN_2$ (S_2 normal), F_3 (S_2 stuck opened), F_4 (S_2 stuck closed)$\}$. As an example, status label for q_1^2, DSL_1^2, is equal to DN_2 (see Fig.5.3);

- $\delta_D^2 : Q_D^2 \times \Sigma_D^2 \rightarrow Q_D^2$: is S_2 state transition function. As an example, $\delta_D^2(q_1^2, CS_2) = q_2^2$ (see Fig.5.3);
- $Init_D^2 : (q_1^2,\ h_{q_1^2}^2 = \tilde{h}_{q_1^2}^2 = 0,\ DSL^2(q_1^2) = DSL_1^2 = DN_2)$.

Finally, discrete automaton DG^3 characterizing switch S_3 discrete dynamics is defined by the tuple (see Fig.5.4):

$$DG^3 = (Q_D^3, h_q^3, \tilde{h}_q^3, \Sigma_D^3, DSL^3, \delta_D^3, Init_D^3) \tag{5.3}$$

where,

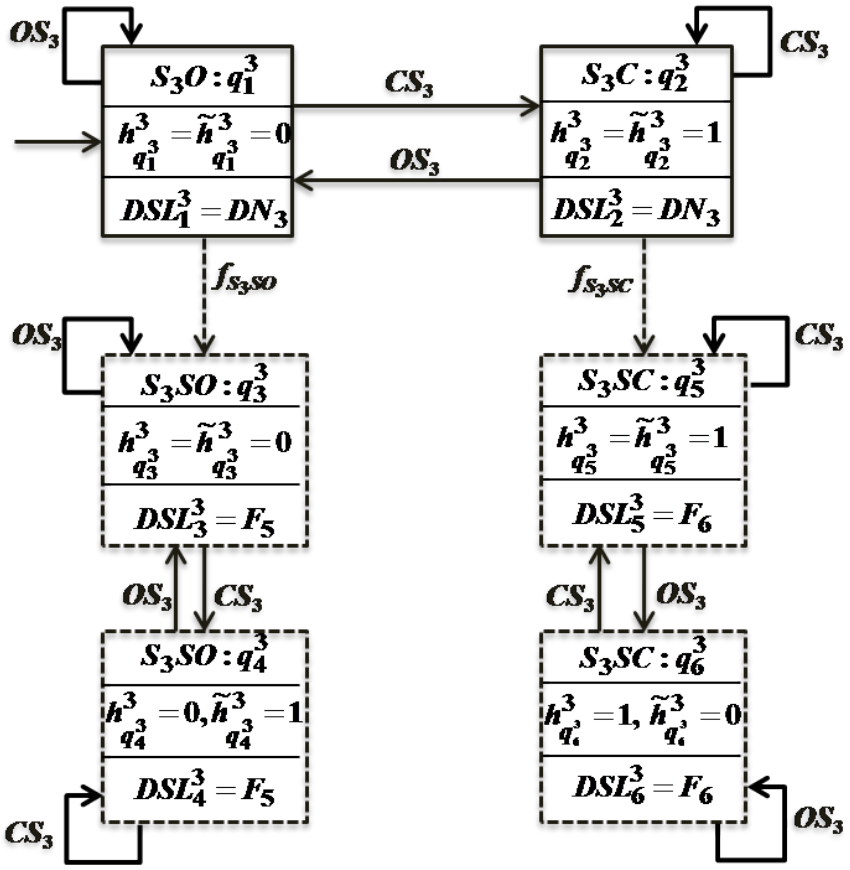

Figure 5.4: Discrete automaton DG^3 for switch S_3.

- $Q_D^3 = \{q_1^3,\ q_2^3,\ q_3^3,\ q_4^3,\ q_5^3,\ q_6^3\}$. q_1^3 and q_2^3 represent, respectively, switch S_3 opened, S_3O, and switch S_3 closed, S_3C, in normal operating conditions. q_3^3 and q_4^3 characterize switch S_3 stuck opened failure mode, S_3SO. q_5^3 and q_6^3 characterize switch S_3 stuck closed failure mode, S_3SC;
- $\Sigma_D^3 = \Sigma_{Do}^3 \bigcup \Sigma_{Du}^3$: is the set of S_3 discrete events. $\Sigma_{Do}^3 = \{CS_3$ (close S_3), OS_3 (open S_3)$\}$, $\Sigma_{Du}^3 = \Sigma_{Df}^3 = \{f_{S_3SO}$ (fault event leading to S_3 stuck opened

failure mode), f_{S_3SC} (fault event leading to S_3 stuck closed failure mode)}. The fault, f_{S_3SO}, can occur at the state where the valve is opened; while f_{S_3SC} can occur at the state where the valve is closed;

- $h_q^3 : Q_D^3 \rightarrow \{0,1\} = \{0$ (S_3 opened), 1 (S_3 closed)$\}$;
- $\tilde{h}_q^3 : Q_D^3 \rightarrow \{0,1\} = \{0$ (S_3 should be opened), 1 (S_3 should be closed)$\}$;
- $DSL^3 = \{DN_3$ (S_3 normal), F_5 (S_3 stuck opened), F_6 (S_3 stuck closed)$\}$. As an example, status label for q_1^3, DSL_1^3, is equal to DN_3 (see Fig.5.4);
- $\delta_D^3 : Q_D^3 \times \Sigma_D^3 \rightarrow Q_D^3$: is S_3 state transition function. As an example, $\delta_D^3(q_1^3, CS_3) = q_2^3$ (see Fig.5.4);
- $Init_D^3 :$ $(q_1^3,\ h_{q_1^3}^3 = \tilde{h}_{q_1^3}^3 = 0,\ DSL^3(q_1^3) = DSL_1^3 = DN_3)$.

5.3.2 Continuous components modeling

Based on (3.8), the real system dynamic evolution of three cell converter is written as follows, Defoort et al. (2011):

$$\begin{cases} \dot{V}c_1 = -h_q^1 \frac{I}{C_1} + h_q^2 \frac{I}{C_1} \\ \dot{V}c_2 = -h_q^2 \frac{I}{C_2} + h_q^3 \frac{I}{C_2} \\ \dot{I} = -\frac{RI}{L} + h_q^1 \frac{1}{L} Vc_1 + h_q^2 \frac{1}{L}(Vc_2 - Vc_1) + h_q^3 \frac{1}{L}(E - Vc_2) \end{cases} \tag{5.4}$$

Based on (3.9), (5.4) is decomposed as follows:

$$\begin{cases} \dot{V}c_1 = \dot{V}c_1^1 + \dot{V}c_1^2 \\ \dot{V}c_2 = \dot{V}c_2^2 + \dot{V}c_2^3 \\ \dot{I} = \dot{I}_c + \dot{I}^1 + \dot{I}^2 + \dot{I}^3 \end{cases} \tag{5.5}$$

where $\dot{V}c_1^1 = -h_q^1 \frac{I}{C_1}$, $\dot{V}c_1^2 = h_q^2 \frac{I}{C_1}$, $\dot{V}c_2^2 = -h_q^2 \frac{I}{C_2}$, $\dot{V}c_2^3 = h_q^3 \frac{I}{C_2}$, $\dot{I}_c = -\frac{RI}{L}$, $\dot{I}^1 = h_q^1 \frac{1}{L} Vc_1$, $\dot{I}^2 = h_q^2 \frac{1}{L}(Vc_2 - Vc_1)$, $\dot{I}^3 = h_q^3 \frac{1}{L}(E - Vc_2)$.
The goal of this decomposition is to show the influence of the discrete state of each discrete component Dc_j, $j \in \{1,2,3\}$, on the continuous dynamic evolutions of Vc_1 (Cc_1), Vc_2 (Cc_2) and I (Cc_3). $\dot{V}c_1^1$ represents the real dynamic evolution of Vc_1 according to the discrete state of S_1 (Dc_1). Likewise, $\dot{V}c_1^2$, $\dot{V}c_2^2$, $\dot{V}c_2^3$, $\dot{I}^1$, $\dot{I}^2$ and $\dot{I}^3$ have the same definition as $\dot{V}c_1^1$. $\dot{I}_c$ represents the part of dynamic evolution of I which does not depend on the discrete state of any switch.

Based on (3.12), and since the parametric faults related to the load (R, L) are not considered ($\tilde{R}$ is equal to R and $\tilde{L}$ is equal to L), the nominal system dynamic evolution of three cell converter is written as follows:

$$\begin{cases} \tilde{\dot{V}}c_1 = -\tilde{h}_q^1 \frac{I}{\tilde{C}_1} + \tilde{h}_q^2 \frac{I}{\tilde{C}_1} \\ \tilde{\dot{V}}c_2 = -\tilde{h}_q^2 \frac{I}{\tilde{C}_2} + \tilde{h}_q^3 \frac{I}{\tilde{C}_2} \\ \tilde{\dot{I}} = -\frac{RI}{L} + \tilde{h}_q^1 \frac{1}{L} Vc_1 + \tilde{h}_q^2 \frac{1}{L}(Vc_2 - Vc_1) + \tilde{h}_q^3 \frac{1}{L}(E - Vc_2) \end{cases} \tag{5.6}$$

where, $\tilde{C}_1$ and $\tilde{C}_2$ are the nominal values of C_1 and C_2.

Based on (3.13), (5.6) is decomposed as follows:

$$\begin{cases} \dot{\tilde{V}}c_1 = \dot{\tilde{V}}c_1^{\,1} + \dot{\tilde{V}}c_1^{\,2} \\ \dot{\tilde{V}}c_2 = \dot{\tilde{V}}c_2^{\,2} + \dot{\tilde{V}}c_2^{\,3} \\ \dot{\tilde{I}} = \dot{\tilde{I}}_c + \dot{\tilde{I}}^1 + \dot{\tilde{I}}^2 + \dot{\tilde{I}}^3 \end{cases} \tag{5.7}$$

where $\dot{\tilde{V}}c_1^{\,1} = -\tilde{h}_q^1 \frac{I}{\tilde{C}_1}$, $\dot{\tilde{V}}c_1^{\,2} = \tilde{h}_q^2 \frac{I}{\tilde{C}_1}$, $\dot{\tilde{V}}c_2^{\,2} = -\tilde{h}_q^2 \frac{I}{\tilde{C}_2}$, $\dot{\tilde{V}}c_2^{\,3} = \tilde{h}_q^3 \frac{I}{\tilde{C}_2}$, $\dot{\tilde{I}}_c = -\frac{RI}{L}$, $\dot{\tilde{I}}^1 = \tilde{h}_q^1 \frac{1}{L} Vc_1$, $\dot{\tilde{I}}^2 = \tilde{h}_q^2 \frac{1}{L}(Vc_2 - Vc_1)$, $\dot{\tilde{I}}^3 = \tilde{h}_q^3 \frac{1}{L}(E - Vc_2)$.

5.3.3 Residuals generation

As developed in subsection 3.2.3 of Chapter 3, residuals r_1, r_2 and r_3 for, respectively, Cc_1, Cc_2 and Cc_3 are generated based on (3.18), (5.4) and (5.6) as follows:

$$\begin{cases} r_1 = \left(-\tilde{h}_q^1 \frac{1}{\tilde{C}_1} + h_q^1 \frac{1}{C_1}\right) I + \left(\tilde{h}_q^2 \frac{1}{\tilde{C}_1} - h_q^2 \frac{1}{C_1}\right) I \\ r_2 = \left(-\tilde{h}_q^2 \frac{1}{\tilde{C}_2} + h_q^2 \frac{1}{C_2}\right) I + \left(\tilde{h}_q^3 \frac{1}{\tilde{C}_2} - h_q^3 \frac{1}{C_2}\right) I \\ r_3 = \left(-\frac{R}{L} I + \frac{R}{L} I\right) + \left(\tilde{h}_q^1 - h_q^1\right) \frac{1}{L} Vc_1 + \left(\tilde{h}_q^2 - h_q^2\right) \frac{1}{L}(Vc_2 - Vc_1) + \\ \qquad \left(\tilde{h}_q^3 - h_q^3\right) \frac{1}{L}(E - Vc_2) \end{cases} \tag{5.8}$$

These residuals take into account the discrete state of switches impacting the continuous dynamics of the corresponding $Cc_i,\ i \in \{1,2,3\}$.

Based on (3.19), (5.8) is decomposed in order to describe the influence of each discrete component $\{Dc_j\},\ j \in \{1,2,3\}$ on the value of residual $\{r_i\},\ i \in \{1,2,3\}$ as follows:

$$\begin{cases} r_1 = r_1^1 + r_1^2 \\ r_2 = r_2^2 + r_2^3 \\ r_3 = r_{c3} + r_3^1 + r_3^2 + r_3^3 \end{cases} \tag{5.9}$$

where, $r_1^1 = \left(-\tilde{h}_q^1 \frac{1}{\tilde{C}_1} + h_q^1 \frac{1}{C_1}\right) I$, $r_1^2 = \left(\tilde{h}_q^2 \frac{1}{\tilde{C}_1} - h_q^2 \frac{1}{C_1}\right) I$, $r_2^2 = \left(-\tilde{h}_q^2 \frac{1}{\tilde{C}_2} + h_q^2 \frac{1}{C_2}\right) I$, $r_2^3 = \left(\tilde{h}_q^3 \frac{1}{\tilde{C}_2} - h_q^3 \frac{1}{C_2}\right) I$, $r_{c3} = -\frac{R}{L} I + \frac{R}{L} I$, $r_3^1 = \left(\tilde{h}_q^1 - h_q^1\right) \frac{1}{L} Vc_1$, $r_3^2 = \left(\tilde{h}_q^2 - h_q^2\right) \frac{1}{L}(Vc_2 - Vc_1)$ and $r_3^3 = \left(\tilde{h}_q^3 - h_q^3\right) \frac{1}{L}(E - Vc_2)$. r_{c3} is ignored since it is always equal to zero (parametric faults related to R and L are not considered). In order to separate the nominal and faulty continuous operating conditions, each continuous component $Cc_i,\ i \in \{1,2,3\}$ is modeled by the automaton, $G_{ci},\ i \in \{1,2,3\}$, depicted in Fig.5.5.

5.3.4 Hybrid components modeling

Based on (5.4), we can conclude that:

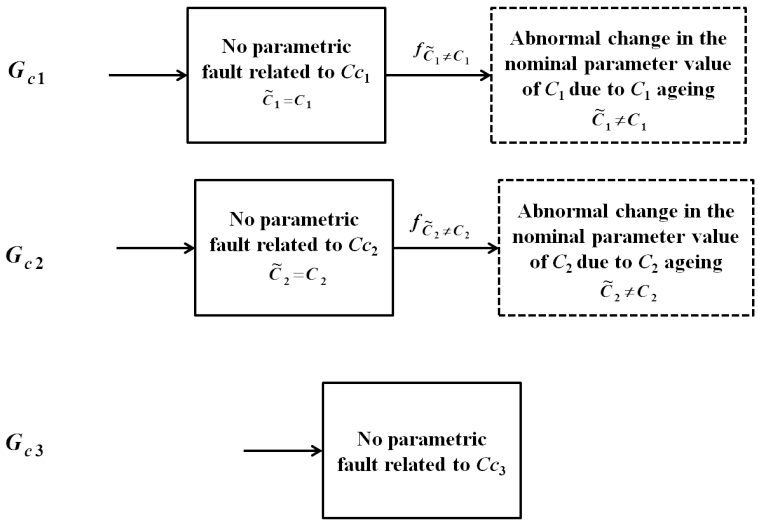

Figure 5.5: Continuous component model $Cc_i,\ i \in \{1,2,3\}$, denoted by $G_{ci},\ i \in \{1,2,3\}$, for the three cell converter.

- The discrete state of S_1, represented by real discrete output h_q^1, influences the dynamic evolution of Vc_1 and I.
- The discrete state of S_2, represented by h_q^2, impacts the dynamic evolution of Vc_1, Vc_2 and I.
- The discrete state of S_3, represented by h_q^3, influences the dynamic evolution of Vc_1 and Vc_2.

Thus, the three cell converter system is decomposed into three interacting hybrid components HCs as shown in Fig.5.6:

- HC_1 is composed of switch S_1 (Dc_1), Vc_1 (Cc_1) and I (Cc_3);
- HC_2 is composed of switch S_2 (Dc_2), Vc_1 (Cc_1), Vc_2 (Cc_2) and I (Cc_3);
- HC_3 is composed of switch S_3 (Dc_3), Vc_2 (Cc_2) and I (Cc_3).

Local hybrid model G^1 of the component HC_1 is obtained by synchronizing the discrete local automaton DG^1 of Dc_1 and the set of local automata G_{c1} and G_{c3} of, respectively, Cc_1 and Cc_3 using parallel or synchronous composition operator (see subsection 3.2.4). Therefore, G^1 is equal to $DG^1||G_{c1}||G_{c3}$. The state corresponding to the multiple faults are removed from G^1.

Based on (3.22), local hybrid automaton G^1 characterizing HC_1 hybrid dynamics is defined by the tuple (see Fig.5.7 and Fig.5.8):

$$G^1 = (Q^1, h_q^1, \tilde{h}_q^1, \Sigma^1, X^1, flux^1, r^1, \delta^1, HSL^1, Init^1) \tag{5.10}$$

where,

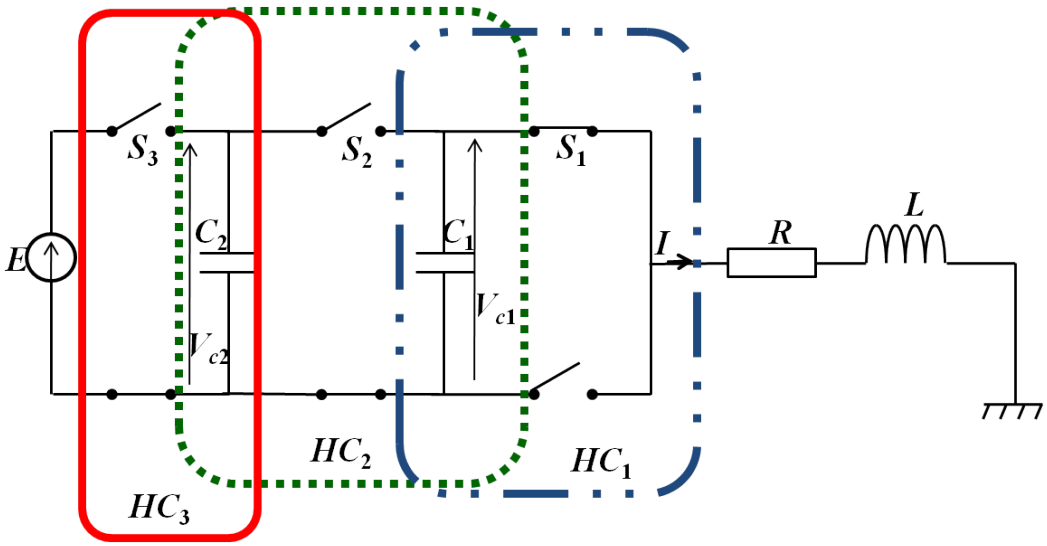

Figure 5.6: Three-cell converter decomposition.

- $Q^1 = \{q_1^1,\ q_2^1,\ q_3^1,\ q_4^1,\ q_5^1,\ q_6^1,\ q_7^1,\ q_8^1\}$. q_1^1 and q_2^1 represent, respectively, switch S_1 closed, S_1C, and switch S_1 opened, S_1O, in normal operating conditions for switch S_1 and capacitor C_1. q_3^1 and q_4^1 characterize S_1 stuck opened discrete failure mode, S_1SO. q_5^1 and q_6^1 characterize S_1 stuck closed discrete failure mode, S_1SC. $Q_c^1 = \{q_7^1,\ q_8^1\}$ characterize the failure mode of C_1 due to its electrical chemical aging in each discrete mode of HC_1, $S_1O(\tilde{C}_1 \neq C_1)$ and $S_1C(\tilde{C}_1 \neq C_1)$;
- $h_q^1 : Q^1 \rightarrow \{0,1\} = \{0\ (S_1 \text{ opened}),\ 1\ (S_1 \text{ closed})\}$;
- $\tilde{h}_q^1 : Q^1 \rightarrow \{0,1\} = \{0\ (S_1 \text{ should be opened}),\ 1\ (S_1 \text{ should be closed})\}$;
- $\Sigma^1 = \Sigma_o^1 \bigcup \Sigma_u^1$: is the set of HC_1 discrete events. $\Sigma_o^1 = \{OS_1\ (\text{open } S_1),\ CS_1\ (\text{close } S_1)\}$, $\Sigma_u^1 = \Sigma_f^1 = \{f_{S_1SO}$ (fault event leading to S_1 stuck opened discrete failure mode), f_{S_1SC} (fault event leading to S_1 stuck closed discrete failure mode), $f_{\tilde{C}_1 \neq C_1}$ (fault event indicating the occurrence of electrical chemical aging of $C_1)\}$. The fault, f_{S_1SO} can occur at the state where S_1 is opened and f_{S_1SC} can occur at the state where S_1 is closed. While $f_{\tilde{C}_1 \neq C_1}$ can occur whatever the discrete mode of HC_1 is.
- $\delta^1 : Q^1 \times \Sigma^1 \rightarrow Q^1$: is the HC_1 state transition function. As an example $\delta^1(q_2^1, OS_1) = q_1^1$ (see Fig.5.8);
- $X^1 = \begin{bmatrix} Vc_1 & I \end{bmatrix}^T$: is a finite set of continuous variables associated to S_1;
- $flux^1 = \{\dot{X}^1,\ \tilde{\dot{X}}^1\}$ are the real $\dot{X}^1 = \begin{bmatrix} \dot{V}c_1^1 & \dot{I}^1 \end{bmatrix}^T$ and nominal $\tilde{\dot{X}}^1 = \begin{bmatrix} \tilde{\dot{V}}c_1^{\,1} & \dot{I}^1 \end{bmatrix}^T$ dynamic evolution parts of X^1 according to each discrete state of switch S_1;

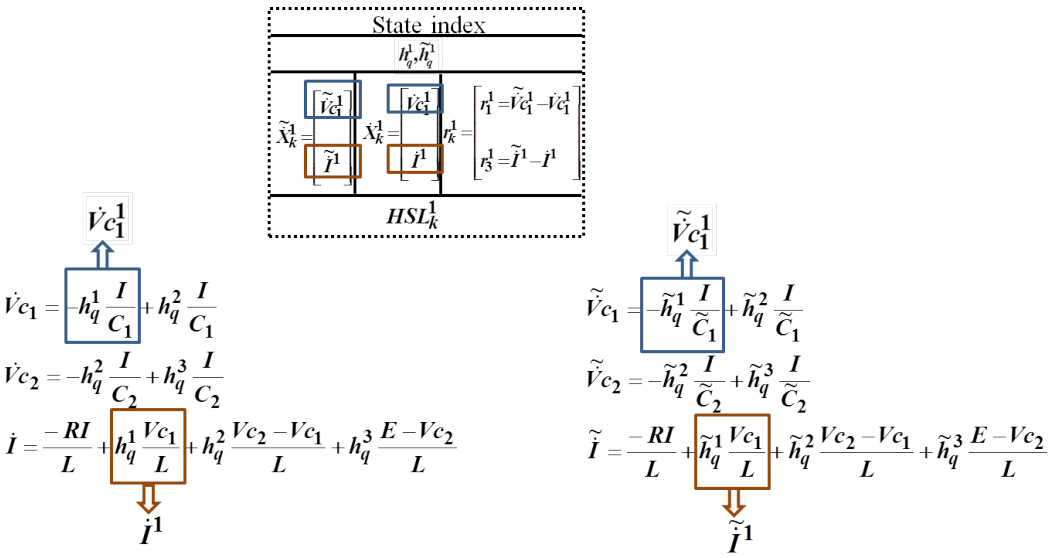

Figure 5.7: Local hybrid state of HC_1.

- $r^1 = \begin{bmatrix} r_1^1 & r_3^1 \end{bmatrix}^T$ is the part of residual r generated in the switch S_1 discrete states;
- $HSL^1 = \{N_1$ (Absence of faults in HC_1), F_1 (S_1 stuck opened), F_2 (S_1 stuck closed), F_7 (parametric fault in C_1 due to its electrical chemical aging)$\}$. As an example, status label for q_1^1, HSL_1^1, is equal to N_1;
- $Init^1$: $(q_1^1,\ h_{q_1^1}^1 = \tilde{h}_{q_1^1}^1 = 1,\ \dot{X}^1 = \dot{\tilde{X}}^1 = \begin{bmatrix} \frac{-I}{\tilde{C}_1} & \frac{Vc_1}{L} \end{bmatrix}^T,\ HSL_{q_1^1} = N_1)$: is the set of initial conditions.

As we have done for constructing G^1, local hybrid automaton G^2 characterizing HC_2 hybrid dynamics is defined by the tuple (see Fig.5.9):

$$G^2 = (Q^2, h_q^2, \tilde{h}_q^2, \Sigma^2, X^2, flux^2, r^2, \delta^2, HSL^2, Init^2) \tag{5.11}$$

where,

- $Q^2 = \{q_1^2,\ q_2^2,\ q_3^2,\ q_4^2,\ q_5^2,\ q_6^2,\ q_7^2,\ q_8^2,\ q_9^2,\ q_{10}^2\}$. q_1^2 and q_2^2 represent, respectively, switch S_2 opened, S_2O, and switch S_2 closed, S_2C, in normal operating conditions for switch S_2, capacitor C_1 and capacitor C_2. q_3^2 and q_4^2 characterize S_2 stuck opened discrete failure mode, S_2SO. q_5^2 and q_6^2 characterize S_2 stuck closed discrete failure mode, S_2SC. $Q_c^2 = \{q_7^2,\ q_8^2,\ q_9^2,\ q_{10}^2\}$. q_7^2 and q_8^2 characterize the failure mode of C_1 due to its electrical chemical aging in each discrete mode of HC_2, $S_2O(\tilde{C}_1 \neq C_1)$ and $S_2C(\tilde{C}_1 \neq C_1)$. q_9^2 and q_{10}^2 characterize the failure mode of C_2 due to its electrical chemical aging in each discrete mode of HC_2, $S_2O(\tilde{C}_2 \neq C_2)$ and $S_2C(\tilde{C}_2 \neq C_2)$;
- $h_q^2 : Q^2 \rightarrow \{0, 1\} = \{0$ (S_2 opened), 1 (S_2 closed)$\}$;

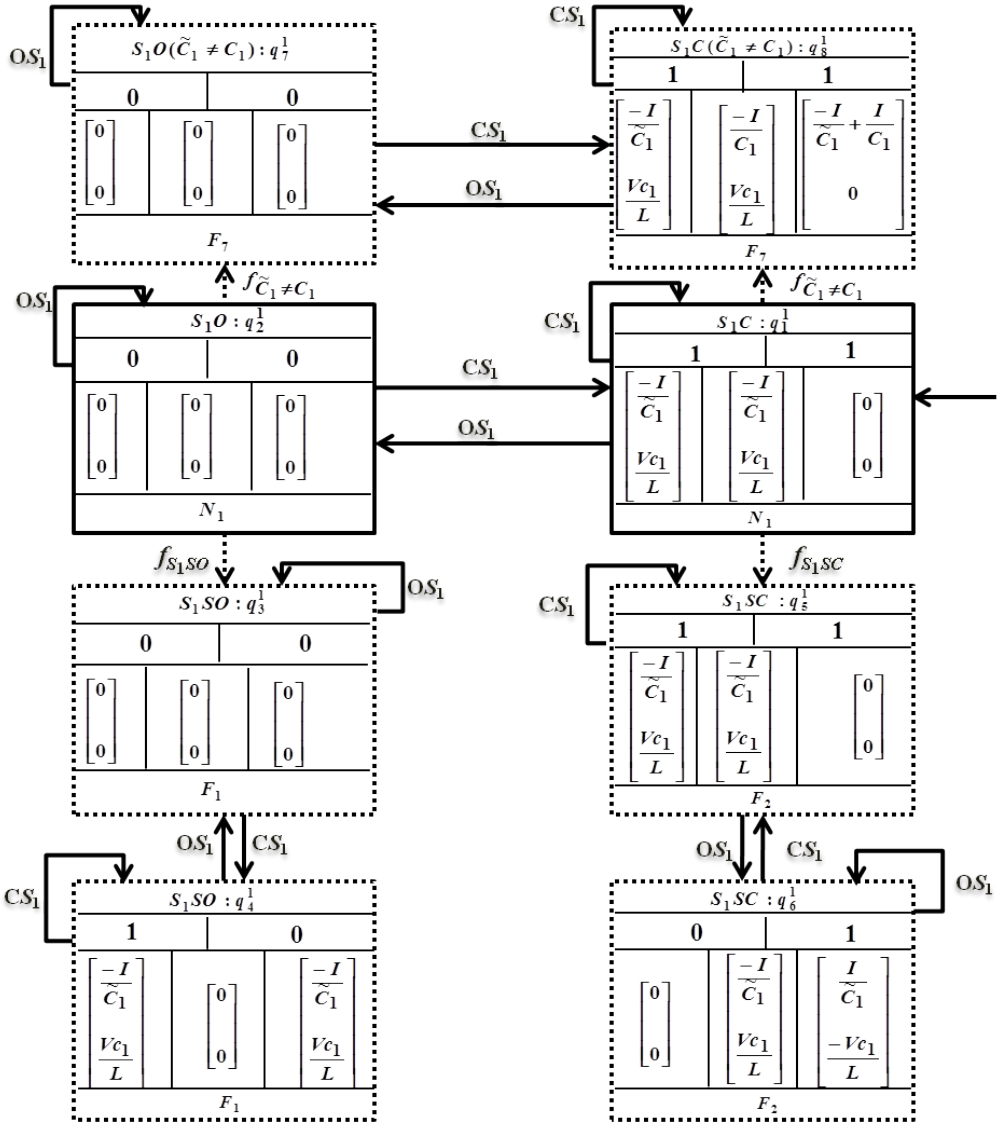

Figure 5.8: Hybrid automaton G^1 for HC_1.

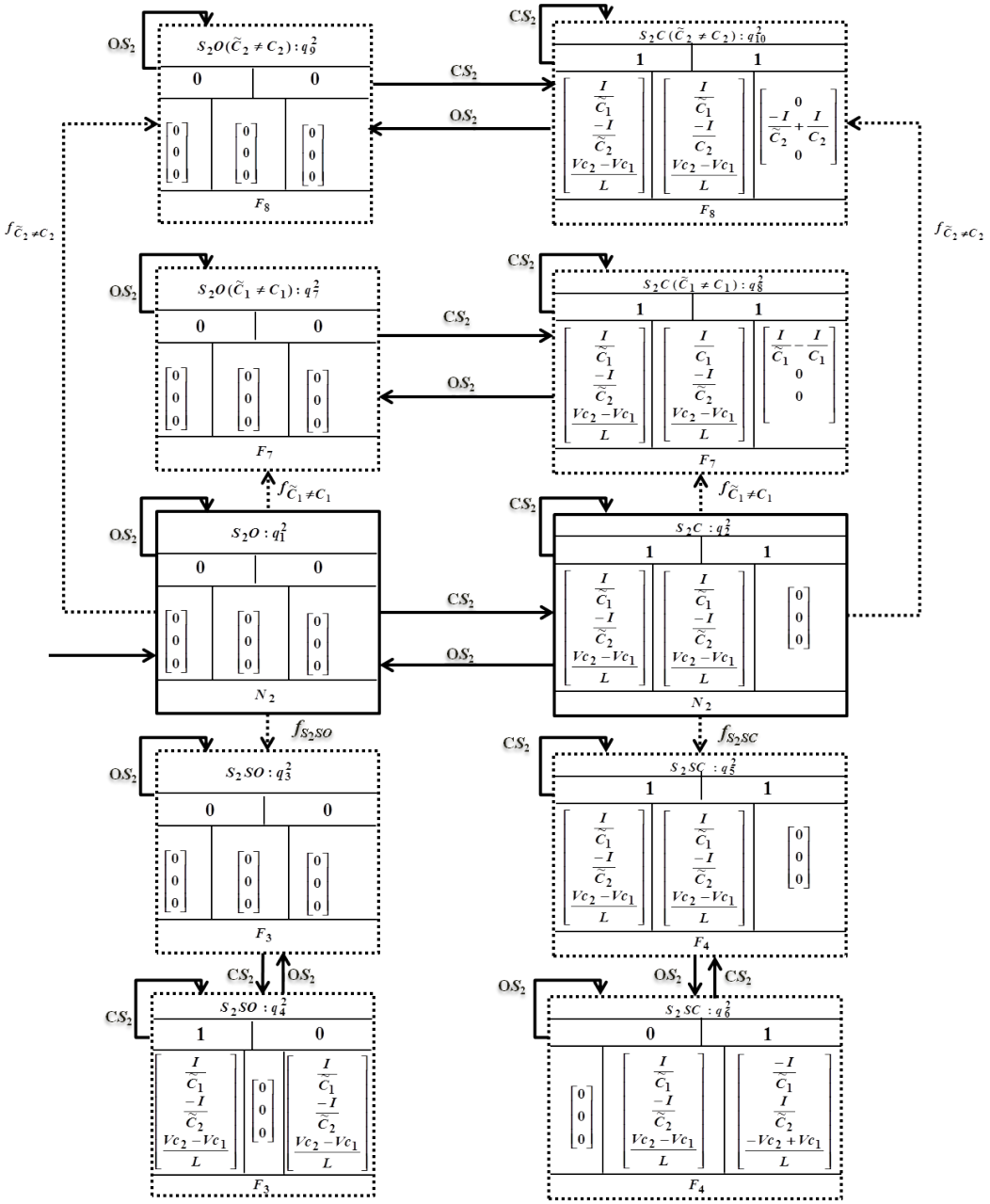

Figure 5.9: Hybrid automaton G^2 for HC_2.

- $\tilde{h}_q^2 : Q^2 \rightarrow \{0,1\} = \{0$ (S_2 should be opened), 1 (S_2 should be closed)$\}$;
- $\Sigma^2 = \Sigma_o^2 \bigcup \Sigma_u^2$: is the set of HC_2 discrete events. $\Sigma_o^2 = \{OS_2$ (open S_2), CS_2 (close S_2)$\}$, $\Sigma_u^2 = \Sigma_f^2 = \{f_{S_2SO}$ (fault event leading to S_2 stuck opened discrete failure mode), f_{S_2SC} (fault event leading to S_2 stuck closed discrete failure mode), $f_{\tilde{C}_1 \neq C_1}$, $f_{\tilde{C}_2 \neq C_2}$ (fault event indicating the occurrence of parametric fault in C_2 due to its electrical chemical aging)$\}$. The fault, f_{S_2SO} can occur at the state where S_2 is opened and f_{S_2SC} can occur at the state where S_2 is closed. While $f_{\tilde{C}_1 \neq C_1}$ and $f_{\tilde{C}_2 \neq C_2}$can occur whatever the discrete mode of HC_2 is.
- $\delta^2 : Q^2 \times \Sigma^2 \rightarrow Q^2$: is the HC_2 state transition function. As an example, $\delta^2(q_1^2, CS_2) = q_2^2$ (see Fig.5.9);
- $X^2 = \begin{bmatrix} Vc_1 & Vc_2 & I \end{bmatrix}^T$: is a finite set of continuous variables associated to S_2;
- $flux^2 = \{\dot{X}^2, \tilde{\dot{X}}^2\}$: are the real $\dot{X}^2 = \begin{bmatrix} \dot{V}c_1^2 & \dot{V}c_2^2 & \dot{I}^2 \end{bmatrix}^T$ and nominal $\tilde{\dot{X}}^2 = \begin{bmatrix} \tilde{\dot{V}}c_1^{\,2} & \tilde{\dot{V}}c_2^{\,2} & \dot{I}^2 \end{bmatrix}^T$ dynamic evolution parts of X^2 according to discrete state of switch S_2;
- $r^2 = \begin{bmatrix} r_1^2 & r_2^2 & r_3^2 \end{bmatrix}^T$ is the part of residual r generated in the switch S_2 discrete states;
- $HSL^2 = \{N_2$ (Absence of the faults in HC_2), F_3 (S_2 stuck opened), F_4 (S_2 stuck closed), F_7, F_8. As an example status label for q_1^2, HSL_1^2, is equal to N_2;
- $Init^2$: $(q_1^2,\ h_{q_1^2}^2 = \tilde{h}_{q_1^2}^2 = 0,\ \dot{X}^2 = \tilde{\dot{X}}^2 = \begin{bmatrix} 0 & 0 & 0 \end{bmatrix}^T,\ HSL_{q_1^2} = N_2)$: is the set of initial conditions.

Likewise, local hybrid automaton G^3 characterizing HC_3 hybrid dynamics is defined by the tuple (see Fig.5.10):

$$G^3 = (Q^3, h_q^3, \tilde{h}_q^3, \Sigma^3, X^3, flux^3, r^3, \delta^3, HSL^3, Init^3) \tag{5.12}$$

where,

- $Q^3 = \{q_1^3,\ q_2^3,\ q_3^3,\ q_4^3,\ q_5^3,\ q_6^3,\ q_7^3,\ q_8^3\}$. q_1^3 and q_2^3 represent, respectively, switch S_3 opened, S_3O, and switch S_3 closed, S_3C, in normal operating conditions for switch S_3 and capacitor C_2. q_3^3 and q_4^3 characterize S_3 stuck opened discrete failure mode, S_3SO. q_5^3 and q_6^3 characterize S_3 stuck closed discrete failure mode, S_3SC. $Q_c^3 = \{q_7^3,\ q_8^3\}$ characterize the failure mode of C_2 due to its electrical chemical aging in each discrete mode of HC_3, $S_3O(\tilde{C}_2 \neq C_2)$ and $S_3C(\tilde{C}_2 \neq C_2)$;
- $h_q^3 : Q^3 \rightarrow \{0,1\} = \{0$ (S_3 opened), 1 (S_3 closed)$\}$;

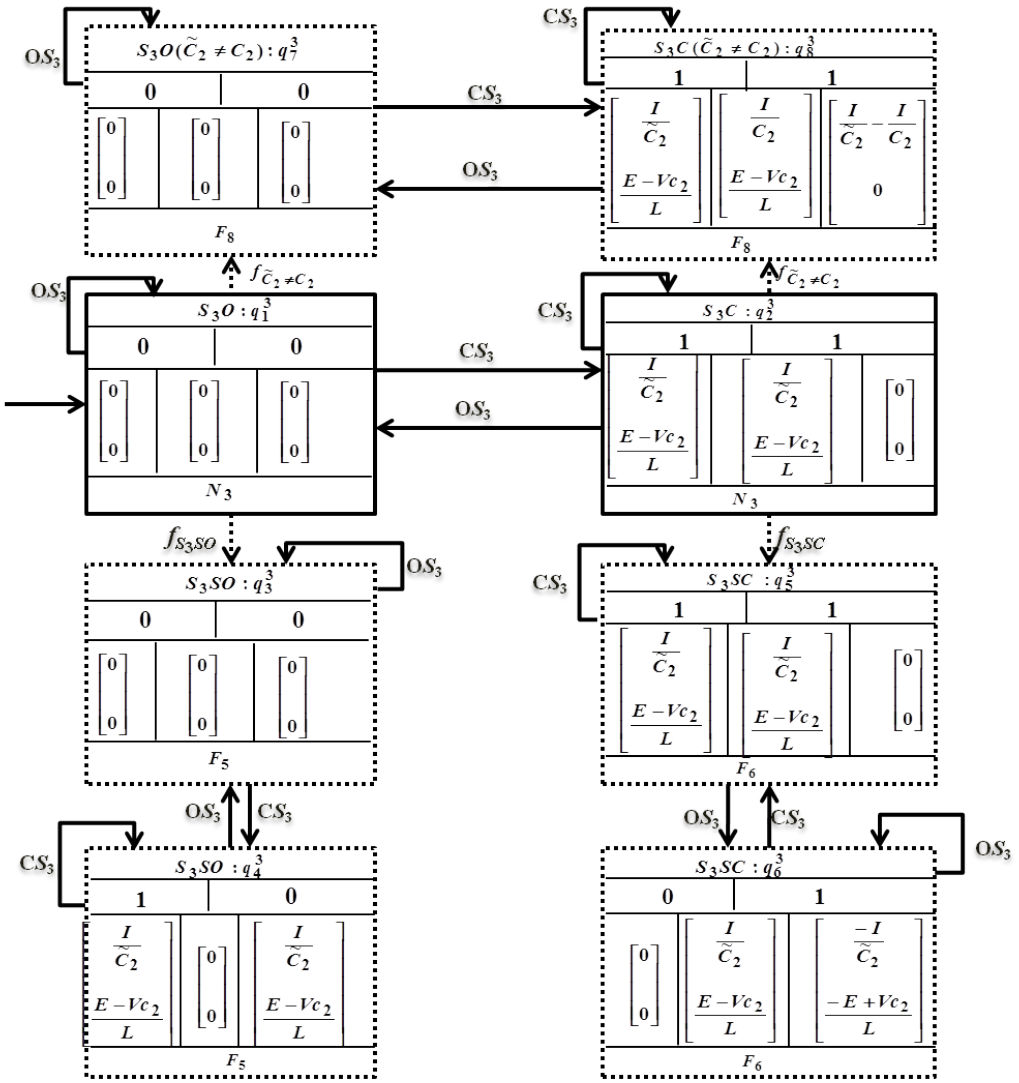

Figure 5.10: Hybrid automaton G^3 for HC_3.

- $\tilde{h}_q^3 : Q^3 \rightarrow \{0,1\} = \{0$ (S_3 should be opened), 1 (S_3 should be closed)$\}$;
- $\Sigma^3 = \Sigma_o^3 \bigcup \Sigma_u^3$: is the set of HC_3 discrete events. $\Sigma_o^3 = \{OS_3$ (open S_3), CS_3 (close S_3)$\}$, $\Sigma_u^3 = \Sigma_f^3 = \{f_{S_3SO}$ (fault event leading to S_3 stuck opened discrete failure mode), f_{S_3SC} (fault event leading to S_3 stuck closed discrete failure mode), $f_{\tilde{C}_2 \neq C_2}\}$. The fault, f_{S_3SO} can occur at the state where S_3 is opened and f_{S_3SC} can occur at the state where S_3 is closed. While $f_{\tilde{C}_2 \neq C_2}$ can occur whatever the discrete mode of HC_3 is.
- $\delta^3 : Q^3 \times \Sigma^3 \rightarrow Q^3$: is the HC_3 state transition function. As an example, $\delta^3(q_2^3, CS_3) = q_1^3$ (see Fig.5.10);
- $X^3 = \left[\begin{array}{cc} Vc_2 & I \end{array} \right]^T$: is a finite set of continuous variables associated to S_3;
- $flux^3 = \{\dot{X}^3, \tilde{\dot{X}}^3\}$: are the real $\dot{X}^3 = \left[\begin{array}{cc} \dot{V}c_2^3 & \dot{I}^3 \end{array} \right]^T$ and nominal $\tilde{\dot{X}}^3 = \left[\begin{array}{cc} \tilde{\dot{V}}c_2^3 & \dot{I}^3 \end{array} \right]^T$ dynamic evolution parts of X^3 according to discrete state of switch S_3;
- $r^3 = \left[\begin{array}{cc} r_2^3 & r_3^3 \end{array} \right]^T$ is the part of residual r generated in the switch S_3 discrete states;
- $HSL^3 = \{N_3$ (Absence of the faults in HC_3), F_5 (S_3 stuck opened), F_6 (S_3 stuck closed), F_8. As an example status label for q_1^3, HSL_1^3, is equal to N_3;
- $Init^3$: $(q_1^3,\ h_{q_1^3}^3 = \tilde{h}_{q_1^3}^3 = 0,\ \dot{X}^3 = \tilde{\dot{X}}^3 = \left[\begin{array}{cc} 0 & 0 \end{array} \right]^T,\ HSL_{q_1^3} = N_3)$: is the set of initial conditions.

5.4 Local hybrid diagnoser

5.4.1 Global fault signature construction

For the three cell converter, the system generates a specific fault signature in each hybrid global state ($q^1q^2q^3$) according to the global residuals $r = \left[\begin{array}{ccc} r_1 & r_2 & r_3 \end{array} \right]^T$. These fault signatures are generated using the continuous dynamic evolutions $\tilde{\dot{X}} = \left[\begin{array}{ccc} \tilde{\dot{V}}c_1 & \tilde{\dot{V}}c_2 & \tilde{\dot{I}} \end{array} \right]^T$ and $\dot{X} = \left[\begin{array}{ccc} \dot{V}c_1 & \dot{V}c_2 & \dot{I} \end{array} \right]^T$.

Based on (5.8), in normal operating mode, the system generates the following normal fault signature:
$sig_0 = (r_1^0, UC_1)\&(r_2^0, UC_2)\&(r_3^0, UC_3)$
The residual in these conditions is equal to zero; there is no fault in the system: $(\tilde{h}_q^1 = h_q^1)$, $(\tilde{h}_q^2 = h_q^2)$, $(\tilde{h}_q^3 = h_q^3)$, $(\tilde{C}_1 = C_1)$ and $(\tilde{C}_2 = C_2)$.

Let us consider the occurrence of a fault of type F_1 (S_1SO), residuals $r = \left[\begin{array}{ccc} r_1 & r_2 & r_3 \end{array} \right]^T$ are computed as follows:

$$\begin{cases} r_1 = \left(-\left(\tilde{h}_q^1 = 1\right)\frac{1}{\tilde{C}_1} + \left(h_q^1 = 0\right)\frac{1}{C_1}\right) I + \left(\tilde{h}_q^2\frac{1}{\tilde{C}_1} - h_q^2\frac{1}{C_1}\right) I \\ r_2 = \left(-\tilde{h}_q^2\frac{1}{\tilde{C}_2} + h_q^2\frac{1}{C_2}\right) I + \left(\tilde{h}_q^3\frac{1}{\tilde{C}_2} - h_q^3\frac{1}{C_2}\right) I \\ r_3 = \left(-\frac{R}{L}I + \frac{R}{L}I\right) + \left(\left(\tilde{h}_q^1 = 1\right) - \left(h_q^1 = 0\right)\right)\frac{1}{L}Vc_1 + \left(\tilde{h}_q^2 - h_q^2\right)\frac{1}{L}(Vc_2 - Vc_1) \\ \quad + \left(\tilde{h}_q^3 - h_q^3\right)\frac{1}{L}(E - Vc_2) \end{cases}$$

Since only simple fault scenario is considered and in the case of the occurrence of a fault of type F_1, i.e., S_1 stuck opened, $\tilde{h}_q^2$ and $\tilde{h}_q^3$ are equal, respectively, to h_q^2 and h_q^3 and $\tilde{C}_1$ and $\tilde{C}_2$ are equal, respectively, to C_1 and C_2. Therefore in this case, residuals r are equal to:

$$\begin{cases} r_1 = -\frac{1}{\tilde{C}_1}I \\ r_2 = 0 \\ r_3 = \frac{1}{L}Vc_1 \end{cases} \tag{5.13}$$

Thus, in response to the abrupt change in r caused by the occurrence of a fault of type F_1, the system generates the following fault signature:

$$sig_1 = (r_1^-, NC_1^1)\&(r_2^0, UC_2)\&(r_3^+, PC_3^1)$$

where $NC_1^1 = -\frac{1}{\tilde{C}_1}I$ and $PC_3^1 = \frac{1}{L}Vc_1$.

Let us now consider the occurrence of a fault of type F_2 (S_1SC), residuals r are computed as follows:

$$\begin{cases} r_1 = \left(-\left(\tilde{h}_q^1 = 0\right)\frac{1}{\tilde{C}_1} + \left(h_q^1 = 1\right)\frac{1}{C_1}\right) I + \left(\tilde{h}_q^2\frac{1}{\tilde{C}_1} - h_q^2\frac{1}{C_1}\right) I \\ r_2 = \left(-\tilde{h}_q^2\frac{1}{\tilde{C}_2} + h_q^2\frac{1}{C_2}\right) I + \left(\tilde{h}_q^3\frac{1}{\tilde{C}_2} - h_q^3\frac{1}{C_2}\right) I \\ r_3 = \left(-\frac{R}{L}I + \frac{R}{L}I\right) + \left(\left(\tilde{h}_q^1 = 0\right) - \left(h_q^1 = 1\right)\right)\frac{1}{L}Vc_1 + \left(\tilde{h}_q^2 - h_q^2\right)\frac{1}{L}(Vc_2 - Vc_1) \\ \quad + \left(\tilde{h}_q^3 - h_q^3\right)\frac{1}{L}(E - Vc_2) \end{cases}$$

Since only simple fault scenario is considered and in the case of the occurrence of a fault of type F_2, i.e., S_1 stuck closed, $\tilde{h}_q^2$ and $\tilde{h}_q^3$ are equal, respectively, to h_q^2 and h_q^3 and $\tilde{C}_1$ and $\tilde{C}_2$ are equal, respectively, to C_1 and C_2. Therefore in this case, residuals r are equal to:

$$\begin{cases} r_1 = \frac{1}{\tilde{C}_1}I \\ r_2 = 0 \\ r_3 = -\frac{1}{L}Vc_1 \end{cases} \tag{5.14}$$

Thus, in response to the abrupt change in r caused by the occurrence of a fault of type F_2, the system generates the following fault signature:

$$sig_2 = (r_1^+, PC_1^1)\&(r_2^0, UC_2)\&(r_3^-, NC_3^1)$$

where $PC_1^1 = \frac{1}{\tilde{C}_1}I$ and $NC_3^1 = -\frac{1}{L}Vc_1$.

Let us now consider the occurrence of a fault of type F_3 (S_2SO), residuals r are computed as follows:

$$\begin{cases} r_1 = \left(-\tilde{h}_q^1 \frac{1}{\tilde{C}_1} + h_q^1 \frac{1}{C_1}\right) I + \left(\left(\tilde{h}_q^2 = 1\right) \frac{1}{\tilde{C}_1} - \left(h_q^2 = 0\right) \frac{1}{C_1}\right) I \\ r_2 = \left(\left(-\tilde{h}_q^2 = 1\right) \frac{1}{\tilde{C}_2} + \left(h_q^2 = 0\right) \frac{1}{C_2}\right) I + \left(\tilde{h}_q^3 \frac{1}{\tilde{C}_2} - h_q^3 \frac{1}{C_2}\right) I \\ r_3 = \left(-\frac{R}{L} I + \frac{R}{L} I\right) + \left(\tilde{h}_q^1 - h_q^1\right) \frac{1}{L} Vc_1 + \left(\left(\tilde{h}_q^2 = 1\right) - \left(h_q^2 = 0\right)\right) \frac{1}{L}(Vc_2 - Vc_1) + \\ \quad \left(\tilde{h}_q^3 - h_q^3\right) \frac{1}{L}(E - Vc_2) \end{cases}$$

Since only simple fault scenario is considered and in the case of the occurrence of a fault of type F_3, i.e., S_2 stuck opened, $\tilde{h}_q^1$ and $\tilde{h}_q^3$ are equal, respectively, to h_q^1 and h_q^3 and $\tilde{C}_1$ and $\tilde{C}_2$ are equal, respectively, to C_1 and C_2. Therefore in this case, residuals r are equal to:

$$\begin{cases} r_1 = \frac{1}{\tilde{C}_1} I \\ r_2 = -\frac{1}{\tilde{C}_2} I \\ r_3 = \frac{1}{L}(Vc_2 - Vc_1) \end{cases} \tag{5.15}$$

Thus, in response to the abrupt change in r caused by the occurrence of a fault of type F_3, the system generates the following fault signature:

$$sig_3 = (r_1^+, PC_1^2) \& (r_2^-, NC_2^2) \& (r_3^+, PC_3^2)$$

where $PC_1^2 = \frac{1}{\tilde{C}_1} I$, $NC_2^2 = -\frac{1}{\tilde{C}_2} I$ and $PC_3^1 = \frac{1}{L}(Vc_2 - Vc_1)$.

Let us now consider the occurrence of a fault of type F_4 (S_2SC), residuals r are computed as follows:

$$\begin{cases} r_1 = \left(-\tilde{h}_q^1 \frac{1}{\tilde{C}_1} + h_q^1 \frac{1}{C_1}\right) I + \left(\left(\tilde{h}_q^2 = 0\right) \frac{1}{\tilde{C}_1} - \left(h_q^2 = 1\right) \frac{1}{C_1}\right) I \\ r_2 = \left(\left(-\tilde{h}_q^2 = 0\right) \frac{1}{\tilde{C}_2} + \left(h_q^2 = 1\right) \frac{1}{C_2}\right) I + \left(\tilde{h}_q^3 \frac{1}{\tilde{C}_2} - h_q^3 \frac{1}{C_2}\right) I \\ r_3 = \left(-\frac{R}{L} I + \frac{R}{L} I\right) + \left(\tilde{h}_q^1 - h_q^1\right) \frac{1}{L} Vc_1 + \left(\left(\tilde{h}_q^2 = 0\right) - \left(h_q^2 = 1\right)\right) \frac{1}{L}(Vc_2 - Vc_1) + \\ \quad \left(\tilde{h}_q^3 - h_q^3\right) \frac{1}{L}(E - Vc_2) \end{cases}$$

Since only simple fault scenario is considered and in the case of the occurrence of a fault of type F_4, i.e., S_2 stuck closed, $\tilde{h}_q^1$ and $\tilde{h}_q^3$ are equal, respectively, to h_q^1 and h_q^3 and $\tilde{C}_1$ and $\tilde{C}_2$ are equal, respectively, to C_1 and C_2. Therefore in this case, residuals r are equal to:

$$\begin{cases} r_1 = -\frac{1}{\tilde{C}_1} I \\ r_2 = \frac{1}{\tilde{C}_2} I \\ r_3 = -\frac{1}{L}(Vc_2 - Vc_1) \end{cases} \tag{5.16}$$

Thus, in response to the abrupt change in r caused by the occurrence of a fault of type F_4, the system generates the following fault signature

$$sig_4 = (r_1^-, NC_1^2) \& (r_2^+, PC_2^2) \& (r_3^-, NC_3^2)$$

where $NC_1^2 = -\frac{1}{\tilde{C}_1} I$, $PC_2^2 = \frac{1}{\tilde{C}_2} I$ and $NC_3^1 = -\frac{1}{L}(Vc_2 - Vc_1)$.

Let us now consider the occurrence of a fault of type F_5 (S_3SO), residuals r is computed as follows:

$$\begin{cases} r_1 = \left(-\tilde{h}_q^1 \frac{1}{\tilde{C}_1} + h_q^1 \frac{1}{C_1}\right) I + \left(\tilde{h}_q^2 \frac{1}{\tilde{C}_1} - h_q^2 \frac{1}{C_1}\right) I \\ r_2 = \left(\tilde{h}_q^2 \frac{1}{\tilde{C}_2} + h_q^2 \frac{1}{C_2}\right) I + \left(\left(\tilde{h}_q^3 = 1\right) \frac{1}{\tilde{C}_2} - \left(h_q^3 = 0\right) \frac{1}{C_2}\right) I \\ r_3 = \left(-\frac{R}{L} I + \frac{R}{L} I\right) + \left(\tilde{h}_q^1 - h_q^1\right) \frac{1}{L} Vc_1 + \left(\tilde{h}_q^2 - h_q^2\right) \frac{1}{L}(Vc_2 - Vc_1) + \\ \quad \left(\left(\tilde{h}_q^3 = 1\right) - \left(h_q^3 = 0\right)\right) \frac{1}{L}(E - Vc_2) \end{cases}$$

Since only simple fault scenario is considered and in the case of the occurrence of a fault of type F_5, i.e., S_3 stuck opened, $\tilde{h}_q^1$ and $\tilde{h}_q^2$ are equal, respectively, to h_q^1 and h_q^2 and $\tilde{C}_1$ and $\tilde{C}_2$ are equal, respectively, to C_1 and C_2. Therefore in this case, residuals r are equal to:

$$\begin{cases} r_1 = 0 \\ r_2 = \frac{1}{\tilde{C}_2} I \\ r_3 = \frac{1}{L}(E - Vc_2) \end{cases} \tag{5.17}$$

Thus, in response to the abrupt change in r caused by the occurrence of a fault of type F_5, the system generates the following fault signature:

$$sig_5 = (r_1^0, UC_1) \& (r_2^+, PC_2^3) \& (r_3^+, PC_3^3)$$

where $PC_2^3 = \frac{1}{\tilde{C}_2} I$ and $PC_3^3 = \frac{1}{L}(E - Vc_2)$.

Let us now consider the occurrence of a fault of type F_6 (S_3SC), residuals r is computed as follows:

$$\begin{cases} r_1 = \left(-\tilde{h}_q^1 \frac{1}{\tilde{C}_1} + h_q^1 \frac{1}{C_1}\right) I + \left(\tilde{h}_q^2 \frac{1}{\tilde{C}_1} - h_q^2 \frac{1}{C_1}\right) I \\ r_2 = \left(\tilde{h}_q^2 \frac{1}{\tilde{C}_2} + h_q^2 \frac{1}{C_2}\right) I + \left(\left(\tilde{h}_q^3 = 0\right) \frac{1}{\tilde{C}_2} - \left(h_q^3 = 1\right) \frac{1}{C_2}\right) I \\ r_3 = \left(-\frac{R}{L} I + \frac{R}{L} I\right) + \left(\tilde{h}_q^1 - h_q^1\right) \frac{1}{L} Vc_1 + \left(\tilde{h}_q^2 - h_q^2\right) \frac{1}{L}(Vc_2 - Vc_1) + \\ \quad \left(\left(\tilde{h}_q^3 = 0\right) - \left(h_q^3 = 1\right)\right) \frac{1}{L}(E - Vc_2) \end{cases}$$

Since only simple fault scenario is considered and in the case of the occurrence of a fault of type F_6, i.e., S_3 stuck closed, $\tilde{h}_q^1$ and $\tilde{h}_q^2$ are equal, respectively, to h_q^1 and h_q^2 and $\tilde{C}_1$ and $\tilde{C}_2$ are equal, respectively, to C_1 and C_2. Therefore in this case, residuals r are equal to:

$$\begin{cases} r_1 = 0 \\ r_2 = -\frac{1}{\tilde{C}_2} I \\ r_3 = -\frac{1}{L}(E - Vc_2) \end{cases} \tag{5.18}$$

Thus, in response to the abrupt change in r caused by the occurrence of a fault of type F_6, the system generates the following fault signature:

$$sig_6 = (r_1^0, UC_1) \& (r_2^-, NC_2^3) \& (r_3^-, NC_3^3)$$

where $NC_2^3 = -\frac{1}{\tilde{C}_2} I$ and $NC_3^3 = -\frac{1}{L}(E - Vc_2)$.

Let us now consider the occurrence of a fault of type F_7, residuals r is computed as follows:

$$\begin{cases} r_1 = \left(-\tilde{h}_q^1 \frac{1}{\tilde{C}_1} + h_q^1 \frac{1}{C_1}\right) I + \left(\tilde{h}_q^2 \frac{1}{\tilde{C}_1} - h_q^2 \frac{1}{C_1}\right) I \\ r_2 = \left(\tilde{h}_q^2 \frac{1}{\tilde{C}_2} + h_q^2 \frac{1}{C_2}\right) I + \left(\tilde{h}_q^3 \frac{1}{\tilde{C}_2} - h_q^3 \frac{1}{C_2}\right) I \\ r_3 = (-\frac{R}{L} I + \frac{R}{L} I) + \left(\tilde{h}_q^1 - h_q^1\right) \frac{1}{L} Vc_1 + \left(\tilde{h}_q^2 - h_q^2\right) \frac{1}{L} (Vc_2 - Vc_1) + \\ \quad \left(\tilde{h}_q^3 - h_q^3\right) \frac{1}{L} (E - Vc_2) \end{cases}$$

Since only simple fault scenario is considered and in the case of the occurrence of a fault of type F_7, i.e., parametric fault in C_1 due to its electrical chemical aging, $\tilde{h}_q^1$, $\tilde{h}_q^2$ and $\tilde{h}_q^3$ are equal, respectively, to h_q^1, h_q^2 and h_q^3 and $\tilde{C}_2$ is equal to C_2. Therefore, residuals r are equal to:

- when $\tilde{h}_q^1 = h_q^1 = \tilde{h}_q^2 = h_q^2 = 0$:

$$\begin{cases} r_1 = 0 \\ r_2 = 0 \\ r_3 = 0 \end{cases} \tag{5.19}$$

- when $\tilde{h}_q^1 = h_q^1 = \tilde{h}_q^2 = h_q^2 = 1$:

$$\begin{cases} r_1 = 0 \\ r_2 = 0 \\ r_3 = 0 \end{cases} \tag{5.20}$$

- when $\tilde{h}_q^1 = h_q^1 = 0$ and $\tilde{h}_q^2 = h_q^2 = 1$:

$$\begin{cases} r_1 = \left(\frac{1}{\tilde{C}_1} - \frac{1}{C_1}\right) I \\ r_2 = 0 \\ r_3 = 0 \end{cases} \tag{5.21}$$

- when $\tilde{h}_q^1 = h_q^1 = 1$ and $\tilde{h}_q^2 = h_q^2 = 0$:

$$\begin{cases} r_1 = -\left(\frac{1}{\tilde{C}_1} - \frac{1}{C_1}\right) I \\ r_2 = 0 \\ r_3 = 0 \end{cases} \tag{5.22}$$

Thus, in response to a change in r caused by the occurrence of a fault of type F_7, the system generates one of the following three fault signatures according to the discrete state of S_1 and S_2:

- when $\tilde{h}_q^1 = h_q^1 = \tilde{h}_q^2 = h_q^2 = 1$ or $\tilde{h}_q^1 = h_q^1 = \tilde{h}_q^2 = h_q^2 = 0$:

  $sig_0 = (r_1^0, UC_1)\&(r_2^0, UC_2)\&(r_3^0, UC_3)$

- when $\tilde{h}_q^1 = h_q^1 = 1$ and $\tilde{h}_q^2 = h_q^2 = 0$:

  $sig_7 = (r_1^-, UC_1)\&(r_2^0, UC_2)\&(r_3^0, UC_3)$

- when $\tilde{h}_q^1 = h_q^1 = 0$ and $\tilde{h}_q^2 = h_q^2 = 1$:

$sig_7 = (r_1^+, UC_1)\&(r_2^0, UC_2)\&(r_3^0, UC_3)$

Let us now consider the occurrence of a fault of type F_8, residuals r is computed as follows:

$$\begin{cases} r_1 = \left(-\tilde{h}_q^1 \frac{1}{\tilde{C}_1} + h_q^1 \frac{1}{C_1}\right) I + \left(\tilde{h}_q^2 \frac{1}{\tilde{C}_1} - h_q^2 \frac{1}{C_1}\right) I \\ r_2 = \left(\tilde{h}_q^2 \frac{1}{\tilde{C}_2} + h_q^2 \frac{1}{C_2}\right) I + \left(\tilde{h}_q^3 \frac{1}{\tilde{C}_2} - h_q^3 \frac{1}{C_2}\right) I \\ r_3 = \left(-\frac{R}{L} I + \frac{R}{L} I\right) + \left(\tilde{h}_q^1 - h_q^1\right) \frac{1}{L} Vc_1 + \left(\tilde{h}_q^2 - h_q^2\right) \frac{1}{L}(Vc_2 - Vc_1) + \\ \qquad \left(\tilde{h}_q^3 - h_q^3\right) \frac{1}{L}(E - Vc_2) \end{cases}$$

Since only simple fault scenario is considered and in the case of the occurrence of a fault of type F_8, i.e., parametric fault in C_2 due to its electrical chemical aging of, $\tilde{h}_q^1$, $\tilde{h}_q^2$ and $\tilde{h}_q^3$ are equal, respectively, to h_q^1, h_q^2 and h_q^3 and $\tilde{C}_1$ is equal to C_1. Therefore, residuals r are equal to:

- when $\tilde{h}_q^2 = h_q^2 = \tilde{h}_q^3 = h_q^3 = 0$:

$$\begin{cases} r_1 = 0 \\ r_2 = 0 \\ r_3 = 0 \end{cases} \tag{5.23}$$

- when $\tilde{h}_q^2 = h_q^2 = \tilde{h}_q^3 = h_q^3 = 1$:

$$\begin{cases} r_1 = 0 \\ r_2 = 0 \\ r_3 = 0 \end{cases} \tag{5.24}$$

- when $\tilde{h}_q^2 = h_q^2 = 0$ and $\tilde{h}_q^3 = h_q^3 = 1$:

$$\begin{cases} r_1 = 0 \\ r_2 = \left(\frac{1}{\tilde{C}_1} - \frac{1}{C_1}\right) I \\ r_3 = 0 \end{cases} \tag{5.25}$$

- when $\tilde{h}_q^2 = h_q^2 = 1$ and $\tilde{h}_q^3 = h_q^3 = 0$:

$$\begin{cases} r_1 = 0 \\ r_2 = -\left(\frac{1}{\tilde{C}_1} - \frac{1}{C_1}\right) I \\ r_3 = 0 \end{cases} \tag{5.26}$$

Thus, in response to the change in r caused by the occurrence of a fault of type F_8, the system generates one of the following three fault signatures according to the discrete state of S_2 and S_3:

- when $\tilde{h}_q^2 = h_q^2 = \tilde{h}_q^3 = h_q^3 = 1$ or $\tilde{h}_q^2 = h_q^2 = \tilde{h}_q^3 = h_q^3 = 0$:

$sig_0 = (r_1^0, UC_1)\&(r_2^0, UC_2)\&(r_3^0, UC_3)$

Table 5.2: Global fault signatures table.

Signature name	*Fault signature*
sig_0	$(r_1^0, UC_1)\&(r_2^0, UC_2)\&(r_3^0, UC_3)$
sig_1	$(r_1^-, NC_1^1)\&(r_2^0, UC_2)\&(r_3^+, PC_3^1)$
sig_2	$(r_1^+, PC_1^1)\&(r_2^0, UC_2)\&(r_3^-, NC_3^1)$
sig_3	$(r_1^+, PC_1^2)\&(r_2^-, NC_2^2)\&(r_3^+, PC_3^2)$
sig_4	$(r_1^-, NC_1^2)\&(r_2^+, PC_2^2)\&(r_3^-, NC_3^2)$
sig_5	$(r_1^0, UC_1)\&(r_2^+, PC_2^3)\&(r_3^+, PC_3^3)$
sig_6	$(r_1^0, UC_1)\&(r_2^-, NC_2^3)\&(r_3^-, NC_3^3)$
sig_7	$(r_1^-, UC_1)\&(r_2^0, UC_2)\&(r_3^0, UC_3)$
	$(r_1^+, UC_1)\&(r_2^0, UC_2)\&(r_3^0, UC_3)$
sig_8	$(r_1^0, UC_1)\&(r_2^+, UC_2)\&(r_3^0, UC_3)$
	$(r_1^0, UC_1)\&(r_2^-, UC_2)\&(r_3^0, UC_3)$

- when $\tilde{h}_q^2 = h_q^2 = 1$ and $\tilde{h}_q^3 = h_q^3 = 0$:

  $sig_8 = (r_1^0, UC_1)\&(r_2^-, UC_2)\&(r_3^0, UC_3)$

- when $\tilde{h}_q^2 = h_q^2 = 0$ and $\tilde{h}_q^3 = h_q^3 = 1$:

  $sig_8 = (r_1^0, UC_1)\&(r_2^+, UC_2)\&(r_3^0, UC_3)$

Table 5.2 shows the global fault signatures generated by the system in response to the occurrence of one of the faults defined in Table5.1.

5.4.2 Local fault signature

5.4.2.1 Local fault signature generated by HC_1

Based on (4.1) and since HC_1 is composed of S_1 (Dc_1), Vc_1 (Cc_1) and I (Cc_3), the masque function $M_1(r)$ is defined as follows:

$$\begin{cases} M_1(r_1) = r_1^1 \\ M_1(r_2) = \Phi \\ M_1(r_3) = r_{c3} + r_3^1 \end{cases} \tag{5.27}$$

where, $r_1^1 = \left(-\tilde{h}_q^1 \frac{1}{C_1} + h_q^1 \frac{1}{C_1}\right) I$, $r_{c3} = -\frac{R}{L} I + \frac{R}{L} I = 0$ and $r_3^1 = \left(\tilde{h}_q^1 - h_q^1\right) \frac{1}{L} Vc_1$. $M_1(r_2)$ is equal to Φ because Vc_2 does not belong to HC_1. r_{c3} is ignored since it is always equal to zero (parametric faults related to R and L are not considered).

Therefore, hybrid component HC_1 is sensitive to faults of type F_1, F_2 and F_7 (see Table 5.1). Consequently, a local fault signature in each local hybrid state ($q^1 \in Q^1$) is defined.

Based on (5.27), in normal operating mode of HC_1 a local normal fault signature sig_0^1 is generated:
$sig_0^1 = (r_1^{1\,0}, UC_1^1)\&(r_3^{1\,0}, UC_3^1)$
The part of residuals associated to HC_1 in these conditions are equal to zero (there is no fault in HC_1: $(\tilde{h}_q^1 = h_q^1)$ and $(\tilde{C}_1 = C_1)$.

Let us consider the occurrence of a fault of type F_1 (S_1SO), the parts of residuals associated to HC_1 in these conditions are computed as follows:
$$\begin{cases} r_1^1 = \left(-\left(\tilde{h}_q^1 = 1\right)\frac{1}{\tilde{C}_1} + \left(h_q^1 = 0\right)\frac{1}{C_1}\right) I \\ r_3^1 = \left(\left(\tilde{h}_q^1 = 1\right) - \left(h_q^1 = 0\right)\right)\frac{1}{L} Vc_1 \end{cases}$$
Therefore, the parts of residuals associated to HC_1 in this case are equal to:
$$\begin{cases} r_1^1 = -\frac{1}{\tilde{C}_1} I \\ r_3^1 = \frac{1}{L} Vc_1 \end{cases}$$
Thus, in response to the abrupt change in the parts of residuals associated to HC_1 caused by the occurrence of a fault of type F_1, the local fault signature sig_1^1 is computed as follows:

$$sig_1^1 = (r_1^{1\,-}, NC_1^1)\&(r_3^{1\,+}, PC_3^1)$$

where $NC_1^1 = -\frac{1}{\tilde{C}_1} I$ and $PC_3^1 = \frac{1}{L} Vc_1$.

Let us now consider the occurrence of a fault of type F_2 (S_1SC), the parts of residuals associated to HC_1 are computed as follows:
$$\begin{cases} r_1^1 = \left(-\left(\tilde{h}_q^1 = 0\right)\frac{1}{\tilde{C}_1} + \left(h_q^1 = 1\right)\frac{1}{C_1}\right) I \\ r_3^1 = \left(\left(\tilde{h}_q^1 = 0\right) - \left(h_q^1 = 1\right)\right)\frac{1}{L} Vc_1 \end{cases}$$
Since only simple fault scenario is considered and in the case of the occurrence of a fault of type F_2, i.e., S_1 stuck closed, $\tilde{C}_1$ is equal to C_1. Therefore, the parts of residuals associated to HC_1 in this case are equal to:
$$\begin{cases} r_1^1 = \frac{1}{\tilde{C}_1} I \\ r_3^1 = -\frac{1}{L} Vc_1 \end{cases}$$
Thus, in response to the abrupt change in r caused by the occurrence of a fault of type F_2 the local fault signature sig_2^1 is computed as follows:

$$sig_2^1 = (r_1^+, PC_1^1)\&(r_3^-, NC_3^1)$$

where $PC_1^1 = \frac{1}{\tilde{C}_1} I$ and $NC_3^1 = -\frac{1}{L} Vc_1$.

Let us now consider the occurrence of fault of type F_7, the part of residuals associated to HC_1 are computed as follows:
$$\begin{cases} r_1^1 = \left(-\tilde{h}_q^1\frac{1}{\tilde{C}_1} + h_q^1\frac{1}{C_1}\right) I \\ r_3^1 = \left(\tilde{h}_q^1 - h_q^1\right)\frac{1}{L} Vc_1 \end{cases}$$
Since only simple fault scenario is considered and in the case of the occurrence of a fault of type F_7, $\tilde{h}_q^1$ is equal to h_q^1. Therefore, when $\tilde{h}_q^1 = h_q^1 = 0$ the parts of residuals associated to HC_1 in this case are equal to:
$$\begin{cases} r_1^1 = 0 \\ r_3^1 = 0 \end{cases}$$

Table 5.3: Local faults signatures table of HC_1.

Signature name	***Fault signature***
sig_0^1	$(r_1^{1\,0}, UC_1^1)\&(r_3^{1\,0}, UC_3^1)$
sig_1^1	$(r_1^{1\,-}, NC_1^1)\&(r_3^{1\,+}, PC_3^1)$
sig_2^1	$(r_1^{1\,+}, PC_1^1)\&(r_3^{1\,-}, NC_3^1)$
sig_7^1	$(r_1^{1\,-}, UC_1^1)\&(r_3^{1\,0}, UC_3^1)$

Table 5.4: Local faults signatures table of HC_2.

Signature name	***Fault signature***
sig_0^2	$(r_1^{2\,0}, UC_1^2)\&(r_2^{2\,0}, UC_2^2)\&(r_3^{2\,0}, UC_3^2)$
sig_3^2	$(r_1^{2\,+}, PC_1^2)\&(r_2^{2\,-}, NC_2^2)\&(r_3^{2\,+}, PC_3^2)$
sig_4	$(r_1^{2\,-}, NC_1^2)\&(r_2^{2\,+}, PC_2^2)\&(r_3^{2\,-}, NC_3^2)$
sig_7^2	$(r_1^{2\,+}, UC_1^2)\&(r_2^{2\,0}, UC_2^2)\&(r_3^{2\,0}, UC_3^2)$
sig_8^2	$(r_1^{2\,0}, UC_1^2)\&(r_2^{2\,-}, UC_2)\&(r_3^{2\,0}, UC_3^2)$

In this case, the obtained local signature is equal to sig_0^1.
when $\tilde{h}_q^1 = h_q^1 = 1$ the part of residuals associated to HC_1 in this case are equal to:
$\begin{cases} r_1^1 = -\left(\frac{1}{\tilde{C}_1} - \frac{1}{C_1}\right) I \\ r_3^1 = 0 \end{cases}$
Thus, in response to the change in the parts of residuals associated to HC_1 caused by the occurrence of a fault of type F_7, the local fault signature sig_7^1 is computed as follows:

$sig_7^1 = (r_1^{1\,-}, UC_1^1)\&(r_3^{1\,0}, UC_3)$

Table 5.3 shows the local fault signatures generated in response to the occurrence fault that can occur in HC_1.

Likewise, Table 5.4 shows the local fault signatures generated in response to the occurrence fault that can occur in HC_2. where, the masque function $M_2(r)$ is defined as follows:

$$\begin{cases} M_2(r_1) = r_1^2 \\ M_2(r_2) = r_2^2 \\ M_2(r_3) = r_{c3} + r_3^2 \end{cases} \tag{5.28}$$

where, $r_1^2 = \left(\tilde{h}_q^2 \frac{1}{\tilde{C}_1} - h_q^2 \frac{1}{C_1}\right) I$, $r_2^2 = \left(-\tilde{h}_q^2 \frac{1}{\tilde{C}_2} + h_q^2 \frac{1}{C_2}\right) I$, $r_{c3} = -\frac{R}{L} I + \frac{R}{L} I$ and $r_3^2 = \left(\tilde{h}_q^2 - h_q^2\right) \frac{1}{L}(Vc_2 - Vc_1)$. r_{c3} is ignored since it is always equal to zero (parametric faults related to R and L are not considered).

Likewise, Table 5.5 shows the local fault signatures generated in response to the occurrence fault that can occur in HC_3. where, the masque function $M_3(r)$ is defined as follows:

Table 5.5: Local faults signatures table of HC_3.

Signature name	***Fault signature***
sig_0^3	$(r_2^{3\,0}, UC_2^3)\&(r_3^{3\,0}, UC_3^3)$
sig_5^3	$(r_2^{3\,+}, PC_2^3)\&(r_3^{3\,+}, PC_3^3)$
sig_6^3	$(r_2^{3\,-}, NC_2^3)\&(r_3^{3\,-}, NC_3^3)$
sig_8^3	$(r_2^{3\,+}, UC_2^3)\&(r_3^{3\,0}, UC_3^3)$

$$\begin{cases} M_3(r_1) = \Phi \\ M_3(r_2) = r_2^3 \\ M_3(r_3) = r_{c3} + r_3^3 \end{cases} \tag{5.29}$$

where, $r_2^3 = \left(\tilde{h}_q^3 \frac{1}{\tilde{C}_2} - h_q^3 \frac{1}{C_2}\right) I$, $r_{c3} = -\frac{R}{L} I + \frac{R}{L} I$, and $r_3^3 = \left(\tilde{h}_q^3 - h_q^3\right) \frac{1}{L}(E - Vc_2)$. $M_3(r_1)$ is equal to Φ because Vc_1 does not belong to HC_3. r_{c3} is ignored since it is always equal to zero (parametric faults related to R and L are not considered).

5.4.3 Local diagnoser construction

For the three cell converter system, three local hybrid diagnosers D_1, D_2 and D_3 are constructed for, respectively, HC_1, HC_2 and HC_3 .

D_1 is constructed based on the use of local hybrid automaton G^1 of Fig.5.8 as follows:

- Initial state z_1^1 (Fig.5.11), characterized by $(Q_1^1,\ \tilde{h}_{z_1^1}^1,\ \tilde{\dot{X}}^1,\ HSL_{z_1^1}^1)$, is composed of the following G^1 states: q_1^1 (G^1 initial state), q_5^1 reached from q_1^1 by the occurrence of fault event f_{S_1SC} (fault of type F_2) and q_8^1 reached from q_1^1 by the occurrence of fault event $f_{\tilde{C}_1 \neq C_1}$ (fault of type F_7). Thus, Q_1^1 is equal to $\{q_1^1,\ q_5^1,\ q_8^1\}$. $\tilde{h}_{z_1^1}^1$ is equal to the nominal output of the states of Q_1^1. As we can see in Fig.5.8 and Fig.5.11, $\tilde{h}_{q_1^1}^1$, $\tilde{h}_{q_5^1}^1$ and $\tilde{h}_{q_8^1}^1$ in, respectively, q_1^1, q_5^1 and q_8^1 are equivalent and equal to 1. Thus, $\tilde{h}_{z_1^1}^1$ is equal to 1. $HSL_{z_1^1}^1$ gathers the normal and fault labels associated to the states belonging to Q_1^1. Therefore, $HSL_{z_1^1}^1$ is equal to $\{N_1,\ F_2,\ F_7\}$. Finally, $\tilde{\dot{X}}^1$ gathers $\dot{\tilde{X}}^1$ of all the states q_k^1 of Q_1^1. Since states q_5^1 and q_8^1 are reached from q_1^1 due to the occurrence of unobservable events (a fault)(see Fig.5.8), $\tilde{\dot{X}}^1$ in q_1^1, q_5^1 and q_8^1 are equivalent and equal to $\begin{bmatrix} \frac{-I}{\tilde{C}_1} & \frac{Vc_1}{L} \end{bmatrix}^T$ (see Fig.5.11).

- Continuous dynamic evolutions of the states belonging to Q_1^1 will allow to generate a set of local fault signatures as we can see in Fig.5.12. These fault signatures allow converting unobservable transitions into observable ones. Consequently, they are used in order to detect and isolate a parametric faults of type F_7 as follows. q_8^1 of G^1 (reached from q_1^1 by the occurrence of fault event $f_{\tilde{C}_1 \neq C_1}$) generates fault signature sig_7^1. sig_7^1 is used as an observable transition

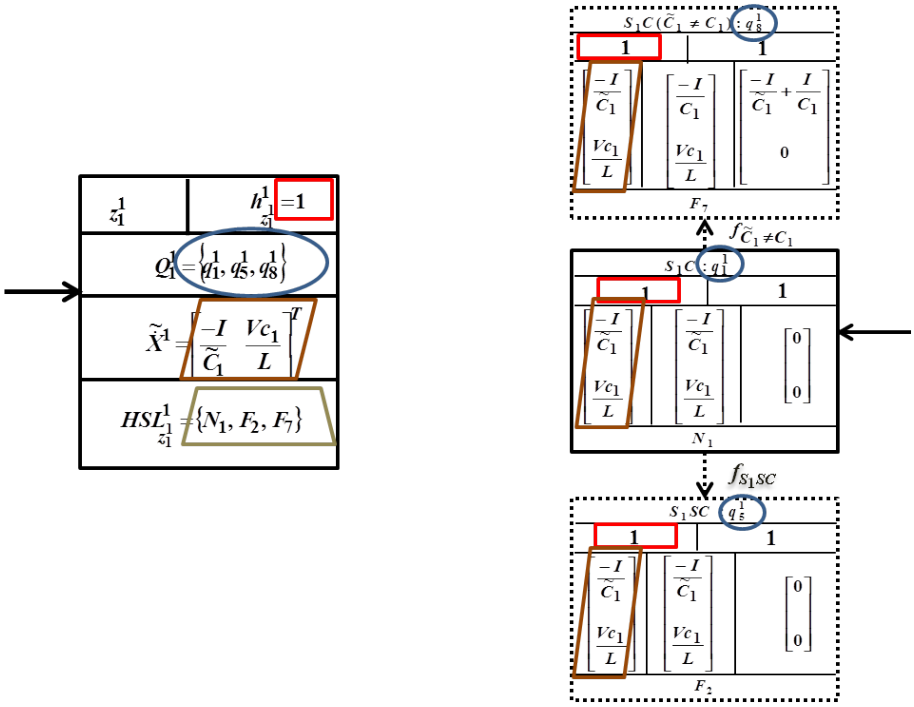

Figure 5.11: Initial state z_1^1 of local hybrid diagnoser D_1.

to isolate the occurrence of a fault of type F_7 by moving the diagnoser to state z_7^1. The other states of Q_1^1, $\{q_1^1,\ q_5^1\}$, generate local fault signature sig_0^1 (the parts of continuous dynamic evolutions in these states do not evolve). sig_0^1 is used as a transition to loop D_1 in state z_1^1.

- The states of D_1 reached due to the occurrence of each control command events are computed. The occurrence of control command OS_1 moves D_1 from z_1^1 to z_2^1 characterized by $(Q_2^1,\ \tilde{h}_{z_2^1}^1,\ \tilde{\dot{X}}^1,\ HSL_{z_2^1}^1)$. Q_2^1 is equal to all the states reached from Q_1^1 due to the occurrence of OS_1. Thus, Q_2^1 is equal to $\{q_2^1,\ q_6^1,\ q_7^1\}$ (see Fig.5.8). Then, all the states of G^1 reached from Q_2^1 due to the occurrence of unobservable event are added to Q_2^1. The unobservable event, other than $f_{\tilde{C}_1 \neq C_1}$, that can occur at q_2^1 is fault event f_{S_1SO}. Therefore, Q_2 is equal to $\{q_2^1,\ q_3^1,\ q_6^1,\ q_7^1\}$. $\tilde{h}_{z_2^1}^1$ is equal to the nominal output of the states of Q_2^1. Consequently, $\tilde{h}_{z_2^1}^1$ is equal to 0 (the switch S_1 should be opened), $HSL_{z_2^1}^1$ is equal to the set of fault labels of the states of Q_2^1. Thus, $HSL_{z_2^1}^1$ is equal to $\{N_1,\ F_1,\ F_2,\ F_7\}$; while $\tilde{\dot{X}}^1$ is equal to the nominal parts of continuous evolutions of X^1 in the states of Q_2^1. Thus, $\tilde{\dot{X}}^1$ is equal to $\begin{bmatrix} 0 & 0 \end{bmatrix}^T$ (see Fig.5.8).

- Continuous dynamic evolutions of the states belonging to Q_2^1 will allow to generate a set of fault signatures as we can see in Fig.5.12. These fault signatures allow converting unobservable transitions into observable ones. Consequently,

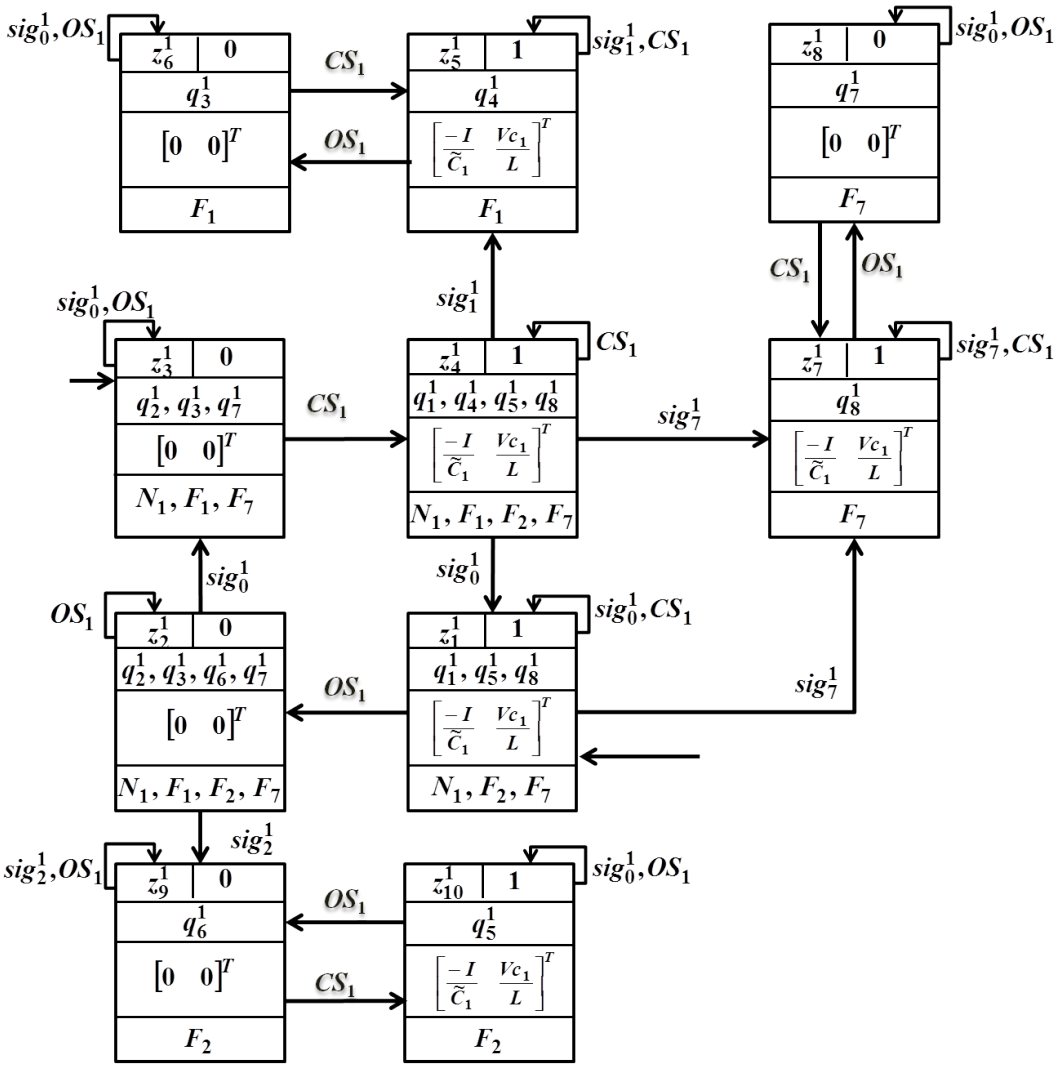

Figure 5.12: Local hybrid diagnoser D_1 of HC_1.

they are used in order to detect and isolate a discrete fault of type F_2 as follows. q_6^1 of G^1 (reached from faulty state q_5^1 due to controllable event OS_1) generates fault signature sig_2^1. sig_2^1 is used as an observable transition to isolate the occurrence of a fault of type F_2 by moving D_1 to state z_9^1. The other states of Q_2^1, $\{q_2^1,\ q_3^1,\ q_7^1\}$, generates fault signature sig_0^1 (the parts of continuous dynamic evolutions in these states do not evolve). sig_0^1 is used to label the transition to local hybrid diagnoser state z_3^1 (see Fig.5.12).

- z_3^1, characterized by $(Q_3^1,\ \tilde{h}_{z_3^1}^1,\ \tilde{\dot{X}}^1,\ HSL_{z_3^1}^1)$, is composed of states of Q_2^1 excluding the state $\{q_6^1\}$ isolated from z_2^1. Thus, Q_3^1 is equal to $\{q_2^1,\ q_3^1,\ q_7^1\}$. $\tilde{h}_{z_3 1^1}^1$ is equal to the nominal output of the states of Q_3^1. As we can see in Fig.5.8, $\tilde{h}_{q_2^1}^1$, $\tilde{h}_{q_3^1}^1$ and $\tilde{h}_{q_7^1}^1$ in, respectively, q_2^1, q_3^1 and q_7^1 are equivalent and equal to 0. Thus, $\tilde{h}_{z_3^1}^1$ is equal to 0. $HSL_{z_3^1}^1$ gathers the normal and fault labels associated to the states belonging to Q_3^1. Therefore, $HSL_{z_3^1}^1$ is equal to $\{N_1,\ F_1,\ F_7\}$. Finally, $\tilde{\dot{X}}^1$ gathers $\tilde{\dot{X}}^1$ of all the states q_k^1 of Q_3^1. Thus, $\tilde{\dot{X}}^1$ in q_2^1, q_3^1 and q_7^1 are equivalent and equal to $\begin{bmatrix} 0 & 0 \end{bmatrix}^T$ (see Fig.5.8).

- The states of D_1 reached due to the occurrence of each control command events are computed. The occurrence of control command CS_1 moves D_1 from z_3^1 to z_4^1 characterized by $(Q_4^1,\ \tilde{h}_{z_4^1}^1,\ \tilde{\dot{X}}^1,\ HSL_{z_4^1}^1)$. Q_4^1 is equal to all the states reached from Q_3^1 due to the occurrence of CS_1. Thus, Q_4^1 is equal to $\{q_1^1,\ q_4^1,\ q_8^1\}$ (see Fig.5.8). Then, all the states of G^1 reached from Q_4^1 due to the occurrence of unobservable event are added to Q_4^1. The unobservable event, other than $f_{\tilde{C}_1 \neq C_1}$, that can occur at q_1^1 is fault event $f_{S_1 SC}$. Therefore, Q_4 is equal to $\{q_1^1,\ q_4^1,\ q_5^1,\ q_8^1\}$. $\tilde{h}_{z_4^1}^1$ is equal to the nominal output of the states of Q_4^1. Consequently, $\tilde{h}_{z_4^1}^1$ is equal to 1 (the switch S_1 should be closed), $HSL_{z_4^1}^1$ is equal to the set of fault labels of the states of Q_4^1. Thus, $HSL_{z_4^1}^1$ is equal to $\{N_1,\ F_1,\ F_2,\ F_7\}$; while $\tilde{\dot{X}}^1$ is equal to the nominal parts of continuous evolutions of X^1 in the states of Q_4^1. Thus, $\tilde{\dot{X}}^1$ is equal to $\begin{bmatrix} \frac{-I}{\tilde{C}_1} & \frac{Vc_1}{L} \end{bmatrix}^T$ (see Fig.5.8).

- Continuous dynamic evolutions of the states belonging to Q_4^1 will allow to generate a set of local fault signatures as we can see in Fig.5.12. These fault signatures allow converting unobservable transitions into observable ones. Consequently, they are used in order to detect and isolate discrete fault of type F_1 and parametric faults of type F_7 as follows. q_4^1 of G^1 (reached from faulty state q_3^1 due to controllable event CS_1) generates fault signature sig_1^1. sig_1^1 is used as an observable transition to isolate the occurrence of a fault of type F_1 by moving the diagnoser to state z_5^1. q_8^1 of G^1 (reached from faulty state q_7^1 due to controllable event CS_1) generates fault signature sig_7^1. sig_7^1 is used as an observable transition to isolate the occurrence of a fault of type F_7 by moving the diagnoser to state z_7^1. The other states of Q_4^1, $\{q_1^1,\ q_5^1\}$, generate

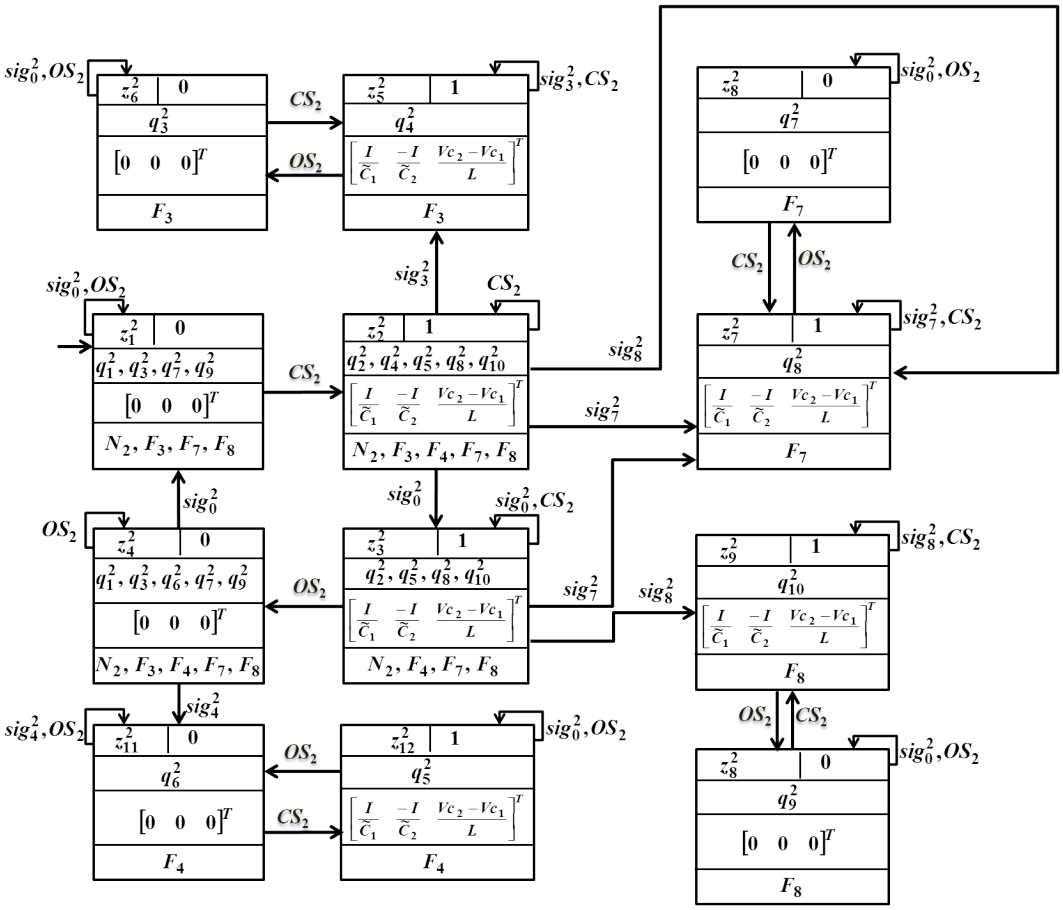

Figure 5.13: Local hybrid diagnoser D_2 of HC_2.

local fault signature sig_0^1 (the parts of continuous dynamic evolutions in these states do not evolve). sig_0^1 is used to is used as a transition to loop D_1 to state z_1^1.

Based on the same reasoning used to construct local diagnoser D_1 of HC_1, D_2 of HC_2 and D_3 of HC_3 can be constructed as we can see in, respectively, Fig.5.13 and Fig.5.14.

5.5 Coordinator construction

5.5.1 Central processing point construction

As shown in subsection 5.3.4, the three cell converter is decomposed into three hybrid components HC_1, HC_2 and HC_3. Therefore, three local hybrid diagnosers D_1, D_2 and D_3 are constructed for, respectively, HC_1, HC_2 and HC_3. Each one of them sends its part of nominal continuous dynamic evolution to the central processing point. Thus, D_1 sends $\tilde{\dot{X}}^1$, D_2 sends $\tilde{\dot{X}}^2$ and D_3 sends $\tilde{\dot{X}}^3$. The central processing

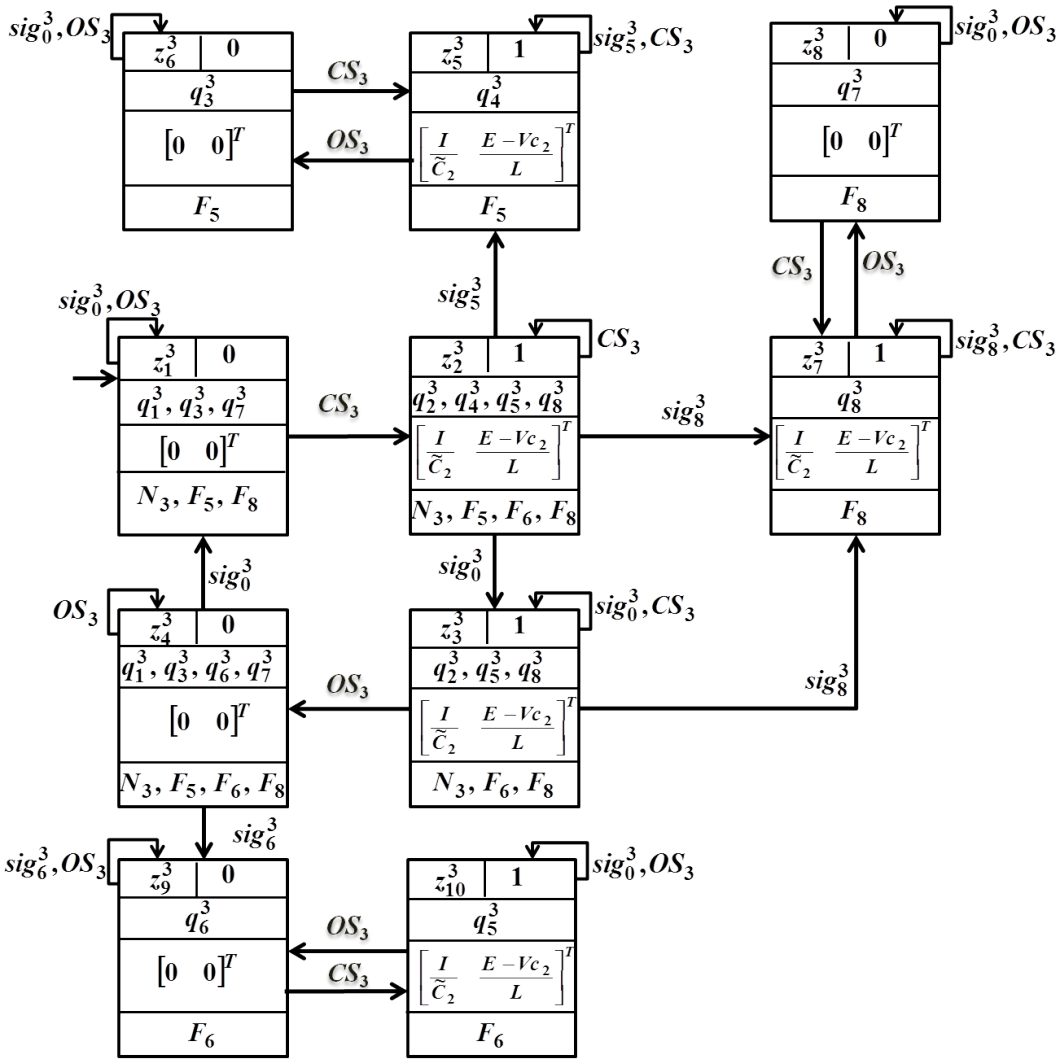

Figure 5.14: Local hybrid diagnoser D_3 of HC_3.

point achieves the following tasks:

1. It calculates the nominal continuous dynamic evolution (see (3.13)) as follows:
   $\tilde{\dot{X}} = \tilde{\dot{X}}^1 + \tilde{\dot{X}}^2 + \tilde{\dot{X}}^3 + \tilde{\dot{X}}_c$
   $\begin{cases} \tilde{\dot{V}}c_1 = \tilde{\dot{V}}c_1^{\,1} + \tilde{\dot{V}}c_1^{\,2} \\ \tilde{\dot{V}}c_2 = \tilde{\dot{V}}c_2^{\,2} + \tilde{\dot{V}}c_2^{\,3} \\ \tilde{\dot{I}} = \tilde{\dot{I}}_c + \tilde{\dot{I}}^1 + \tilde{\dot{I}}^2 + \tilde{\dot{I}}^3 \end{cases}$
   where $\tilde{\dot{V}}c_1^{\,1} = -\tilde{h}_q^1 \frac{I}{\tilde{C}_1}$, $\tilde{\dot{V}}c_1^{\,2} = \tilde{h}_q^2 \frac{I}{\tilde{C}_1}$, $\tilde{\dot{V}}c_2^{\,2} = -\tilde{h}_q^2 \frac{I}{\tilde{C}_2}$, $\tilde{\dot{V}}c_2^{\,3} = \tilde{h}_q^3 \frac{I}{\tilde{C}_2}$, $\tilde{\dot{I}}_c = -\frac{RI}{L}$, $\tilde{\dot{I}}^1 = \tilde{h}_q^1 \frac{1}{L} Vc_1$, $\tilde{\dot{I}}^2 = \tilde{h}_q^2 \frac{1}{L}(Vc_2 - Vc_1)$, $\tilde{\dot{I}}^3 = \tilde{h}_q^3 \frac{1}{L}(E - Vc_2)$.
   $\tilde{\dot{X}}^1 = \begin{bmatrix} \tilde{\dot{V}}c_1^1 & \tilde{\dot{I}}^1 \end{bmatrix}^T$, $\tilde{\dot{X}}^2 = \begin{bmatrix} \tilde{\dot{V}}c_1^2 & \tilde{\dot{V}}c_2^2 & \tilde{\dot{I}}^2 \end{bmatrix}^T$ and $\tilde{\dot{X}}^3 = \begin{bmatrix} \tilde{\dot{V}}c_2^3 & \tilde{\dot{I}}^3 \end{bmatrix}^T$.
   $\tilde{\dot{X}}_c = \begin{bmatrix} 0 & 0 & \tilde{\dot{I}}_c \end{bmatrix}^T$.
   It is worthy to note that $\tilde{\dot{X}}$ is already recorded in the central processing point (see Fig.5.15).
   Real continuous evolution $\dot{X}$ is obtained through the continuous sensors measuring the floating voltages Vc_1 and Vc_2 of, respectively, capacitors C_1 and C_2 as well as the current I.

2. It calculates residuals r as the difference between the nominal and real continuous dynamic evolutions of X ($r = \tilde{\dot{X}} - \dot{X}$).

3. Finally, the central processing point calculates the local residuals as follows (see Fig.5.15):

   - In the case of the occurrence of a discrete fault of type F_1 in Dc_1 (see Table 5.1) belonging to HC_1, residuals r are equal to (see (5.13)):
     $\begin{cases} r_1 = -\frac{1}{\tilde{C}_1} I \\ r_2 = 0 \\ r_3 = \frac{1}{L} Vc_1 \end{cases}$
     In the case of the occurrence of a discrete fault of type F_2 in Dc_1 (see Table 5.1) belonging to HC_1, residuals r are equal to (see (5.14)):
     $\begin{cases} r_1 = \frac{1}{\tilde{C}_1} I \\ r_2 = 0 \\ r_3 = -\frac{1}{L} Vc_1 \end{cases}$
     Based on (4.5), in the case of the occurrence of a fault in a discrete component of HC_1, residuals r are equal to the local ones of HC_1. The local residuals are computed as follows:
     $$\begin{cases} r_1^1 = r_1,\ r_1^2 = 0,\ r_1^3 = \Phi \\ r_2^1 = \Phi,\ r_2^2 = r_2^3 = 0 \\ r_3^1 = r_3,\ r_3^2 = r_3^3 = 0 \end{cases} \tag{5.30}$$

   - In the case of the occurrence of a discrete fault of type F_3 in Dc_2 (see Table 5.1) belonging to HC_2, residuals r are equal to (see (5.15)):

$$\begin{cases} r_1 = \frac{1}{\tilde{C}_1} I \\ r_2 = -\frac{1}{\tilde{C}_2} I \\ r_3 = \frac{1}{L}(Vc_2 - Vc_1) \end{cases}$$

In the case of the occurrence of a discrete fault of type F_4 in Dc_2 (see Table 5.1) belonging to HC_2, residuals r are equal to (see (5.16)):

$$\begin{cases} r_1 = -\frac{1}{\tilde{C}_1} I \\ r_2 = \frac{1}{\tilde{C}_2} I \\ r_3 = -\frac{1}{L}(Vc_2 - Vc_1) \end{cases}$$

Based on (4.5) which indicates that in the case of the occurrence of a fault in a discrete component of HC_2, residuals r are equal to the local ones of HC_2. The local residuals are computed as follows:

$$\begin{cases} r_1^1 = 0,\ r_1^2 = r_1,\ r_1^3 = \Phi \\ r_2^1 = \Phi,\ r_2^2 = r_2,\ r_2^3 = 0 \\ r_3^1 = 0,\ r_3^2 = r_3,\ r_3^3 = 0 \end{cases} \tag{5.31}$$

- In the case of the occurrence of a discrete fault of type F_5 in Dc_3 (see Table 5.1) belonging to HC_3, residuals r are equal to (see (5.17)):

$$\begin{cases} r_1 = 0 \\ r_2 = \frac{1}{\tilde{C}_2} I \\ r_3 = \frac{1}{L}(E - Vc_2) \end{cases}$$

- In the case of the occurrence of a discrete fault of type F_6 in Dc_3 (see Table 5.1) belonging to HC_3, residuas r are equal to (see (5.18)):

$$\begin{cases} r_1 = 0 \\ r_2 = -\frac{1}{\tilde{C}_2} I \\ r_3 = -\frac{1}{L}(E - Vc_2) \end{cases}$$

Based on (4.5) which indicates that in the case of the occurrence of a fault in a discrete component of HC_3, residuals r are equal to the local ones of HC_3. The local residuals are computed as follows:

$$\begin{cases} r_1^1 = 0,\ r_1^2 = 0,\ r_1^3 = \Phi \\ r_2^1 = \Phi,\ r_2^2 = 0,\ r_2^3 = r_2 \\ r_3^1 = r_3^2 = 0,\ r_3^3 = r_3 \end{cases} \tag{5.32}$$

- In the case of the occurrence of a parametric fault of type F_7 in Cc_1 (see Table 5.1) belonging to HC_1 and HC_2 and residuals r are equal to:
  - when $\tilde{h}_q^1 = h_q^1 = \tilde{h}_q^2 = h_q^2 = 0$ (see (5.19)):

$$\begin{cases} r_1 = 0 \\ r_2 = 0 \\ r_3 = 0 \end{cases}$$

  - when $\tilde{h}_q^1 = h_q^1 = \tilde{h}_q^2 = h_q^2 = 1$ (see (5.20)):

$$\begin{cases} r_1 = 0 \\ r_2 = 0 \\ r_3 = 0 \end{cases}$$

- when $\tilde{h}_q^1 = h_q^1 = 0$ and $\tilde{h}_q^2 = h_q^2 = 1$ (see (5.21)):
$$\begin{cases} r_1 = \left(\frac{1}{\tilde{C}_1} - \frac{1}{C_1}\right) I \\ r_2 = 0 \\ r_3 = 0 \end{cases}$$
- when $\tilde{h}_q^1 = h_q^1 = 1$ and $\tilde{h}_q^2 = h_q^2 = 0$ (see (5.22)):
$$\begin{cases} r_1 = -\left(\frac{1}{\tilde{C}_1} - \frac{1}{C_1}\right) I \\ r_2 = 0 \\ r_3 = 0 \end{cases}$$

Based on (4.6), in the case of the occurrence of a fault in a continuous component belonging to HC_1 and HC_2, residuals r are equal to the local ones of HC_1 and HC_2. The local residuals are computed as follows:

$$\begin{cases} r_1^1 = r_1^2 = r_1,\ r_1^3 = \Phi \\ r_2^1 = \Phi,\ r_2^2 = r_2^3 = 0 \\ r_3^1 = r_3^2 = r_3^3 = 0 \end{cases} \tag{5.33}$$

- In the case of the occurrence of a parametric fault of type F_8 in Cc_2 (see Table 5.1) belonging to HC_2 and HC_3, residuals r are equal to:
  - when $\tilde{h}_q^2 = h_q^2 = \tilde{h}_q^3 = h_q^3 = 0$ (see (5.23)):
$$\begin{cases} r_1 = 0 \\ r_2 = 0 \\ r_3 = 0 \end{cases}$$
  - when $\tilde{h}_q^2 = h_q^2 = \tilde{h}_q^3 = h_q^3 = 1$ (see (5.24)):
$$\begin{cases} r_1 = 0 \\ r_2 = 0 \\ r_3 = 0 \end{cases}$$
  - when $\tilde{h}_q^2 = h_q^2 = 0$ and $\tilde{h}_q^3 = h_q^3 = 1$ (see (5.25)):
$$\begin{cases} r_1 = 0 \\ r_2 = \left(\frac{1}{\tilde{C}_1} - \frac{1}{C_1}\right) I \\ r_3 = 0 \end{cases}$$
  - when $\tilde{h}_q^2 = h_q^2 = 1$ and $\tilde{h}_q^3 = h_q^3 = 0$ (see (5.26)):
$$\begin{cases} r_1 = 0 \\ r_2 = -\left(\frac{1}{\tilde{C}_1} - \frac{1}{C_1}\right) I \\ r_3 = 0 \end{cases}$$

Based on (4.6), in the case of the occurrence of a fault in a continuous component belonging to HC_3 and HC_3, residuals r are equal to the local ones of HC_2 and HC_3. The local residuals are computed as follows:

$$\begin{cases} r_1^1 = r_1^2 = 0,\ r_1^3 = \Phi \\ r_2^1 = \Phi,\ r_2^2 = r_2^3 = r_2 \\ r_3^1 = r_3^2 = r_3^3 = 0 \end{cases} \tag{5.34}$$

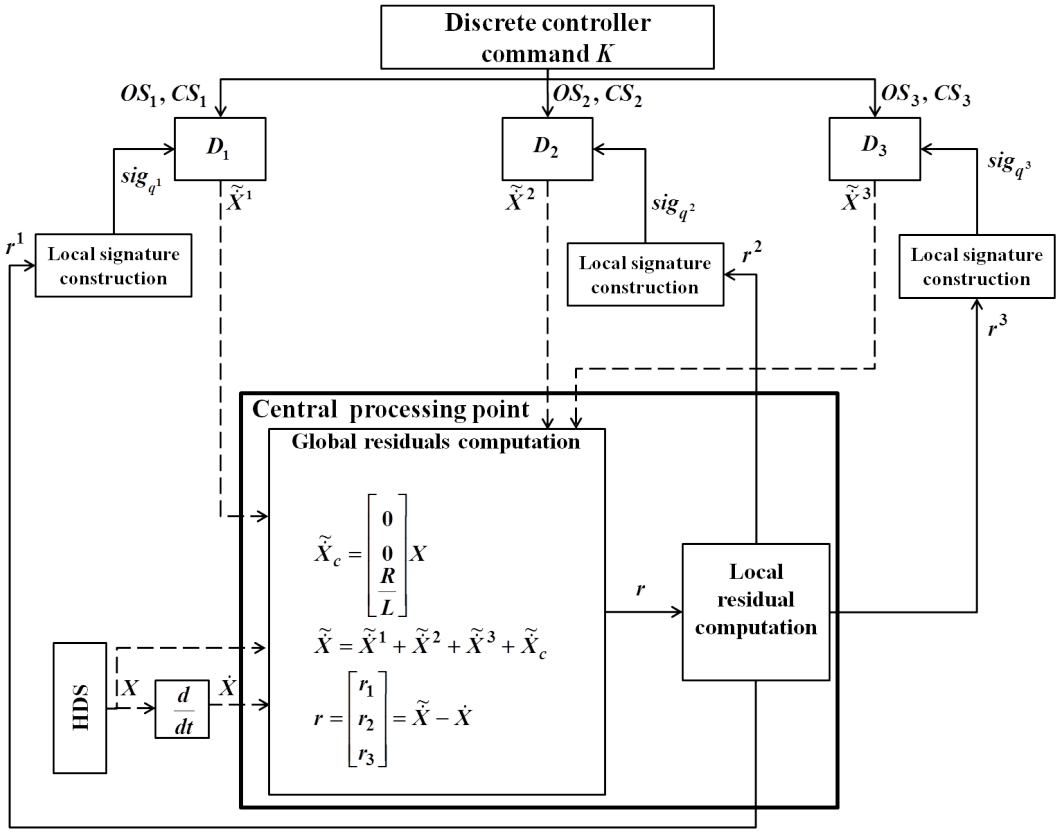

Figure 5.15: Central processing point for the three cell converter.

- In the case of the nominal conditions, residuals r are equal to:
$$\begin{cases} r_1 = 0 \\ r_2 = 0 \\ r_3 = 0 \end{cases}$$
Based on (4.7), the local residuals are computed as follows:

$$\begin{cases} r_1^1 = r_1^2 = 0,\ r_1^3 = \Phi \\ r_2^1 = \Phi,\ r_2^2 = r_2^3 = 0 \\ r_3^1 = r_3^2 = r_3^3 = 0 \end{cases} \tag{5.35}$$

5.5.2 Decision merging point construction

As we have seen before (see subsection 5.4.3), local diagnoser D_1 of HC_1 is sensitive to faults of types F_1, F_2 and F_7 (see Fig.5.12), local diagnoser D_2 of HC_2 is sensitive to faults of types F_3, F_4, F_7 and F_8(see Fig.5.13) and local diagnoser D_3 of HC_3 is sensitive to faults of types F_5, F_6 and F_8 (see Fig.5.14). In order to obtain one global diagnosis decision DD for the three cell converter, the local diagnosis decisions are merged using Table 5.6 (see the rules defined in subsection 4.3.2).

Table 5.6: Global diagnosis decision DD for the three cell converter.

Rules	***Local hybrid diagnoser*** D_1	***Local hybrid diagnoser*** D_2	***Local hybrid diagnoser*** D_3	***Global decision*** DD
2	F_1	Nothing	Nothing	F_1
	F_2	Nothing	Nothing	F_2
	Nothing	F_3	Nothing	F_3
	Nothing	F_4	Nothing	F_4
	Nothing	Nothing	F_5	F_5
	Nothing	Nothing	F_6	F_6
3	F_7	F_7	Nothing	F_7
	Nothing	F_8	F_8	F_8
4	Nothing	Nothing	Nothing	Nothing

Table 5.6 comprises three rules. The first rule (rule 2), indicates the case of the occurrence of a fault of type F_j declared by only one local diagnoser. As an example, a fault of type F_1 is declared by only D_1 since the latter is the only local diagnoser sensitive to the occurrence of this type of faults. When more than one local diagnoser are sensitive to the occurrence of a fault of type F_j, these local diagnosers will declare this fault. This is the case of rule 3 for faults of type F_7 declared by D_1 and D_2 and faults of type F_8 declared by D_2 and D_3. Rule 4 indicates the case when all the local diagnosers are not yet able to diagnose a fault. Thus, they remain all silent.

5.6 Experimentation and obtained results

In order to evaluate the proposed approach, simulations were carried out for the three-cell converter using Matlab-Simulink^{TM} environment and Stateflow^{TM} toolbox. The parameters used in these simulations are:
$E = 60V,\ \tilde{C}_1 = \tilde{C}_2 = 40\,\mu F,\ R = 200\Omega,\ L = 0.1H.$

In order to highlight the efficiency of the diagnoser, the simulations take into account the set of faults defined in Table 5.1 for the three-cell converter.

Discrete controller commands are assured by a pulse width modulation (PWM) signal, Defoort et al. (2011). Fig.5.16 depicts the control of the three switches S_1, S_2 and S_3. When the triangular signal is below the reference signal (ref in Fig.5.16), the associated switch is controlled to be opened. When the triangular signal is above the reference signal, the associated switch is controlled to be closed. This sequence of control is periodic with a period of $T_{PWM} = 0.02s$.

5.6.1 Normal conditions scenario

Fig.5.17 depicts, respectively, the signals of floating voltages Vc_1 and Vc_2 and the current I. These signals correspond to the normal conditions. Moreover, one can see in Fig.5.17 that Vc_1 (respectively Vc_2) has a periodic signal corresponding to load and unload of capacitor C_1 (respectively C_2) around the mean value $Vc_{1ref} = \frac{E}{3} =$

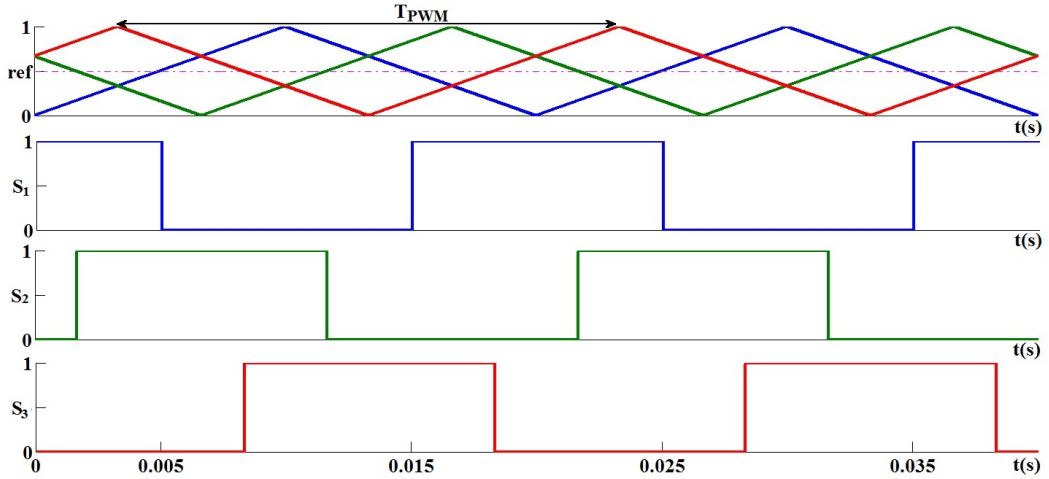

Figure 5.16: PWM for control of three switches S_1, S_2 and S_3.

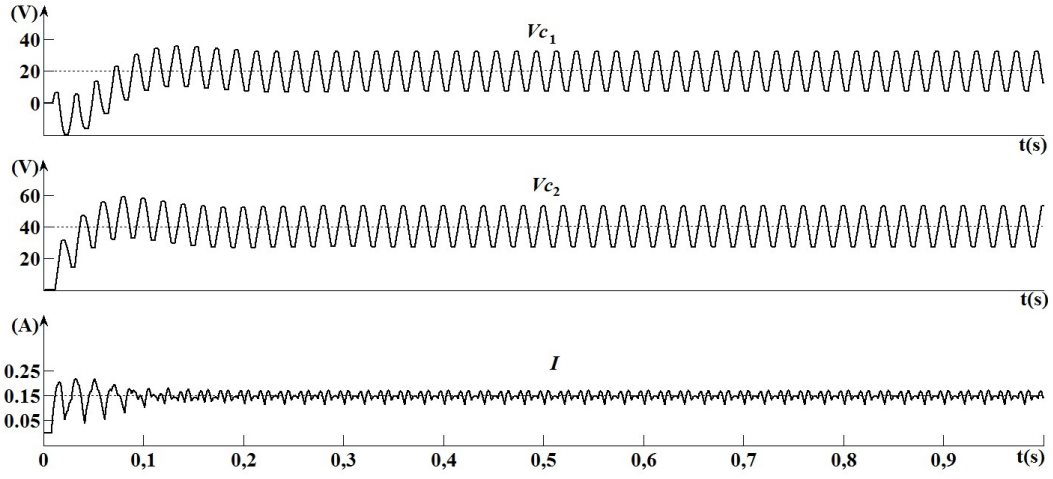

Figure 5.17: Real signals corresponding to Vc_1, Vc_2 and I in normal conditions.

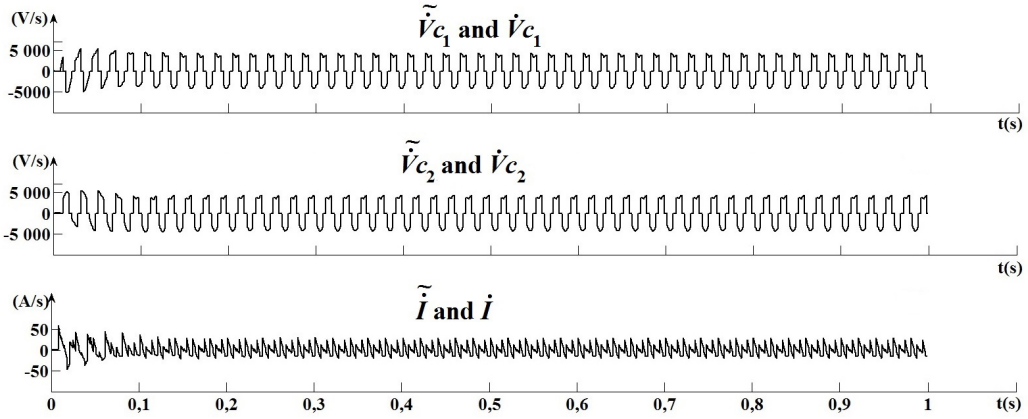

Figure 5.18: Real and nominal dynamic evolutions of Vc_1, Vc_2 and I in normal conditions.

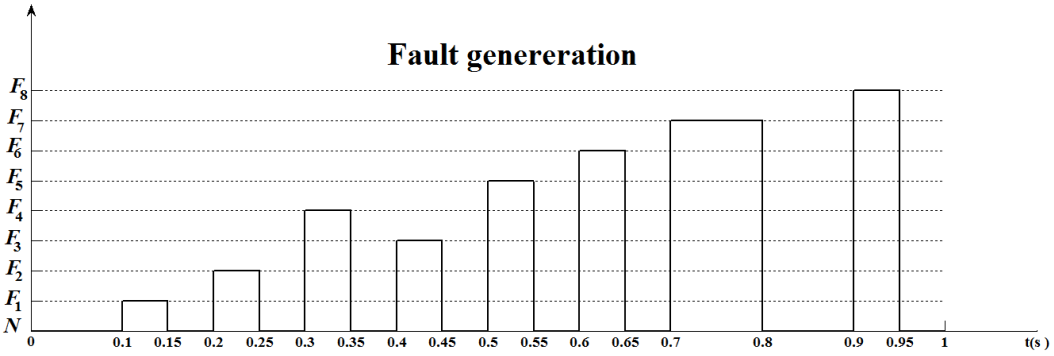

Figure 5.19: Time of appearance, injection, of faults during the simulation of three cell converter.

$20V$ (respectively $Vc_{2ref} = \frac{2E}{3} = 40V$) and that the current I remains constant in the region of its reference value ($0.15A$).

Fig.5.18 shows the real and nominal dynamic evolutions of Vc_1 ($\dot{V}c_1$ and $\tilde{\dot{V}}c_1$), Vc_2 ($\dot{V}c_2$ and $\tilde{\dot{V}}c_2$) and I ($\dot{I}$ and $\tilde{\dot{I}}$). We can notice that the curves representing the real and nominal dynamic evolutions are superposed. Consequently, residuals r_1, r_2 and r_3 are equal to zero in these conditions.

5.6.2 Faulty conditions scenario

The test scenario is generated as follows (see Fig.5.19). Each fault f, belonging to one of the fault labels of Table 5.1, is generated starting at time t_{sf} and ending at time t_{ef}. Then, the system returns to normal operating conditions before generating a new fault for a certain predefined time. Parametric faults of types F_7 and F_8 are simulated by changing gradually the real values of C_1, respectively C_2, in negative

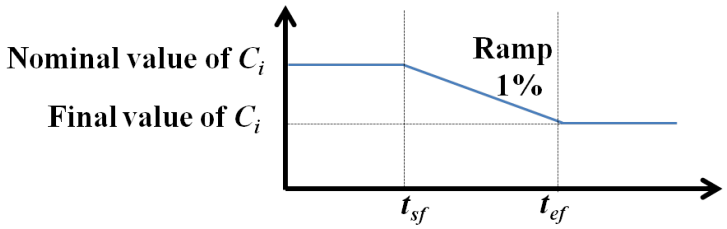

Figure 5.20: Ramp signal applied to simulate the gradual change of C_1 value, respectively ,C_2 value.

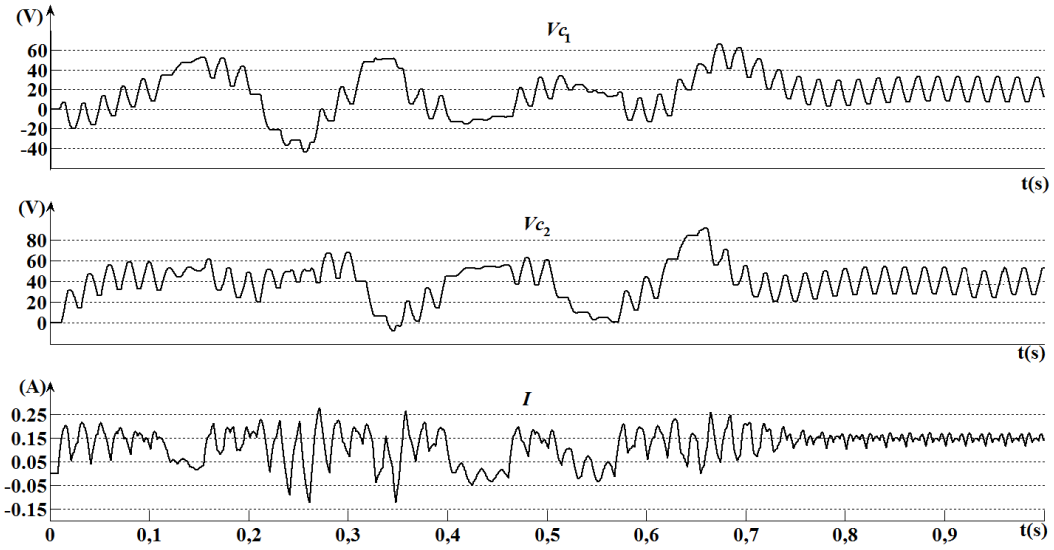

Figure 5.21: Real signals of Vc_1, Vc_2 and I in simulated normal and faulty conditions of Fig.5.19.

direction (aging) using a ramp signal (see Fig.5.20). Vc_1, Vc_2 and I simulated signals including these faults are represented in Fig.5.21. The ramp signal is used in order to generate a slow gradual change in the value of C_1, respectively, C_2.

One can see in Fig.5.21 that Vc_1 (respectively Vc_2) has lost the periodic aspects in the case of a fault and that the current I has become inconstant in the region of its reference value. r_1, r_2, r_3 are represented in Fig.5.22 and Fig.5.23. As expected, r_1 is sensitive to the faults of types F_1, F_2, F_3, F_4 and F_7, r_2 is sensitive to the faults of types F_3, F_4, F_5, F_6 and F_8; while r_3 is sensitive to the faults of types F_1, F_2, F_3, F_4, F_5 and F_6.

Fig.5.24, Fig.5.25, Fig.5.26 and Fig.5.6.2 show, respectively, local decision DD_1 of diagnoser D_1, local decision DD_2 of diagnoser D_2, local decision DD_3 of diagnoser D_3 and global decision (DD). we can see that, The first local diagnoser (D_1) is sensitive to faults of types F_1, F_2 and F_7 (diagnosis with certainty their occurrence), the second local diagnoser (D_2) is sensitive to faults of types F_3, F_4, F_7 and F_8;

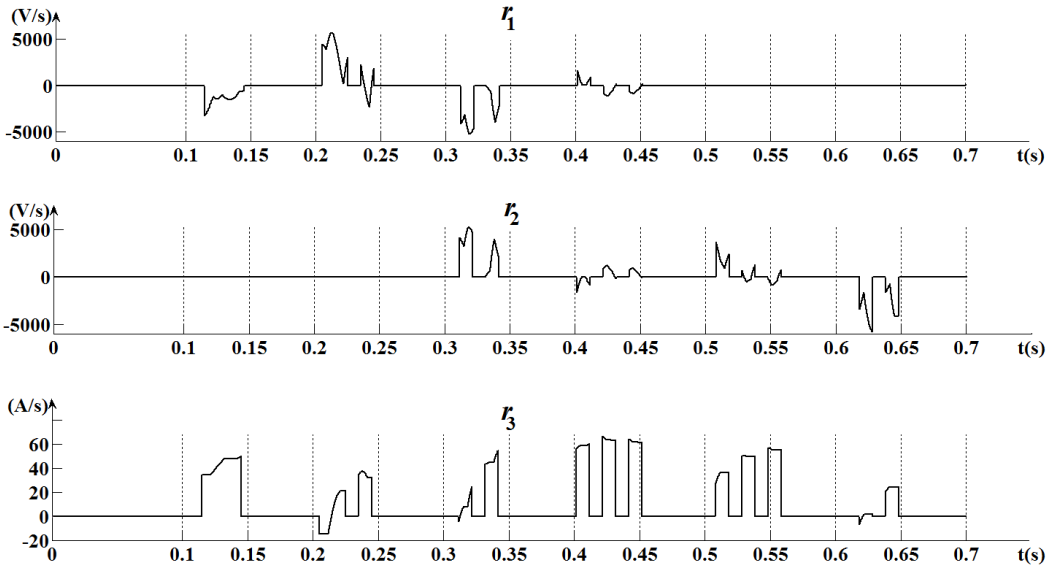

Figure 5.22: Residuals corresponding to the generated discrete faults of Fig.5.19.

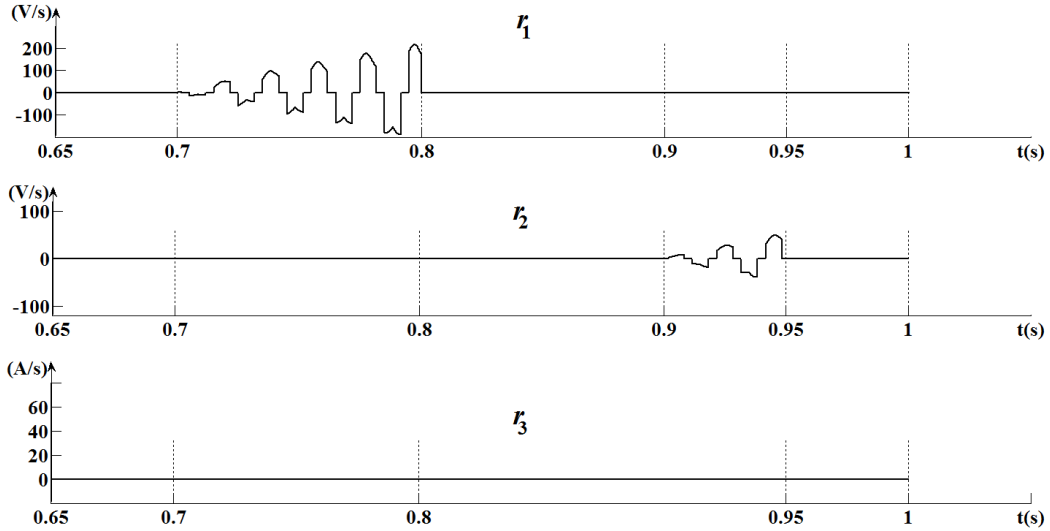

Figure 5.23: Residuals corresponding to the generated parametric faults of Fig.5.19.

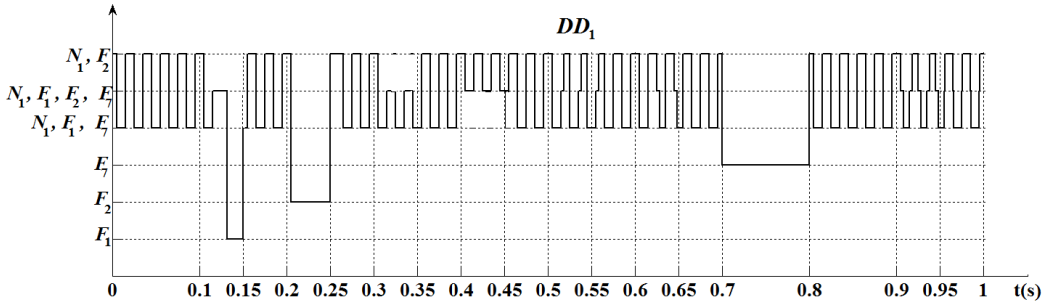

Figure 5.24: Local decision DD_1 of D_1.

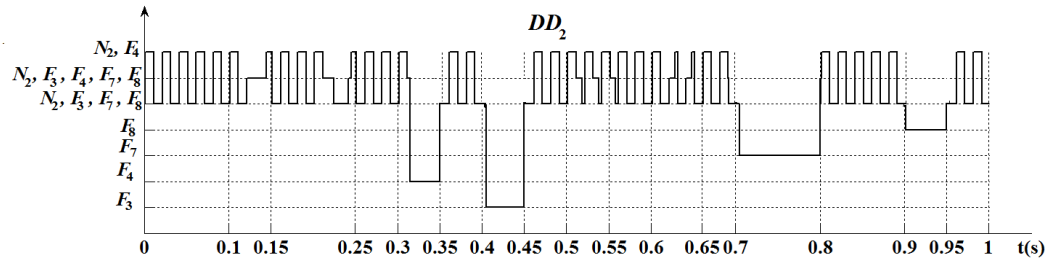

Figure 5.25: Local decision DD_2 of D_2.

while the third local diagnoser (D_3) is sensitive to faults of types F_5, F_6 and F_8. We can conclude that the global decision indicates with certainty the occurrence of each of the generated faults of Fig.5.19. The diagnosis delay, Δ_F, (see Fig.5.28) is defined as the difference between the time of the occurrence of a fault and the time of the diagnosis of this fault. If the fault is occurred when hybrid component HC_j is in a local hybrid state (q^j), this fault is diagnosed if the continuous dynamics of q^j generates a fault signature sensitive to this fault. In this case, the generated fault signature moves the diagnoser D_j from an uncertain state to a certain state with only one fault label indicating the occurrence of this fault. However, if the continuous dynamics of q^j does not allow the generation of a fault signature sensitive to this fault, the latter cannot be isolated. As an example in Fig.5.12, if a fault of type F_7 occurs when HC_1 is in local state q_2^1, HC_1 reach q_7^1 due to the occurrence of this fault. The continuous dynamics in q_7^1 does not allow the generation of a fault signature sensitive to this fault. The local diagnoser D_1 cannot diagnose with certainty the occurrence of this fault (see states z_2^1 or z_3^1 of Fig.5.12); while if a fault of type F_7 occurs when HC_1 is in local state q_1^1, HC_1 reach q_8^1 due to the occurrence of this fault. The continuous dynamic in q_8^1 allow generating a fault signature sig_7^1 sensitive to this fault. Local diagnoser D_1 moves to z_7^1 (see states z_1^1, z_4^1 and z_7^1 of Fig.5.12).

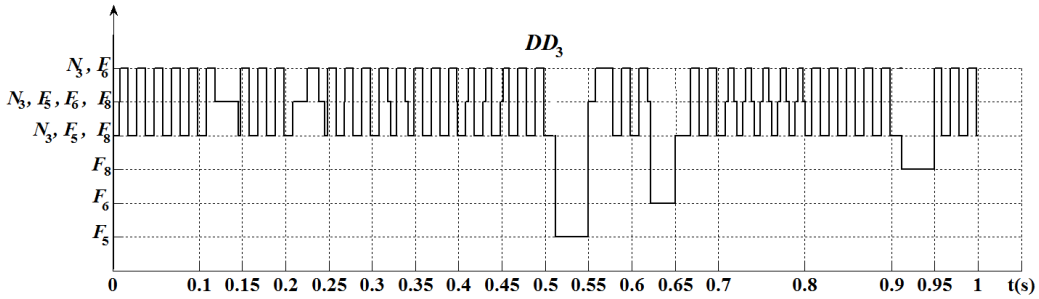

Figure 5.26: Local decision DD_3 of D_3.

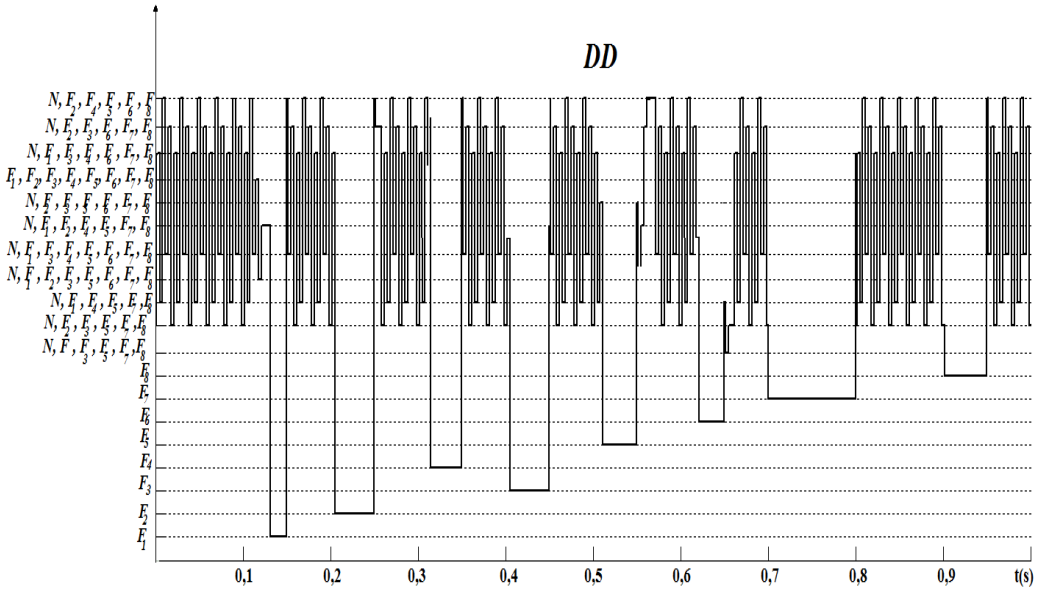

Figure 5.27: Global diagnosis decision issued by the coordinator.

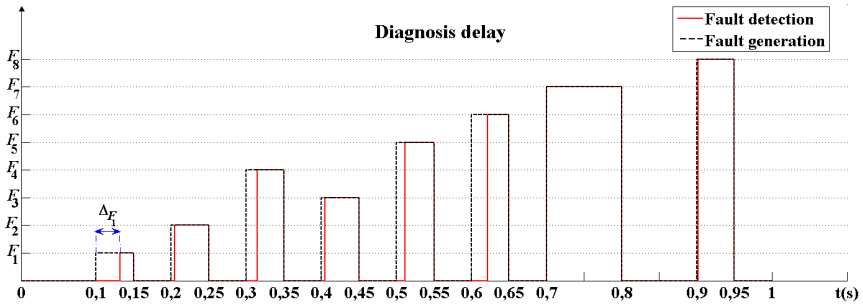

Figure 5.28: Diagnosis delay, Δ_{F_d}, $d \in \{1, \cdots, 8\}$, for the fault scenario of Fig.5.19. Δ_{F_d} depends on the discrete mode in which a fault occurred.

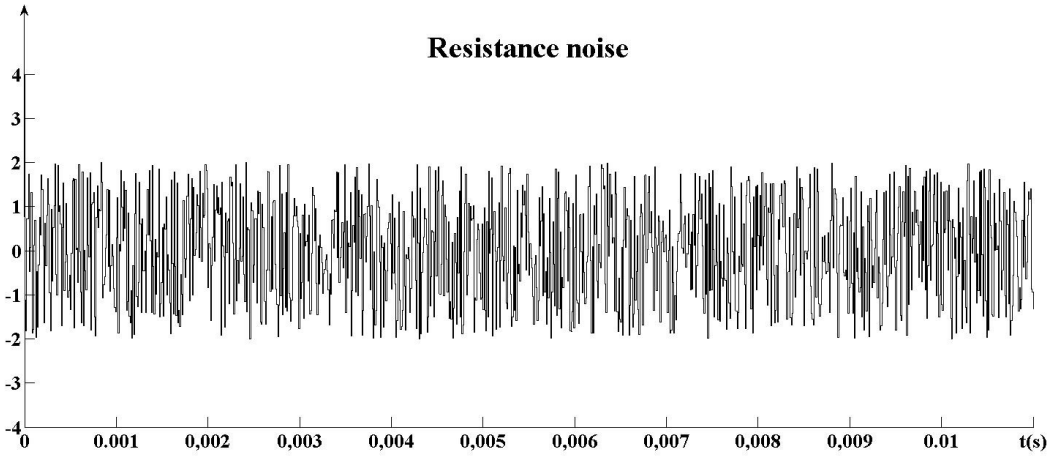

Figure 5.29: Noises added to the load resistor, R.

5.6.3 Normal conditions scenario with noises added to load resistor R

Diagnosis algorithms should be tested and evaluated on real systems with practical significance. In these systems, factors such as noises make diagnosis challenging. Therefore, there is a need to evaluate the robustness of the diagnosis algorithms for different faults and noises magnitudes. Accurate simulation models of the system are required for this purpose. Further, it is important to execute the diagnosis algorithms on systems, where the noises model is always present, and complicates the diagnosis task. In order to examine the robustness of our approach, a parametric noises (see for example Fig.5.29), applied on parameters, is used. From an electrical point of view, the resistors are the most disturbing elements in the three cell converter systems. For this reason, we added noises to the nominal value of resistor R. In order to take into account the noises added to R, the residuals of (5.8) is written as follows:

$$\begin{cases} r_1 = \left(-\tilde{h}_q^1 \frac{1}{\tilde{C}_1} + h_q^1 \frac{1}{C_1}\right) I + \left(\tilde{h}_q^2 \frac{1}{\tilde{C}_1} - h_q^2 \frac{1}{C_1}\right) I \\ r_2 = \left(-\tilde{h}_q^2 \frac{1}{\tilde{C}_2} + h_q^2 \frac{1}{C_2}\right) I + \left(\tilde{h}_q^3 \frac{1}{\tilde{C}_2} - h_q^3 \frac{1}{C_2}\right) I \\ r_3 = \left(-\tilde{R} + R_b\right) \frac{I}{L} + \left(\tilde{h}_q^1 - h_q^1\right) \frac{Vc_1}{L} + \left(\tilde{h}_q^2 - h_q^2\right) \frac{(Vc_2 - Vc_1)}{L} + \\ \qquad \left(\tilde{h}_q^3 - h_q^3\right) \frac{(E - Vc_2)}{L} \end{cases} \tag{5.36}$$

where $\tilde{R}$ is the nominal value of R without noises; while R_b is the real value of R. R_b corresponds to the nominal value of R with noises. r_1, r_2, r_3 are represented in Fig.5.30. As expected, r_1 and r_2 are not sensitive to this perturbation in normal conditions (R does not influence the dynamic evolutions of Vc_1 and Vc_2; while r_3 is impacted by these noises. r_3 changes between $-0.4\,A/s$ and $0.4\,A/s$ as we can see in Fig.5.30.

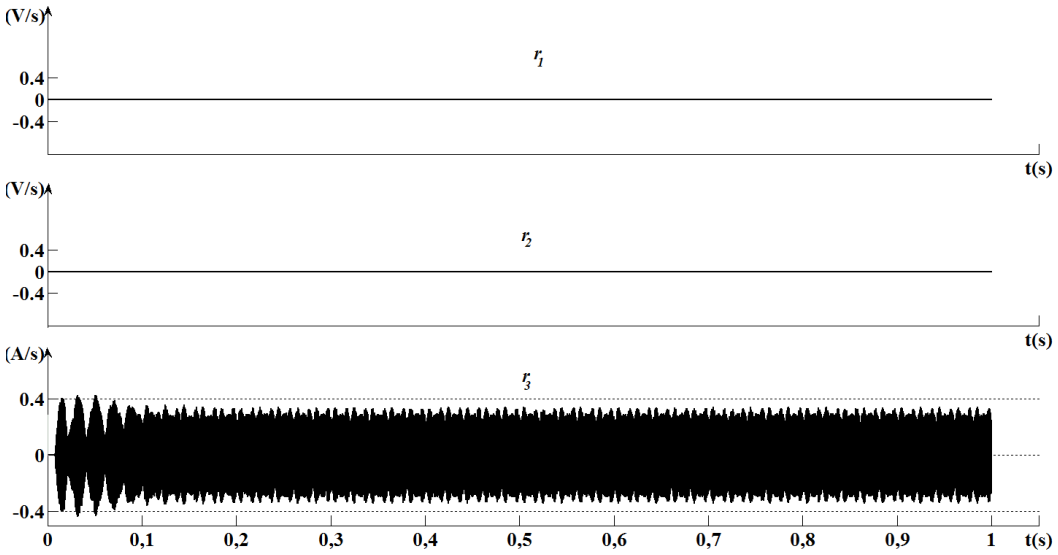

Figure 5.30: Set of residuals with noises corresponding to the normal conditions.

Ideally, any non-zero residual value implies a fault, which should trigger the fault isolation system. Therefore, statistical techniques are required for reliable fault detection. The fault detection system is based on a Z-test that uses the estimated variance of the residuals and a pre-specified confidence level to establish the significance of observed nonzero residuals. To cope with noises, we compute the mean and the variance at different time points, Biswas et al. (2003), Khorasgani et al. (2014). The Z-test is a statistical inference test employed to establish the signification of the deviation. It requires the mean and standard deviation of the population, and the mean and size of the samples. These values are estimated using sliding windows over the residual for a variable. A small sliding window of size W_1 samples, is used to estimate the current mean $\mu_{r_i}(t)$ of residual r_i related to the variable x_i:

$$\mu_{r_i}(t) = \frac{1}{W_1} \sum_{v=t-W_1+1}^{t} r_i(v) \tag{5.37}$$

We suppose the mean of the population is equal to zero, since the residual should be zero when the system is free of faults. We compute the variance from data history of the nominal residual signal over a window W_2 proceeding W_1, where $W_2 \gg W_1$, as an estimate of the true variance:

$$\mu'_{r_i}(t) = \frac{1}{W_2} \sum_{v=t-W_2-W_1+1}^{t-W_1} r_i(v) \tag{5.38}$$

$$\sigma_{r_i}(t) = \frac{1}{W_2} \sum_{v=t-W_2-W_1+1}^{t-W_1} (r_i(v) - \mu'_{r_i}(v))^2 \tag{5.39}$$

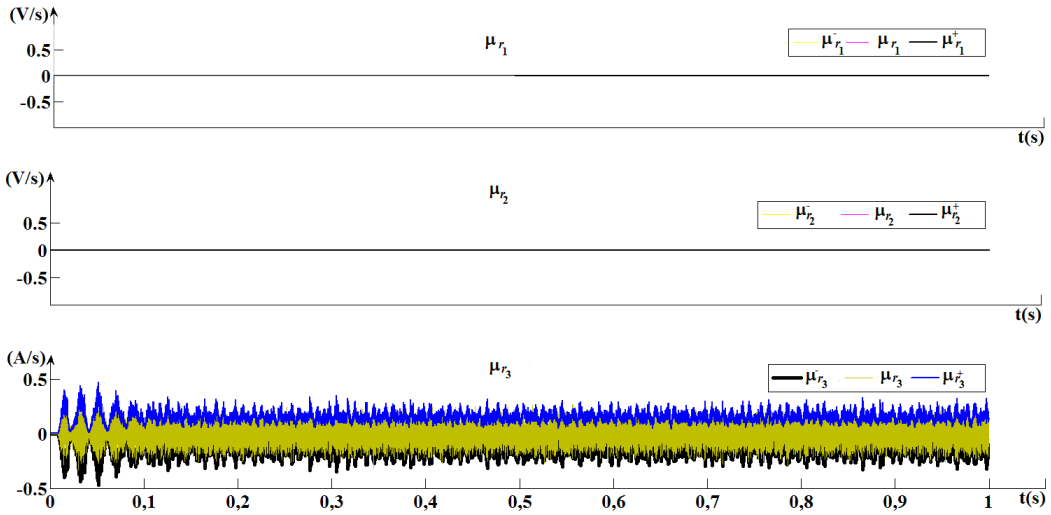

Figure 5.31: Set of residuals and thresholds with noises corresponding to the normal conditions.

The size of W_2 must contain enough of measurements in order to estimate correctly the residuals mean and variance in the normal operating conditions and therefore to reduce the rate of false alarms. The size of W_1 must also be selected as a tradeoff between the delay of fault detection and the rate of false alarms. The size of W_2, respectively W_1, is chosen experimentally to be equal to 25, respectively 5, measurements.

Since the distribution of residuals mean is supposed to follow the normal distribution, a confidence level, α, is defined by determining the bound $\left[\mu_{r_i}^-, \mu_{r_i}^+\right]$ within which $\mu_{r_i}(t)$ is considered to correspond to normal operating conditions. $\left[\mu_{r_i}^-, \mu_{r_i}^+\right]$ is defined using Z-test table and the approximation σ_{r_i}:

$$\begin{cases} \mu_{r_i}^-(t) = \frac{z_{vi}^- \sigma_{r_i}}{W_1} \\ \\ \mu_{r_i}^+(t) = \frac{z_{vi}^+ \sigma_{r_i}}{W_1} \end{cases} \tag{5.40}$$

For α equal to 0.95, z_{vi}^- and z_{vi}^+ are equal to, respectively, -1.64 and 1.64.

The Z-test is employed in the following manner:

- $\mu_{r_i}^- < \mu_{r_i} < \mu_{r_i}^+ \Rightarrow$ No fault;
- Otherwise $\Rightarrow$ Fault;

Fig.5.31 depicts the mean of residual μ_{r_3} and the negative and positive thresholds of this residual defined by the Z-test. The mean and true variance of residuals r_1 and r_2 are equal to zero. Thus, their thresholds are also equal to zero (μ_{r_1}, $\mu_{r_1}^+$ and $\mu_{r_1}^-$, respectively, μ_{r_2}, $\mu_{r_2}^+$ and $\mu_{r_2}^-$ are superposed).

Table 5.7: Local fault signatures generated due to the occurrence of faults in HC_1 in the case of parametric noise.

Local fault signature symbol	***Equivalent global fault signatures***
sig_0^1	$\left(\mu_{r_1}^- < \mu_{r_1} < \mu_{r_1}^+\right) \& \left(\mu_{r_2}^- < \mu_{r_2} < \mu_{r_2}^+\right)$ $\& \left(\mu_{r_3}^- < \mu_{r_3} < \mu_{r_3}^+\right)$
sig_1^1	$\left(NC_1^1 + \mu_{r_1}^- < \mu_{r_1} < NC_1^1 + \mu_{r_1}^+\right) \& \left(\mu_{r_2}^- < \mu_{r_2} < \mu_{r_2}^+\right)$ $\& \left(PC_3^1 + \mu_{r_3}^- < \mu_{r_3} < PC_3^1 + \mu_{r_3}^+\right)$
sig_2^1	$\left(PC_1^1 + \mu_{r_1}^- < \mu_{r_1} < PC_1^1 + \mu_{r_1}^+\right) \& \left(\mu_{r_2}^- < \mu_{r_2} < \mu_{r_2}^+\right)$ $\& \left(NC_3^1 + \mu_{r_3}^- < \mu_{r_3} < NC_3^1 + \mu_{r_3}^+\right)$
sig_7^1	$\left(\mu_{r_1}^+ < \mu_{r_1}\right) \& \left(\mu_{r_2}^- < \mu_{r_2} < \mu_{r_2}^+\right) \& \left(\mu_{r_3}^- < \mu_{r_3} < \mu_{r_3}^+\right)$
	$\left(\mu_{r_1}^- > \mu_{r_1}\right) \& \left(\mu_{r_2}^- < \mu_{r_2} < \mu_{r_2}^+\right) \& \left(\mu_{r_3}^- < \mu_{r_3} < \mu_{r_3}^+\right)$

Table 5.8: Local fault signatures generated due to the occurrence of faults in HC_2 in the case of parametric noise.

Local fault signature symbol	***Equivalent global fault signatures***
sig_0^2	$\left(\mu_{r_1}^- < \mu_{r_1} < \mu_{r_1}^+\right) \& \left(\mu_{r_2}^- < \mu_{r_2} < \mu_{r_2}^+\right)$ $\& \left(\mu_{r_3}^- < \mu_{r_3} < \mu_{r_3}^+\right)$
sig_3^2	$\left(PC_1^2 + \mu_{r_1}^- < \mu_{r_1} < PC_1^2 + \mu_{r_1}^+\right)$ $\& \left(NC_2^2 + \mu_{r_2}^- < \mu_{r_2} < NC_2^2 + \mu_{r_2}^+\right)$ $\& \left(PC_3^2 + \mu_{r_3}^- < \mu_{r_3} < PC_3^2 + \mu_{r_3}^+\right)$
sig_4^2	$\left(NC_1^2 + \mu_{r_1}^- < \mu_{r_1} < NC_1^2 + \mu_{r_1}^+\right)$ $\& \left(PC_2^2 + \mu_{r_2}^- < \mu_{r_2} < PC_2^2 + \mu_{r_2}^+\right)$ $\& \left(NC_3^2 + \mu_{r_3}^- < \mu_{r_3} < NC_3^2 + \mu_{r_3}^+\right)$
sig_7^2	$\left(\mu_{r_1}^+ < \mu_{r_1}\right) \& \left(\mu_{r_2}^- < \mu_{r_2} < \mu_{r_2}^+\right) \& \left(\mu_{r_3}^- < \mu_{r_3} < \mu_{r_3}^+\right)$
	$\left(\mu_{r_1}^- > \mu_{r_1}\right) \& \left(\mu_{r_2}^- < \mu_{r_2} < \mu_{r_2}^+\right) \& \left(\mu_{r_3}^- < \mu_{r_3} < \mu_{r_3}^+\right)$
sig_8^2	$\left(\mu_{r_1}^- < \mu_{r_1} < \mu_{r_1}^+\right) \& \left(\mu_{r_2}^- > \mu_{r_2}\right) \& \left(\mu_{r_3}^- < \mu_{r_3} < \mu_{r_3}^+\right)$
	$\left(\mu_{r_1}^- < \mu_{r_1} < \mu_{r_1}^+\right) \& \left(\mu_{r_2}^+ < \mu_{r_2}\right) \& \left(\mu_{r_3}^- < \mu_{r_3} < \mu_{r_3}^+\right)$

Table 5.9: Local fault signatures generated due to the occurrence of faults in HC_3 in the case of parametric noise.

Local fault signature symbol	***Equivalent global fault signatures***
sig_0^3	$\left(\mu_{r_1}^- < \mu_{r_1} < \mu_{r_1}^+\right) \& \left(\mu_{r_2}^- < \mu_{r_2} < \mu_{r_2}^+\right)$ $\& \left(\mu_{r_3}^- < \mu_{r_3} < \mu_{r_3}^+\right)$
sig_5^3	$\left(\mu_{r_1}^- < \mu_{r_1} < \mu_{r_1}^+\right) \& \left(PC_2^3 + \mu_{r_2}^- < \mu_{r_2} < PC_2^3 + \mu_{r_2}^+\right)$ $\& \left(PC_3^3 + \mu_{r_3}^- < \mu_{r_3} < PC_3^3 + \mu_{r_3}^+\right)$
sig_6^3	$\left(\mu_{r_1}^- < \mu_{r_1} < \mu_{r_1}^+\right) \& \left(NC_2^3 + \mu_{r_2}^- < \mu_{r_2} < NC_2^3 + \mu_{r_2}^+\right)$ $\& \left(NC_3^3 + \mu_{r_3}^- < \mu_{r_3} < NC_3^3 + \mu_{r_3}^+\right)$
sig_8^2	$\left(\mu_{r_1}^- < \mu_{r_1} < \mu_{r_1}^+\right) \& \left(\mu_{r_2}^- > \mu_{r_2}\right) \& \left(\mu_{r_3}^- < \mu_{r_3} < \mu_{r_3}^+\right)$
	$\left(\mu_{r_1}^- < \mu_{r_1} < \mu_{r_1}^+\right) \& \left(\mu_{r_2}^+ < \mu_{r_2}\right) \& \left(\mu_{r_3}^- < \mu_{r_3} < \mu_{r_3}^+\right)$

Tables 5.3, 5.4 and 5.5 are modified by replacing r_1 by μ_{r_1}, r_2 by μ_{r_2} and r_3 by μ_{r_3}. Thus, Tables 5.3, 5.4 and 5.5 become as, respectively, Tables 5.7, 5.8 and 5.9 in order to integrate the noises added to resistor R.

5.6.4 Faulty conditions scenario with noises added to load resistor R

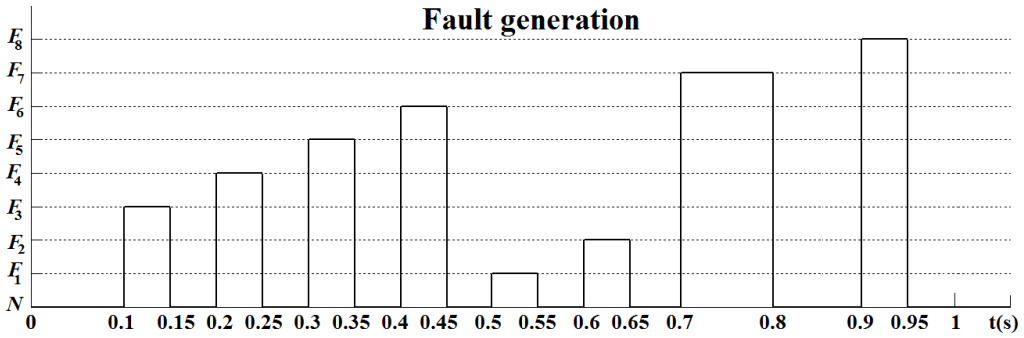

Figure 5.32: Time of appearance, injection, of faults during the simulation of three cell converters with noise.

In order to evaluate the proposed approach in the case of noises, fault scenario is generated (see Fig.5.32). The order of the occurrence of faults according to the one of Fig.5.19 has been changed in order to show the robustness of the proposed approach according to the order of fault occurrence. The corresponding μ_{r_1}, μ_{r_2} and μ_{r_3} for this scenario is represented in Fig.5.33 and Fig.5.34. In this case, noises are observed only in μ_{r_3} at normal and faulty conditions (see zoom in Fig.5.35). As we said before, only μ_{r_3} is impacted by noises since the noisy parameter R is included only in the dynamic evolution $\dot{I}$ of I (see (5.36)). To overcome this noises problem, a threshold is defined for each residual using Z-test. These thresholds are used during the fault detection and isolation in order to avoid the false alarms (residuals are different from zero due to the noises and not because of the occurrence of a fault) as well as the missed fault detection (The discrete symbols PC^j and NC^j in the faults signatures must take into account the presence of the noises) caused by noises.

Fig.5.36, Fig.5.37, Fig.5.38 and Fig.5.39 show, respectively, local decision DD_1 of diagnoser D_1, local decision DD_2 of diagnoser D_2, local decision DD_3 of diagnoser D_3 and global decision DD. The first local diagnoser D_1 is sensitive to faults of types F_1, F_2 and F_7 (diagnosis with certainty their occurrence), the second local diagnoser D_2 is sensitive to faults of types F_3, F_4, F_7 and F_8; while the third local diagnoser D_3 is sensitive to faults of types F_5, F_6 and F_8. We can conclude that the global decision indicates with certainty the occurrence of each of the generated faults of Fig.5.32 regardless of the existence of noises.

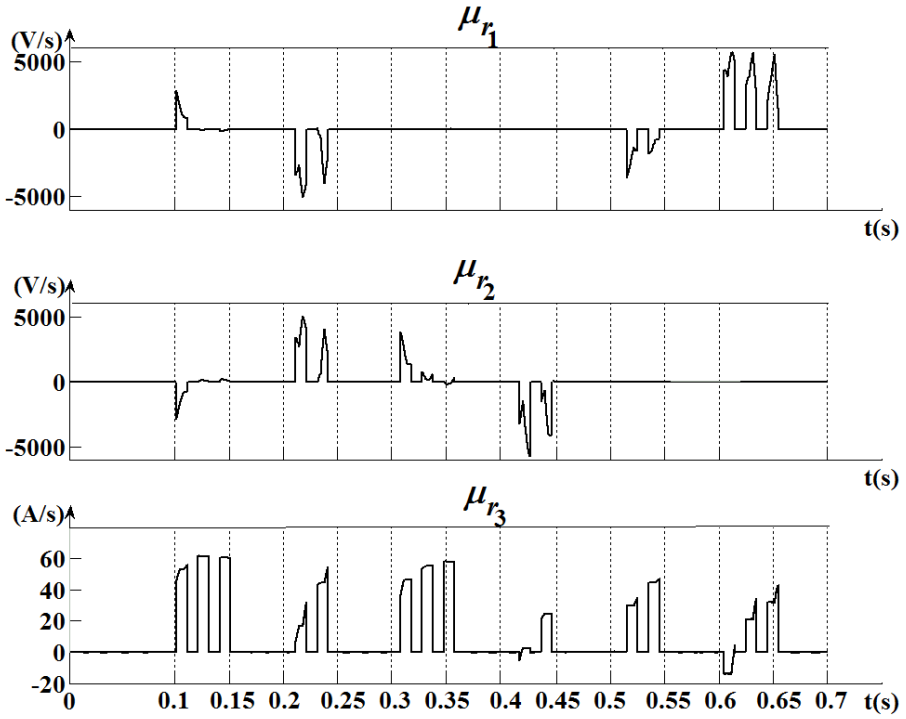

Figure 5.33: Residuals corresponding to the generated discrete faults of Fig.5.32 in the case of noises added to R.

5.6.5 Normal conditions scenario with noises added to capacitor C_1

In order to test the diagnosis approach performance, noises are added to the nominal value of the three cell converter capacitor C_1. Fig.5.40 depicts the mean of residual μ_{r_1} and the negative and positive thresholds of this residual defined by the Z-test. The mean and true variance of residuals r_2 and r_3 are equal to zero. Thus, their thresholds are also equal to zero. In the case of noises added to C_1, only μ_{r_1} is impacted by noises since the noisy parameter C_1 is included only in the dynamic evolution $\dot{V}c_1$ of Vc_1.

5.6.6 Faulty conditions scenario with noises added to capacitor C_1

In order to evaluate the proposed approach in the case of noises added to capacitor C_1, the fault scenario generated previously (see Fig.5.32) is used but by adding noises to capacitor C_1 and not to resistor R. The corresponding μ_{r_1}, μ_{r_2} and μ_{r_3} for this scenario are represented in Fig.5.41. In this case, noises are observed only in μ_{r_1} at normal and faulty conditions. As we said before, only μ_{r_1} is impacted by noises since the noisy parameter C_1 is included only in dynamic evolution $\dot{V}c_1$ of Vc_1. Fig.5.42 shows the global decision DD in the case of noises added to capacitor C_1. In this case, the decentralized approach allows to diagnose the set of the generated fault of Fig5.32. By comparing DD for C_1 without noises (see Fig.5.39) and DD for

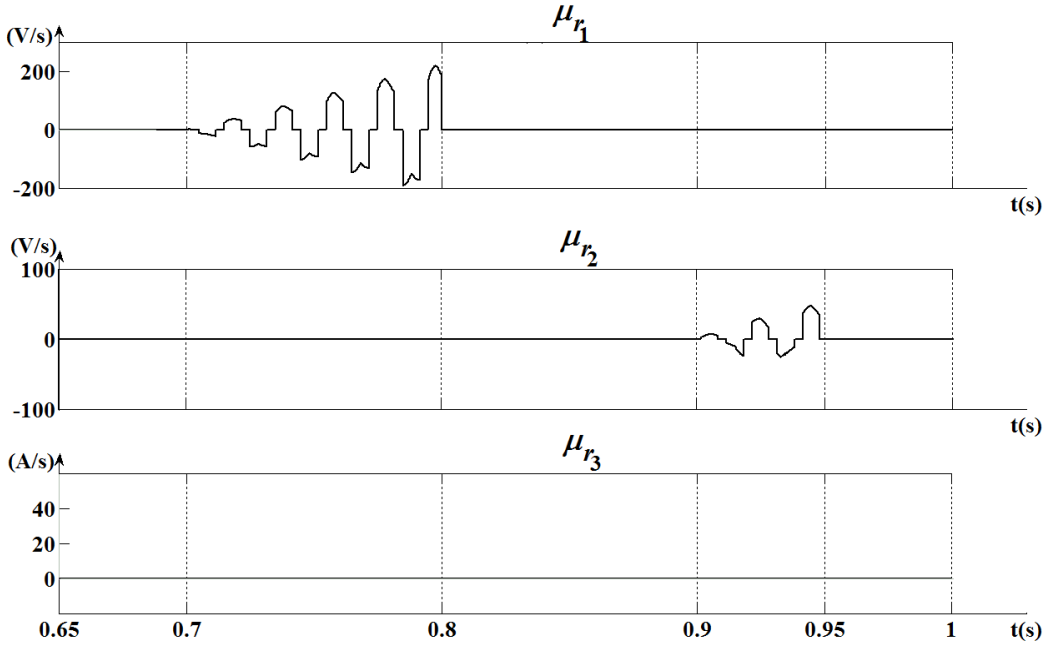

Figure 5.34: Residuals corresponding to the generated parametric faults of Fig.5.32 in the case of noises added to R.

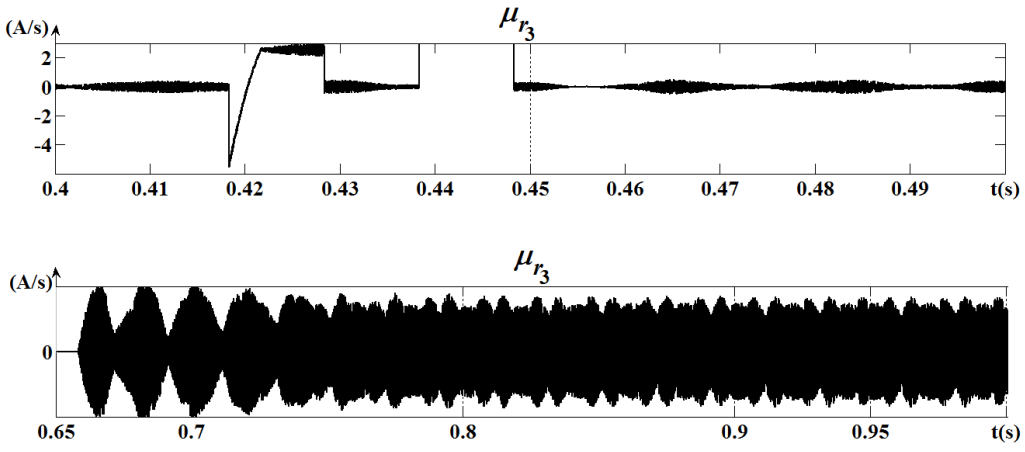

Figure 5.35: Zoom of μ_{r_3} with noises corresponding to normal and faulty conditions scenario of Fig.5.32.

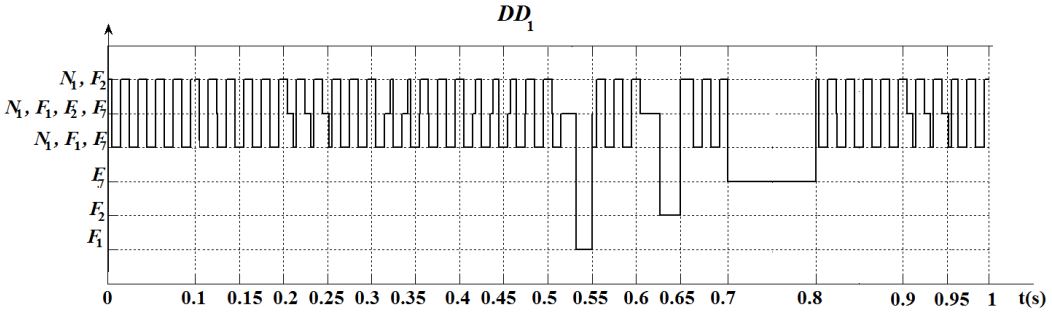

Figure 5.36: Local decisions DD_1 of D_1 in the case of noises.

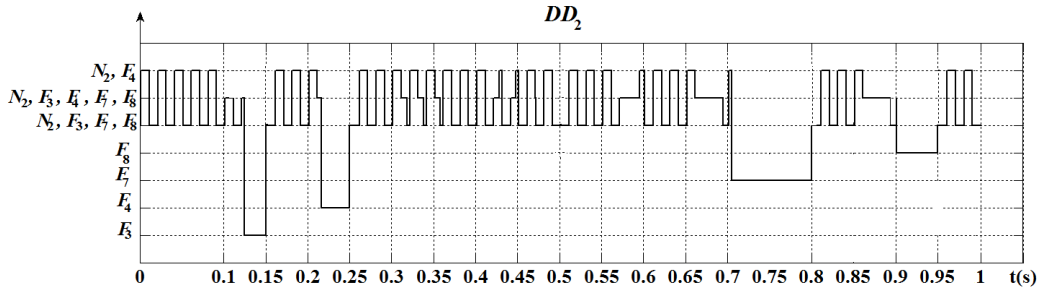

Figure 5.37: Local decisions DD_2 of D_2 in the case of noises added to R.

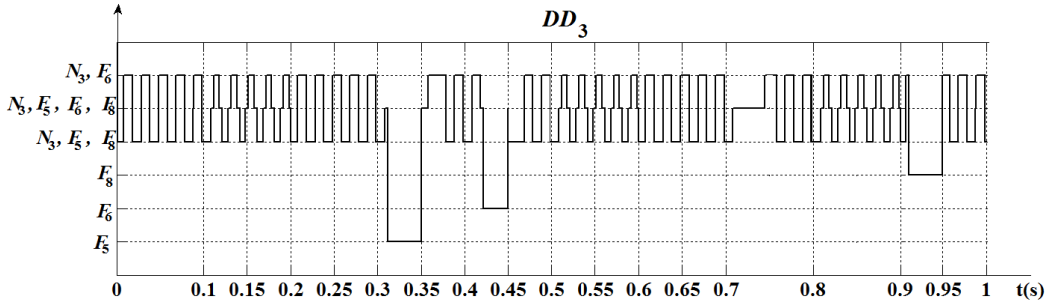

Figure 5.38: Local decisions DD_3 of D_3 in the case of noises added to R.

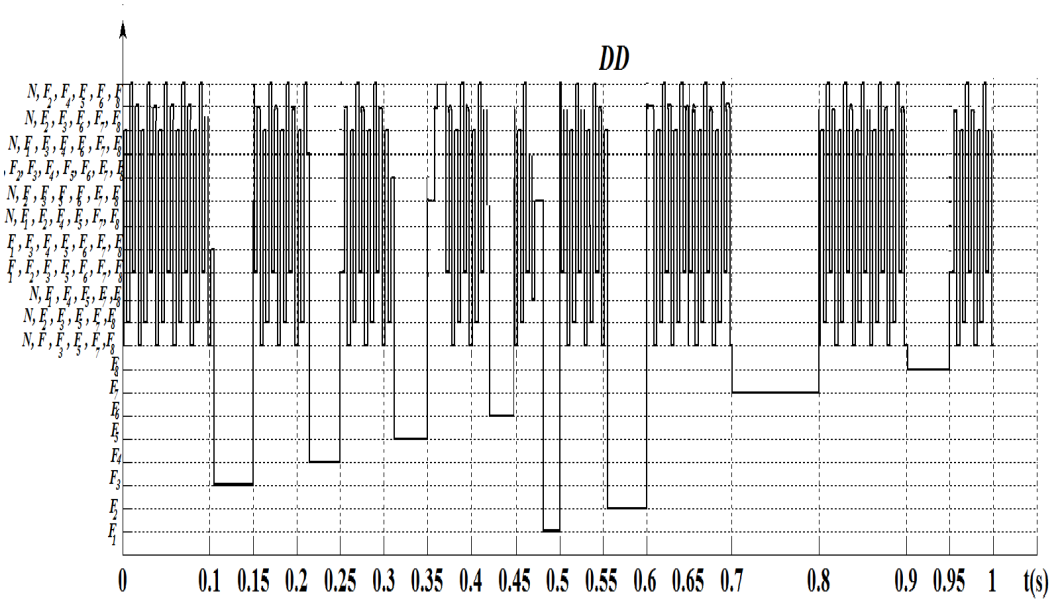

Figure 5.39: Global diagnosis decision issued by the coordinator in the case of noises added to R.

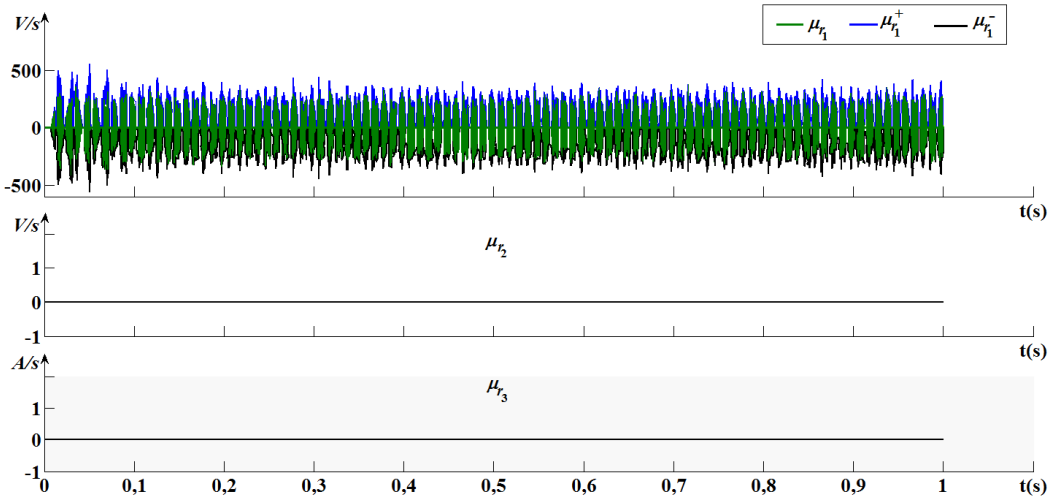

Figure 5.40: Set of residuals corresponding to the normal conditions in the case of noises added to the nominal value of the three cell converter capacitor C_1.

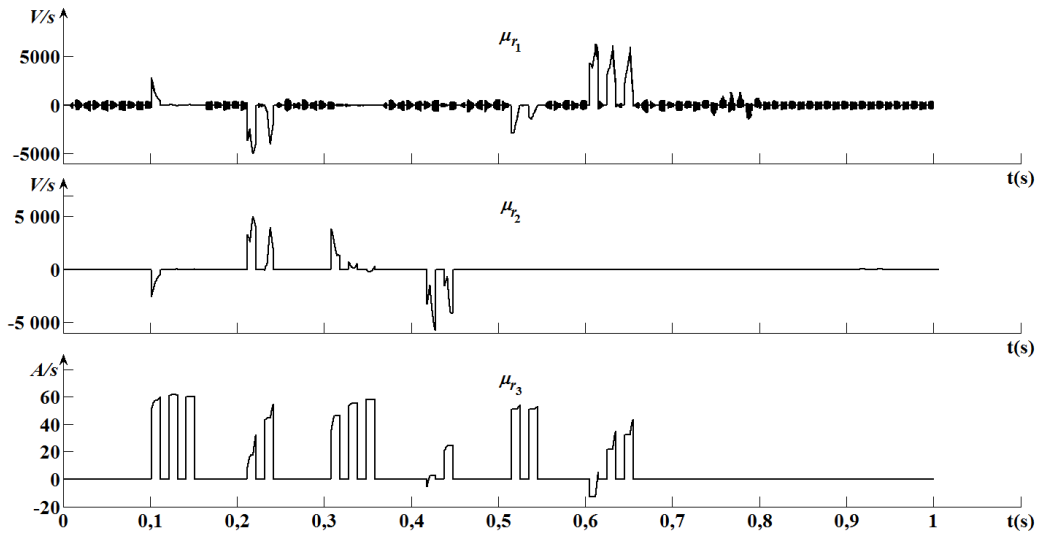

Figure 5.41: Set of residuals corresponding to the generated faults of Fig.5.32 in the case of noises added to the nominal value of the three cell converter capacitor C_1.

C_1 with noises (see Fig.5.42), we can see that the diagnosis delay for the diagnosis of a fault of type F_7 is bigger in the later than the one of the former. This is due to the fact that the diagnosers wait μ_{r_1} to exceed the thresholds in order to detect the occurrence of this fault.

5.7 Comparison between the proposed centralized and decentralized approaches for the three cell converter system

In this chapter, the decentralized hybrid diagnosis approach is applied to achieve the diagnosis of the parametric and discrete faults (see Table 5.1) that can occur in the three cell converter system. Table 5.10 represents the comparison between the major characteristics of the centralized and decentralized proposed approaches for the three cell converter system.

Based on remark 4.1, the decentralized proposed approach has the advantage to be robust because when D_1 fails, D_2, respectively D_3, diagnoses the occurrence of faults of types F_3, F_4, F_7 and F_8, respectively F_5, F_6 and F_8; while when D_2 fails, D_1, respectively D_3, assures the diagnosis of the occurrence of faults of types F_1, F_2 and F_7, respectively F_5, F_6 and F_8. Likewise, when D_3 fails, D_1, respectively D_2, assures the diagnosis of the occurrence of faults of types F_1, F_2 and F_7, respectively F_3, F_4, F_7 and F_8.

Let $|G^j|$, $j \in \{1,2,3\}$, be the number of states of local model G^j, $j \in \{1,2,3\}$, and $|G|$ be the number of states of global model G of the three cell converter system. Let $|\Sigma^j|$, $j \in \{1,2,3\}$, be the number of events in Σ^j, $j \in \{1,2,3\}$, and $|\Sigma|$ be the

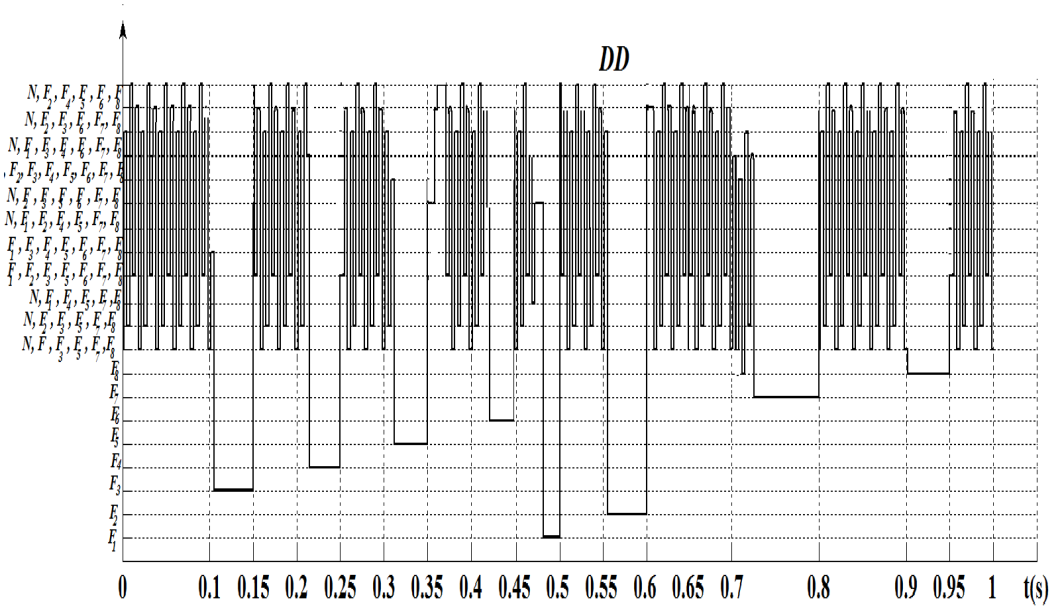

Figure 5.42: Global diagnosis decision issued by the coordinator in the case of noises added to C_1.

number of events in Σ, i.e., events generated in the three cell converter system. The number of transitions is equal to $|G^j| \times |\Sigma^j|$, $j \in \{1,2,3\}$, for G^j and $|G| \times |\Sigma|$ for G. Consequently, the complexity for constructing D_j, $j \in \{1,2,3\}$, is of the order $O\left(|G^j| \times |\Sigma^j|\right)$, e.g., the complexity for constructing D_1 is of the order $O\left(8 \times 5\right)$ ((8 hybrid states)$\times$(2 controller command events and 3 events indicating the occurrence of faults (see Fig.5.8))). Likewise, the complexity for constructing D_2 is of the order $O\left(10 \times 5\right)$ ((10 hybrid states)$\times$(2 controller command events and 3 events indicating the occurrence of faults (see Fig.5.9))) and the complexity for constructing D_3 is of the order $O\left(8 \times 5\right)$ ((8 hybrid states)$\times$(2 controller command events and 3 events indicating the occurrence of faults (see Fig.5.10))). The complexity for constructing D is of the order $O\left(|G| \times |\Sigma|\right)$. i.e, the complexity for constructing D is of the order $O\left(640 \times 125\right)$ ((8$\times$10$\times$8 hybrid states$\times$(5$\times$5$\times$5 events)). Therefore, the complexity of the proposed decentralized diagnosis approach is polynomial in the number of the system components and in the size of local model G^j; while the complexity of the proposed centralized diagnosis approach is exponential in the number of the system components and the size of local model G^j.

5.8 Summary

In this chapter, the decentralized hybrid diagnosis approach for discretely controlled continuous systems, developed in Chapter 4, is applied using the three cell converter. This application demonstrated the capacitor of the hybrid models to represent intrinsically the interactions between the continuous and the discrete dynamics of

Table 5.10: Comparison between the proposed centralized and decentralized approaches for the three cell converter.

Characteristics	***Centralized approach***	***Decentralized approach***
Decomposition of the system	Yes Into 3 hybrid components HC_1, HC_2 and HC_3	Yes Into 3 hybrid components HC_1, HC_2 and HC_3
The use of global model	Yes	No
The complexity of the diagnoser	$\|G^1\| \times \|G^2\| \times \|G^3\|$	$\|G^1\| + \|G^2\| + \|G^3\|$
Diagnosis of discrete faults	Yes F_1, F_2, F_3, F_4, F_5 and F_6	Yes F_1, F_2, F_3, F_4, F_5 and F_6
Diagnosis of parametric faults	Yes F_7 and F_8	Yes F_7 and F_8
Robustness	Weak robustness (see remark 4.1)	Strong robustness (see remark 4.1)

the system. The diagnosis task is accomplished by a set of local hybrid diagnosers D_1, D_2 and D_3. Each of the latter is responsible of the diagnosis of a specific part of the system. These local hybrid diagnosers are built without the use of the system global model but only the local models. The decisions of the local hybrid diagnosers are merged using a coordinator in order to diagnose the set of generated faults in the system.

In order to highlight the efficiency of the decentralized diagnosis approach, developed in Chapter 4, several simulation scenarios are generated for the three cell converter. These scenarios represent several parametric and discrete faults impacting the discrete switches (S_1, S_2 and S_3) and the capacities (C_1 and C_2). In the first time, the faults are generated without considering the noises in the parameters of the three cell converter. The diagnosers diagnosed with certainty the occurrence of the set of generated parametric and discrete faults. In the second time, noises are added to load resistor (R) and to capacitor (C_1). The obtained results showed that the decentralized fault diagnosis structure continues to diagnose with certainty the occurrence of parametric and discrete generated faults in the presence of noises. This proves the robustness of the proposed decentralized approach against the noises in the converter parameters.

Based on Fig.5.8 and Fig.5.10, we can conclude that the models of the first and the third hybrid components, HC_1 and HC_3, representing the first and third cells of converter are similar. Therefore their local diagnosers D_1 and D_2 are also similar

(see Fig.5.12 and Fig.5.12). consequently, in the case of multi-cell converter with n cells, the local diagnosers for the impair cells will be similar. Likewise, the local diagnosers of the pair cells will be similar. This can help to reduce significantly the computation efforts to construct the local diagnosers for n multi-cell converter.

In the future work, this approach will be applied to a physical real three cell converter with different types of controllers. The goal is to apply the proposed approach to the converters used in wind turbines. In the latter, the controller is used to change the current frequency in order to obtain different relation speeds for the generator. The goal is to optimize the generated electricity by the generator according to the wind speed.

Chapter 6

Conclusion

6.1 Summary of contributions and discussion

The work presented in this dissertation focused on the development of a model based approach to achieve the discrete and parametric faults diagnosis in hybrid dynamic systems (HDS), in particular discretely controlled continuous systems (DCCS). In Chapter 2, the basic definitions and the classes of HDS are presented. Then, the different approaches of the literature to achieve the fault diagnosis of HDS, in particular DCCS, are studied and compared using a simple example of one tank system. As shown in Chapter 2, these approaches are classified into three main categories:

1. approaches for the diagnosis of parametric faults. They take benefit of the discrete dynamics in order to enhance the diagnosis capacity (i.e., diagnosability) of only parametric faults. They cannot diagnose discrete faults because they consider the discrete events as observable events while the discrete faults are unobservable discrete events;

2. approaches for the diagnosis of discrete faults. They use the continuous dynamics in each normal or fault discrete mode in order to generate observable events. The latter, generated thanks to the continuous dynamics, are used to enhance the diagnosability of only discrete faults. These approaches cannot diagnose parametric faults. This is due to the fact that they use the events generated by the continuous dynamics in order to distinguish between normal and fault discrete modes;

3. approaches for the diagnosis of both parametric and discrete faults. In these approaches, discrete and parametric faults are represented by different states in the system model. Thus, the system model size is more complex than the one built by the approaches of the two previous categories. This increases the complexity to diagnose these faults since the diagnoser, based on the same observability, needs to distinguish between a higher number of normal and faulty states (i.e., distinguishing discrete and continuous fault behaviors from the normal ones using the same observation of the system). For this reason, few approaches have been proposed in the literature to achieve both the parametric and discrete faults.

However, the approaches of these three categories suffer from the drawback that they do not scale well to large scale systems with huge number of discrete modes. This is due to the fact that they need a global model of the system. The construction of this global model may become unfeasible in the case of large scale systems because of the state space complexity.

Consequently, the contributions of this dissertation aim at developing an approach to achieve the diagnosis of parametric and discrete faults in large scale DCCS. To this end, two approaches have been proposed. The first approach is a modular parametric and discrete faults centralized diagnosis approach that takes benefit of the system modularity in order to facilitate the construction of the system global model. The second approach is based on the use of a decentralized diagnosis structure to achieve the parametric and discrete faults diagnosis without the use of a global model but only the local models of the systems components. The major advantages of these two approaches are as follows:

1. **Exploitation of the modularity of the system**: The system is decomposed into a set of discrete and continuous components. The discrete components present the discrete behaviors of the systems while the continuous components present the continuous behaviors of the system. The hybrid components are built as a combination of one discrete component and the continuous components interacting with it (i.e. the components that change their continuous dynamic evolutions due to the discrete mode of these discrete components). The local hybrid model of each hybrid component is built by synchronizing the local models of discrete and continuous components belonging to this hybrid components.

2. **Modular construction of the global model as well as the centralized diagnoser**. The global model is constructed based on the synchronous composition between the different hybrid local models. This facilitates the construction of the system global model. Then, the centralized diagnoser is constructed systematically based on the global model of the system.

3. **Decentralized parametric and discrete faults diagnosis strcuture**. In this approach a set of local diagnosers are built based on the local hybrid models of the system hybrid components. The aim of this approach is to diagnose the discrete and parametric faults without the use of global model. Each hybrid local diagnoser is sensitive to the fault occurring in its associated hybrid component. The local decisions issued from the local diagnosers are merged throughout a coordinator in order to obtain one global decision equivalent to the one of the centralized diagnoser. The advantage of this approach is that local hybrid diagnosers as well as the coordinator are built using local models. Consequently the decentralized parametric and discrete faults diagnosis approach scales well to large scale systems with multiple discrete modes.

Experimental case study to achieve the decentralized diagnosis of the three cell converter is devloped. In order to evaluate the proposed decentralized fault diagnosis approach, simulations are carried out for the three-cell converter using Matlab-Simulink^{TM} environment and Stateflow^{TM} toolbox. Several simulation scenarios are generated for the three cell converter in order to test the capacity of the proposed approach to diagnose the discrete and parametric faults impacting the system. The noises are added to be as close as possible to real operating conditions. The obtained results showed that the decentralized fault diagnosis structure continues to diagnose

with certainty the occurrence of the parametric and the discrete generated faults in the presence of noises. This proves the robustness of the proposed decentralized approach against the noises.

6.2 Future directions

The proposed approaches of this dissertation do have some limitations which provide directions for future work. These future directions are summarized as follows:

1. **Diagnosis of drift-like faults**. A system can change its operation conditions from normal to faulty either abruptly or gradually. In the case of gradual change, the system begins to malfunction (degraded behavior) until the failure takes over completely. Early or advanced warning of failures can help providing a time to achieve appropriate corrective actions and to reduce the maintenance costs. The discrete faults are abrupt failures and thus can be caused by exogenous actions; while parametric faults are caused by a deviation (variation) in some system parameters. We considered in this dissertation that the parametric faults are gradual ones that may lead the system, after a certain time, to a failure mode. This failure is diagnosed when its importance (the abnormal change amplitude of the parameter nominal value) is enough to allow the sensitive residuals to be greater than the predefined failure detection thresholds. The gradual dynamics of the parametric faults can be represented as a drift in the system operating conditions from normal to faulty ones. This drift leads to a gradual change in the characteristics of the system dynamics. Detecting this drift as early as possible may allow warning human supervision operators about the fault occurrence in early stage. Therefore, one future work is to integrate in the proposed approaches drift indicators allowing monitoring any serious change in the characteristics of the discrete and/or the continuous dynamics of the system in each discrete mode or configuration. These indicators observe some statistical properties of the observed discrete events and/or the continuous measurements in a discrete mode. When at least one characteristic statistical property of these discrete events or measurements changes, a warning is activated. Then, this warning is confirmed as soon as this drift is confirmed. As an example, the data indicating the time of events occurrences in the case of normal operating conditions are gathered to form a historic or learning set. Then, a histogram is constructed to show the frequency distribution of the occurrence of the various events in response to actions (commands). This histogram can be used to calculate the mean and the spread of the normal variation of the component behavior. When the system begins to malfunction, the time occurrence of events starts to drift (increases or decreases). This drift leads to a change in the frequency distribution of time event occurrences. Therefore, an indicator monitoring the change in the mean and spread of the normal variation of the system behavior, or one of its components, can be used to detect this drift and alarm a human operator. Same reasoning can be applied for the continuous measurements in

each discrete mode, e.g. the time for filling or draining a tank or for charging or discharging a capacitor. Fig.6.1 shows an example of the change of the frequency distributions of the maximum, respectively minimum, tension of a capacitor during the charge, respectively discharge, of this capacitor.

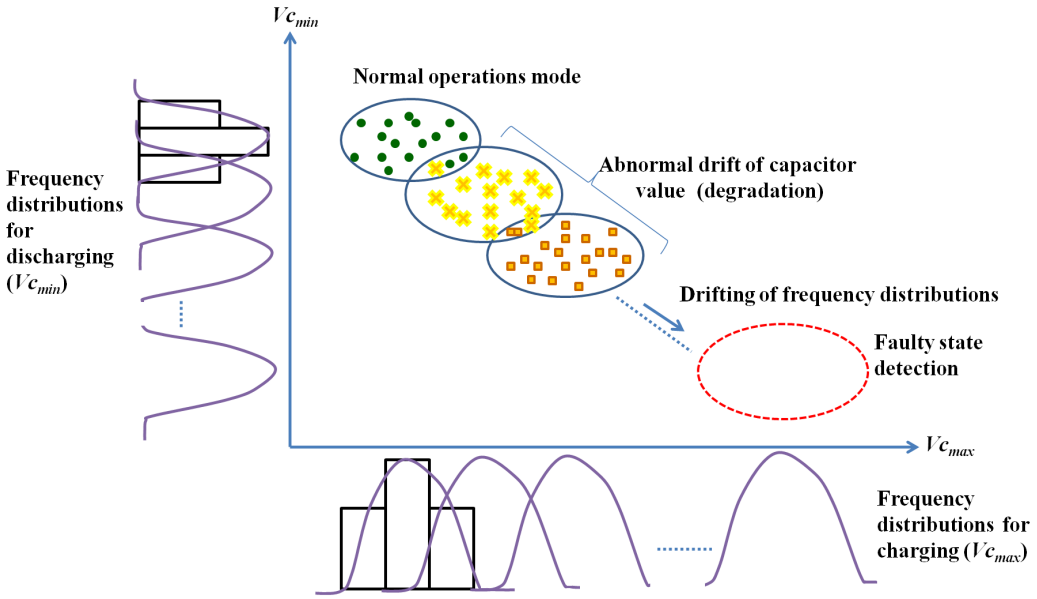

Figure 6.1: Abnormal drift from normal to faulty operation conditions of a capacitor representing its degradation (aging effect).

2. **Multiple faults diagnosis**. In this dissertation, the proposed approaches are based on the single fault hypothesis. In this case, only one fault (parametric or discrete) can occur. However, sometimes a set of faults may occur together. This case is termed as multiple faults scenario and the diagnosis method must be able to infer their occurrence together in order to explain the observed fault behavior. The multiple faults diagnosis is a challenging task due to the interaction between the different faults. This interaction may generate new fault behaviors or cause fault masking. In addition, the same set of multiple faults can manifest in different ways, depending on which fault occurs first, and on the fault propagation delays in the system. This will increase exponentially the state space with the number of potential faults. Therefore, one future direction of our work is to extend the proposed decentralized hybrid diagnosis approach in order to achieve the diagnosis of parametric and discrete faults occurring in multiple faults scenarios. To this end, the multiple faults modes will be included as states in the local hybrid models. The goal is to be able to include the effect of multiple faults on the system behavior as well as on the generated fault signatures. In addition, the processing capacity of the coordinator will be increased in order to generate new information useful to

improve the discrimination power of the different normal and fault behaviors of the decentralized diagnosis structure. Example of this useful information is the integration, in the fault signatures, of the time ordering deviations impacting continuous variables. This ordering is useful to distinguish between the occurrence of a single fault and the effect of its propagation towards other components from the occurrence of multiple faults. Finally, the incremental inference used by the proposed approaches can be used here in order to reduce the set of fault candidates in response to the occurrence of new observable events.

3. **Application of the proposed decentralized diagnosis structure to a physical three cell converter**. The proposed decentralized diagnosis structure were tested and evaluated using a bench-mark of three cell converter developed using Matlab-Simulink^{TM} environment and Stateflow^{TM} toolbox. A future direction is to apply these approaches using a physical three cell converter. The challenge is to incorporate parametric and discrete faults on the physical converter (changing artificially the values of capacitors and forcing switches to change or to remain in their current discrete mode, i.e. 'stuck-closed' or 'stuck-opened'). To this end, the scheme of Fig.6.2 will be used.

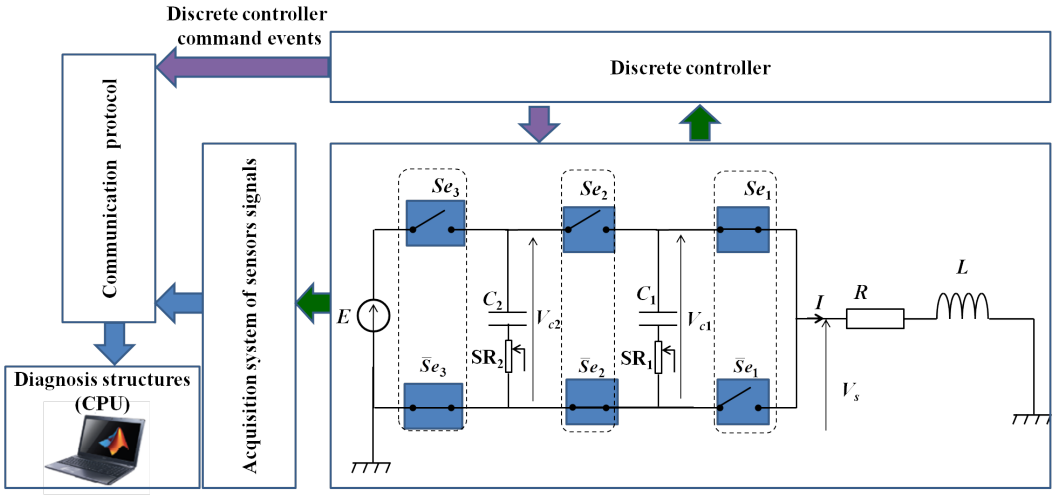

Figure 6.2: General scheme of the physical three cell converter.

In this scheme, the decentralized diagnosis structure (local diagnosers and the coordinator) are implemented using a calculator (CPU) equipped with Matlab-Simulink^{TM} environment and Stateflow^{TM} toolbox. The sensors readings as well as the discrete control command events will be communicated to the calculator (CPU) in order to allow the evolving of the decentralized diagnosis structure. Then, discrete faults are incorporated using the scheme of Fig.6.3. In this scheme, the 'stuck-closed' discrete fault in switch S_j, $j \in \{1, 2, 3\}$, is

generated by closing the additional parallel related switch $SC_j,\ j \in \{1,2,3\}$. Likewise, the 'stuck-on' discrete fault in switch $S_j,\ j \in \{1,2,3\}$ is generated by opening the additional serial switch $SO_j,\ j \in \{1,2,3\}$. Similarly, parametric faults in capacitors will be incorporated by changing artificially the tensions $(Vc_i,\ i \in \{1,2\})$ of capacitors $C_i,\ i \in \{1,2\}$. To achieve that, the value of resistor $SR_i,\ i \in \{1,2\}$, (see Fig.6.2) will be increased gradually from its initial value (i.e., zero corresponding to the normal operation conditions of $C_i,\ i \in \{1,2\}$). This increase of SR_i will decrease the value of C_i leading to generate an artificial abnormal change in the value of C_i.

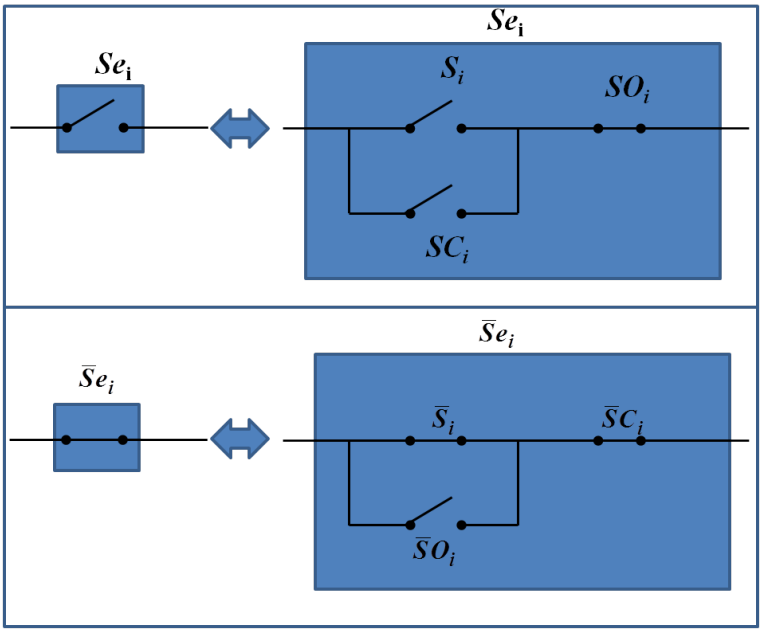

Figure 6.3: Discrete faults generated in switch S_i in the physical three cell converter.

4. **Integrating the decentralized diagnosis structure in an advanced supervision scheme and its application to achieve the monitoring of wind turbines**. One future direction of our work is to develop the proposed decentralized fault diagnosis approach in order to be integrated in an advanced supervision scheme. The latter contains a fault management module that aims at deciding the actions to be taken (to stop or to change the operation, to reconfigure the system or to achieve an adequate maintenance procedure) in response to the occurrence of a fault. These actions lead to maximize the system performance (availability, production, security) and to reduce its maintenance costs. One potential application of this advanced supervision scheme is the monitoring of wind turbines, in particular the converters. Indeed, the converter used in wind turbines is similar to the three cell converter used in Chapter 5 of this dissertation. The difference is that the converter in the wind turbine has 3 arms; each one of them is a three cell converter (see Fig.6.4).

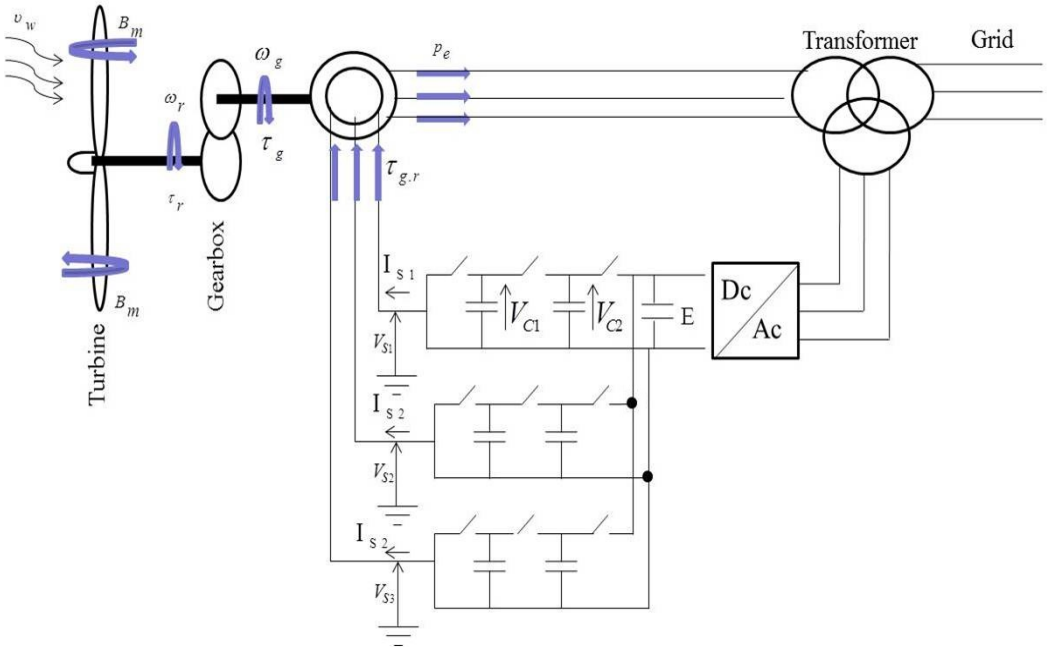

Figure 6.4: Wind turbine with its corresponding converter.

Bibliography

Alavi, M., Luo, M., Wang, D., and Zhang, D. H. (2011). Fault diagnosis for power electronic inverters: A model-based approach. In *IEEE International Symposium on Diagnostics for Electric Machines, Power Electronics & Drives (SDEMPED)*, pages 221–228. IEEE. (Cited on page 18.)

Bayoudh, M., Travé-Massuyes, L., and Olive, X. (2006). Hybrid systems diagnosability by abstracting faulty continuous dynamics. In *Proceedings of the 17th International Principles of Diagnosis Workshop*, pages 9–15. Citeseer. (Cited on pages 22 and 23.)

Bemporad, A., Garulli, A., Paoletti, S., and Vicino, A. (2005). A bounded-error approach to piecewise affine system identification. *IEEE Transactions on Automatic Control*, 50(10):1567–1580. (Cited on page 8.)

Benzineb, O., Taibi, F., Laleg-Kirati, T. M., Seghir Boucherit, M., and Tadjine, M. (2013). Control and fault diagnosis based sliding mode observer of a multicellular converter: Hybrid approach. *Journal of Electrical Engineering*, 64(1):20–30. (Cited on page 110.)

Bhowal, P., Sarkar, D., Mukhopadhyay, S., and Basu, A. (2007). Fault diagnosis in discrete time hybrid systems–a case study. *Information Sciences*, 177(5):1290–1308. (Cited on pages 5, 24 and 26.)

Biswas, G., Simon, G., Mahadevan, N., Narasimhan, S., Ramirez, J., and Karsai, G. (2003). A robust method for hybrid diagnosis of complex systems. In *Proceedings of the 5th Symposium on Fault Detection, Supervision and Safety for Technical Processes*, pages 1125–1131. (Cited on page 151.)

Biswas, S., Sarkar, D., Mukhopadhyay, S., and Patra, A. (2006). Diagnosability analysis of real time hybrid systems. In *IEEE International Conference on Industrial Technology, 2006*, pages 104–109. IEEE. (Cited on page 24.)

Bouibed, K., Seddiki, L., Guelton, K., and Akdag, H. (2014). Actuator and sensor fault detection and isolation of an actuated seat via nonlinear multi-observers. *Systems Science & Control Engineering: An Open Access Journal*, 2(1):150–160. (Cited on page 14.)

Brito Palma, L., Coito, F. V., and Neves da Silva, R. (2005). Diagnosis of parametric faults based on identification and statistical methods. In *44th IEEE Conference on Decision and Control, European Control Conference*, pages 3838–3843. IEEE. (Cited on page 73.)

Cassandras, C. G. and Lafortune, S. (2008). *Introduction to discrete event systems*. Springer. (Cited on page 43.)

Cha, Y.-J. and Agrawal, A. K. (2014). Robustness studies of sensor faults and noises for semi-active control strategies using large-scale magnetorheological dampers. *Journal of Vibration and Control*. (Cited on page 15.)

Cocquempot, V., El Mezyani, T., and Staroswiecki, M. (2004). Fault detection and isolation for hybrid systems using structured parity residuals. In *5th Proceedings of Control Conference*, volume 2, pages 1204–1212. IEEE. (Cited on pages 6, 18, 19 and 49.)

Daigle, M. J. (2008). *A qualitative event-based approach to fault diagnosis of hybrid systems*. PhD thesis, Vanderbilt University. (Cited on pages 13 and 16.)

Daigle, M. J., Koutsoukos, X. D., and Biswas, G. (2010a). An event-based approach to integrated parametric and discrete fault diagnosis in hybrid systems. *Transactions of the Institute of Measurement and Control*, 32(5):487–510. (Cited on page 30.)

Daigle, M. J., Roychoudhury, I., Biswas, G., Koutsoukos, X. D., Patterson-Hine, A., and Poll, S. (2010b). A comprehensive diagnosis methodology for complex hybrid systems: A case study on spacecraft power distribution systems. *IEEE Transactions on Systems, Man and Cybernetics, Part A: Systems and Humans*, 40(5):917–931. (Cited on pages 30 and 33.)

Defoort, M., Djemai, M., Floquet, T., and Perruquetti, W. (2011). Robust finite time observer design for multicellular converters. *International Journal of Systems Science*, 42(11):1859–1868. (Cited on pages 21, 110, 115 and 143.)

Derbel, H. (2009). *Diagnostic à base de modèles des systèmes temporisés et d'une sous-classe de systèmes dynamiques hybrides*. PhD thesis, Université Joseph-Fourier-Grenoble I. (Cited on pages 28 and 29.)

Ding, F., Liu, X., Chen, H., and Yao, G. (2014). Hierarchical gradient based and hierarchical least squares based iterative parameter identification for cararma systems. *Signal Processing*, 97:31–39. (Cited on page 13.)

Eren, Y., Shen, J., and Camlibel, K. (2014). Quadratic stability and stabilization of bimodal piecewise linear systems. *Automatica*, 50(5):1444–1450. (Cited on page 8.)

Farhood, M. and Beck, C. L. (2014). On the balanced truncation and coprime factors reduction of markovian jump linear systems. *Systems & Control Letters*, 64:96–106. (Cited on page 7.)

Fichou, P. (2004). Technologie n 133, ch. bond graphs: une méthode pluridisciplinaire. *Sciences et techniques industrielles*, 33:37–46. (Cited on page 12.)

Fourlas, G., Kyriakopoulos, K. J., and Krikelis, N. (2002). Diagnosability of hybrid systems. In *Proceedings of the 10th IEEE Mediterranean Conference on Control and Automation*. (Cited on page 34.)

Fourlas, G. K. (2009). Multiple faults diagnosability of hybrid systems. In *17th Mediterranean Conference on Control and Automation, MED'09.*, pages 365–370. IEEE. (Cited on page 34.)

Fourlas, G. K. (2014). Application of hybrid systems multiple faults diagnosis to a four–wheeled mobile robot. In *Proceedings of the 25th International Workshop on Principles of Diagnosis DX'14*. (Cited on pages 34 and 35.)

Gomez, L., Ramirez-Trevino, A., Gomez-Gutierrez, D., Ramirez-Prado, G., and Ruiz-Leon, J. (2010). *Diagnosability in Switched Linear Systems*. INTECH Open Access Publisher. (Cited on pages 9 and 70.)

Gray, C. S., Koitz, R., Psutka, S., and Wotawa, F. (2014). An abductive diagnosis and modeling concept for wind power plants. In *Proceedings of the 25th International Workshop on Principles of Diagnosis DX'14*. (Cited on page 110.)

Gupta, V., Murray, R. M., Shi, L., and Sinopoli, B. (2009). Networked sensing, estimation and control systems. *California Institute of Technology Report*. (Cited on page 8.)

Isermann, R. (2006). *Fault-diagnosis systems*. Springer. (Cited on page 16.)

Kamel, T., Diduch, C., Bilestkiy, Y., and Chang, L. (2012). Fault diagnoses for the dc filters of power electronic converters. In *Energy Conversion Congress and Exposition (ECCE), IEEE*, pages 2135–2141. IEEE. (Cited on page 18.)

Kan John, P., Blackhall, L., and Grastien, A. (2009). Diagnosing hybrid dynamical systems. In *Fault Detection, Supervision and Safety of Technical Processes*, pages 983–988. (Cited on page 17.)

Khorasgani, H., Eriksson, D., Biswas, G., Frisk, G., and Krysander, M. (2014). Offline robust residual selection using sensitivity analysis. In *Proceedings of the 25th International Workshop on Principles of Diagnosis DX'14*. (Cited on page 151.)

Koutsoukos, X., Kurien, J., and Zhao, F. (2002). Monitoring and diagnosis of hybrid systems using particle filtering methods. In *International Symposium on Mathematical Theory of Networks and Systems*. (Cited on page 17.)

Lezana, P., Aguilera, R., and Rodríguez, J. (2009). Fault detection on multicell converter based on output voltage frequency analysis. *IEEE Transactions on Industrial Electronics*, 56(6):2275–2283. (Cited on page 110.)

Louajri, H. and Sayed-Mouchaweh, M. (2014a). Decentralized approach for fault diagnosis of three cell converters. In *Annual Conference of the Prognostics and Health Management Society, PHM Society*. (Cited on pages 2 and 109.)

Louajri, H. and Sayed-Mouchaweh, M. (2014b). Decentralized diagnosis and diagnosability of a class of hybrid dynamic systems: Application to the three cell converter. In *Proceedings of the11th International Conference on Informatics in Control, Automation and Robotics (ICINCO)*. (Cited on pages 2 and 77.)

Louajri, H. and Sayed-Mouchaweh, M. (2014c). Decentralized structure for fault diagnosis of a class of hybrid dynamic systems. In *22nd IEEE Mediterranean Conference on Control & Automation*. (Cited on page 2.)

Louajri, H. and Sayed-Mouchaweh, M. (2014d). Modular approach for the diagnosis of a class of hybrid dynamic systems: Application to three cell converters. In *Proceedings of the 25th International Workshop on Principles of Diagnosis DX'14*. (Cited on pages 2, 39 and 77.)

Louajri, H., Sayed-Mouchaweh, M., and Labbare, C. (2013). Diagnoser with hybrid structure for fault diagnosis of a class of hybrid dynamic systems. *Chemical Engineering Transactions*, 33:85–90. (Cited on pages 2, 39 and 77.)

Lynch, N., Segala, R., and Vaandrager, F. (2003). Hybrid i/o automata. *Information and Computation*, 185(1):105–157. (Cited on page 10.)

Palejiya, D., Shaltout, M., Yan, Z., and Chen, D. (2014). stability of wind turbine switching control. *International Journal of Control*, (ahead-of-print):1–11. (Cited on page 8.)

Pencolé, Y. and Cordier, M.-O. (2005). A formal framework for the decentralised diagnosis of large scale discrete event systems and its application to telecommunication networks. *Artificial Intelligence*, 164(1):121–170. (Cited on page 77.)

Pisano, A., Rapaić, M. R., and Usai, E. (2014). Discontinuous dynamical systems for fault detection. a unified approach including fractional and integer order dynamics. *Mathematics and Computers in Simulation*, 95:111–125. (Cited on page 14.)

Rahiminejad, M., Diduch, C., Stevenson, M., and Chang, L. (2012). Open-circuit fault diagnosis in 3-phase uncontrolled rectifiers. In *3rd IEEE International Symposium on Power Electronics for Distributed Generation Systems (PEDG)*, pages 254–259. IEEE. (Cited on page 21.)

Rodrigues, L. and How, J. P. (2003). Observer-based control of piecewise-affine systems. *International Journal of Control*, 76(5):459–477. (Cited on page 8.)

Roychoudhury, I., Biswas, G., and Koutsoukos, X. (2009). Designing distributed diagnosers for complex continuous systems. *IEEE Transactions on Automation Science and Engineering*, 6(2):277–290. (Cited on page 11.)

Sampath, M. (1995). *A discrete event systems approach to failure diagnosis*. PhD thesis, The University of Michigan. (Cited on page 70.)

Sampath, M., Sengupta, R., Lafortune, S., Sinnamohideen, K., and Teneketzis, D. C. (1996). Failure diagnosis using discrete-event models. *IEEE Transactions on Control Systems Technology*, 4(2):105–124. (Cited on pages 3 and 70.)

Savkin, A. V. and Evans, R. J. (2002). *Hybrid dynamical systems: controller and sensor switching problems*. Springer. (Cited on page 15.)

Shahbazi, M., Jamshidpour, E., Poure, P., Saadate, S., and Zolghadri, M. R. (2013). Open-and short-circuit switch fault diagnosis for nonisolated dc–dc converters using field programmable gate array. *IEEE Transactions on Industrial Electronics*, 60(9):4136–4146. (Cited on page 110.)

Sun, B., Luh, P. B., Jia, Q.-S., O'Neill, Z., and Song, F. (2014). Dept. of autom., tsinghua univ., beijing, china. *IEEE Transactions on Automation Science and Engineering*, 11(1):215–229. (Cited on page 16.)

Uzunova, M., Bouamama, B. O., and Djemai, M. (2012). Hybrid bond graph diagnostic and localisation-signal signature study of three-cell converter. In *20th Mediterranean Conference on Control & Automation (MED)*, pages 966–971. IEEE. (Cited on page 110.)

Van Der Schaft, A. J., Schumacher, J. M., van der Schaft, A. J., and van der Schaft, A. J. (2000). *An introduction to hybrid dynamical systems*, volume 251. Springer London. (Cited on pages 6, 8 and 9.)

Van Gorp, J. (2013). *Diagnostic et observation d'une classe de systèmes dynamiques hybrides. Application au convertisseur multicellulaire série*. PhD thesis, Université de Valenciennes et du Hainaut-Cambresis. (Cited on pages 18, 19 and 20.)

Xu, Q., Yang, H., Jiang, B., Zhou, D., and Zhang, Y. (2014). Fault tolerant formations control of uavs subject to permanent and intermittent faults. *Journal of Intelligent & Robotic Systems*, 73(1-4):589–602. (Cited on page 16.)

Yoo, S. J. (2014). Fault detection and accommodation of a class of nonlinear systems with unknown multiple time-delayed faults. *Automatica*, 50(1):255–261. (Cited on page 15.)

Zhang, L. and Boukas, E.-K. (2009). Stability and stabilization of markovian jump linear systems with partly unknown transition probabilities. *Automatica*, 45(2):463–468. (Cited on page 7.)

Zouari, T., Pekpe, K. M., Cocquempot, V., and Ksouri, M. (2014). Active mode recognition of switched nonlinear systems: application to fault detection and isolation. *Asian Journal of Control*, 16(2):345–357. (Cited on page 14.)

Abstract: This thesis aims at defining a diagnosis approach for hybrid dynamic systems in particular Discretely Controlled Continuous Systems. The goal is to build a diagnosis module called, diagnoser, able to diagnose parametric and discrete faults. Parametric faults affect the system continuous dynamics and are characterized by abnormal changes in some system parameters; whereas discrete faults affect the system discrete dynamics and are considered either as the occurrence of unobservable events and/or reaching discrete fault modes. This approach is based on modular modeling in order to take into account the interactions between continuous and discrete dynamics. This approach is developed through two approaches. A modular diagnosis approach in which the diagnoser is built based on the use of the global model and a decentralized approach in which a set of local diagnosers are built based on the local model of the system components. The three-cell converter is used to demonstrate the efficacy of these two approaches.

Keywords: Mots clefs : Hybrid fault diagnosis, Hybrid dynamic systems, discretely controlled continuous systems, Parametric faults, Discrete fault, Hybrid dynamic system modeling, Power electronics.

Rśumé Les travaux de ma thèse ont pour but la définition d'une dḿarche modulaire permettant le diagnostic des df́auts liés conjointement aux dynamiques continue et discrète des Systèmes Dynamiques Hybrides (SDH), en particulier les systèmes continus à commande discrète (SCCD). L'objectif est de construire un modèle de diagnostic appelé, diagnostiqueur, permettant de diagnostiquer à la fois les défauts paramétriques et discrets des SDH de grande taille. Les défauts paramétriques sont caractérisés par un changement anormal de certains paramètres tandis que les défauts discrets sont caractérisés par un changement inattendu du mode discret du système. Cette démarche est basée sur une modélisation modulaire orientée composant permettant de tenir compte de la nature composite du système. Elle tient compte également des interactions entre les dynamiques discrète et continue. Cette démarche est développée à travers deux approches. Une approche de diagnostique modulaire dont le diagnostiqueur est construite à partir du modèle global de système, et une approche de diagnostique décentralisé dont d'un ensemble des diagnostiqueurs locaux sont construits à partir des modèles locaux du système. Ces deux approches sont validées en utilisant un convertisseur à trois cellules.

Mots clefs: Diagnostique des défauts, Systèmes dynamiques hybrides, System continus a commande discrète, Défauts paramétriques et discrets, Modélisation hybride, Electronique de puissance.